Technical Publication SJ2022-02

AQUIFER RECHARGE POTENTIAL OF A SINKHOLE: SUNNYHILL RESTORATION AREA, MARION COUNTY, FLORIDA

by

Donald J. Lee, P.G.
Jeffrey B. Davis, P.G.
Paul Bremner, Ph.D.
Wei Jin, P.E., Ph.D.

St. Johns River Water Management District
Palatka, Florida

2022

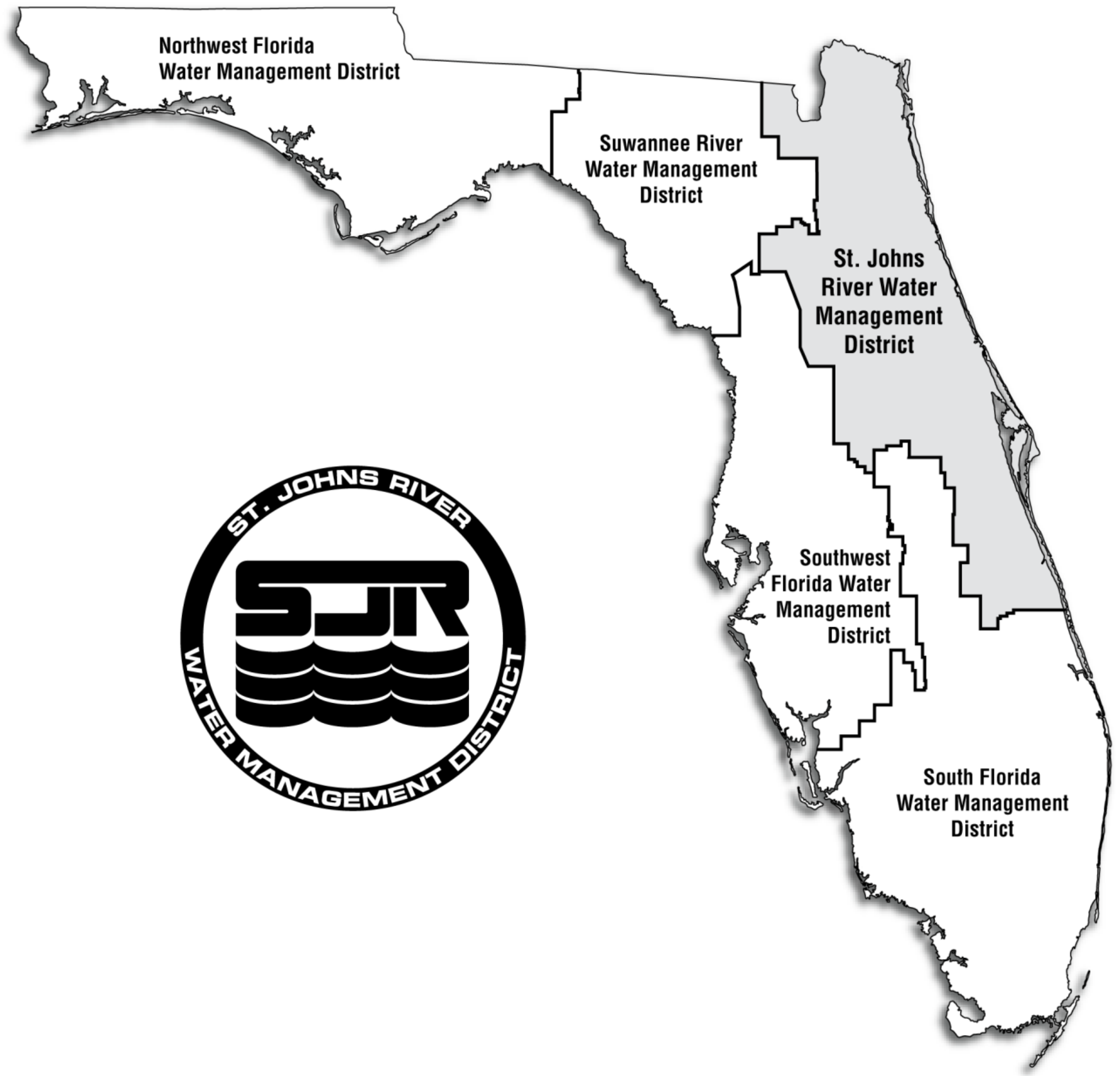

The St. Johns River Water Management District was created in 1972 by passage of the Florida Water Resources Act, which created five regional water management districts. The St. Johns District includes all or part of 18 counties in northeast and east-central Florida. Its mission is to preserve and manage the region's water resources, focusing on core missions of water supply, flood protection, water quality and natural systems protection and improvement. In its daily operations, the district conducts research, collects data, manages land, restores and protects water above and below the ground, and preserves natural areas.

This document is published to disseminate information collected by the district in pursuit of its mission. Electronic copies are available at *www.sjrwmd.com/technicalreports* or by calling the district at the number below.

Scientific Reference Center
St. Johns River Water Management District
4049 Reid Street/P.O. Box 1429
Palatka, FL 32178-1429 (32177 for street deliveries)
386-329-4500

EXECUTIVE SUMMARY

The St. Johns River Water Management District (District) owns 8,355 acres in Marion and Lake counties known as the Sunnyhill Restoration Area (Figure 1). The District is evaluating sites having the potential for groundwater recharge using surface water that may not otherwise recharge due to flow paths or geologic conditions. One recharge scenario under consideration is to provide surface water to existing sinkholes that may have a direct hydraulic connection to the Upper Floridan aquifer (UFA).

Two sinkholes at the Sunnyhill property were evaluated in phases. The first phase was an investigation to confirm that the physical conditions at the sinkholes are conducive to recharge. The second phase of investigation was a hydraulic loading test of the Site 1 sinkhole to evaluate its capacity to recharge the UFA and to estimate the hydraulic characteristics of the sinkhole.

The following methods were used in this investigation that were progressively more site-specific.

- Conducted a desktop review of available regional hydrogeological data.
- Designed and obtained an electrical resistivity survey over both sinkhole sites identified at the Sunnyhill Restoration Area.
- Acquired lithologic information from within the Site 1 sinkhole with a test borehole using the standard penetration test (SPT) method.
- Calibrated the electrical resistivity survey model using lithologic information from the Site 1 sinkhole borehole.
- Installed monitor wells peripheral to the Site 1 sinkhole to confirm subsurface lithology and to monitor both surficial aquifer system (SAS) and UFA water levels.
- Collected aerial imagery with an unmanned aerial vehicle (UAV) equipped with high resolution camera to create a digital terrain model to estimate the sinkhole storage volume.
- Conducted a hydraulic load test by pumping surface water from a flooded former agricultural field approximately 1,000 feet west of the Site 1 sinkhole.
- Released fluorescein dye into the sinkhole at the onset of the hydraulic load test to aid in evaluating the UFA recharge potential.
- Performed statistical analysis of water level data collected during the load test to evaluate recharge to the UFA.

The results of the investigation demonstrated that there was a likely hydraulic connection between the SAS and UFA beneath the cover-collapse type sinkhole identified as Site 1. Approximately 14 million gallons (MG) of water percolated into the subsurface or evaporated and approximately 6.6 MG staged up inside the sinkhole during the 13-day hydraulic load test, which delivered 20.6 MG. Approximately 1.4 MG per day may be able to recharge the UFA at the Site 1 sinkhole. An estimated volume of 6.6 MG beneath the 70-foot elevation contour within the Site 1 sinkhole could store water until it percolates downward. Given the pumped volume during load test was 20.6 MG, approximately 13.9 MG of pumped water infiltrated into the sinkhole.

CONTENTS

LIST OF FIGURES

LIST OF TABLES

1. INTRODUCTION

The St. Johns River Water Management District (District) owns 8,355 acres in Marion and Lake counties known as the Sunnyhill Restoration Area (Figure 1). The District is evaluating sites that may have the potential for groundwater recharge using surface water that may not otherwise recharge due to flow paths or geologic conditions. Depending on their origin, sinkholes may provide recharge pathways to the subsurface if conditions exist that caused a breach in the confining unit that separate the surficial aquifer system (SAS) from the underlying Upper Floridan aquifer (UFA). The Sunnyhill site has numerous large closed topographic depressions, one of which is a mature cover-collapse type sinkhole (Site 1). Another area contains an apparent cover-subsidence type sinkhole (Site 2).

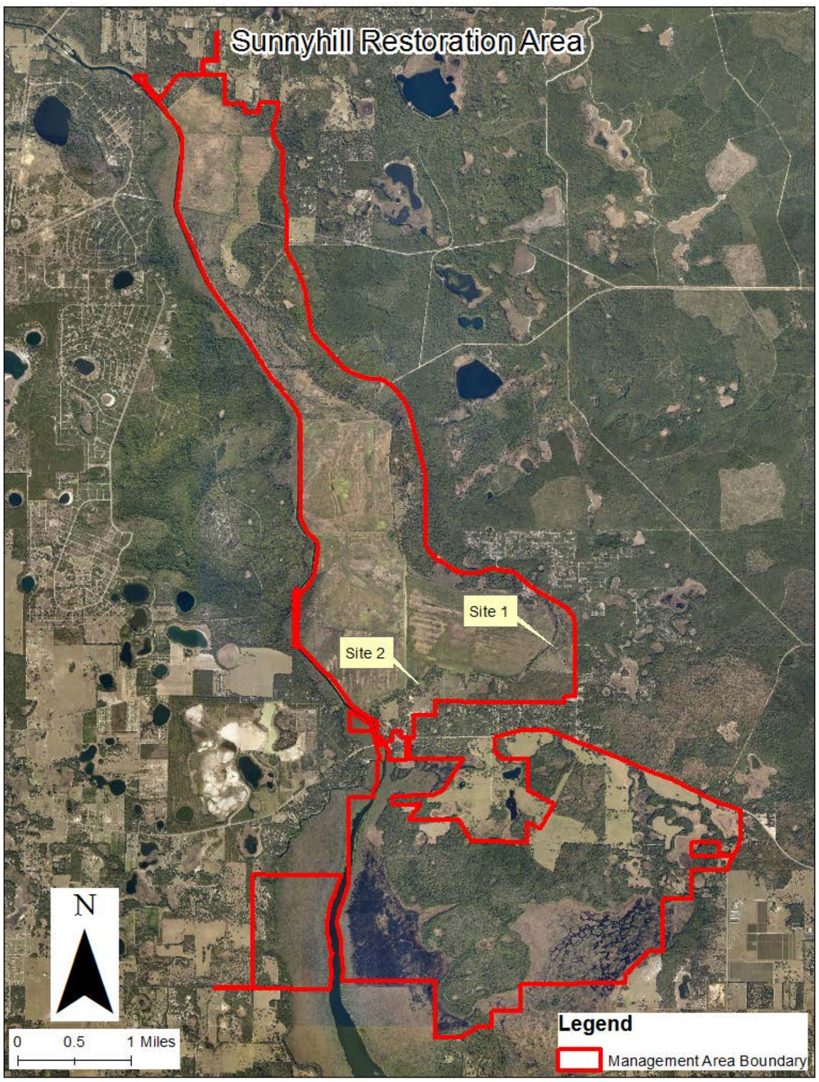

Figure 1. Location of potential sinkhole recharge sites at Sunnyhill Restoration Area. Site 1 was identified as having the most potential for recharge

Once the confining unit is breached in cover-collapse type sinkholes, the sand-sized siliciclastic sediment above the collapse will infill the throat of the sinkhole (Figure 2). These sand-sized grains have relatively high porosity and higher hydraulic conductivity than the confining units, which allow water to flow downward and recharge the SAS and UFA.

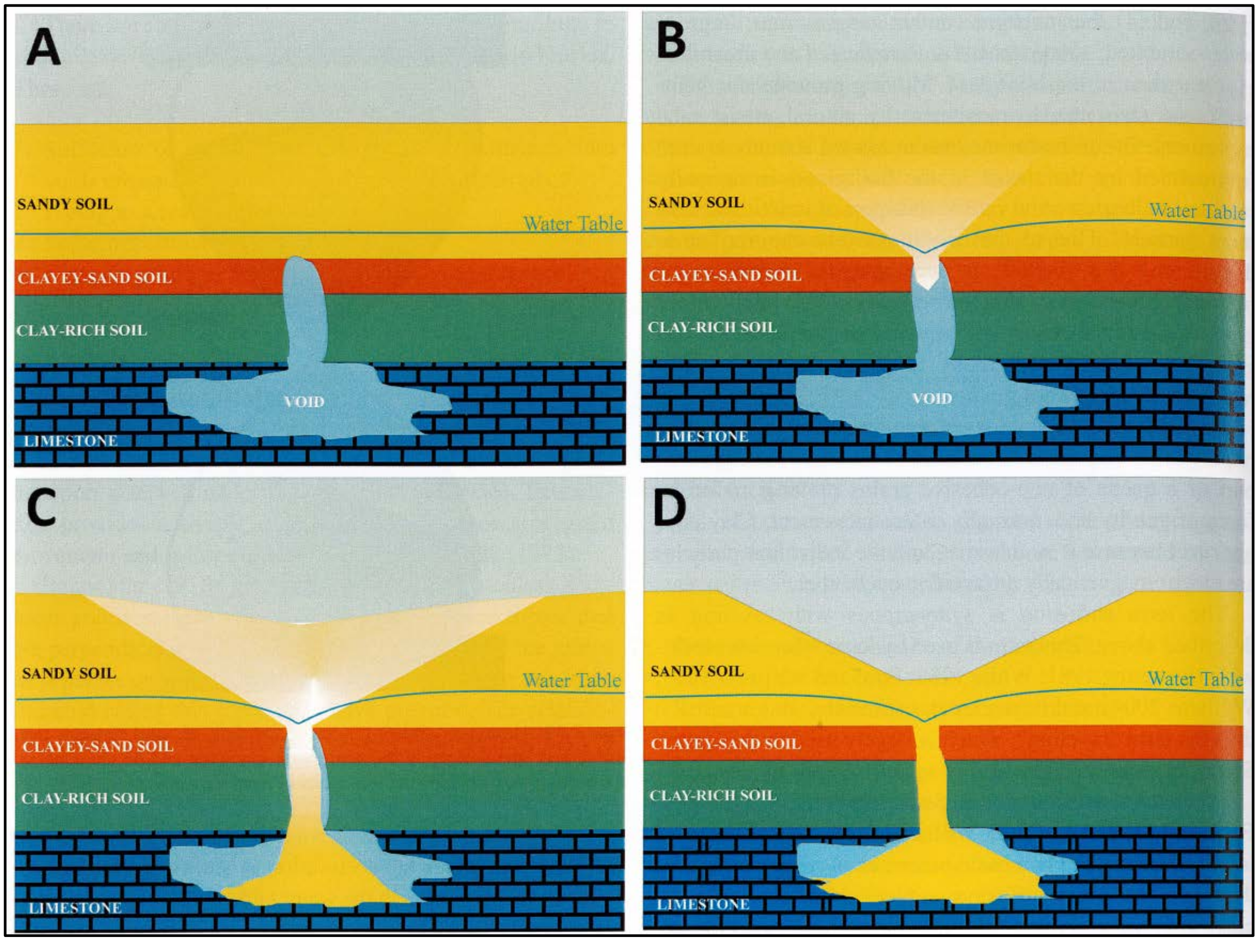

Figure 2. Development sequence of cover-collapse sinkhole: (A) pathway through confining unit above limestone developed, (B) sand dilatation with downward movement through confining unit like in an hourglass, (C) continued sand dilatation and downward migration, (D) sand completes downward migration resulting in land surface depression (adapted from Upchurch, et al. 2019)

Cover-subsidence sinkholes may not have as high hydraulic conductivity as cover-collapse sinkholes (Figure 3). However, the confining unit may be disturbed sufficiently to increase vertical hydraulic conductivity. Other sites within the District are being considered for similar sinkhole-related recharge projects. A feasibility study should be completed before designing and building the infra-structure needed for a recharge project. This report summarizes techniques that were used to evaluate the effectiveness of using a sinkhole for recharge.

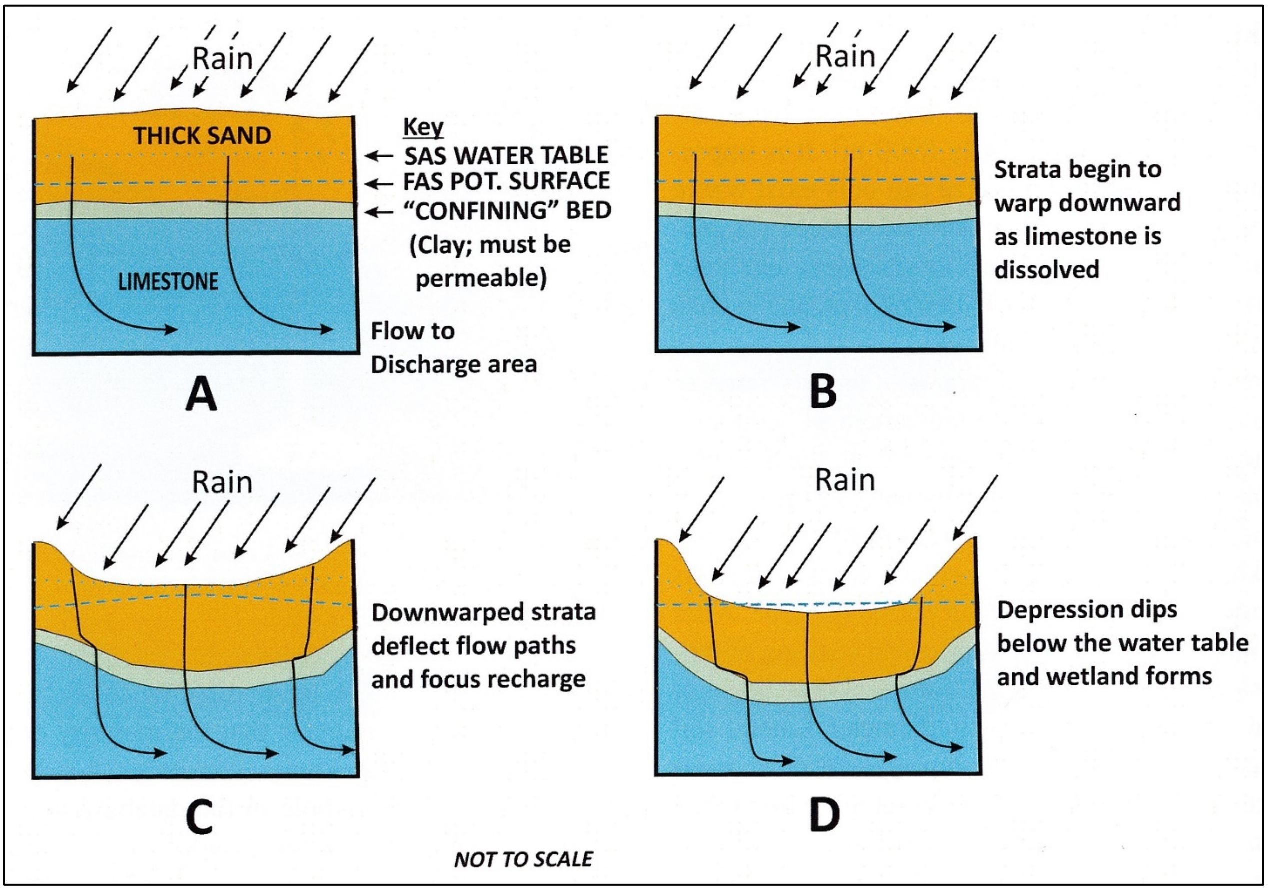

Figure 3. Development of cover-subsidence sinkhole (adapted from Upchurch, et al. 2019)

The Sunnyhill sinkholes were evaluated in two phases. The first phase was a site investigation to confirm that the physical conditions of the sinkholes are conducive to recharge. The second phase of investigation was a hydraulic loading test of the sinkhole to evaluate its capacity to recharge the UFA and to estimate the hydraulic characteristics of the sinkhole.

The District investigated two Sunnyhill sinkholes in the first phase to characterize the subsurface and assess the potential for use as an UFA recharge site. Results of the first phase indicated that Site 1 was the best sinkhole for potential recharge. A testing plan was designed and implemented for the Site 1 sinkhole during the second phase of investigation to further evaluate if the cover-collapse sinkhole could provide a site for recharge to the UFA.

2. METHODS

To investigate the recharge potential of the sinkholes at the Sunnyhill Restoration Area several methods were used that were progressively more site-specific. A summary of the investigation performed follow with details of the investigation methods provided below.

- Conducted a desktop review of available regional hydrogeological data.
- Designed and obtained an electrical resistivity survey over both sinkhole sites identified at the Sunnyhill Restoration Area and calibrated the electrical resistivity survey model using lithologic information from Site 1 sinkhole borehole.
- Acquired lithologic information from within the Site 1 sinkhole with a test borehole using the standard penetration test (SPT) method.
- Calibrated the electrical resistivity survey model using lithologic information from the Site 1 sinkhole borehole.
- Installed monitor wells peripheral to the Site 1 sinkhole to confirm subsurface lithology and to monitor both SAS and UFA water levels.
- Collected aerial imagery with an unmanned aerial vehicle (UAV) equipped with high resolution camera to create a digital terrain model to estimate the sinkhole storage volume.
- Conducted a hydraulic load test by pumping surface water from a flooded former agricultural field approximately 1,000 feet west of the Site 1 sinkhole.
- Released fluorescein dye into the sinkhole at the onset of the hydraulic load test to aid in evaluating UFA recharge potential.
- Performed statistical analysis of water level data collected during load test to evaluate recharge to UFA.

DESKTOP REGIONAL HYDROGEOLOGICAL INVESTIGATION

The sinkhole recharge investigation began by compiling existing data to gain an understanding of the local hydrogeologic conditions. Borehole data, such as nearby lithologic and geophysical log data and well completion reports were reviewed to establish the thickness of the SAS, the Intermediate Confining Unit (ICU) and the top of the UFA. UFA potentiometric surface maps and United States Geological Survey (USGS) topographic maps were also reviewed. Closed topographic depressions on the Sunnyhill site were mapped using available digital elevation models (DEMs). This information was then used to plan a site-specific investigation of the Sunnyhill sinkhole sites identified that have the potential for recharge.

ELECTRICAL RESISTIVITY IMAGING

Direct current (DC) electrical resistivity imaging (ERI) surveys were conducted to identify the configuration of the material that is beneath the Site 1 and Site 2 sinkholes (referenced as Area 1 and Area 2 in Geohazards report), (Appendix A and Figure 4). These ERI surveys were designed to reach the expected depth of the top of the UFA with maximum depth of penetration from approximately 175 to 180 feet. Profile 1 was significantly longer than Profile 2. It was extended to the abandoned irrigation well (M-0357) to the southwest of the Site 1 sinkhole and included areas that were not disturbed by sinkhole activity.

ERI Profile 1 was used to locate the site of the test borehole that was drilled on the southwest side near the bottom of the sinkhole along the profile line to aid in interpretation of the resistivity values. Continuous split spoon samples were collected in the test borehole to a depth of 50 feet and then every 2 feet thereafter. A BF51 drilling rig mounted on a Marooka off road rubber tracked machine (Figure 5) was used to construct the borehole due to the steep-sided slope of the sinkhole.

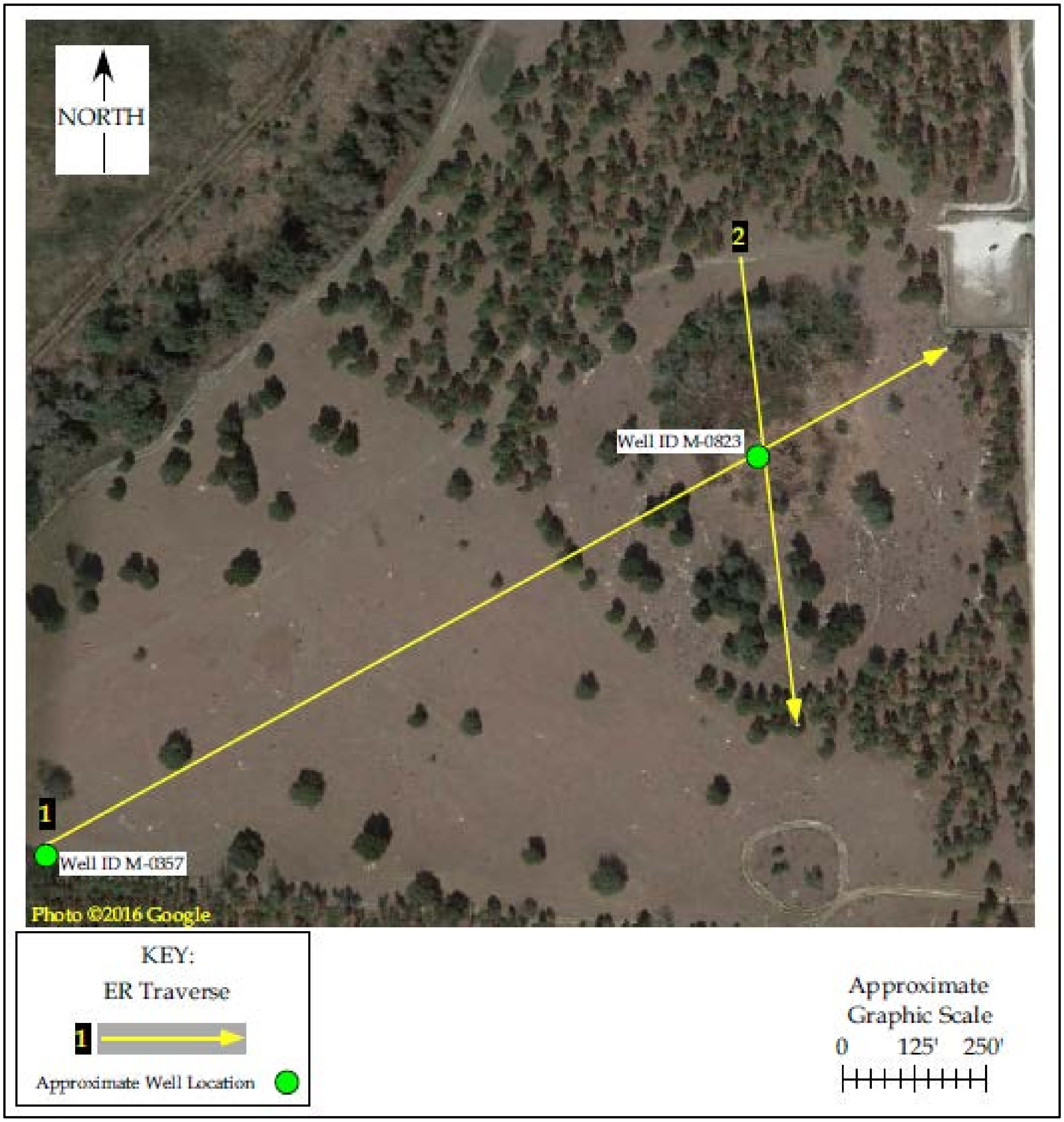

Figure 4. Location of Electrical Resistivity Imaging profiles at Site 1 sinkhole, abandoned well M-0357 with geophysical logs and borehole M-0823 in the sinkhole (modified from Appendix A – Jones Edmunds/Geohazards report)

SUBSURFACE LITHOLOGICAL INVESTIGATION

The District issued a Work Order to Huss Drilling, Inc. for the test hole construction and provided field oversight of the drilling and site preparations to ensure safety and support for access to the steep terrain of the sinkhole. The water well contractor used a track-mounted drill rig to navigate the steep slope of the sinkhole and for drilling of the borehole. Geophysical borehole logging was completed using the District's equipment.

Figure 5. Track mounted drilling rig used to drill the test hole in the bottom of the sinkhole (left image). Right image shows District staff John Lombardi deploying the cable from the geophysical logging truck stationed at the rim of the sink.

MONITOR WELL INSTALLATION AND WATER LEVEL MONITORING

Monitor wells were constructed for obtaining water level measurements and for water quality sampling points (Figure 6). Monitor well construction began with the preparation of construction specifications to provide to the water well contractor. The data collected in the desktop analysis and ERI investigation were used to design the monitor wells and insure the hydrogeologic intervals of interest were monitored. At Site 1, both the SAS and the UFA are present. There is a downward hydraulic gradient from the SAS to the UFA, so water recharged into the SAS will eventually migrate downward through whatever pathway may exist.

Ideally for a dye trace test, there would be multiple wells for sampling in several directions believed to be preferred flow paths evidenced by regional karst features. Each sample site should have wells installed in the SAS and UFA. For this investigation budget constraints resulted in one UFA well and two SAS wells being constructed.

Locating the wells presented a challenge. To ensure the SAS and the UFA wells were monitoring just those aquifers a confining unit needs to be between them. In the sinkhole no confining unit (ICU) was identified. To the north, there is a large topographic depression which could be related to a disrupted ICU or the ICU may be missing entirely. The one area where it could be likely that the confining unit would be encountered is to the northwest of the Site 1 sinkhole near the now-abandoned irrigation well M-0357 location.

The UFA potentiometric surface is relatively flat locally but has a low gradient to the northeast or northwest. A comparison of water levels of the UFA well (M-0831) to the existing UFA water level in M-0483 (aka The Blue House well) indicated about a 0.4-foot difference. Because the Blue House well is over 1.5 miles away from M-0831, the gradient is so low it is insignificant compared to the gradient between the sinkhole water level and the well.

Water levels in the sinkhole and the monitor wells were recorded before pumping water into the sinkhole to establish a baseline. A continuous water level record was available for the Blue House monitor site (M-0483) as a regional reference location. Water level in the sinkhole was recorded using a pressure transducer connected to a telemetry system that transmitted the data back to the District server in Palatka in real time. The pressure transducer was installed below the water surface and the depth below water surface was set as a reference so correction to true elevation could be calculated after an elevation survey was completed.

A data cable was installed up the slope of the sinkhole to a telemetry station attached to a steel pole. The elevation of the station was designed to not be submerged when water was pumped into the sinkhole. Monitoring of the sinkhole water levels began on August 8, 2019, and was initially recorded every hour. Once the monitor wells were constructed, the frequency of water level measurements was increased to every five minutes to match the monitor well recording frequency.

Water level monitoring for the wells began on November 21, 2019, and was set at a frequency of every five minutes. In-Situ, Inc. Level TROLL 700 series transducers were installed in the monitor wells without real-time telemetry. Staff periodically visited the site and downloaded data as necessary from the Level TROLL 700 transducers. The measure point on each monitor well was surveyed so the recorded water levels could be corrected to elevation in feet NAVD 88.

As previously stated, transducers were installed in the wells and data was downloaded periodically. This typically coincided with a dye sampling event to minimized trips to the site and disturbances in the data. The effects of removing the sampler could be seen in the water level data. These effects were removed before analysis was done.

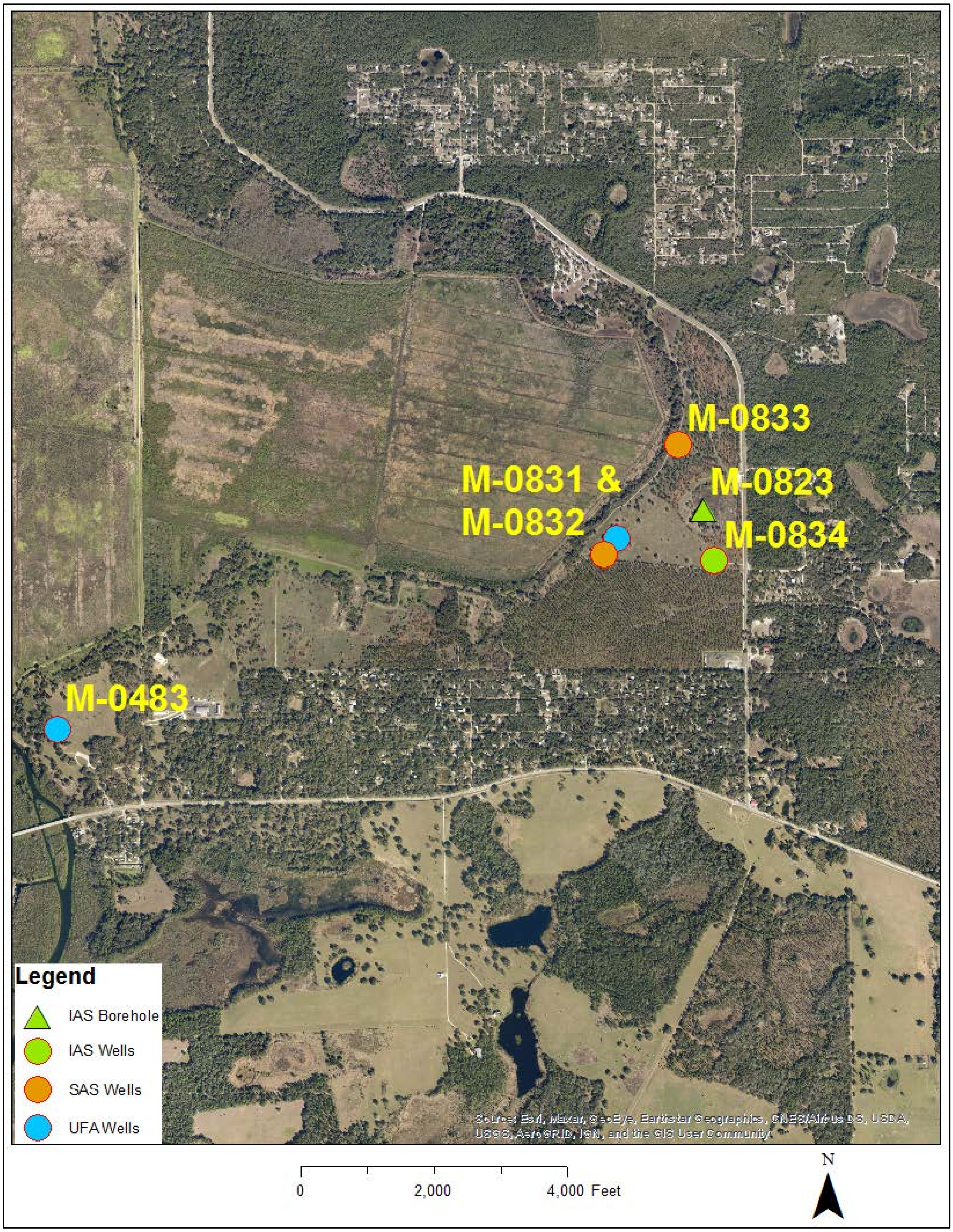

Figure 6. Location of wells used for water level monitoring and sampling.

UNMANNED AERIAL VEHICLE IMAGERY ACQUISITION AND PROCESSING

Aerial imagery of the site was captured using District equipment and personnel to document the initial conditions, test equipment layout, and to create a digital terrain model (DTM) of the sink. Surveyed ground control points were used to transform the altitude above land surface collected by the unmanned aerial vehicle (UAV) to true elevation NAVD 88. Pix4D software was used to process the images into a bare earth, 3-dimensional model corrected to the surveyed elevation points.

A UAV flight of the sinkhole was also used to document visible gopher tortoise burrows inside the sinkhole. This data was used to assist with a pre-pumping gopher tortoise survey.

HYDRAULIC LOAD TEST

Physical conditions typically conducive to sinkhole recharge were identified during the subsurface lithologic and geophysical testing of the Site 1 sinkhole. A hydraulic load test was designed to estimate the rate of potential recharge to the sinkhole and to evaluate the hydraulic connection to the UFA. A metered quantity of water was pumped into the sinkhole and the change in water levels in the sinkhole, the UFA and SAS were monitored.

Prior to setting up the pump and pipe to move water from the rim canal bordering a flooded agricultural field, Sunnyhill land management staff excavated a sump within the rim canal to place the pump intake (Figure 7). Approximately 850 feet of nominal 12-inch diameter discharge pipe was installed from the rim canal sump to the inside slope of the sinkhole. The elevation difference between the sump to the edge of the sinkhole was approximately 38 feet.

The pump used for conveying the water from the rim canal sump to the edge of the sinkhole was a Duraflo HTC012 hydraulic submersible trash pump powered by a diesel drive unit. A 300-gallon capacity diesel fuel tank was used to provide enough fuel to run the pump for a day. This pump was able to provide a discharge of over 4,000 gallons per minute with a total dynamic head of over 40 feet. Pump unit specifications are provided in Appendix B.

A calibrated, non-resettable propeller type flowmeter was installed in the discharge pipe to measure the flow into the sinkhole. The pipe and pump were installed on December 3 and 4, 2019, and the pumping system was tested for a couple of days prior to the dye being introduced on December 6, 2019, as is discussed below.

Figure 7. UAV view of surface water pump and intake location in rim canal sump excavated by District staff.

The hydraulic load test pumping began on Monday, December 9, 2019. Low pump discharge rates required that a replacement pump be installed on December 10, 2019. During the early morning hours of December 15, 2019, the pump stopped working. District staff discovered that the fuel tank was empty, and the fuel was suspected of being stolen. Pumping began again around noon on December 15, 2019. The pumping phase of the hydraulic load test was concluded on December 15, 2019, at approximately 17:10 after the pump fuel supply was stolen again. Water levels were monitored during the recovery phase as the water infiltrated the sinkhole after pumping stopped.

DYE TRACE STUDY

Dye tracing involves injecting a concentrated amount of non-toxic dye (fluorescein at this site) in one place and sampling to detect dye to verify that the water traveled to a destination point. In this study, one UFA well (M-0831) and two SAS (M-0832, M-0833) wells were drilled and used for monitoring water levels and to sample for dye. An additional existing well (M-0834) that was located to the south of the Site 1 sinkhole, was monitored but not included in the final analysis since the well construction details could not be verified.

Multiple factors affect the success of dye detection in a dye trace study. Ideally, there are enough sampling points so that no matter which direction the groundwater flows, one of the sampling sites will detect the dye. In this study, budget constraints allowed for only one location for sampling the UFA interval (M-0831).

There was a large volume of water planned for injection into the sinkhole. The material the water should flow through is a permeable, homogeneous quartz sand. Based on this scenario, the injected water containing the dye was expected to create a local mound and flow radially away from the sinkhole and dominate the local groundwater flow direction. The hydraulic gradient between the dye injection source and monitor well sampling destinations was expected to be higher than under static conditions.

The detection limit for the dye is in parts per billion, so it was important that no dye contamination occur at the sampling sites. To avoid potential contamination, only one person was designated for dye emplacement and was not allowed near the sampling sites before or after the dye was released. All equipment, clothing, vehicle, and anything that could possibly be contaminated with the dye arrived on site and left with the individual designated for dye emplacement.

The dye injection began on December 6, 2019. Personnel and equipment provided by Karst Environmental Services were set up at the end of the discharge pipe that was conveying surface water from the flooded agricultural fields to the east into the sinkhole (Figure 8). The pump was turned on at 10:55 hours and ran until 11:31 hours to saturate the ground prior to releasing the dye. Pumping was restarted at 11:39 hours. A total of 12 pounds of premixed fluorescein dye was brought to the discharge pipe and released into the water flow.

Figure 8. UAV view of surface water discharge pipe with dye being introduced into the flowing water by Karst Environmental Services staff.

Prior to releasing the dye, specially designed packets containing activated charcoal were inserted into the four nearby monitor wells and at a remote monitor well at the Sunnyhill Blue House monitoring station M-0483. The packets were lowered into the wells to a depth that placed the packets in the open hole interval of the wells.

Initially, the charcoal sampling packets were switched out weekly. The samples were later collected every two weeks, which was then increased to monthly (Table 1). Samples were collected from each of the four monitoring well sites near the sinkhole and at the District's UFA Blue House monitor well (M-0483) approximately 1.5 miles to the southwest of the Site 1 sinkhole. A water sample was collected along with each charcoal packet; however, the water sample was to be analyzed only if dye was detected in the charcoal packet. All samples were sent to Ozark Underground Laboratories in Protem, MO for analysis.

Table 1. Dye sampling summary

DATE SAMPLER DEPLOYED	DURATION (days)	DESCRIPTION
11/21/2019	5	Background
11/26/2019	10	Background
12/06/2019	7	Well Sampling
12/13/2019	6	Well Sampling
12/19/2019	8	Well Sampling
12/27/2019	10	Well Sampling
01/06/2020	11	Well Sampling
01/17/2020	13	Well Sampling
01/30/2020	14	Well Sampling
02/13/2020	13	Well Sampling
02/26/2020	20	Well Sampling
03/17/2020	14	Well Sampling
03/31/2020	13	Well Sampling
04/13/2020	21	Well Sampling
05/04/2020	22	Well Sampling
05/26/2020	20	Well Sampling
06/15/2020	22	Well Sampling
07/07/2020	20	Well Sampling

Note: Dye was injected on December 6, 2019.

STATISTICAL ANALYSIS OF DATA COLLECTED

A statistical analytical technique was used to quantify the visual observations that water level increases measured in the sinkhole were correlated to observed water level increases in the UFA monitor well (M-0381). The daily median water level recorded in the sinkhole and in well M-0381 were calculated from the water level datasets and were plotted. Using the SAS/STAT software package, the CORR Procedure was used to calculate the Pearson product-moment correlation between the daily median water levels calculated for the sinkhole and well M-0381.

In addition, a technique from seismology known as “Seismic Ambient Noise” was adapted and used for the purpose of determining a correlation of water level between the sinkhole and adjacent wells, and between the adjacent wells. A positive correlation of the sinkhole to a well implies a hydraulic connection to the aquifer that the well monitors. The methodology adopted to do this work involved analyzing the frequency content of the water level time-series data followed by performing traditional seismic ambient noise processing steps outlined in Bremner et al. (2019).

For hydrogeology, this is a new method that previously has not been applied to water level data for this kind of analysis. Thus, a second goal of this work was to determine the technique’s feasibility to correlate the data from different measurement sites, as is routinely done for seismic data, as well as to determine what other information about the site’s hydraulic properties might be accessible through this process.

Water level time-series data from four monitoring wells surrounding the sinkhole were processed and cross-correlated between the sinkhole and monitoring wells, and between the monitoring wells. Two of the monitoring wells measured the SAS, one measured the UFA, and one well measured an uncertain portion of the aquifer.

Because this technique is new to analyzing water level time-series data, and new to the District, the methods, results, and the interpretations were laid out in such a way as to provide a blueprint that can be further developed or used for future projects.

3. RESULTS AND DISCUSSION

The results of the initial investigations demonstrated that there was a likely hydraulic connection between the SAS and UFA beneath the cover-collapse type sinkhole identified as Site 1. A limited hydraulic loading test designed to evaluate the volume of water that could be recharged through the Site 1 sinkhole confirmed that recharge to the UFA was attainable by discharging a water source into the Site 1 sinkhole. Following are the results of the various methods used during this aquifer recharge study.

DESKTOP REGIONAL HYDROGEOLOGICAL INVESTIGATION

The regional setting of the Sunnyhill property does not have the typical ideal attributes conducive to direct recharge of the UFA, such as a thin confining unit between the SAS and the UFA and a high downward hydraulic head gradient between the surface water in the sinkhole and the potentiometric surface of the UFA. The field investigation was designed to specifically target the Sunnyhill sinkholes to evaluate if the stratigraphic layers providing regional confinement to the UFA are breached within the sinkholes.

Site 1 is a large, mature cover-collapse sinkhole (Figures 1 and 2). It is approximately 780 feet in diameter and 50 feet deep. There is no inlet or outlet so all the material that existed before the collapse of the sinkhole has filled voids in the subsurface. The volume of material that is now in the subsurface is approximately 12,253,230 cubic meters (432,718,734 cubic feet).

The recharge potential of the sinkhole was evaluated by identifying subsurface sediment and lithologic composition that could potentially provide a pathway for downward flow of water to the UFA. At Site 1 (Figure 1) the elevation of the bottom of the sinkhole is approximately 55 feet (NAVD 88), based on an elevation survey conducted by District staff after construction of all monitor wells. Geophysical logs were historically run on a now abandoned irrigation well, M-0357, located approximately 1,400 feet southwest of Site 1 (Figure 4). At that location, the elevation of the top of the UFA is -111 feet NAVD 88 or approximately 190 feet below land surface (bls).

The logs from the former irrigation well indicated that the elevation of the top of the intermediate confining unit (ICU) is approximately -12 NAVD 88 (91 feet bls). Above the ICU is mostly clean quartz sand with a 10-foot-thick layer of clayey sand from 60-50 feet NAVD 88 (19-49 feet below land surface).

A review of the potentiometric surface of the UFA from September 2005 (a relatively high period) indicates an elevation of 57 feet NAVD 88, which is slightly higher that the elevation measured at the Site 1 sinkhole during this investigation. An initial evaluation based on the regional hydrogeologic mapping, indicates the area surrounding the Sunnyhill sinkhole sites are not conducive to providing natural recharge to the UFA. The thickness of the ICU could be a significant hydraulic barrier to water flow if it were not breached.

A 2-inch diameter well, M-0834, is located approximately 300 feet south of the southern rim of the Site 1 sinkhole that could have the potential to be used to measure the potentiometric surface at Site 1. However, when geophysical probes were lowered in the well the total depth that could be logged was 145 feet bls. The top of the ICU in this well was approximately 111 feet bls where the gamma response indicated significant clay material. The clay continued until the total depth logged indicating that the well penetrated the ICU, but the UFA was not encountered above 145 feet bls. It is likely that the well was drilled deeper but caved in or had some other blockage at 145 feet bls. Although there is uncertainty in which aquifer water level this well represents, water level data was collected during the hydraulic loading testing phase to evaluate its response.

Based on the results of the desktop regional investigation more site-specific detailed data acquisition was recommended and implemented as follows. An electrical resistivity profiling geophysical investigation technique was used in the vicinity of the Site 1 sinkhole to penetrate to the depth of where the top of the UFA was expected to occur based on the regional hydrogeological investigation. Standard penetration test (SPT) split-spoon borehole sampling and geophysical borehole logging was obtained and provided additional site-specific lithologic information to inform the electrical resistivity profile interpretation and to identify subsurface conditions specific to the Site 1 sinkhole.

ELECTRICAL RESISTIVITY IMAGING

A full report of the ERI investigation is included as Appendix A. Following is a summary of the findings of the ERI investigation.

The ERI profiles are color mapped from low resistivity (dark blue) to high resistivity (red/yellow) based on ohm-m values. Low resistivity areas correspond to high conductivity areas, where an electrical current may flow more unimpeded than in more resistive areas. In the subsurface, the higher conductivity (lower resistivity) areas typically correlate with higher water-filled porosity.

In Profile 1 (Figure 9) the sinkhole area is clearly seen by the depression in the surface to the northeast (right). The area to southwest (left) shows a distinct horizon of high resistivity material (red/yellow) which correlates to dry mostly quartz sand material to an elevation of 40 feet NAVD 88 and is labeled “A” horizon in Figure 9.

Below the dry sand is clayey sand and clay in the “B” horizon. Areas where sand has migrated downward into a possible solution pipe or local depressions are reddish yellow finger-like features into the green/blue zone. The upper dashed line delineates where the material becomes more clayey. The lower dashed line indicates where the UFA limestone was encountered and is labeled “C” horizon. The “D” horizon is dark blue and is believed to represent cavernous porosity in the limestone related to the collapse into the sinkhole.

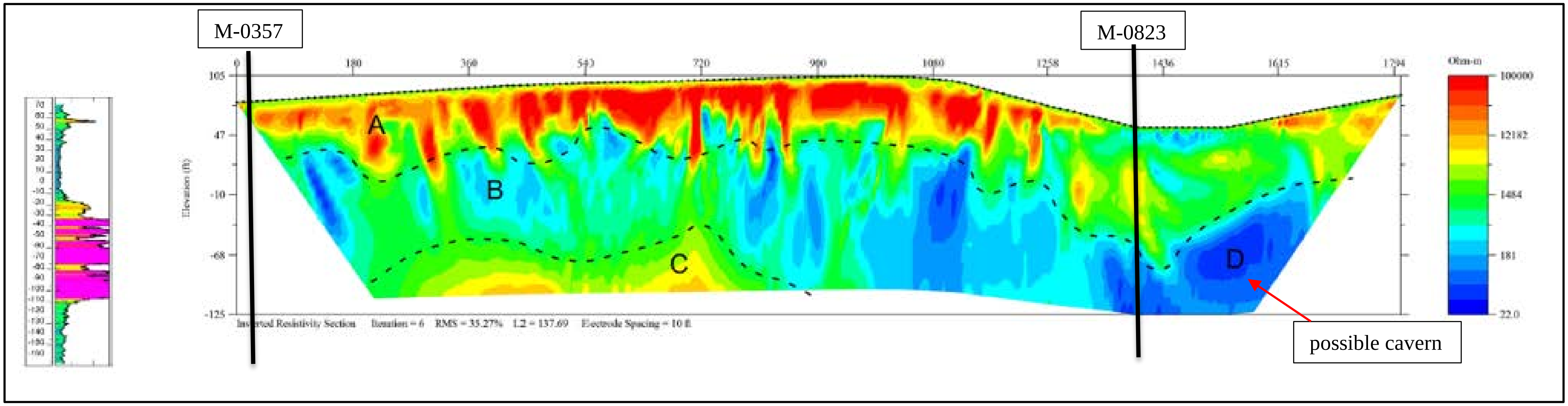

Figure 9. DC Electrical Resistivity Profile 1 from Site 1 (modified from Jones Edmunds/ Geohazards report included in Appendix A) with Natural Gamma log from borehole M-0357 (left)

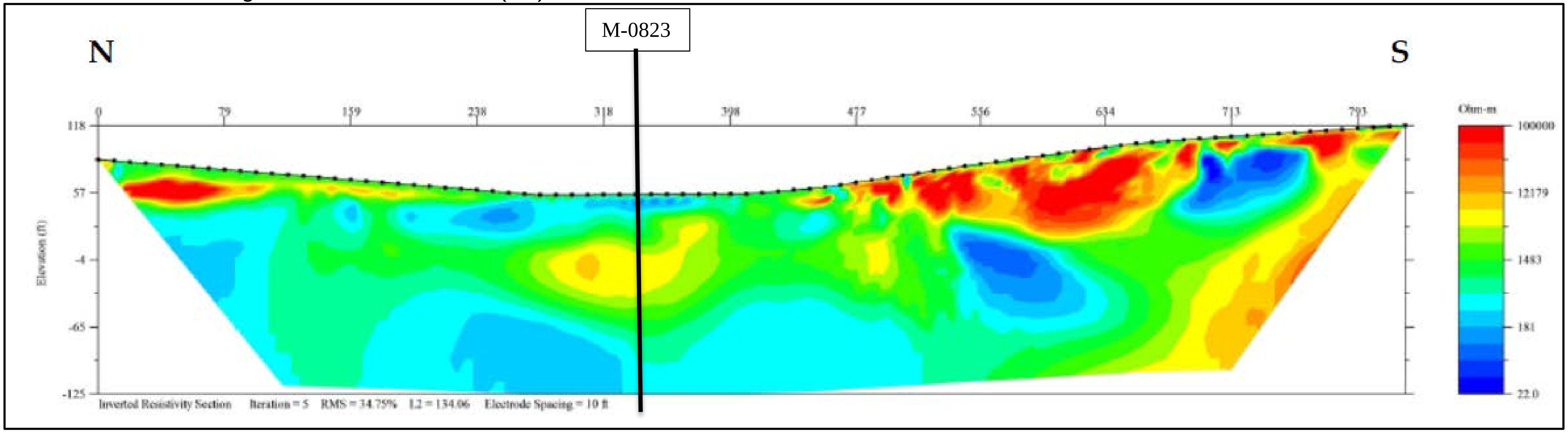

Figure 10. Site 1 Line 2 Electrical Resistivity profile (modified from Jones Edmunds/ Geohazards) report included in Appendix A)

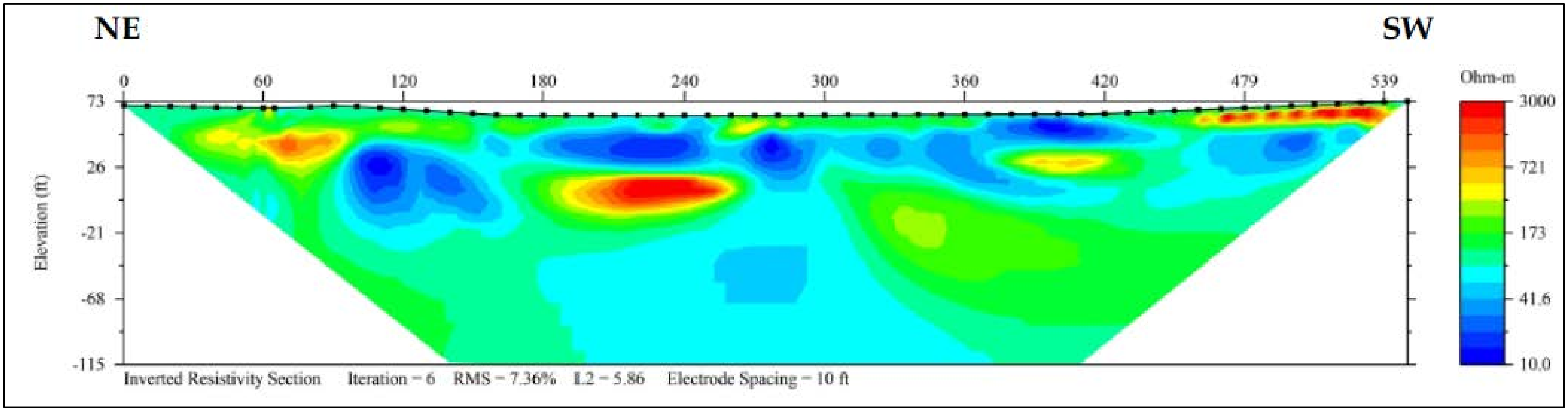

Figure 11. Site 2 Electrical Resistivity Profile 3 (adapted from Jones Edmunds/Geohazards report Appendix A)

The resistivity profile correlates well with the natural gamma log from the old former irrigation well M-0357. The very high intensity red peaks in the gamma log are an indication of clay mineral and accessory minerals containing naturally occurring radioactivity content and the lower values below that are a typical response seen in limestones of the UFA.

The area directly below the sinkhole is significantly different than in the profile to the southwest. Note the absence of the very high resistivity sand (red orange and yellow) which indicates some mixing between sand and clay and may also be affected by the water saturation. Below the sinkhole the material is very low resistivity (dark blue) and may represent the clay material seen in the high gamma peaks from the irrigation well shown on the left of Figure 9. No evidence of the UFA limestone was detected in the borehole below the sinkhole though it was expected to be seen somewhere below an elevation of -68 feet. The profiles indicate less clay material on the southwest side.

ERI Profile 2 was collected at an approximately 70° angle to Profile 1 along the west side of the sinkhole (Figure 10). The high resistivity, clean, dry sands (red and yellow) were only encountered on the flanks of the sinkhole with most of it occurring on the southeastern side of the sinkhole. The lower resistivity unit below 1,500 ohm-m (blue and green) is predominately sand and clayey sand. Profile 2 crosses the site of the test borehole that encountered sand to its total depth. There is sporadic evidence of the very low resistivity (dark blue) clay as was also seen in the northeastern section of Profile 1. No evidence of the UFA limestone was detected along Profile 2.

The sinkhole at Site 2 is topographically less distinct than the sinkhole at Site 1. It was considered as an alternative site in case conditions at Site 1 were not suitable. The color mapping scale was set by Geohazards from 10–3,000 ohm-m at Site 2 instead of 22- 100,000 ohm-m that was used in the Site 1 profiles (Figure 11). A direct color comparison between the two sites is not possible owing to the scale differences. The lower values encountered at Site 2 are an indication of the presence of more clay versus sandy sediment and therefore less permeable conditions.

The ends of the profile represent a relatively undisturbed area; whereas, the central portion shows signs of disturbance to the total depth investigated. This central portion has a lens of clean sand indicated by the red area at 26 feet NAVD 88 and 240 feet from start of the profile. In this profile there is no evidence of the thick clay seen in well M-0357 or evidence of the UFA limestone. The low resistivity values (blue) represent either higher clay content or less consolidated saturated sands. A test borehole would be needed to verify the exact composition and depth to the top of the UFA at sinkhole Site 2.

SUBSURFACE LITHOLOGICAL INVESTIGATION

Test borehole M-0823 was in the base of the Site 1 sinkhole and was advanced to a total depth of 201 feet (Figure 6). The borehole encountered mostly clean quartz sand for its entire depth. This indicates that the sand originally situated above, before formation of the sinkhole, collapsed downward and filled to a depth of at least 201 feet.

The sands were unconsolidated, fine to very fine grained, with little indication of clay (Figure 12). Some of the quartz sand grains have iron staining and are associated with black fine-grained heavy minerals or phosphate grains, which originated from Hawthorn Group sediments during collapse. There is some evidence of clay material as some of the samples show slight cohesion when compacted; however, it is very difficult to see much clay matrix.

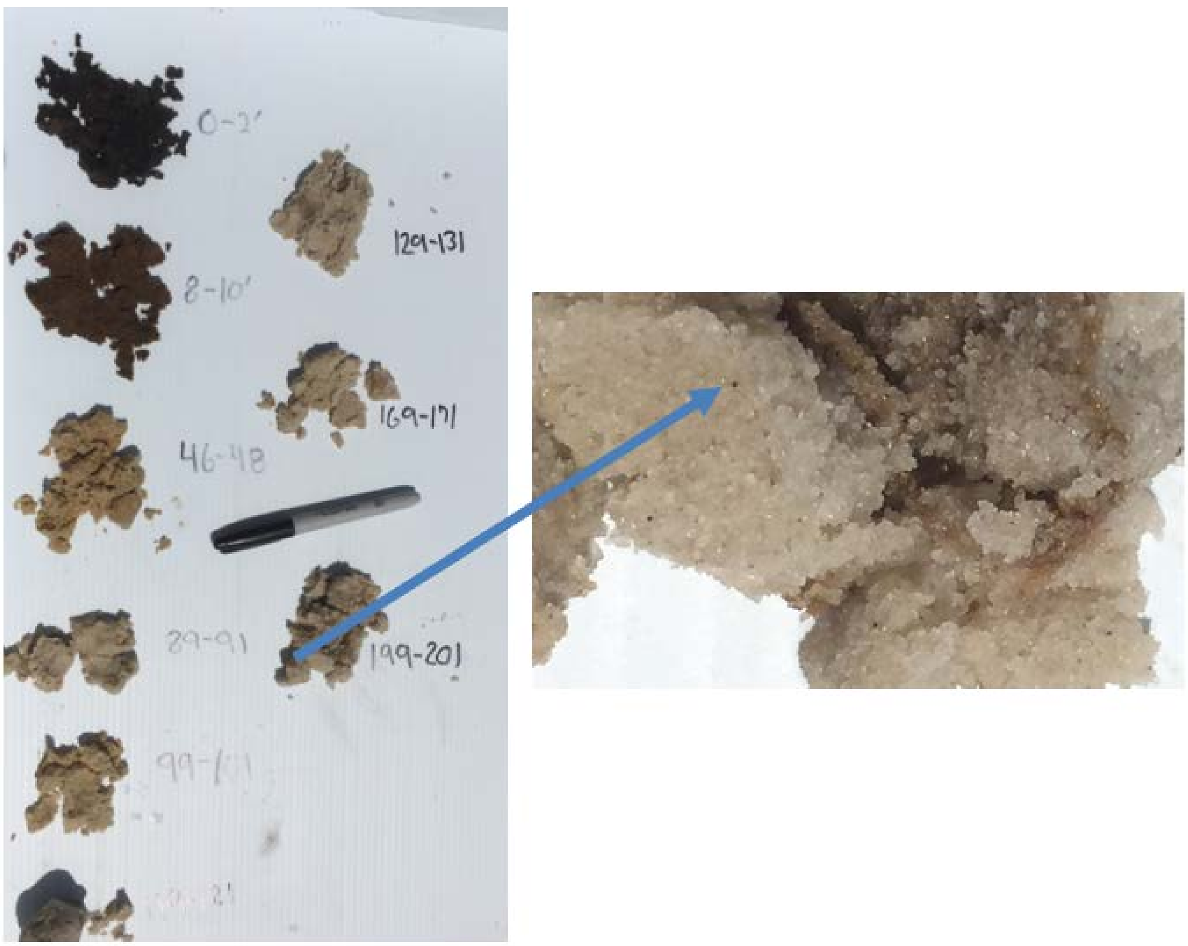

Figure 12. Samples of unconsolidated sand from test borehole M-0823 with zoomed view of sample from 199 to 201 feet on the right with arrow pointing to black fine-grained phosphate or heavy mineral.

A natural gamma log (Figure 13 right image) was run through a 2-inch diameter PVC pipe that was inserted inside the borehole to prevent it from collapsing. The gamma log has a slight increase in intensity below -80 feet NAVD 88, which is normally associated with increased clay mineral content or radioactive minerals. The samples below -80 feet NAVD 88 may contain a low percentage of phosphate or uranium mineral grains that could cause the increased gamma response.

In borehole M-0823 there is no evidence of the 100 feet of clay detected in borehole M-0357 between 10 feet to -110 feet NAVD 88 (Figure 13 gamma left image) so it presumably lies below 201 feet if it is present at all. The dark blue area labeled “D” in the resistivity profile (Figure 9) is probably that clay. A distinct breach in the clay as interpreted from the ERI profiles has occurred where M-0823 is located.

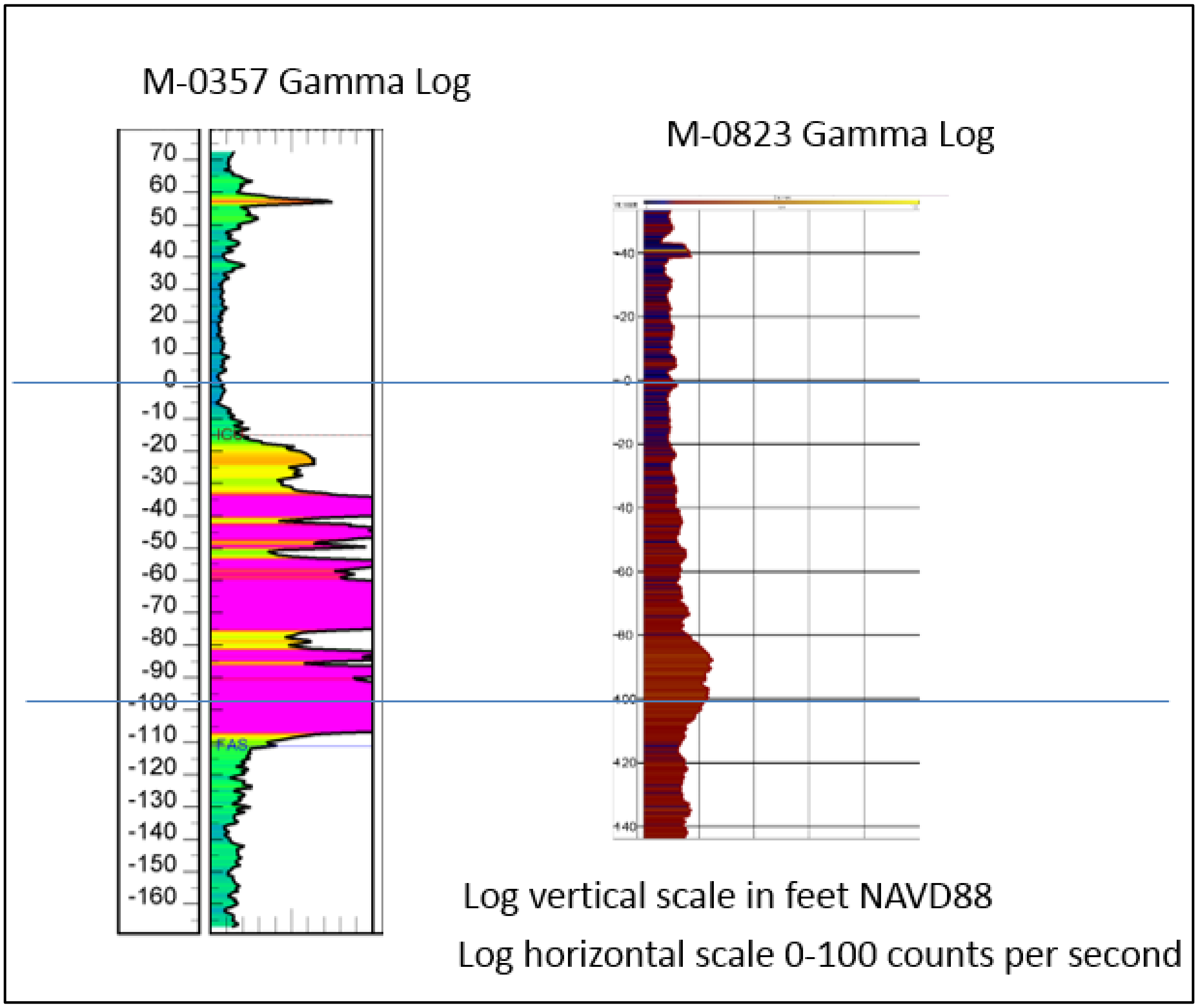

Figure 13. Natural gamma logs from old irrigation well M-0357 to the southwest of sinkhole and recent test hole M-0823 drilled in the bottom of the Site 1 sinkhole. Vertical scale is elevation (feet NAVD 88).

MONITOR WELL INSTALLATION AND WATER LEVEL MONITORING

As part of this investigation three existing nearby wells (M-0483, M-0834 and M-0357) on the Sunnyhill property were used. In addition, one borehole was constructed inside the sinkhole (M-0823) and three monitor wells (M-0831, M-0832 and M-0833) were constructed. Well and borehole construction details are provided in the Table 2 and Table 3 below.

Table 2. Well and borehole construction details Sunnyhill Recreation Area

Well ID	Site Description	Land Elevation (feet NAVD 1988)	ICU Depth (feet)	UFA Depth (feet)	Total Depth (feet)	Casing Depth (feet)	Casing Elevation (feet NAVD 1988)	Total Depth Elevation (feet NAVD 1988)
M-0483	Blue House UFA monitor well	68	40	184	240	192	-124	-172
M-0823	Sinkhole bottom test borehole	56	NA	NA	201	NA	NA	-145
M-0831	UFA monitor well to west	76	110	188	255	201	-125	-179
M-0832	SAS west monitor well to west	79	NA	NA	60	30	49	19
M-0833	SAS monitor well to north	65	NA	NA	40	20	45	25
M-0834	2-inch well to south	122	115	NA	>145	133	-11	>-23
M-0357	Sinkhole old irrigation well to west	80	95	191	172	116	-91	-109

Table 3. Monitor well survey information.

Well ID	Aquifer	Latitude	Longitude	UTM East (meters)	UTM North (meters)	Elevation Top of Casing (feet NAVD 88)
M-0831	UFA	29° 00’ 05.961” N	81° 48’ 46.268” W	420828	3208441	79.62
M-0832	SAS	29° 00’ 05.930” N	81° 48’ 46.328” W	420826	3208440	79.41
M-0833	SAS	29° 00’ 18.015” N	81° 48’ 37.270” W	421074	3208810	68.47
M-0834	UFA	29° 00’ 02.939” N	81° 48’ 32.137” W	421209	3208345	123.39

Figure 14. UAV view of drill rig and equipment used to construct monitor wells for water level monitoring and dye sampling.

The following plots of water levels are from the sinkhole (Figure 15) and wells (Figures 16 through 22) that were monitored before testing, during recharge pumping, and during the recovery phase after the water level had stabilized in the sinkhole at approximately 70 feet NGVD 88. Note that the water elevation scales are customized for each plot to maximize the details of the plots.

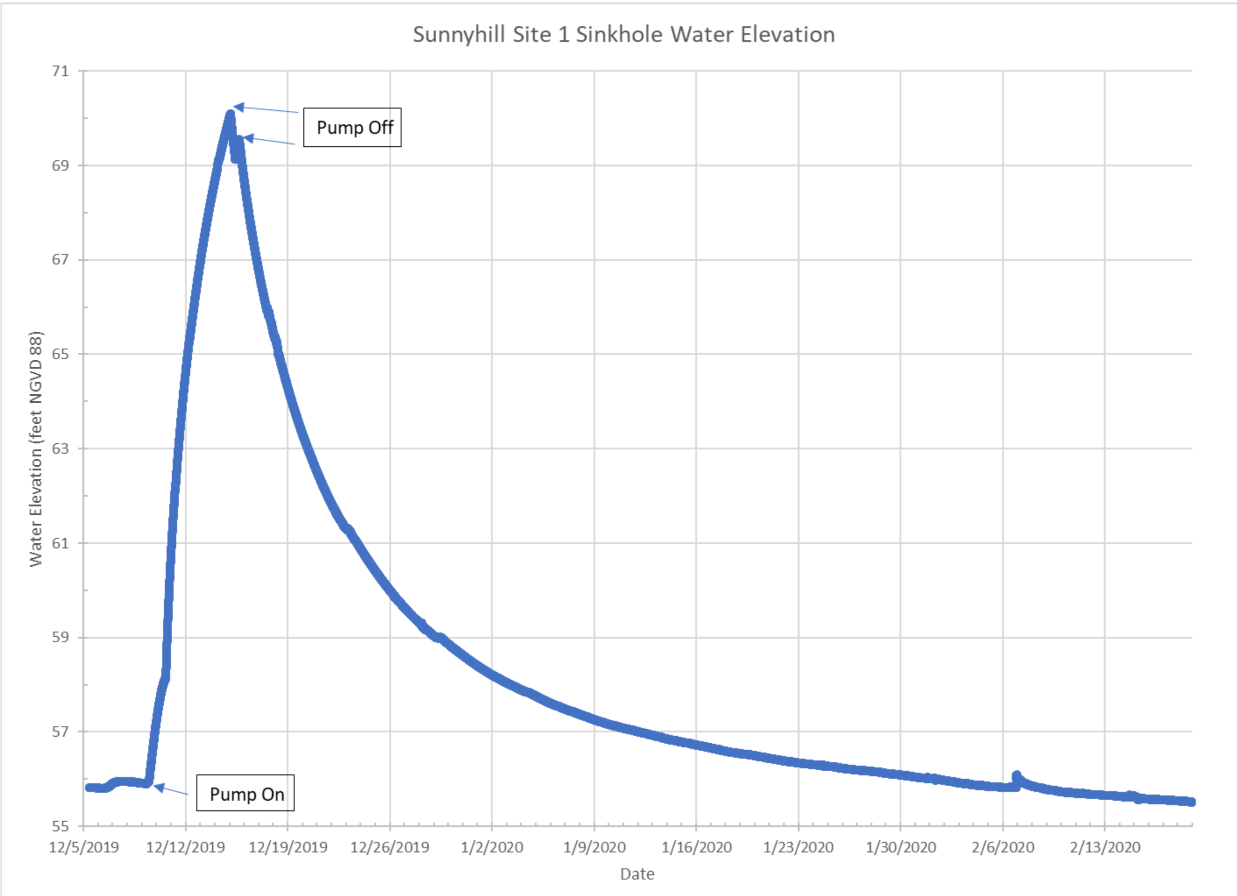

Figure 15. Surface water elevation measured in the sinkhole before, during, and after pumping water into the sinkhole.

The water elevation plot for the sinkhole shows the results of the monitoring by the transducer station that was installed in the sinkhole prior to the surface water being pumped into the sinkhole. Pumping began at 12:30 on December 9, 2019. The first pump had problems and was changed on December 10, 2019. This is followed by a steeper increase in water elevations in the water elevation curve.

The pump was off on December 15, 2019, at 03:15, was briefly back on at 11:30 and then was off again at 16:55 on the same day. Fuel was missing from the pump fuel supply tank in both instances and was believed to be due to theft. Water elevations subsided after the pump was off after staff decided to end the recharge test pumping phase.

Figure 16. Water elevations (feet) measured in all monitor wells with daily rain shown at bottom.

To understand how the water elevations in the SAS and UFA responded to the recharge into the sinkhole, Figure 16 was created with all water levels expressed as feet of elevation. Daily rainfall was plotted at the bottom to understand the response due to several significant storm events that occurred after the sinkhole pumped recharge stopped.

The uppermost curve in blue is the only UFA monitor well (M-0831) near the sinkhole, which was located approximately 1,260 feet to the west of the sinkhole (Figure 6) and was paired with the SAS monitor well M-0832 shown in green. Another SAS monitor well shown in yellow, M-0833, was located approximately 870 feet north of the sinkhole (Figure 6).

Water elevations from the "Blue House" UFA monitor well (M-0483), shown in dark blue above, were collected to understand the local influence that recharging the sinkhole would have on the UFA, as compared to a well over 1.5 miles to the southwest that would presumably not be influenced by the sinkhole recharging event.

There is an obvious increase in water elevation in the UFA near the sinkhole as compared to the background well M-0483. Figure 19 below shows this relationship in detail. The SAS wells show good responses to the rain events, which mask any influence seen due to the sinkhole recharge.

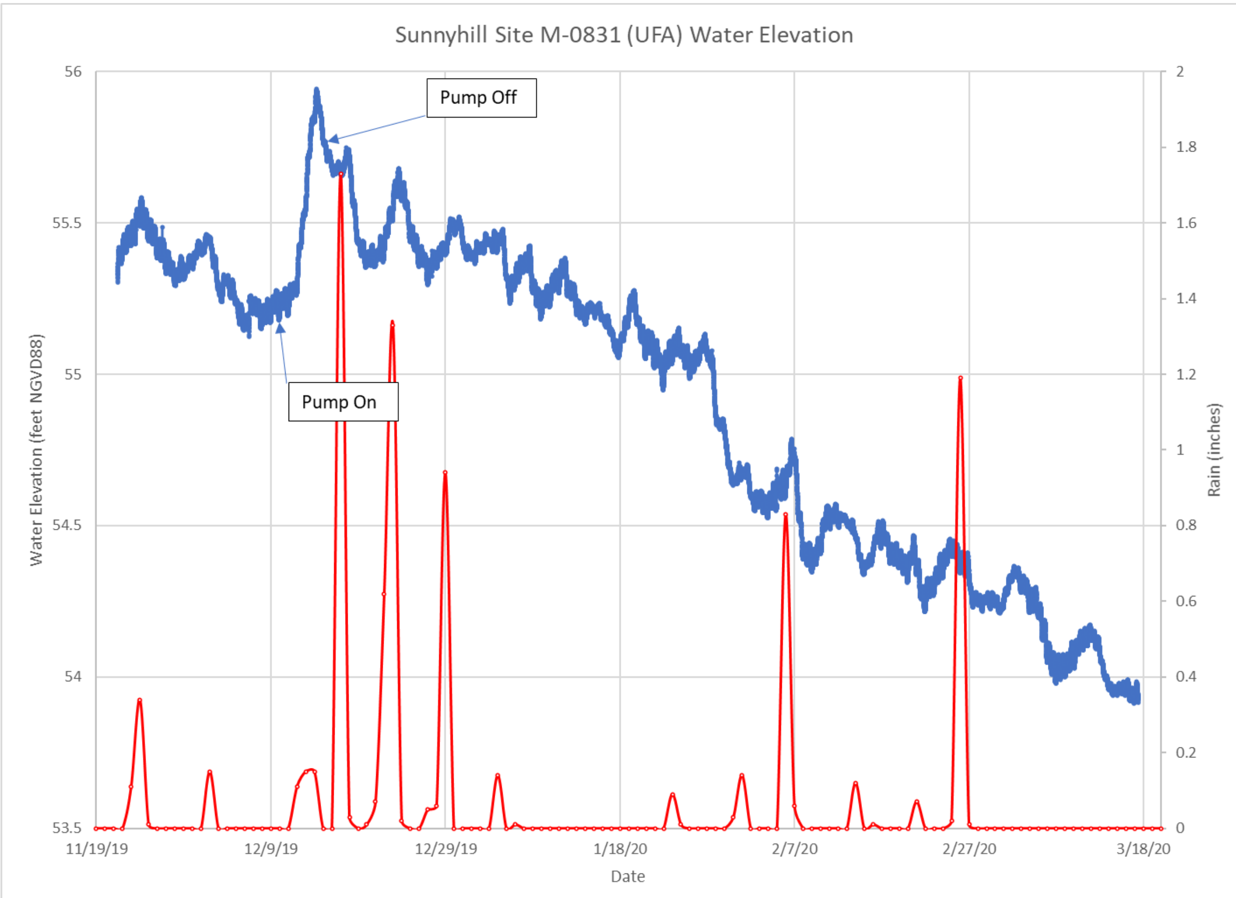

Figure 17. Water elevation measured in the Upper Floridan aquifer monitor well M-0831.

Figure 17 shows the details of the water elevation changes in the UFA monitor well located 1,260 feet to the west of the sinkhole (Figure 6). Prior to the recharge in the sinkhole, the water elevation trend was downward, which was reversed when the pump started discharging into the sinkhole. The downward trend resumed after the pumping stopped.

Superimposed on the downward elevation trend is a sinusoidal elevation change that has a 3–5-day periodicity. This most likely a response to irrigation pumpage in the vicinity.

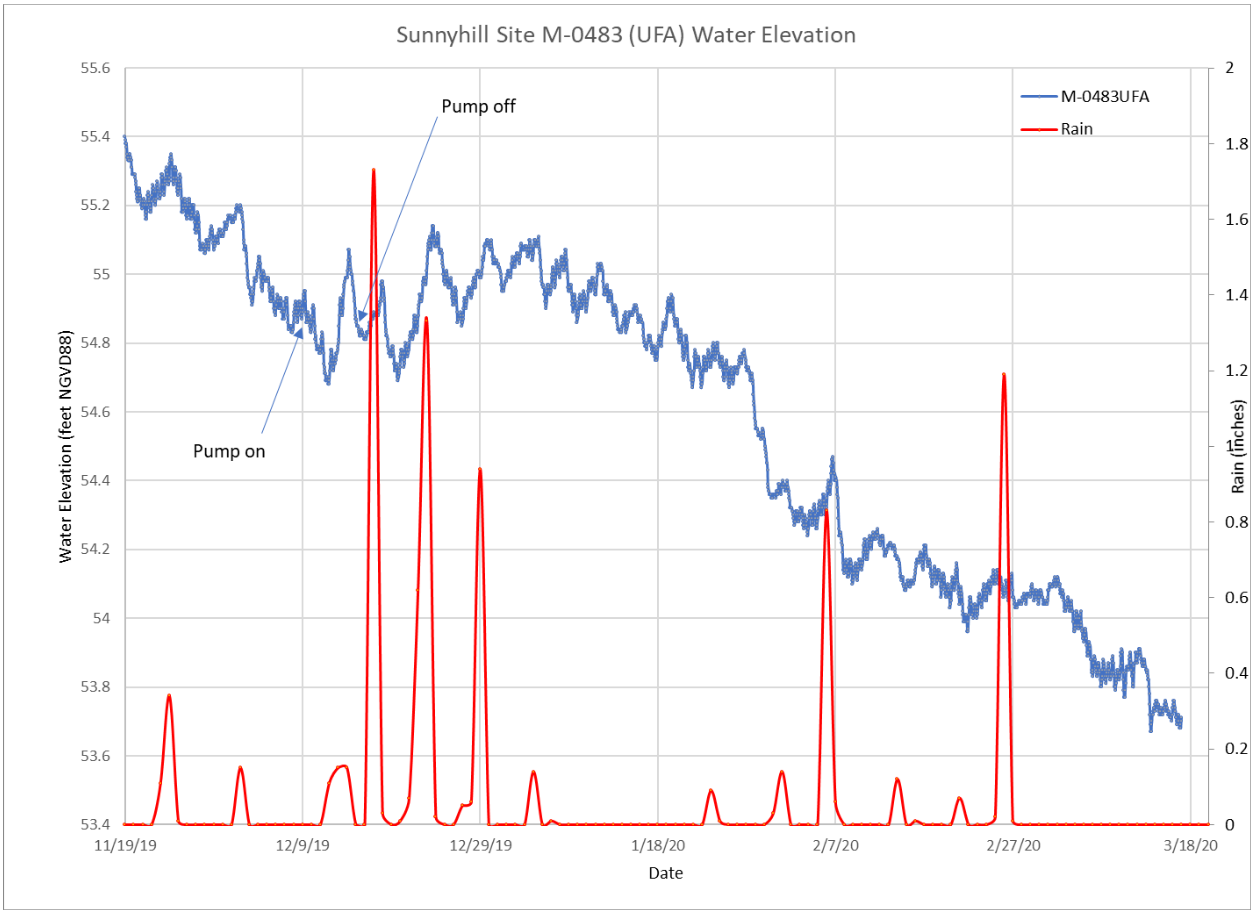

Figure 18. Water elevation measured in the Upper Floridan aquifer monitor well M-0483 (Blue House well), which functions as a background water level monitor well.

Figure 18 shows the details of the water elevation changes in the UFA “Blue House” monitor well M-0483 located 1.5 miles to the southwest of the sinkhole (Figure 6). Prior to the recharge in the sinkhole, the water elevation trend was downward, which continued for a while after the pump started discharging into the sinkhole. The downward trend resumed after the pumping stopped.

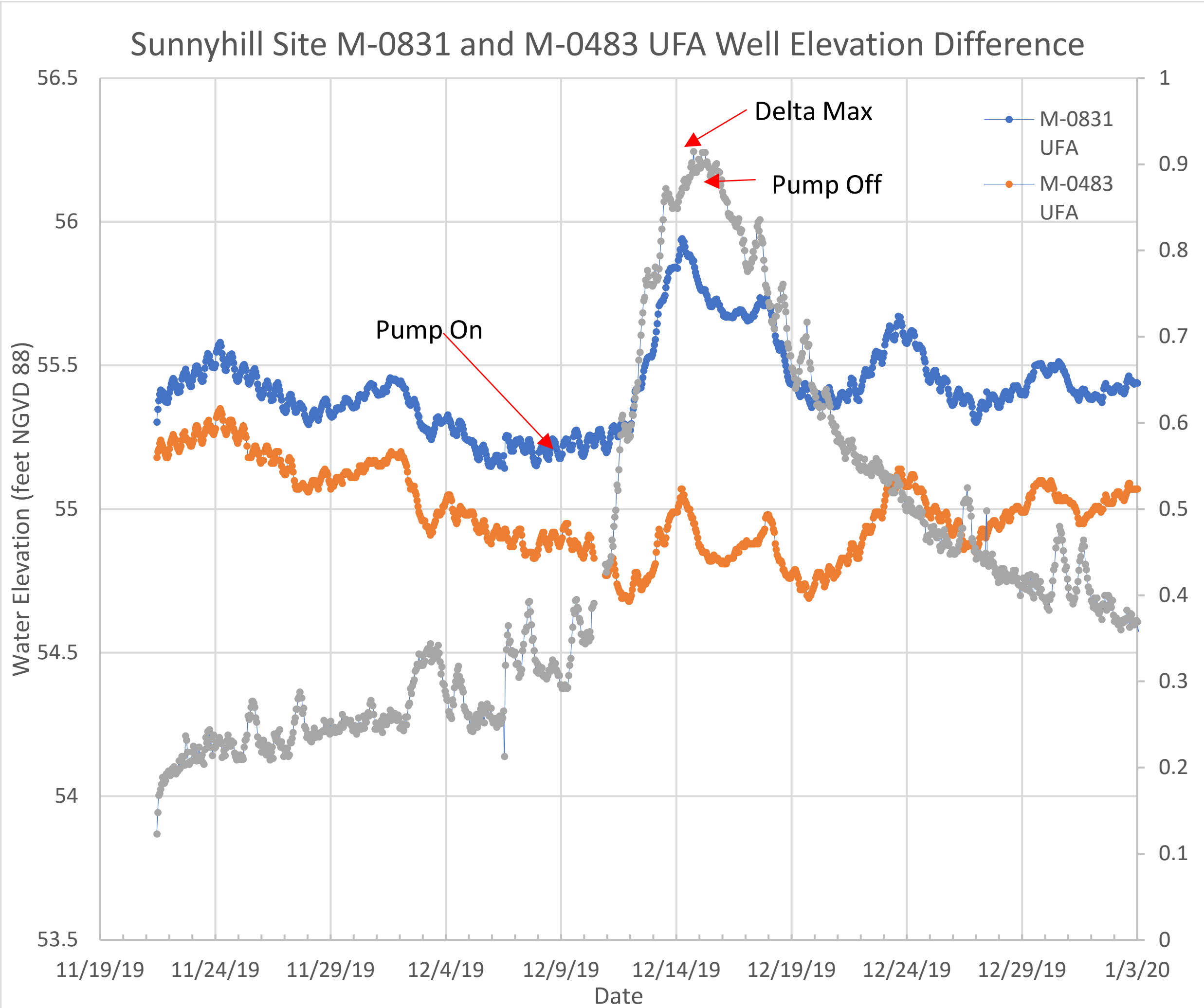

Figure 19. Water elevation difference between UFA M-0831 at sinkhole and M-0483 “Blue House” background monitor well.

Figure 19 was created to better understand the potential recharge that occurred to the UFA during the recharge test, the water elevations in the UFA monitor well M-0831, located 1,260 feet to the west of the sinkhole were compared to those recorded in the “background Blue House” monitor well M-0483, which was 1.5 miles to the southwest of the sinkhole (Figure 6).

Prior to the recharge pumping, both wells appeared to track each other with the well at the sinkhole having a slightly higher elevation. Once pumping began, the elevation difference (delta) between the two wells increased to a maximum of just over 0.9 feet. This delta decreased as the recharge to the sinkhole stopped.

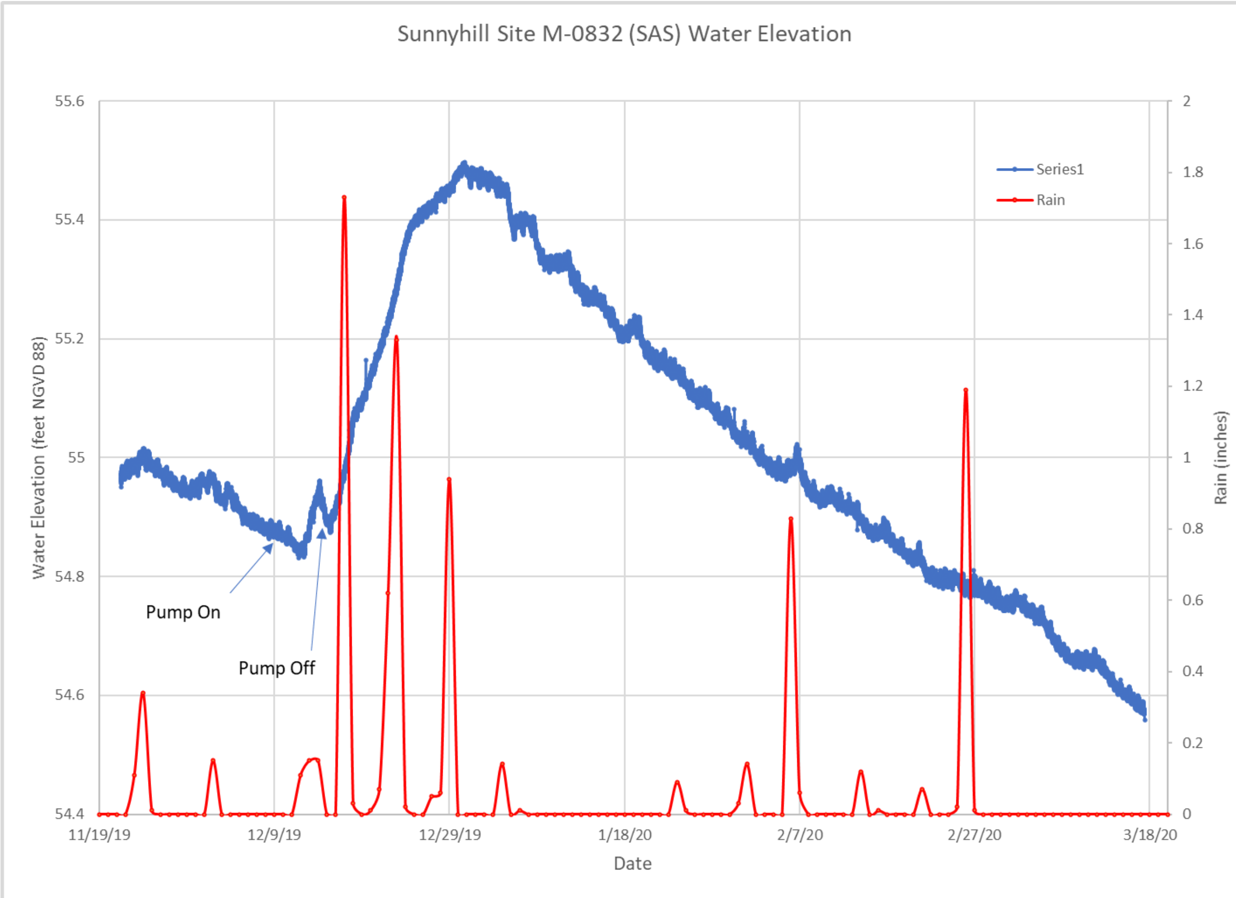

Figure 20. Water elevation measured in the Surficial aquifer monitor well M-0832.

Figure 20 shows the water elevation recorded in the SAS monitor well that was clustered with the UFA monitor well that was located 1,260 feet to the west of the sinkhole. A slight upturn in the water level was noticed as pumping began, which may be attributable to recharge into the sinkhole.

Approximately 0.2 inches of rain was recorded at the Blue House monitoring station shortly after pumping began, which could have increased the water elevation in this SAS monitor well (refer to Figure 6). After December 17, 2019, three significant rainfall events, each with over 1 inch recorded, were the main cause for the approximate 0.7-foot increase in water elevation in the SAS monitor well.

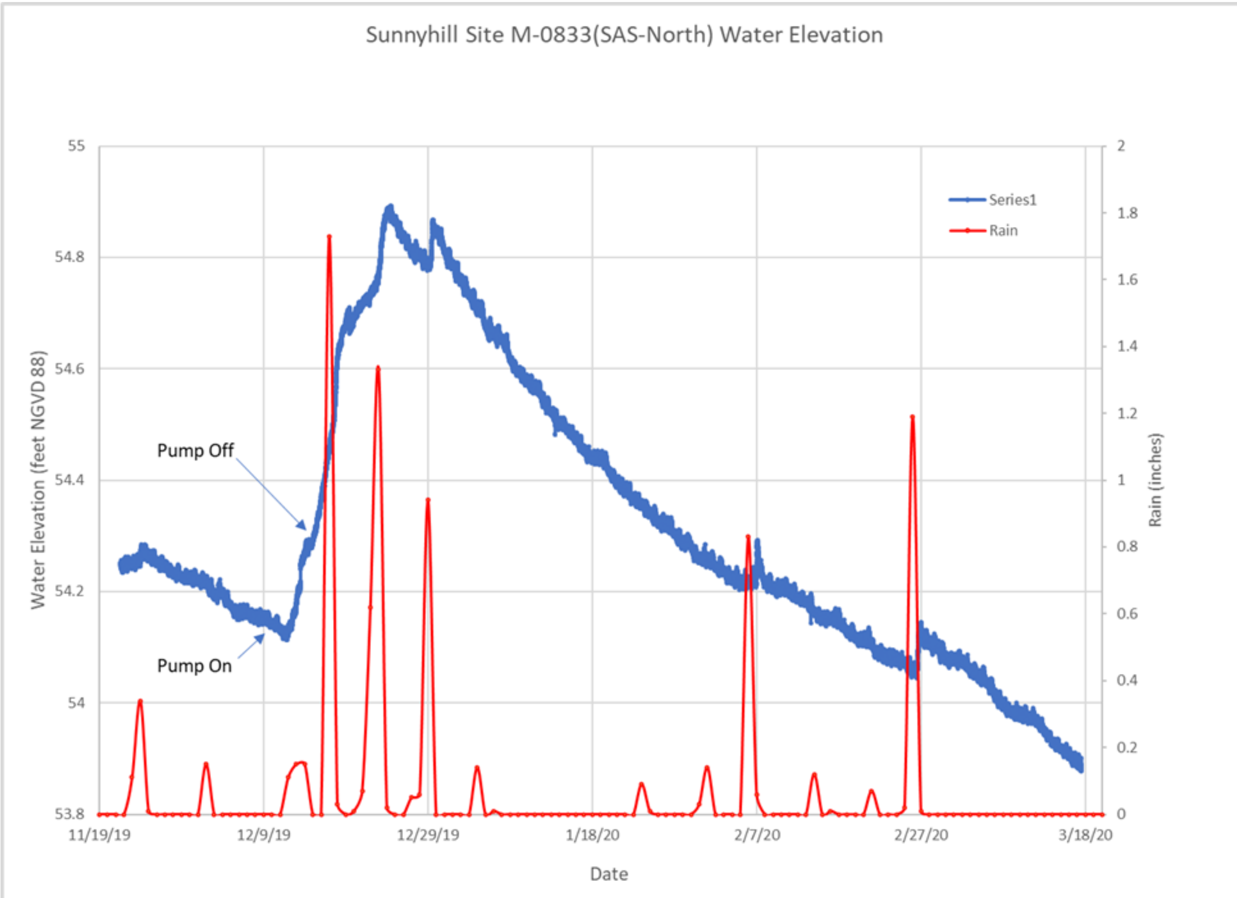

Figure 21. Water elevation measured in the Surficial aquifer north monitor well M-0833.

Figure 21 shows the water elevation recorded in the SAS monitor well that was located 870 feet to the north of the sinkhole. The slight upturn in the water level that was noticed in M-0832 once pumping began was not detected in this well.

Approximately 0.2 inches of rain was recorded at the Blue House monitoring station shortly after pumping began, which could have increased the water elevation in this SAS monitor well (refer to Figure 6). After December 17, 2019, three significant rainfall events, each with over 1 inch recorded, were the main cause for the approximate 0.7-foot increase in water elevation in the SAS monitor well.

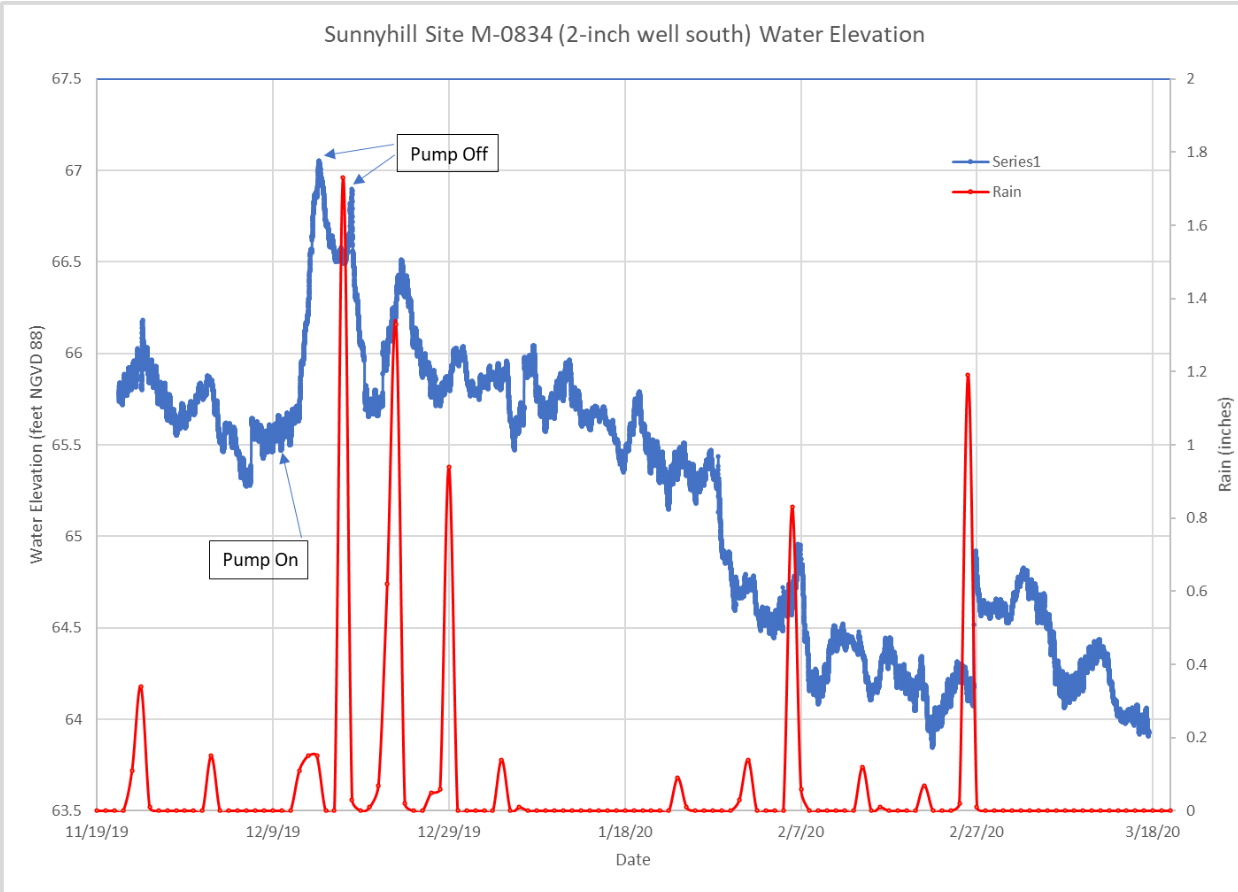

Figure 22. Water elevation measured in the 2-inch well (M-0834) south of Site 1 sinkhole.

This well (M-0834) was a former water supply well that has a 2-inch diameter casing set at 133 feet and has an open hole to 145 feet where an obstruction was identified. The original total depth was not known. Figure 22 shows that the shape of the water elevation curve looks more like the UFA wells than the SAS wells. The well was monitored primarily to see if dye would be detected.

UNMANNED AERIAL VEHICLE IMAGERY ACQUISITION AND PROCESSING

Post processing of imagery collected during the UAV flight resulted in a 3D model that was used to estimate the volume of water that seeped into the ground while pumping into the Site 1 sinkhole (Figure 23). During the pumping phase, a total of 20,617,509 gallons were pumped into the sinkhole based on data obtained from a calibrated non-resettable totalizing flow meter. This volume filled the sinkhole to an elevation of approximately 70 feet NAVD 1988.

The volume of water in the sinkhole at the 70-foot elevation contour was estimated to be 6,645,184 gallons (Figure 26). By subtracting the total volume pumped from the volume at the 70-foot contour an estimated 13,972,325 gallons seeped into the subsurface during the load test.

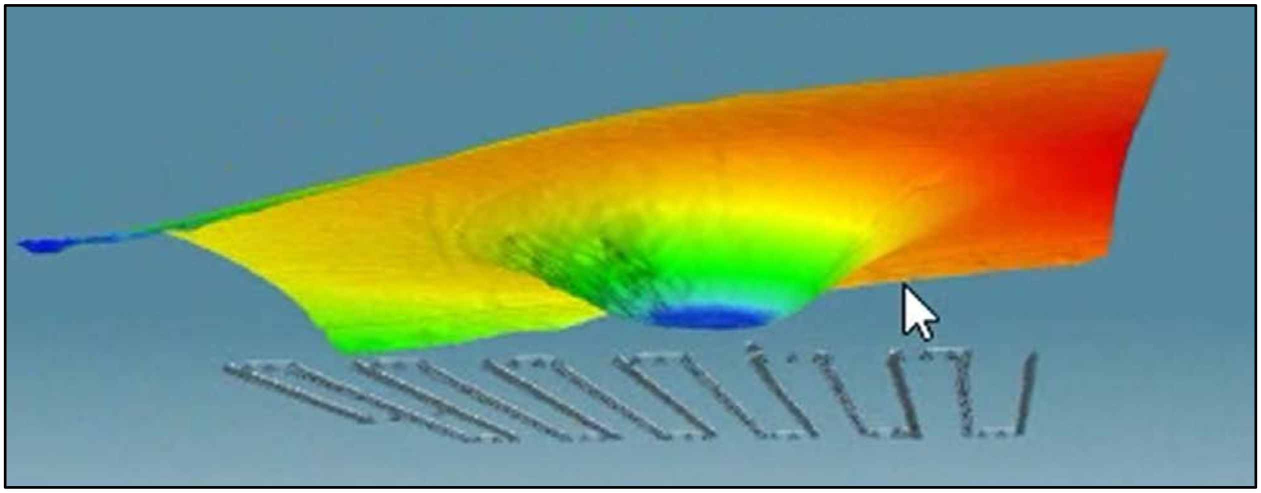

Figure 23. View from below the digital terrain model made with processed UAV imagery collected on the grid shown used for estimating Sunnyhill Site 1 sinkhole storage volume.

Imagery was also collected by the UAV as part of an initial reconnaissance to document the locations of gopher tortoise burrows (Figures 24 and 25). This data was used by a District ecologist who performed a detailed gopher tortoise survey prior to the hydraulic load test. The District ecologist also performed a detailed post pumping gopher tortoise survey.

The DEM was used to identify which burrows had the potential to be inundated based on the anticipated elevation of water in the sinkhole during pumping. Because the inundation was going to be short term and occur slowly, the hydraulic test was considered to not be a threat to the gopher tortoises. The post hydraulic test gopher tortoise survey detected fresh tracks at the burrows after the water receded.

Figure 24. Pre-pumping UAV imagery of Sunnyhill Site 1 sinkhole used for initial reconnaissance for gopher tortoise survey and to create a digital terrain model corrected to true elevation.

The effectiveness of the UAV survey is illustrated in the image below of a gopher tortoise entering a burrow (Figure 25).

Figure 25. Zoomed in view of UAV aerial imagery showing gopher tortoise entering a burrow.

HYDRAULIC LOAD TEST

Physical conditions that are typically conducive to sinkhole recharge were identified during the subsurface lithologic investigation that included borehole lithologic information and interpretation of ERI profiles and geophysical borehole logging.

Approximately 20.6 million gallons (MG) of surface water was pumped into the Site 1 sinkhole over 13 days from December 3 to December 16, 2019. Most of the water (20.3 MG) was pumped into the sinkhole over eight days from December 9, 2019, to December 16, 2019 (Figure 27).

During the hydraulic load test, water level in the sinkhole rose to the 70-foot elevation contour. Based on interpretation of a digital elevation model created with UAV collected imagery combined with land and elevation survey data, the volume of water stored in the sinkhole at the elevation of 70 feet NAVD 88 was approximately 6.7 MG (Figure 26). Given the pumped volume over the 13-day hydraulic load test was 20.6 MG, approximately 13.9 MG of pumped water infiltrated into the sinkhole over the 13-day test.

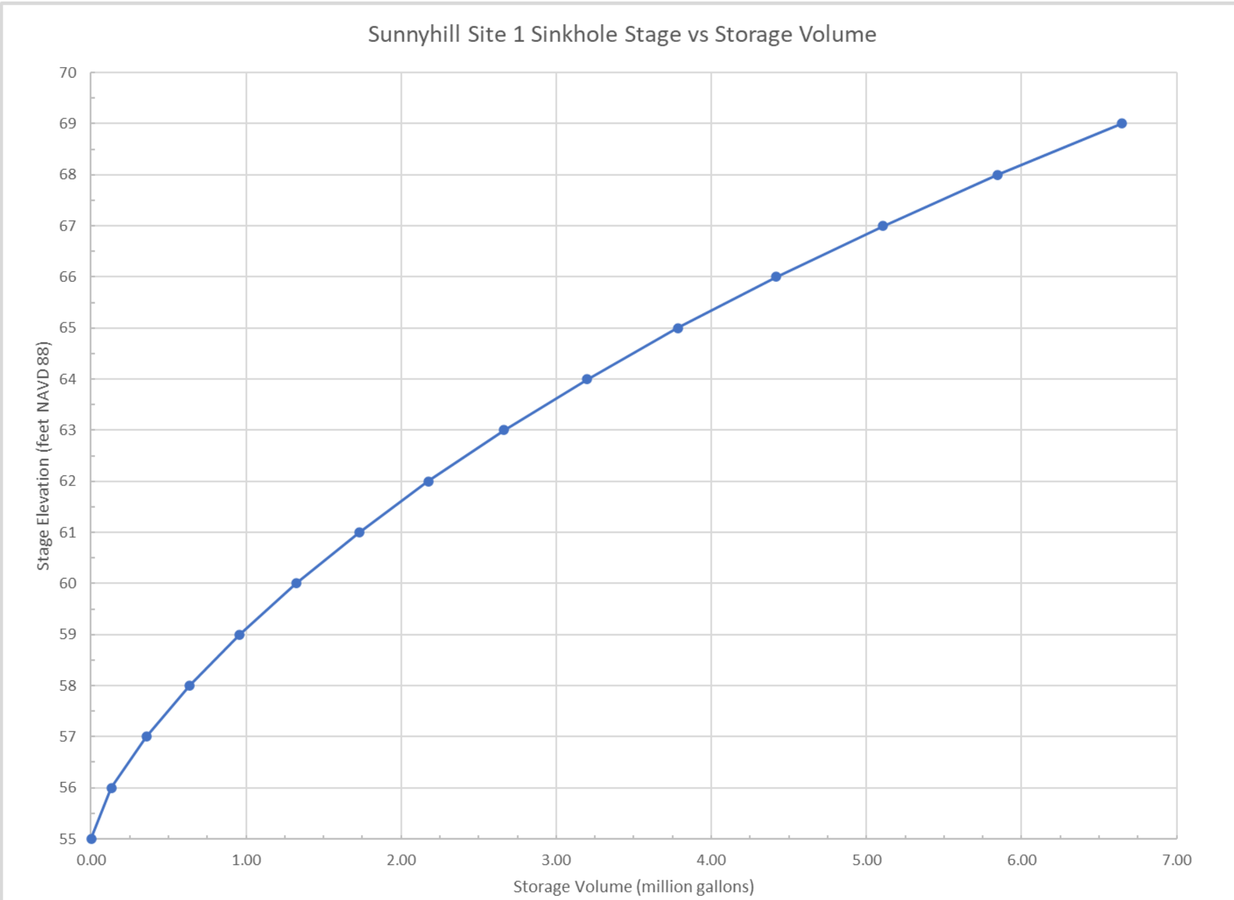

Figure 26. Storage volume at water stage elevation in Sunnyhill Site 1 sinkhole during hydraulic load test based on UAV digital terrain model results.

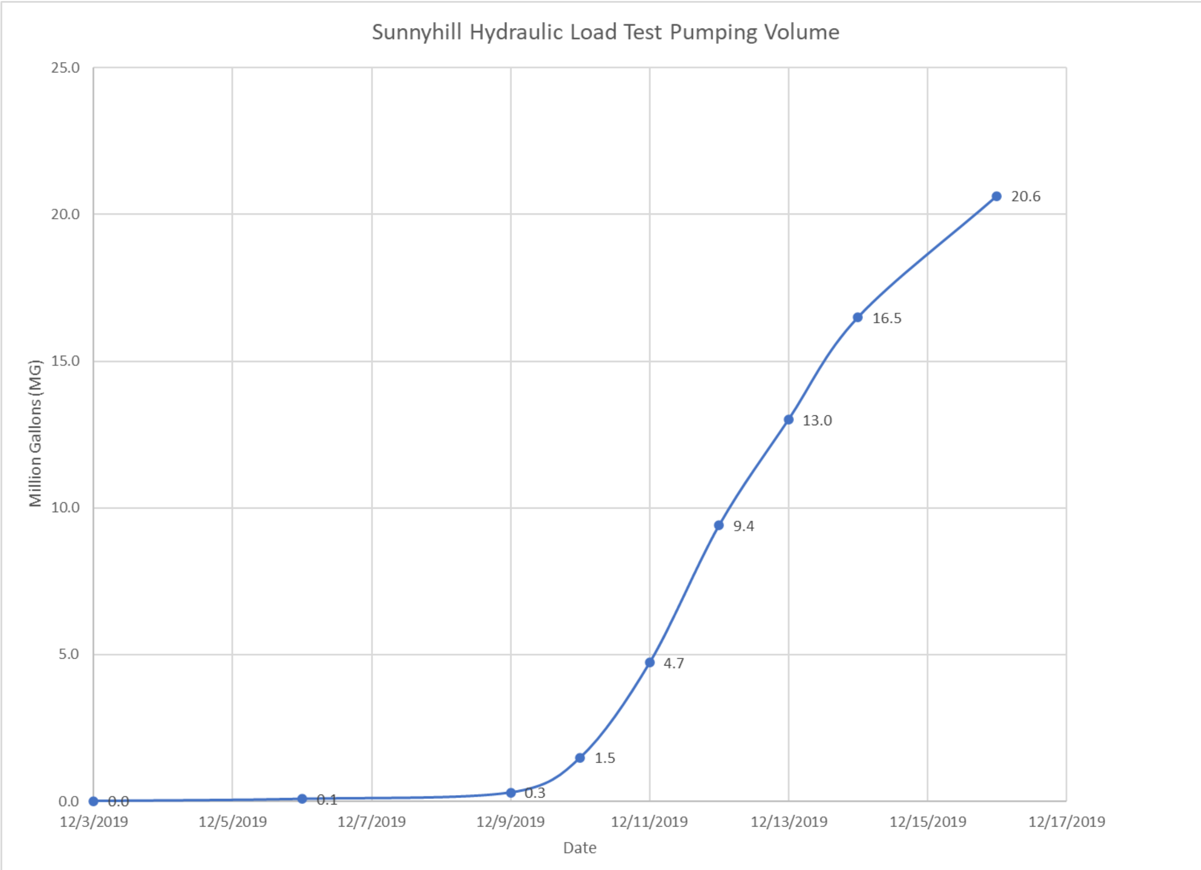

Figure 27. Volume of water pumped into Sunnyhill Site 1 sinkhole during hydraulic load test.

During the eight days after the pump was replaced, when 20.3 MG was pumped into the sinkhole, approximately 13.6 MG infiltrated the sinkhole for an average rate of 1.9 MG per day.

After pumping stopped, the water level recovery in the sinkhole was monitored. During the 10.6 hours after pumping stopped the second time, the water level receded from 69 to 68 feet NAVD 88. Based on the UAV imagery digital terrain model, approximately 740,697 gallons infiltrated into the sinkhole (Figure 28). This infiltration rate was approximately 69,440 gallons per hour or 1.67 MG per day. As expected by Darcy's law, the infiltration rate decreased as the elevation (head) decreased over time.

The potential volume of water that could be stored in the sinkhole at each one-foot interval is shown in Figure 26. As shown on the digital terrain model in Figure 23, the sinkhole is funnel-shaped and therefore stores more water per foot at the higher elevations.

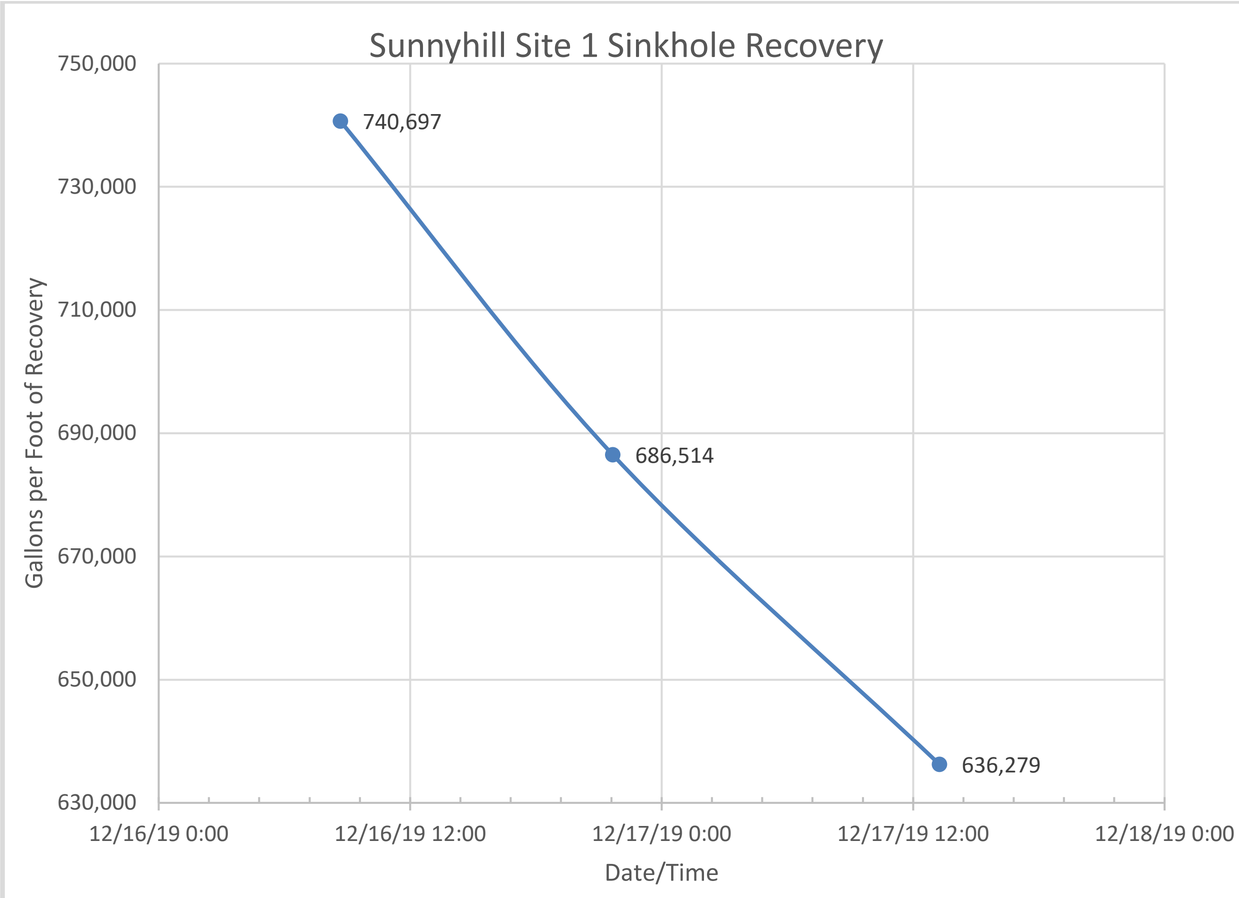

Figure 28. Infiltration volume in gallons per foot of elevation change of sinkhole as water level receded after pumping stopped based on UAV digital elevation model.

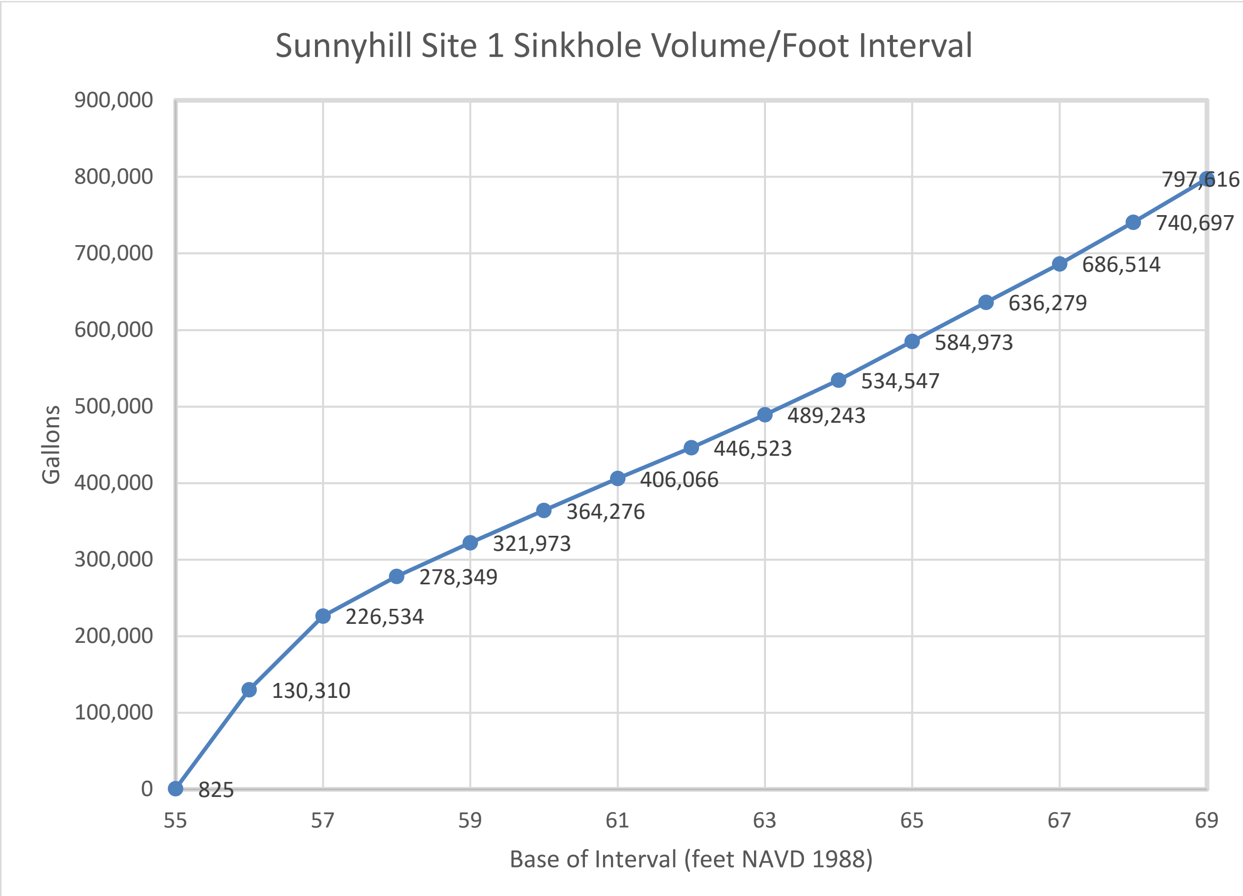

Figure 29. Volume of water stored in each foot interval of Sunnyhill Site 1 sinkhole based on UAV digital terrain model results.

Dye Trace Study

No dye was detected in any of the monitor wells during this study. This could be related to the limited number of monitor well sample points that were available.

Statistical Analysis of Data Collected

Water level elevations monitored in the sinkhole and monitor wells during the hydraulic load test were analyzed by two methods to evaluate whether the water entering the sinkhole recharged the UFA. Analysis of the water level data indicated that the water pumped into the sinkhole did recharge the UFA using a parametric statistical correlation analysis. A cross correlation analytical technique confirmed that water discharged into the sinkhole recharged the UFA in the vicinity of the monitor wells.

SAS/STAT CORR Procedure

The summary of the simple statistics from analyzing the daily median water level for the sinkhole (skmed) and UFA monitor well M-0381 (wlmed) is shown in the table below. Note the variables are defined as: wlmed (well median daily water level) and skmed (sinkhole median daily water level). The SAS/STAT CORR Procedure yielded the following results.

Table 4. Simple statistics summary using SAS/STAT CORR procedure

Variable	N	Mean	Standard Deviation	Sum	Minimum	Maximum
wlmed	117	54.92774	0.53310	6427	53.94550	55.87600
skmed	117	57.24587	3.12620	6698	55.01200	69.37950

Note: N=number of samples, wlmed=median daily water level in UFA well, skmed=median daily water level in sinkhole

The Pearson Correlation Coefficients tested the null hypothesis that there was no correlation between the variables wlmed and skmed. The correlation coefficient was calculated to be 0.62402, which shows that the variables are moderately positively correlated, and the null hypothesis of zero correlation was rejected.

Seismic Ambient Noise Cross-Correlation Procedure

A detailed report in Appendix C provides information about how the seismic ambient noise cross-correlation procedure was adapted to the analysis water level fluctuations during the hydraulic load test. Following is a summary of the results of that detailed analysis.

The cross-correlations revealed a 12-hour period oscillation, potentially caused by solid earth tides from the sun and moon’s gravitational influence. The observed oscillation for some correlated measurement station pairs were out of phase with others, implying a delay in diffusive water level changes, and could possibly be used to estimate transmissivity between monitoring sites. Additionally, local correlated signals appeared to occupy a different, higher, frequency band than lower frequency background signals.

Site characteristics were determined from both the analysis of the raw water level time-series data and the cross-correlations. Well M-0834 did not measure the SAS, but potentially measured the UFA or an aquifer that was partially isolated from the SAS and UFA (potentially within the ICU). Furthermore, the UFA at well M-0831 appeared to possess a connection, though limited, to the aquifer that well M-0834 measures. Recall that the specific construction specifications of well M-0834 are not known and geophysical logs were limited in depth because of an obstruction below the casing depth.

The sinkhole did not appear directly connected to the SAS but did appear connected to the aquifer measured by well M-0834, as well as some connection to the portion of the UFA that well M-0831 measured. The SAS appeared buffered from the UFA (via the ICU). However, that buffer was not absolute, perhaps due to thick sandy infill into the sinkhole. Finally, local correlated signals appeared to occupy a different, higher, frequency band than lower frequency background signals.

4. CONCLUSIONS AND RECOMMENDATIONS

The investigation of the two sinkhole sites located on the Sunnyhill property provided evidence of permeable siliciclastic sand-sized material lying between the bottom of the sinkholes and the UFA. The continuous section of unconsolidated sand confirmed at Site 1 in borehole M-0823 is a possible pathway for downward waterflow to recharge the UFA.

The borehole lithologic information and electrical resistivity imaging survey identified a breach in the confinement between the SAS and UFA and a permeable sand infill that would be conducive to recharge. The Site 1 cover-collapse type of sinkhole typically provides significant disturbance of the subsurface material, including the confining unit.

An estimated volume of 6.6 million gallons (MG) was stored in the Site 1 sinkhole beneath the 70-foot elevation contour at the conclusion of the hydraulic load test. Approximately 14 MG of water percolated into the subsurface or evaporated during the hydraulic load test, which delivered 20.6 MG of water over 10 days. The balance of the water delivered to the sinkhole was still inside the sinkhole and eventually percolated downward after pumping stopped. Assuming negligible evaporation, approximately 1.4 MG per day may be able to recharge the UFA at the Site 1 sinkhole.

The methods used in this investigation are appropriate to qualitatively identify potential recharge pathways but are not designed to calculate leakance or vertical hydraulic conductivity.

The depth to the UFA potentiometric surface from the bottom of the Site 1 sinkhole has a degree of uncertainty because the monitor wells used to create the potentiometric surface maps are located a significant distance from the sinkhole site. Evaluation of the nearby wells or drilling of a UFA monitor well could provide additional information regarding the UFA potentiometric surface.

Statistical analysis of the water levels measured in the Site 1 sinkhole and the UFA monitor well M-0831 during the hydraulic load test indicated a moderately positive correlation coefficient using the Pearson Correlation Coefficient method.

An innovative cross-correlation method, typically used in the analysis of seismic ambient noise, was used to analyze the water level data collected in the sinkhole and all monitor wells. This method indicated that the water levels in the sinkhole correlated better with the monitor well completed in the UFA and not as well with the SAS monitor wells.

To evaluate the recharge potential of the Site 1 sinkhole at the Sunnyhill property, and to better quantify the hydraulic properties of the subsurface, another hydraulic loading test may be useful. This test would benefit from having a pump that could deliver at least 3,500 gallons per minute with a secure fuel source that would allow for continuous pumping. A site-scale groundwater model would aid site hydraulic property characterization and quantification.

LITERATURE CITED

Bremner, P., W. Jin, and M. Brown. 2020 (draft). Cross-correlation of Sunnyhill recharge water level data. St. Johns Water Management District, Palatka, Fla.

Geohazards, Inc. 2016. Electrical resistivity imaging investigation of the geological subsurface at the Sunnyhill Restoration Area, Ocklawaha, Florida. Gainesville, FL

Upchurch, S., T, Scott, M. Alfieri, B. Fratesi, T. Dobecki. 2019. The karst systems of Florida. Springer, Switzerland.

APPENDIX A – GEOHAZARDS FINAL REPORT OF ELECTRICAL RESISTIVITY PROFILING

GEOHAZARDS™

ENGINEERING AND GEOLOGY

Expert Solutions. Exceptional Service.

May 23, 2016

Geohazards, Inc., Investigation No. 2016210

ELECTRICAL RESISTIVTY IMAGING INVESTIGATION OF THE GEOLOGICAL SUBSURFACE AT THE SUNNYHILL RESTORATION AREA, OCKLAWAHA, FLORIDA

INTRODUCTION

Purpose

Geohazards, Inc. was tasked by Jones Edmunds & Associates, Inc. to conduct a geophysical investigation at the above referenced locality. This investigation was conducted to provide a geophysical characterization of the geological subsurface on portions of the Sunnyhill Restoration Area, southeast of Ocklawaha, Florida. This investigation was conducted via electrical resistivity imaging (ERI). In particular, our efforts were designed to identify lithologies and subsurface features near two depressions located on the site.

Scope

The investigation conducted and reported herein included the following:

- A review of available geologic maps and other published data to establish the general probable lithology and regional conditions for the site of investigation.

- A reconnaissance of the site of investigation to recognize and identify surface conditions pertinent to the purpose of the investigation.

C.A. 9396, G.B. 10 1204 NW 13th St. Gainesville FL 32601 Telephone: 800.770.9990 Admin@GeohazardsInc.com

- An Electrical Resistivity Imaging (ERI) investigation of the site to assist in the recognition of site-specific geological conditions at the subject property and to determine evidence for the presence of subsurface features or conditions.

- A final report summarizing results and conveying professional opinions.

Site Information

The initial reconnaissance and the geophysical field investigation were conducted on May 3 and 5, 2016. Two areas were tested as part of this investigation. The surface in both areas was relatively clear of trees and brush, consisting of grass-covered, loose sandy soils.

The first area, Area 1, was located in and near a large, an approximate 50 feet depth, circular depression in the eastern portion of the property. Standing water was encountered in the base of the depression. A St. Johns River Water Management District well (ID M-0357) is located approximately 1,000 feet to the southwest of the depression.

The second area, Area 2, was located in a shallow circular depression north of the Sunnyhill maintenance building.

REGIONAL CONDITIONS

Geology

Based on map consultations, as defined by the USGS, and personal inspection, the surficial geologic material at the study site is the Pliocene-age Cypresshead Formation overlying the Coosawhatchie Formation. Holocene sediments, composed largely of a varying thickness of siliciclastics, are present at the surface in the northwest portion of the site. The Cypresshead Formation is a shallow marine, near shore deposit consisting of reddish brown to reddish orange, unconsolidated to poorly consolidated, fine to very coarse grained, clean to clayey sands. Cross bedded sands are common within the formation. Discoid quartzite pebbles and mica are often present. Clay beds are scattered and not areally extensive. Original fossil material is not present in the sediments although poorly preserved molds and casts of mollusks and burrow structures are occasionally present.

The Miocene-age Coosawhatchie Formation varies from a light gray to olive gray, poorly consolidated, variably clayey and phosphatic sand with few fossils, to an olive gray, poorly to moderately consolidated, slightly sandy, silty clay with few to no fossils. Occasionally, the sands will contain a dolomitic component and, rarely, the dominant lithology will be dolostone or limestone. Silicified nodules are often present in the Coosawhatchie Formation sediments in the outcrop region. The sediment may contain 20 percent or more phosphate. Where they occur near the surface in significant thickness and lateral continuity, shrink/swell clays are a particularly troublesome characteristic of the Coosawhatchie Formation in some areas. Concrete slabs and foundations can be severely damaged where such a geologic condition occurs.

The Eocene-age Ocala Limestone underlies the Coosawhatchie Formation. The Ocala Limestone consists of nearly pure limestones and occasional dolostones. It can be subdivided into lower and upper facies on the basis of lithology. The lower member is composed of a white to cream-colored, fine to medium grained, poorly to moderately indurated, very fossiliferous limestone (grainstone and packstone). The lower facies may not be present throughout the areal extent of the Ocala Limestone and may be partially to completely dolomitized in some regions. The upper facies is a white, poorly to well indurated, poorly sorted, very fossiliferous limestone (grainstone, packstone and wackestone). Silicified limestone (chert) is common in the upper facies. Fossils present in the Ocala Limestone include abundant large and smaller foraminifers, echinoids, bryozoans and mollusks. In these areas where the formation is at or near the surface, the Ocala Limestone exhibits extensive karstification. Problems in the development of sinkholes are related to the size and nearness to the surface of the limestone and these underground cavities. The upper surface of the Ocala Limestone may be highly irregular.

FIELD TEST METHODS: GEOPHYSICAL SURVEYS

Electrical Resistivity Imaging

An electrical resistivity imaging (ERI) survey was completed for the purpose of identifying possible subsurface anomalies, which may be related to karst or sinkhole activity, and to aid in the positioning of any test borings to be performed at the site. Color prints of the modeled ERI cross sections are included. The ERI survey was conducted in general accordance with ASTM D-6431 “Standard Guide for Using Direct Current Resistivity Method for Subsurface Investigations,” as applied to a multi-electrode Resistivity system.

The ERI data was collected using Pole-Dipole array type sequencing. The depth limits of the modeled ER data are primarily dependent on the type of array (Pole-Dipole, Dipole-Dipole, Schlumberger, Wenner, etc.) and the total spread of the electrode array.

Measurements of ERI were made with Advanced Geosciences, Inc. SuperSting R8 8-channel Resistivity Meter with an incorporated switchbox and a passive electrode cable system. The resulting data were processed utilizing EarthImager 2D, a computer program that produces two-dimensional vertical cross section models of the subsurface. The quality of these models was assessed by root mean square (RMS) and L2 values.

Electrical resistivity measurements involve the passing of an electric current underground and measuring its resistance to flow. Different earth materials (e.g. clay, sand, limestone) and subsurface cavities will resist the flow of electrical current differently. Substantially greater contrasts in the degree of resistance (anomalies) are used to identify and locate boundaries among different materials as well as the presence of cavities. When minor contrasts are not observable within the traverse profile, specific point data is analyzed to differentiate transition zones (see attachment).

The orientation, configuration and distribution of the ERI traverses were designed to provide representative coverage of the site of investigation (see ERI location map). Three traverses were measured in the survey area. Maximum depth of penetration ranged from approximately 175 to 180 feet.

GPS Location Table

Name	Latitude	Longitude
Trav1 end	29.00333622	-81.8081734
Trav1 start	29.00095486	-81.81310914
trav2 start	29.0037591	-81.80929639
trav2 end	29.00153276	-81.80897493
Trav3 end	28.99648014	-81.83009139
Trav3 start	28.99761356	-81.82896641

RESULTS

Electrical Resistivity

1. Color print-outs of the modeled two-dimensional ERI cross sections are included. The quality of the resistivity models is considered to be very good to adequate based on RMS and L2 error values.

2. The data collected were interpreted as indicative of a variable cover of sandy soils overlying less resistive clayey and/or saturated materials, and limestone at depth.

3. The southwest portion of the ERI cross section for traverse 1 depicts a zone of high resistivity materials indicative of limestone at depth of approximately -60 to -125 feet MSL. The upper limestone surface was only detected within the first 800 linear feet of traverse 1 and is represented by light orange to green colors in the traverse.

4. The northeast portion of the ERI cross section for traverse 1 (~1,258 to 1,615 feet from the start) depicts a zone of higher resistivity materials to a depth of approximately -120 feet MSL. These materials are interpreted to be sandy soils in-filling deeper karst activity. Limestone was not detected in the northeast portion of traverse 1.

5. Traverse 2 crossed traverse 1 at approximately 1,430 feet along traverse 1 and 350 feet along traverse 2.

6. The ERI cross section for traverse 2, near 360 feet from the start, depicts a zone of higher resistivity materials (light orange to green) to a depth of approximately -120 feet MSL. These materials are interpreted to be sandy soils in-filling deeper karst activity. The upper limestone surface was not detected in traverse 2.

7. The central portion of the ERI cross section for traverse 3 depicts a zone of higher resistivity materials (red to yellow) from approximately 20 to -20 feet MSL. These materials are interpreted to be sandy soils. Less resistive materials, consistent with clayey soils or very loose sandy soils, were detected to -115 feet MSL, within the central portion of traverse 3. The upper limestone surface was not detected in traverse 3.

CONCLUSIONS

The site of this investigation was located at the Sunnyhill Restoration Area, southeast of Ocklawaha, Florida. Two areas of the site were tested as part of this investigation. The surface in both areas was relatively clear of trees and brush, consisting of grass-covered, loose sandy soils. The first area, Area 1, was located in and near a large, deep circular depression in the eastern portion of the property. Standing water was encountered in the base of the depression. A St. Johns River Water Management District well (ID M-0357), drilled to approximately -125 feet MSL, is located approximately 1,000 feet to the southwest of the depression and also the approximate location of the start of ERI traverse 1. The second area, Area 2, was located in a shallow circular depression north of the Sunnyhill maintenance building. Well M-0823 was located to further investigate the lithology within the depression in Area 1.

Electrical resistivity results are interpreted as indicative of sands, overlying clayey materials and a variable upper limestone surface. Within the depression in Area 1, raveled sands were detected to a depth of -120 feet MSL. The final lithologic description by the FGS for Well M-0823 is in production as of this report date, but initial examination indicates sands throughout the entire depth of the well. The gamma log for Well M-0357 corresponds very well with the interpreted results of ERI traverse 1; specifically the depths related to lithology changes of the sand to clayey materials, and clayey materials to limestone.

CERTIFICATION

This report was prepared under the direction and supervision of Registered Professional Geologists, licensed in the State of Florida, whose field of expertise is geology and sinkhole evaluation. The geologists' signatures and seals with Florida Registration Numbers appear on the report.

LIMITATIONS

While due care has been exercised in the performance of these measurements and their interpretation, Geohazards, Inc. can make no representations, warranties, or guarantees with respect to latent or concealed conditions which may exist that may be beyond the limits of detection with the methodologies used.

JAMES D. OLSON LICENSE No. 2795 STATE OF FLORIDA PROFESSIONAL GEOLOGIST
5-23-16

James D. Olson, P.G.
Professional Geologist
Florida License No. PG2795

SCOTT E. PURCIFULL LICENSE No. 2328 STATE OF FLORIDA PROFESSIONAL GEOLOGIST
5-23-16

Scott E. Purcifull, P.G.
Professional Geologist
Florida License No. PG2328

Appendix A

Maps and Figures

GEOHAZARDS™
ENGINEERING AND GEOLOGY

1204 NW 13th Street, Gainesville, FL 32601
(352) 371-7243 1-800-770-9990
www.geohazardsinc.com

SITE PLAN OF GEOPHYSICAL INVESTIGATION

TWO-DIMENSIONAL ELECTRICAL RESISTIVITY IMAGING SURVEY

Sunnyhilll Restoration Area - Area 1
Ocklawaha, Florida

FOR: Jones Edmunds & Associates, Inc.

DATE: 5-9-16

BY: R. Emslie, Geologist
Investigation #2016210

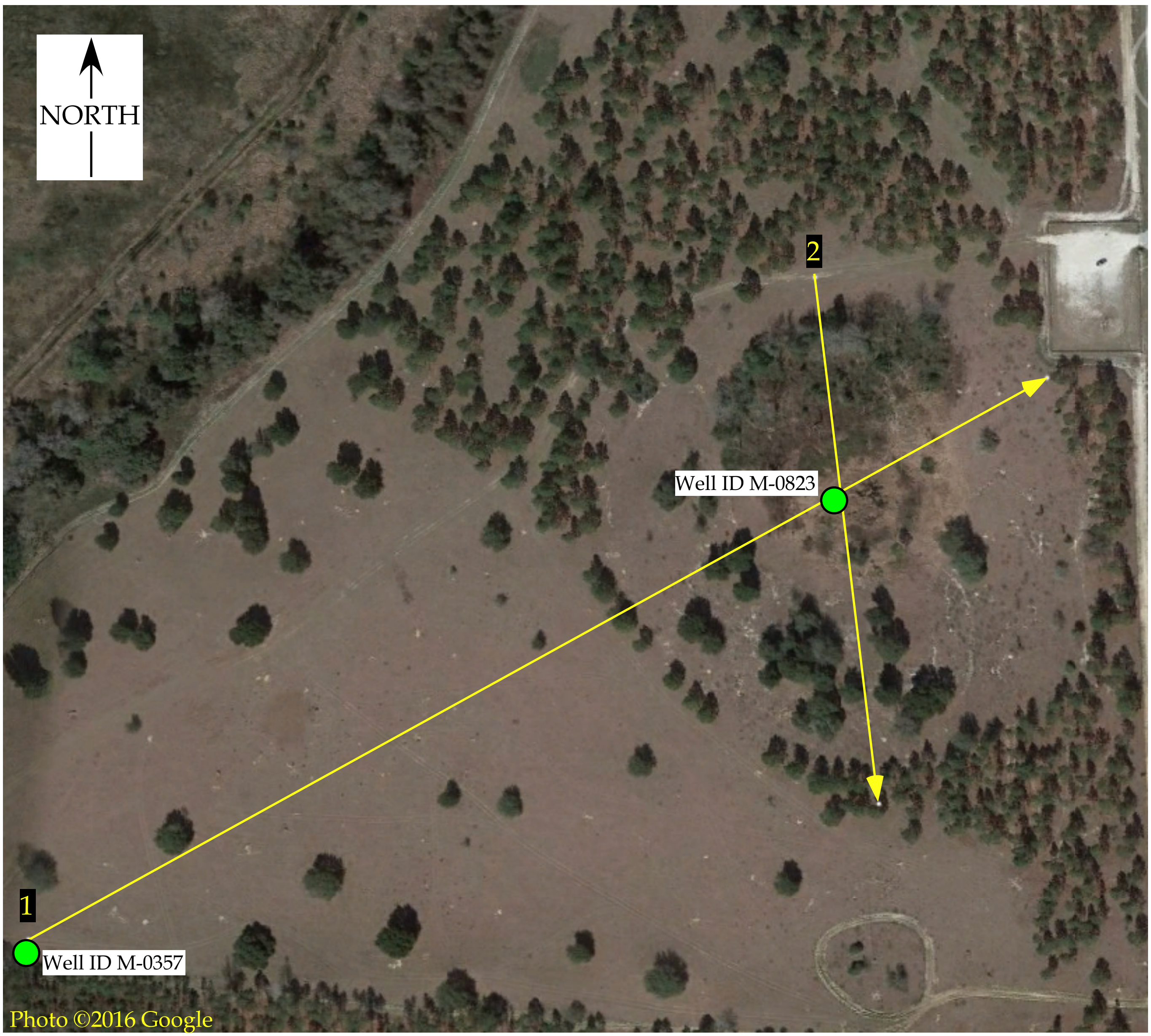

KEY:
ER Traverse
1
Approximate Well Location

Approximate
Graphic Scale
0 125' 250'

GEOHAZARDS™
ENGINEERING AND GEOLOGY

1204 NW 13th Street, Gainesville, FL 32601
(352) 371-7243 1-800-770-9990
www.geohazardsinc.com

SITE PLAN OF GEOPHYSICAL INVESTIGATION

TWO-DIMENSIONAL ELECTRICAL RESISTIVITY IMAGING SURVEY

Sunnyhilll Restoration Area - Area 2
Ocklawaha, Florida

FOR: Jones Edmunds & Associates, Inc.

DATE: 5-9-16

BY: R. Emslie, Geologist
Investigation #2016210

KEY:
ER Traverse
1

Approximate Graphic Scale
0 100' 200'

SW **NE**

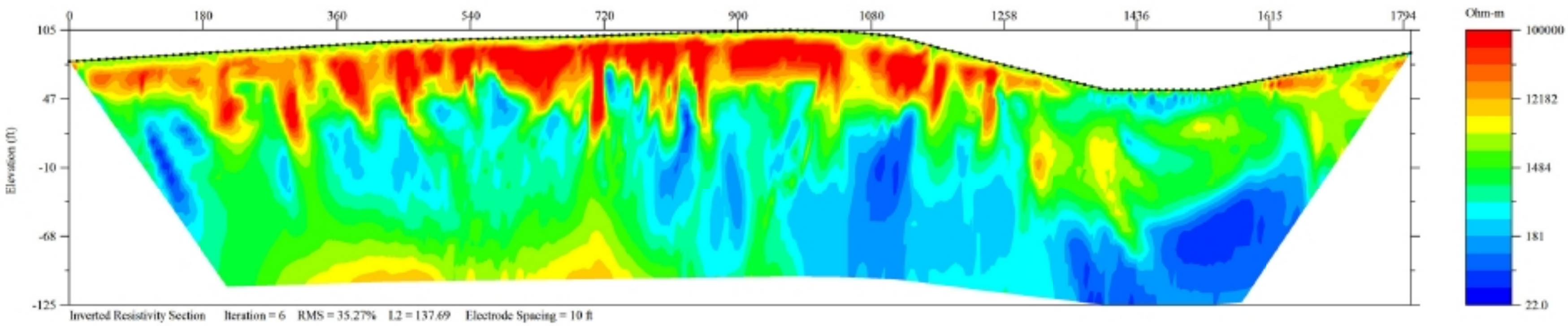

BEARING: 60°

ARRAY: POLE-DIPOLE

GEOHAZARDS™
ENGINEERING AND GEOLOGY

1204 NW 13th Street, Gainesville, FL 32601
(352) 371-7243 1-800-770-9990
www.geohazardsinc.com

TWO-DIMENSIONAL ELECTRICAL RESISTIVITY PROFILE TRAVERSE 1

Sunnyhilll Restoration Area - Area 1
Ocklawaha, Florida

FOR: Jones Edmunds & Associates, Inc.

DATE: 5-18-16

BY: R. Emslie, Geologist
Investigation #2016210

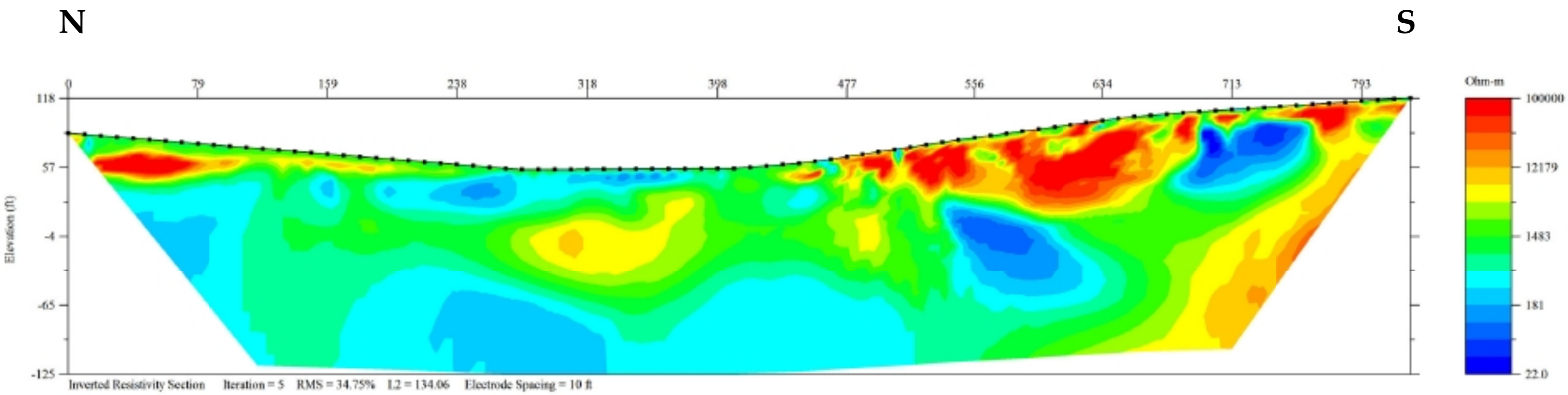

BEARING: 172°

ARRAY: POLE-DIPOLE

GEOHAZARDS™
ENGINEERING AND GEOLOGY

1204 NW 13th Street, Gainesville, FL 32601
(352) 371-7243 1-800-770-9990
www.geohazardsinc.com

TWO-DIMENSIONAL ELECTRICAL RESISTIVITY PROFILE TRAVERSE 2

Sunnyhilll Restoration Area - Area 1
Ocklawaha, Florida

FOR: Jones Edmunds & Associates, Inc.

DATE: 5-18-16

BY: R. Emslie, Geologist
Investigation #2016210

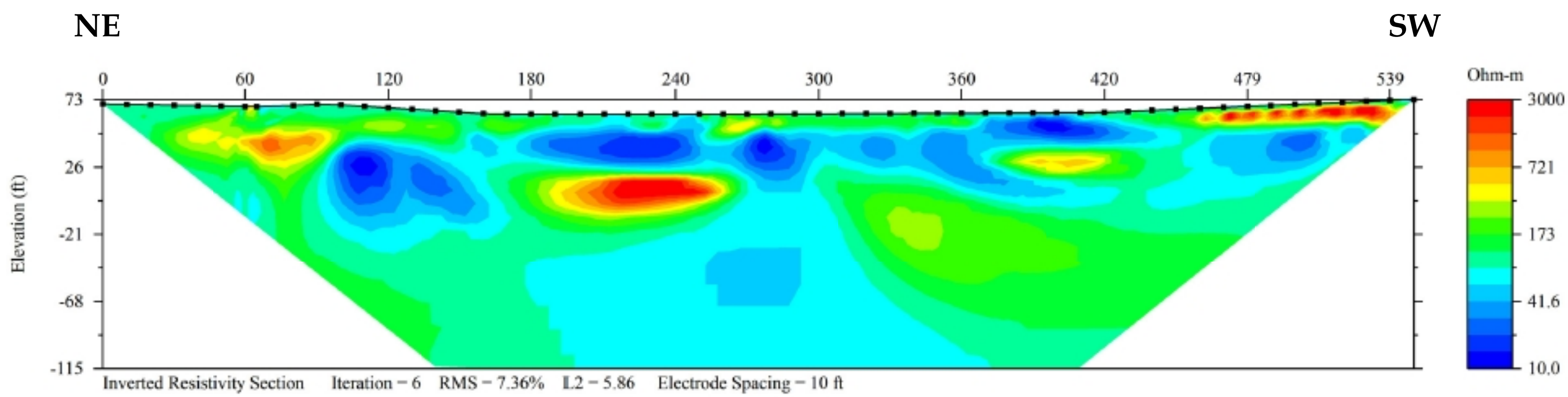

BEARING: 220°

ARRAY: POLE-DIPOLE

GEOHAZARDS™
ENGINEERING AND GEOLOGY

1204 NW 13th Street, Gainesville, FL 32601
(352) 371-7243 1-800-770-9990
www.geohazardsinc.com

TWO-DIMENSIONAL ELECTRICAL RESISTIVITY PROFILE TRAVERSE 3

Sunnyhilll Restoration Area - Area 2
Ocklawaha, Florida

FOR: Jones Edmunds & Associates, Inc.

DATE: 5-18-16

BY: R. Emslie, Geologist
Investigation #2016210

Example point resistivity log:

x = 1300.000(Ft)		traverse 1
Depth(Feet)		Resistivity(Ohm-m)
69.555		3372.726
68.856		4175.805
66.562		6401.39
63.961		13530.363
61.023		24786.452
57.715		12986.501
54		7680.839
49.84		5050.65
45.191		3363.957
40.005		2532.035
34.23		2335.195
27.81		2849.025
20.681		3751.726
12.776		3394.355
4.018		6599.007
5.673		13908.328
16.39		9236.088
28.229		2215.162
41.302		700.163
55.726		454.846
71.633		467.743
89.167		427.228
108.488		446.677
118.816		456.786

APPENDIX B – HYDRAULIC SUBMERSIBLE PUMP SPECIFICATIONS

DURAFLO™ HTC012

HYDRAULIC SUBMERSIBLE TRASH PUMP AND 2400D DRIVE UNIT

MWI PUMPS
The Power to Move Water®

APPLICATIONS

Flood Control

Industrial

Bypass Pumping

Stormwater Drainage

Construction Dewatering

Agriculture

Aquaculture

Quarries

The MWI Duraflo™ hydraulic submersible trash pumps coupled with their diesel or electric drive units are an unbeatable combination for drying out construction excavations, quarry dewatering, sewage bypass, general municipal use and industrial work. These units are designed and manufactured for the toughest environments with the best combination of ruggedness, reliability, performance, operational costs and initial price. These pumps never quit – positively affecting your success and bottom line.

FEATURES

Duraflo™ - HTC012

- Open 3 bladed impeller for handling trash and sewage
- Easily passes 3.125” solids
- Runs dry indefinitely with oil lubricated seals and bearings
- Reliable, rugged vane hydraulic motor
- Lifting point
- Weldable and shock proof cast steel volute
- Manufactured in the USA

2400D Diesel Engine Drive Unit

- Skid mounted unit standard
- Trailer mounted unit available with optional fenders, DOT light kit and braking system
- Engine and hydraulic safety shutdowns
- Complete hydraulic system with control panel, pump, filters, tank and gauges
- Small hydraulic tank reduces fluid replacement costs
- Reliable, efficient vane hydraulic pump
- Environmentally friendly - inherently biodegradable hydraulic fluid
- Auto start/stop panel available with floats
- Manufactured in the USA

QUICK SPECIFICATIONS	
Delivery connection	12” ANSI Pattern Flange
Max capacity	7200 GPM
Max solids handling	3.125”
Max impeller diameter	16.75”
Max head (TDH)	130’
Max hydraulic system pressure	2700 PSI
Dimensions	Unit: 39 x 81” / Drive: 48 x 79 x 125.5”
Sound levels w/ enclosure	67 dBA at 7M / 23’
Max fuel consumption	8.3 gal/hr at 156 HP; 22.3 hr run time

PERFORMANCE CURVE

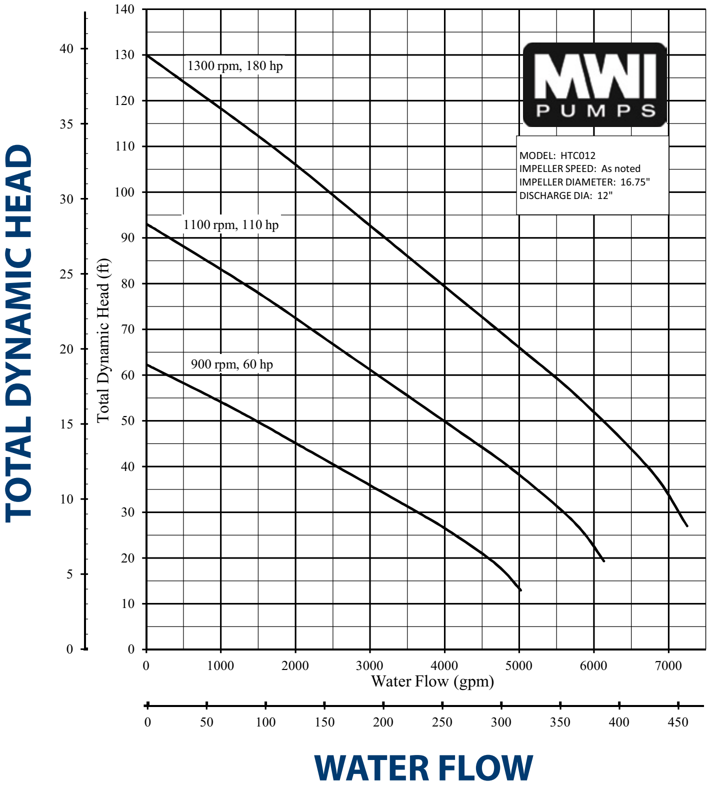

DIMENSIONS

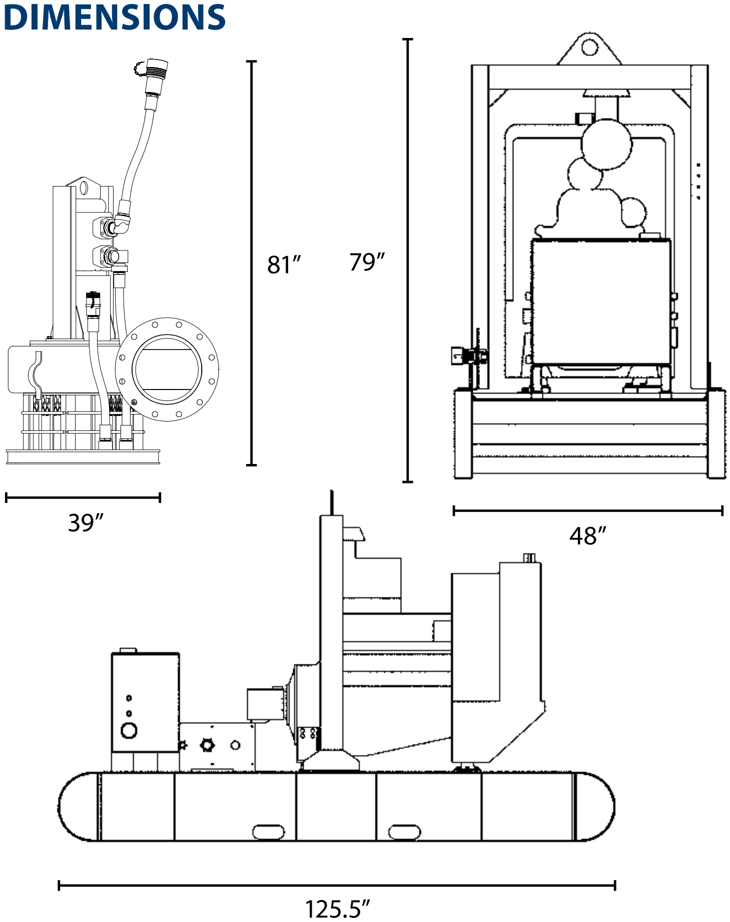

MATERIALS & SPECIFICATIONS	
DURAFLO™ HTC012	
Hydraulic motor	Vane type
Impeller	3 Bladed open - A36 steel
Shaft material	300 Series stainless steel
Volute	High strength, cast steel-nautilus design
Wear plates	A36 Steel - upper and lower
Delivery connection	12″ ANSI Pattern Flange
Hose ports	1.5″ Supply, 1.5″ return, .75″ case drain
Mechanical seal	Silicone carbide - hydraulic-fluid bathed
Bearings	Hydraulic-fluid lubricated - 50,000 hrs minimum life
Weight	1230 lbs
Coating	Epoxy

2000D DRIVE UNIT	
Engine	John Deere 6068HF285
Engine power	156 HP
Control panel with safety shutdowns	Including tach, hour meter, high coolant temperature and high/low oil pressure/temperature, excessive vacuum shutdowns plus over speed protection
Fuel tank	187 Gallon vented fuel tank with extra large filler and fuel gauge
Fluid tank	22 Gallon hydraulic
Equipped standard	Internal suction strainer, return filter, external sight gauge for hydraulic oil and vented hydraulic oil filler cap
Hydraulic oil	AW 68
Weight	4900 lbs (skid)

MWI Pumps Headquarters
33 NW 2nd St | Deerfield Beach, FL 33441

Inquiries: 954-426-1500 | Fax: 954-426-8938 | Email: info@mwipumps.com | **mwipumps.com**

APPENDIX C - CROSS-CORRELATIONS OF SUNNYHILL RECHARGE WATER LEVEL DATA

CROSS-CORRELATIONS OF SUNNYHILL RECHARGE WATER LEVEL DATA

By:
Paul Bremner, Ph.D.
Wei Jin, Ph.D., P.E.
Michelle Brown, P.E.

St. Johns River Water Management District
Palatka, Florida

2020

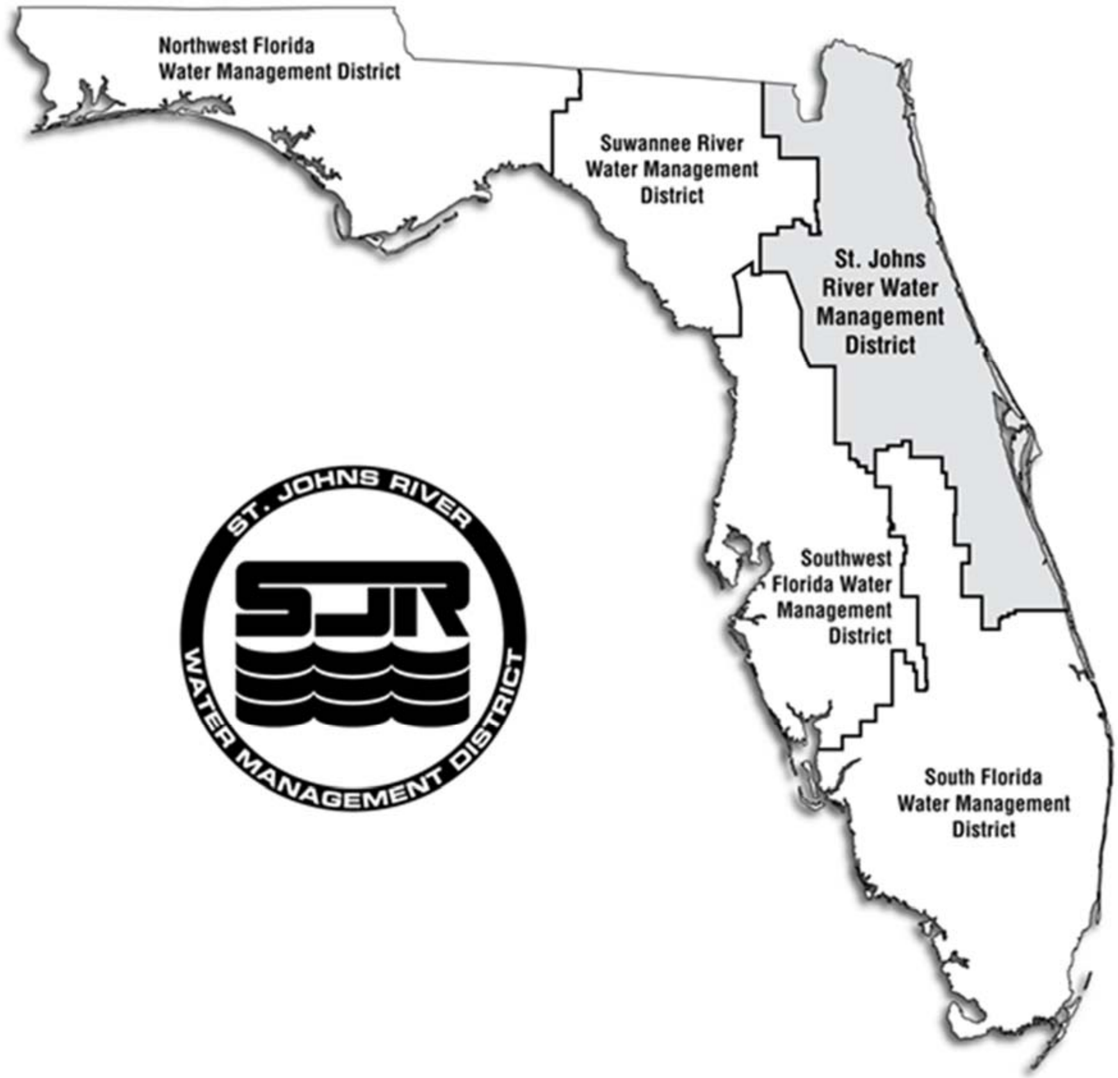
Northwest Florida
Water Management District
Suwannee River
Water Management
District
St. Johns
River Water
Management
District
Southwest
Florida Water
Management
District
South Florida
Water Management
District
ST. JOHNS RIVER
SJR
WATER MANAGEMENT DISTRICT

EXECUTIVE SUMMARY

In this work, a common seismic investigation methodology known as seismic ambient noise, which correlates different time-series, was extended to correlate time-series of water level measurements from a sinkhole and surrounding monitoring wells spanning a recharge test at a selected sinkhole located at the Sunnyhill Restoration Area. The overarching goal of this part of the Sunnyhill recharge project was to positively identify which aquifer was recharged when water was pumped into the sinkhole. The results demonstrated that cross-correlation techniques regularly applied in seismology also successfully determined a correlation of water level changes between the sinkhole and adjacent wells, and between the adjacent wells. The results also demonstrated that, with further development of the methodology and utilizing more advanced techniques, other hydraulic properties might be accessible, as well, such as: estimating the leakance and transmissivity between measurement sites, and constructing and removing a common background signal from a group of measurement sites to reveal local changes in water levels. Thus, the goals of this portion of the Sunnyhill recharge project were met.

Water level time-series data from four monitoring wells surrounding the sinkhole were processed and cross-correlated between the sinkhole and monitoring wells, and between the monitoring wells. Two of the monitoring wells measured the surficial aquifer system (SAS), one measured the upper Floridan Aquifer system (UFA), and one well measured an uncertain portion of the aquifer.

The cross-correlations revealed a 12-hour period oscillation, potentially caused by solid Earth tides from the Sun and Moon's gravitational influence. The observed oscillation for some correlated measurement station pairs were out of phase with others, implying a delay in diffusive water level changes, and could be used to determine transmissivity between monitoring sites. Additionally, local correlated signals appeared to occupy a different, higher, frequency band than lower frequency background signals.

Site characteristics were determined from both the analysis of the raw water level time-series data and the cross-correlations. The well that measured an uncertain portion of the aquifer apparently did not measure the SAS, but potentially measured the UFA or an aquifer partially isolated from the SAS and UFA, potentially within the Intermediate Confining Unit (ICU). The sinkhole did not appear directly connected to the SAS but did appear connected to an aquifer potentially within the ICU, as well as some connection to the UFA. The SAS appeared buffered from the UFA (via the ICU). However, that buffer was not absolute, perhaps due to a thick sandy infill into the sinkhole.

Table of Contents

List of Figures

List of Tables

Chapter 1. INTRODUCTION OR BACKGROUND

The Sunnyhill recharge project was designed to test the effectiveness of using a sinkhole to recharge the Floridan Aquifer and to develop and evaluate techniques to analyze that effectiveness (Davis et al., 2020). Results of a successful test could be used to evaluate the feasibility and design of a water delivery system through a sinkhole. The goal of the analysis was to verify that the sinkhole is hydraulically connected to the Floridan Aquifer system (FAS) and to what part, as well as attempt to estimate the leakance between the sinkhole and the aquifer system, the leakance of the ICU near the sinkhole, and the transmissivity of the aquifer system between the sinkhole and nearby wells. The evaluation of methods used real data collected during a recharge test at a selected sinkhole located at the Sunnyhill Restoration Area to determine the optimal analysis techniques.

A technique from seismology known as “Seismic Ambient Noise” was adapted and used for the purpose of determining a correlation of water level between the sinkhole and adjacent wells, and between the adjacent wells. A positive correlation of the sinkhole to a well implies a hydraulic connection to the aquifer that the well monitors. The methodology adopted to do this work involved analyzing the frequency content of the water level time-series data followed by performing traditional seismic ambient noise processing steps outlined in Bremner et al. (2019). For hydrogeology, this is a new method that previously has not been applied to water level data for this kind of analysis. Thus, a second goal of this work was to determine the technique’s feasibility to correlate the data from different measurement sites, as is routinely done for seismic data, as well as to determine what other information about the site’s hydraulic properties might be accessible through this process.

Since this technique is new to analyzing water level time-series data, and new to the District, the methods, results, and the interpretations were laid out in such a way as to provide a blueprint that can be further developed or used for future projects.

STUDY SITE AND DATA CHARACTERISTICS

Time-series data from four measurement wells were processed and compared with the time-series of water level within the sinkhole (Table 1). Two wells, M0832 and M-0833 measured the SAS, whereas M-0831 measured the UFA. Well M-0834 was thought to also measure the UFA, however that was uncertain due to observed irregularities in the well (Davis et al., 2020). Figure 1 is an aerial image of the test site displaying the sinkhole and spatial distribution of the wells about the sinkhole.

Recording of water level at the sinkhole began in mid-August of 2019, followed by the monitoring wells in late-November of 2019 (Figure 2). Each site measured at a rate of 1 sample per 5 minutes. Starting in early December of 2019, water was pumped into the sinkhole from outside the system to elevate the water level. Pumping ceased in mid-December, at which point the sinkhole water level rapidly fell. Each of the monitoring wells recorded an increase, followed by decrease, in water level at a similar time period suggesting a hydraulic link between water draining from the sinkhole and entering the aquifer system.

*Table 1. Properties of each measurement site. Times are based in 24hr format. * indicates cluster well*

Measurement Site Name	Major Aquifer and Site Characteristics	Casing / Total Depth Elevation (ft NAVD88) Davis et al. (2020)	Water Level Measurement Sampling Rate	Measurement Start Date/Time	Measurement End Date/Time
SINK	Sinkhole	NA / -145	1 sample / 5 min	8/16/2019 11:00	3/17/2020 12:35
M-0831*	UFA cluster	-125 / -179	1 sample / 5 min	11/21/2019 11:00	3/17/2020 9:55
M-0832*	SAS cluster	49 / 19	1 sample / 5 min	11/21/2019 11:15	3/17/2020 9:45
M-0833	SAS	45 / 25	1 sample / 5 min	11/21/2019 23:55	3/17/2020 13:00
M-0834	Unknown (potentially UFA)	<-11 / <-23	1 sample / 5 min	11/21/2019 23:55	3/17/2020 12:35

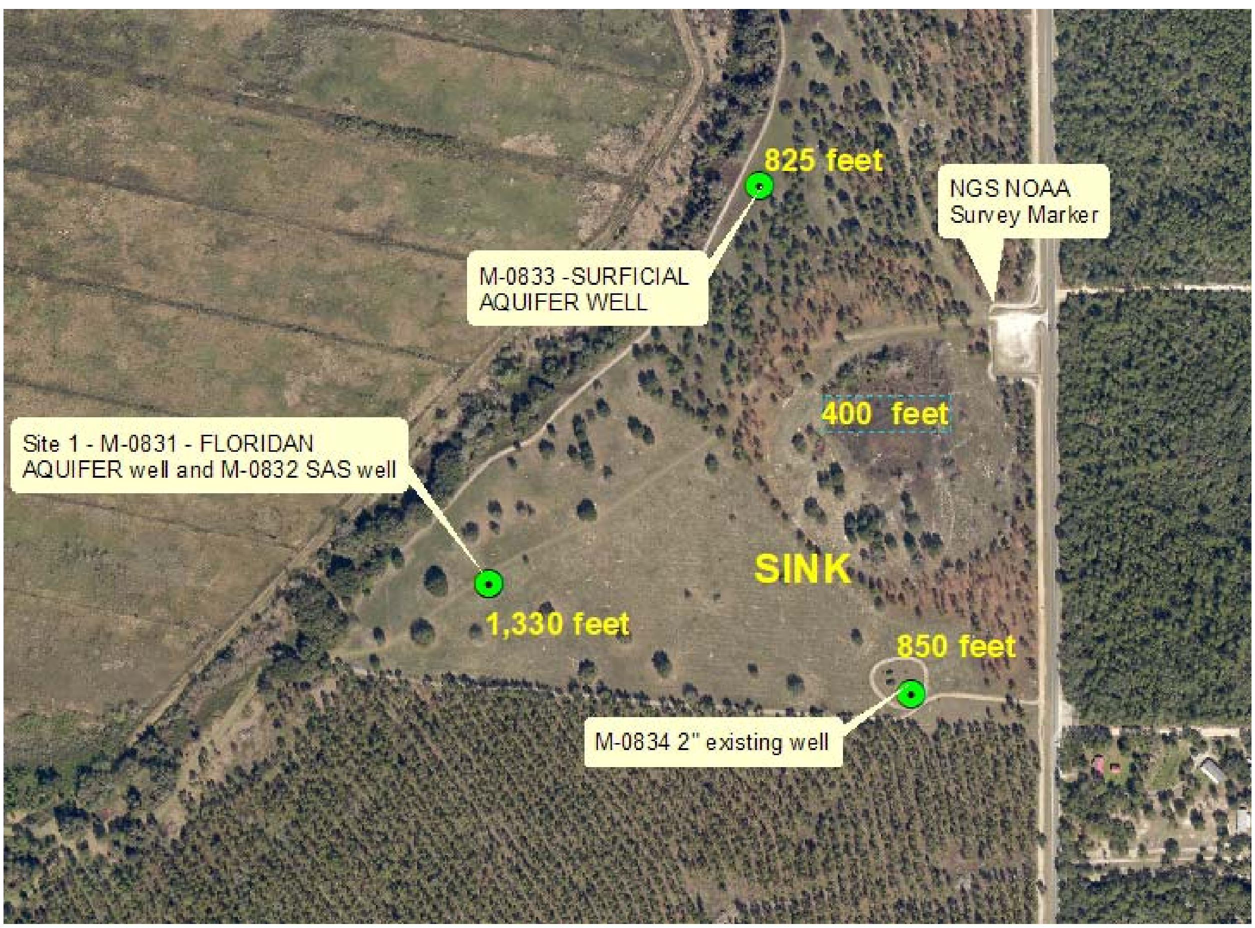

Figure 1. Aerial view of the Sunnyhill recharge project site. The sinkhole is near the center of the photo beneath the "400 feet" labeled scalebar north-northeast of the label SINK. The four nearby monitoring wells roughly surround the sinkhole, and are each marked with distance from the from the sinkhole in yellow. Site 1, on the west side of view, is a cluster well of two nearly co-located wells: M-0831 montoring the UFA and M-0832 monitoring the SAS. M-0834 was a preexisting well that monitored an uncertain portion of the FAS due to a physical obstruction within the well. Photo and labels courtesy of Jeff Davis (personal communication).

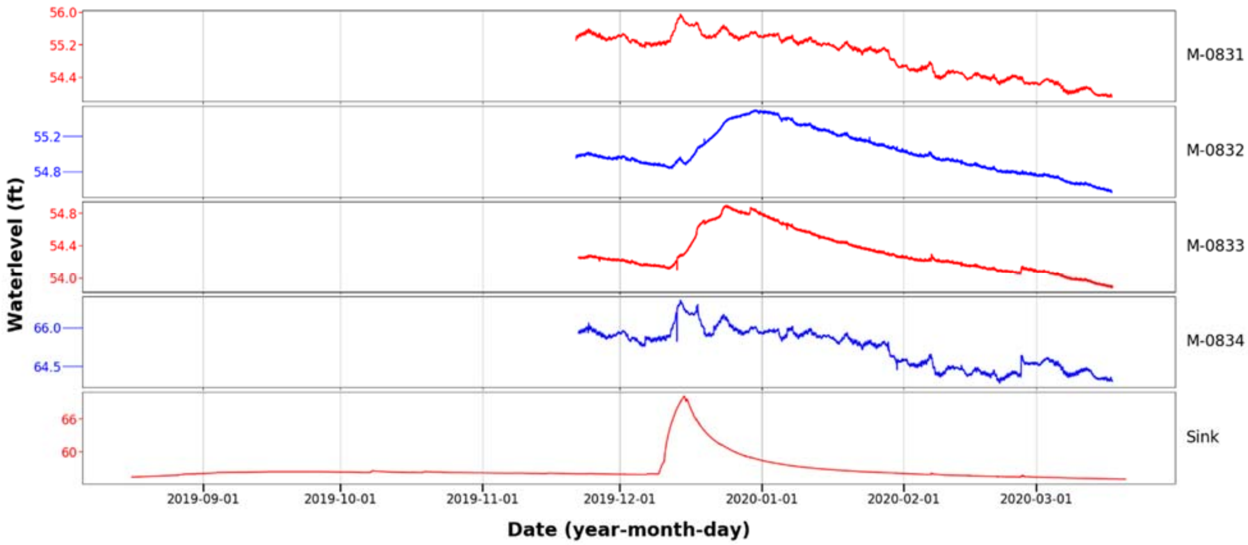

Figure 2. Time-series of water level measurements for each of the monitoring wells and the sinkhole. Water actively pumped into the sinkhole corresponds to the rapid rise in sinkhole water level. Likewise, the gradual drop in water level began once active pumping ceased.

Chapter 2. METHODS

In order to conduct and process the cross-correlations, the water level time-series data for each of the monitoring wells and the sinkhole had to be formatted and preprocessed. The sections below describe the procedures used to format the raw time-series data, as well as the data preprocessing and the cross-correlations steps.

CONSTRUCTING TIME-SERIES SEGMENTS

The full-length raw water level records were split into a series of consecutive, non-overlapping, and equal length data segments. Each segment of one measurement site was later correlated with synchronous segments of the other measurement sites. For this application to water level data, the appropriate length of data segments was uncertain. Data segments of a single hour or 24 hours in length are common in traditional seismic ambient noise data processing, which provide an adequate number of time points to attempt correlation between two records, as well as enough records to correlate and average together. However, seismic data typically possesses a ≥ 40 Hz sampling rate, a much higher point density than the data used here. Therefore, it was decided to evaluate three different segment lengths: 24-hour segments (daily), 7-day segments (weekly), and 30-day segments (monthly). Additionally, the results of cross-correlation that are shown in this report utilized a software toolkit known as SAC (Seismic Analysis Code) (Goldstein, 2003; Goldstein, P., & Snoke, A., 2005), which uses its own binary file format. Thus, all constructed data segments were translated into the SAC binary file format and specific SAC utilities were highlighted where appropriate in the description of the methods below.

PREPROCESS THE DATA

Below are the descriptions of the preprocessing steps applied to each data segment prior to cross-correlations in the order they were applied:

- Make the time-series evenly-spaced: Many of the SAC tools require evenly-spaced data, where each subsequent data point falls on the expected point in time in the record, according to the sampling rate. Missing or shifted data points are not permitted. Therefore, each data segment was interpolated in SAC using the built-in Wiggins' weighted average-slopes interpolation method (Wiggins, 1976) to produce an evenly-spaced time-series from the unevenly-spaced data. The base sampling rate was unchanged.
- Remove the mean and trend: Next, both the mean and trend were removed. For this step, the arithmetic mean of water levels was calculated for the given data segment, then subtracted from each data point to yield the residual values. The trend was calculated via least-squares linear fit of the given data segment, and then subsequently subtracted from the data points. The SAC commands “rmean” and “rtrend” were applied to remove the data mean and trends, respectively.
- Bandpass filter: In traditional seismic and acoustic cross-correlation methods, the time-series data is band-pass filtered to exclude frequency content outside of the band of interest. This step is most important to remove short period noise. The water level sampling rate recorded by the instruments limited the high frequency content. The sampling rate of 1 sample per 5 minutes, or ~0.0033 Hz (300 second period; five-minute period), gave a Nyquist frequency of ~0.001667 Hz (600 second period; 10-minute period). Acoustic pressure waves in open water propagate at the bulk sound speed (on the order of 1.5 km/sec at 20 °C, 68 °F), though velocity is modified in porous media. Thus, 600 seconds exceeds the time necessary for pressure waves to pass through the system, and a higher frequency recording would be needed to capture them. Therefore, band-pass filtering was not applied here.
- Data resampling: The cross-correlation processing time depends upon the number of data points within the data segments. Both seismic and acoustic data typically have a data sampling rate of ≥ 40 Hz, and the number of records to cross-correlate typically exceeds one thousand, for modern studies. Thus, the data is downsampled in order to speed cross-correlation calculations. The data used for this report possessed a sampling rate of 1 sample per 5 minutes, much lower than typical seismic data. Therefore, downsampling was not necessary and was not applied.
- Normalize the amplitude: In traditional seismic ambient noise cross-correlation, the time domain amplitude (measure of water level, here) is normalized to reduce the effects of high energy (high amplitude) temporally localized events, such as earthquakes. It is still unclear if this is necessary for water level measurements. Thus, amplitude was handled two different ways and both cases were compared:
    - Normalize the amplitude
    - Preserve the amplitude

- Spectral whitening: Spectral whitening was the final preprocessing step, where the power of each frequency in the band of interest was normalized in the frequency domain. The SAC command "whiten" was applied to do this. Spectral whitening reduces bias introduced by dominant frequencies inherent in the data that may mask the signal of interest.

Cross-Correlations and Post-Processing

Correlation is a method to detect like patterns between multiple time-series. The definition adopted for seismic ambient noise, and for the work outlined here, is that cross-correlation is the process of correlating multiple time-series from different measurement locations but synchronous in time, though a more general definition allows correlating asynchronous time segments. Auto-correlation is the process of correlating multiple synchronous time-series from the same measurement location.

To provide an illustrative way to understand the process, imagine correlating two time-series, A and B. Calculating the cross-correlation in the time-domain entails holding time-series A in place (the master) and systematically shifting time-series B (the secondary) along time-series A both forward and backward in time. At each shift, the correlation coefficient is calculated, and the final output is a new time-series of correlation coefficients called an auto- or cross-correlogram, and collectively called correlograms. Thus, the time position of a high correlation coefficient within the correlogram provides the traveltime (also known as the offset, delay, or lag time) for a common signal to propagate from one measurement site to another.

Each of the preprocessed data segments were both auto and cross-correlated with synchronous segments. Correlograms as function of traveltime (*t*) were calculated in the frequency domain via multiplication of the master series with the complex conjugate of the secondary series (**Equation 1**):

$$xcorr(t) = F^{-1}[F_{stn1}(\text{v}) \cdot F^{*}_{stn2}(\text{v})], \tag{1}$$

where *F* is the Fourier transform of the time-series, *v* is the frequency, * denotes the complex conjugate, and F^{-1} is the inverse Fourier transform used to revert the correlogram, *xcorr*, to the time domain.

Following correlation, correlograms for each pair of measurement sites were linearly stacked (averaged). Stacking proceeded in the time domain via point-by-point addition over traveltime (*t*) of individual correlograms and then divided by the number of summed traces (**Equation 2**):

$$StackedXcorr(t) = \frac{1}{N}\sum_{i=0}^{N} xcorr_i(t), \tag{2}$$

where the increment *i* denotes an individual correlogram, and *N* is the total number of correlograms to be stacked for a given pair of measurement sites. Summarized below are the steps used to produce stacked correlograms for each pair of measurement sites:

1. Match simultaneous data segments from a pair of stations
2. Auto- or cross-correlate the pair of simultaneous time-series data segments to produce a new correlogram
3. Stack the correlograms for the current pair of measurement sites

Chapter 3. RESULTS

The correlation process outlined above resulted in stacked correlograms, and are presented below organized first by auto- then cross-correlograms from both cases of water level amplitude (normalized or preserved amplitudes). For each water level amplitude case, stacked correlograms were produced from four scenarios: from all three data segment lengths; the 30-day segment lengths (~monthly), 7-day lengths (weekly), and 1-day lengths (daily); as well as stacks that consisted of daily data segments which bracketed the period of active water pumping into the sinkhole. The stacked correlograms between measurement sites were used as a proxy to assess the correlation between hydrogeologic site properties, such as M-0831 to M-0833 addressed correlation between the UFA and SAS at those locations. In the following sections, the results were listed as apparent signals (or lack thereof) observed within the correlograms and spectrograms, with all interpretations relegated to the Discussion and Interpretations.

The correlograms of site *A*-to-*B* are the mirror of site *B*-to-*A*. Thus, for simplicity, only one direction (*A*-to-*B*) of each station pair is shown. The correlograms are displayed with traveltime along the x-axis and the scale is symmetric about a traveltime equal to zero. A positive traveltime (the causal branch) denotes a signal that traveled from site *A*-to-*B*, while a negative traveltime (the acausal branch) denotes the reverse, a signal that traveled from site *B*-to-*A*. Throughout the remainder of the report the site names of monitoring wells have been shortened to: 831, 832, 833, and 834. Table 2 lists the start/end dates of correlograms included into each stack, as well as the total number of correlograms incorporated.

Table 2. The start date of the first correlogram, and the end date of the last correlogram included in the stack for each pair of measurement locations are listed for each scenario. Dates are formatted as Year-Month-Day. The columns labeled # Stacked denote the total number of correlograms incorporated into each stack.

Station Pair	**30-Day Increments**		**7-Day Increment**		**Daily – All Segments**		**Daily – Pumping Period**	
	Start/End Date	**# Stacked**	**Start/End Date**	**# Stacked**	**Start/End Date**	**# Stacked**	**Start/End Date**	**# Stacked**
Sink-Sink	2019-12-07 2020-03-05	3	2019-12-07 2020-03-13	14	2019-12-06 2020-03-16	101	2019-12-08 2019-12-17	10
831-831	2019-12-07 2020-03-05	3	2019-11-23 2020-03-13	16	2019-11-22 2020-03-16	116	2019-12-08 2019-12-17	10
832-832	2019-12-07 2020-03-05	3	2019-11-23 2020-03-13	16	2019-11-22 2020-03-16	116	2019-12-08 2019-12-17	10
833-833	2019-12-07 2020-03-05	2	2019-11-23 2020-03-13	15	2019-11-22 2020-03-16	115	2019-12-08 2019-12-17	10
834-834	2019-12-07 2020-03-05	3	2019-11-23 2020-03-13	16	2019-11-22 2020-03-16	116	2019-12-08 2019-12-17	10
Sink-831	2019-12-07 2020-03-05	3	2019-12-07 2020-03-13	14	2019-12-06 2020-03-16	101	2019-12-08 2019-12-17	10

Sink-832	2019-12-07 2020-03-05	3	2019-12-07 2020-03-13	14	2019-12-06 2020-03-16	101	2019-12-08 2019-12-17	10
Sink-833	2019-12-07 2020-03-05	2	2019-12-07 2020-03-13	13	2019-12-06 2020-03-16	100	2019-12-08 2019-12-17	10
Sink-834	2019-12-07 2020-03-05	3	2019-12-07 2020-03-13	14	2019-12-06 2020-03-16	101	2019-12-08 2019-12-17	10
831-832	2019-12-07 2020-03-05	3	2019-11-23 2020-03-13	16	2019-11-22 2020-03-16	116	2019-12-08 2019-12-17	10
831-833	2019-12-07 2020-03-05	2	2019-11-23 2020-03-13	15	2019-11-22 2020-03-16	115	2019-12-08 2019-12-17	10
831-834	2019-12-07 2020-03-05	3	2019-11-23 2020-03-13	16	2019-11-22 2020-03-16	116	2019-12-08 2019-12-17	10
832-833	2019-12-07 2020-03-05	2	2019-11-23 2020-03-13	15	2019-11-22 2020-03-16	115	2019-12-08 2019-12-17	10
832-834	2019-12-07 2020-03-05	3	2019-11-23 2020-03-13	16	2019-11-22 2020-03-16	116	2019-12-08 2019-12-17	10
833-834	2019-12-07 2020-03-05	2	2019-11-23 2020-03-13	15	2019-11-22 2020-03-16	115	2019-12-08 2019-12-17	10

AUTO-CORRELOGRAMS

Stacked auto-correlograms and their associated spectrograms were calculated for each station pair, for each scenario, and both normalized and preserved water level amplitude cases, forty in all. Figure 3 shows a representative set of stacked auto-correlograms obtained from stacking all the correlations of the daily length data segments which preserved the water level amplitudes (without normalization). The remaining auto-correlograms are shown in Appendix A, Auto-Correlograms and Associated Spectrograms. Although techniques exist to extract information about the local physical system utilizing auto-correlograms, that was not done for this work. Instead the stacked auto-correlograms were used solely as a diagnostic tool to ensure the quality of the correlations. All the auto-correlograms displayed characteristics indicative of good quality correlations, including:

- A characteristic “spike” at 0 second traveltime, which was expected since signals arrive instantaneously in an auto-correlation.
- Moving out symmetrically from the central peak, the signals tapered toward zero amplitude with minor oscillations, which was expected since auto-correlated signals are identical with no delay between them.

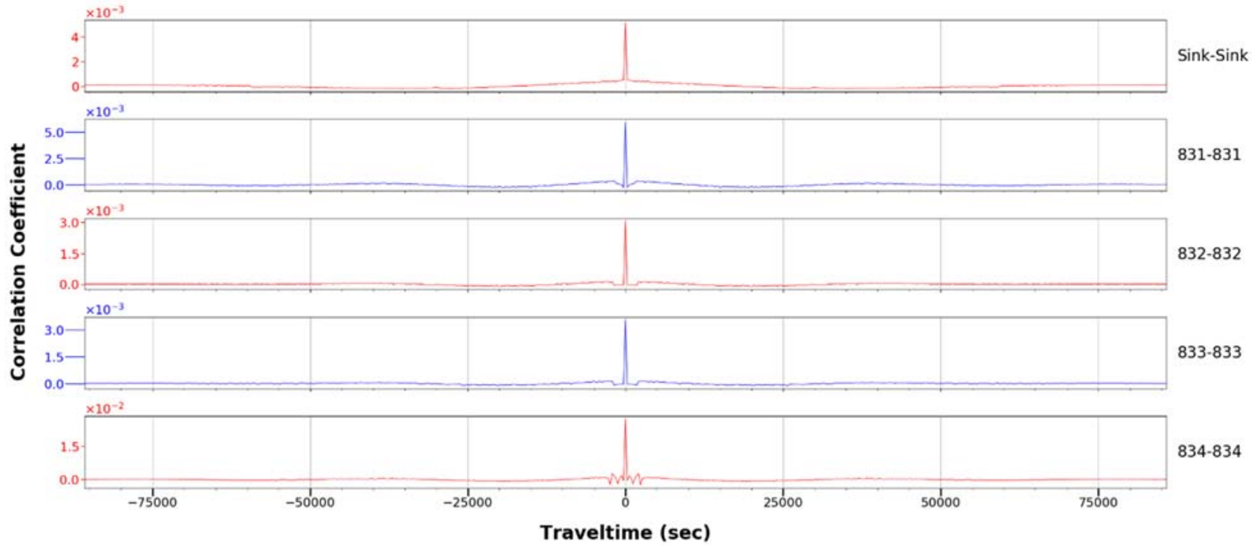

Figure 3. Stacked auto-correlograms for all the daily segment lengths with preserved water level amplitudes (without normalization). Each panel displays a single stacked correlogram with the measurement site pair labeled on the righthand side as "site1"-"site2". Traveltime is featured along the x-axis in units of seconds and scaled such that negative and positive time is symmetric about zero seconds. Unitless correlation coefficients are along the y-axis. For y-axis values in scientific notation, the base and exponent is displayed atop the left-side of the panel.

Figure 4 shows a spectrogram calculated for the station pair Sink-Sink of the stacked auto-correlogram seen in Figure 3, and is representative of all the auto-correlated spectrograms calculated. All remaining auto-correlated spectrograms are shown in Auto-Correlograms and Associated Spectrograms in Appendix A. The spectrogram figures consist of two panels:

1. The top panel displays the stacked correlogram with traveltime featured along the top-*x*-axis and unitless correlation coefficients marked on the *y*-axis. Horizontal lines reference the estimated signal to noise ratio (SNR) values 1, 3, or 6 (shown in the legend to the right of the panel). The measurement station pair is labeled on the top and to the right of the panel.
2. The bottom panel displays the spectrogram of the correlogram featured in the top panel. The spectrogram is aligned along the *x*-axis to the correlogram. Frequency in units of Hertz is marked along the *y*-axis, and the color scales with relative power (scalebar to the right of the panel) where increasing color intensity corresponds to increasing power.

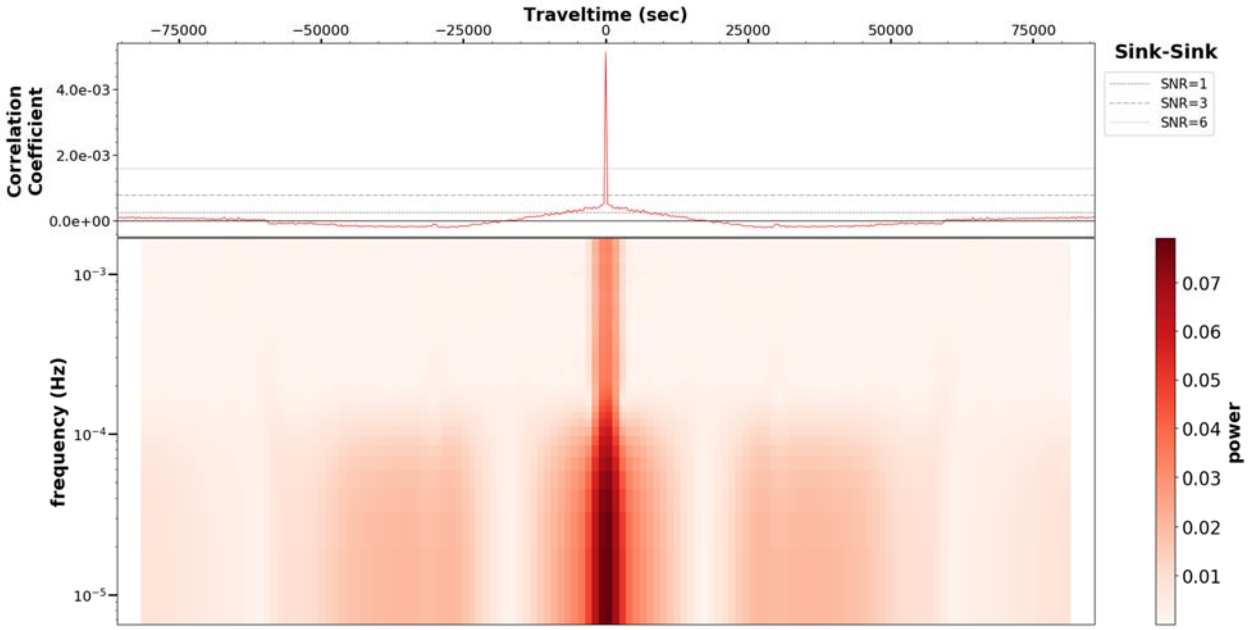

Figure 4. Spectrogram from stacked auto-correlated daily length data segments with preserved amplitudes (not normalized), all segments. Station pair: Sink-Sink

What is considered a high SNR value is not standardized, therefore this work relied on definitions used in seismic ambient noise, where SNR≥6 were considered high values (Gallego et al., 2010; James et al., 2017; Bremner et al., 2019). For a given correlogram, SNR levels were calculated at multiples of the estimated noise floor. Ideally, the noise floor would be calculated based on the correlogram minus the signal of interest. However, the signal and its traveltime were unknown. Therefore, the noise floor was calculated as the RMS of the entire record, including both true noise and signal. This method overestimated the noise floor, as well as the amplitude of the correlation coefficient corresponding to the SNR values referenced in Figure 4 (SNR = 1, 3, or 6). However, this was considered a conservative estimate since the true noise floor would be lower than the RMS of the entire record, and that identified signals would be more significant if only the true noise level was used. All spectrograms of the auto-correlograms displayed similar characteristics; that signal power was concentrated at zero traveltime for all frequencies and was the only place where SNR>6. Furthermore, at high frequencies signal power was only visible at zero traveltime, indicative that no other significant short wavelength signals existed away from this point. Both of these characteristics were expected features of good quality auto-correlograms.

Cross-Correlograms from Normalized Amplitudes

The stacked cross-correlograms calculated from data segments whose water level amplitudes were normalized are shown below for all four scenarios. They are organized as: the 30-day segment lengths, 7-day lengths, daily, followed by those from the pumping period. Supporting figures are shown in Figure A- 47 - Figure A- 94.

Figure 5 shows cross-correlograms stacked from the 30-day segment length normalized data. The stacked cross-correlograms either displayed long wavetrains or numerous shorter bursts, each with similar SNR across its respective record. A semi-regular beat pattern was observed for the pairs Sink-

831, Sink-833, Sink-834, 833-834, and less noticeable for Sink-832 and 831-833. The remaining pairs possessed long wavetrains with amplitudes that generally were higher for short and mid-length traveltimes, then progressively tapered toward the ends. The rate of tapering for these pairs were not symmetric about zero traveltime.

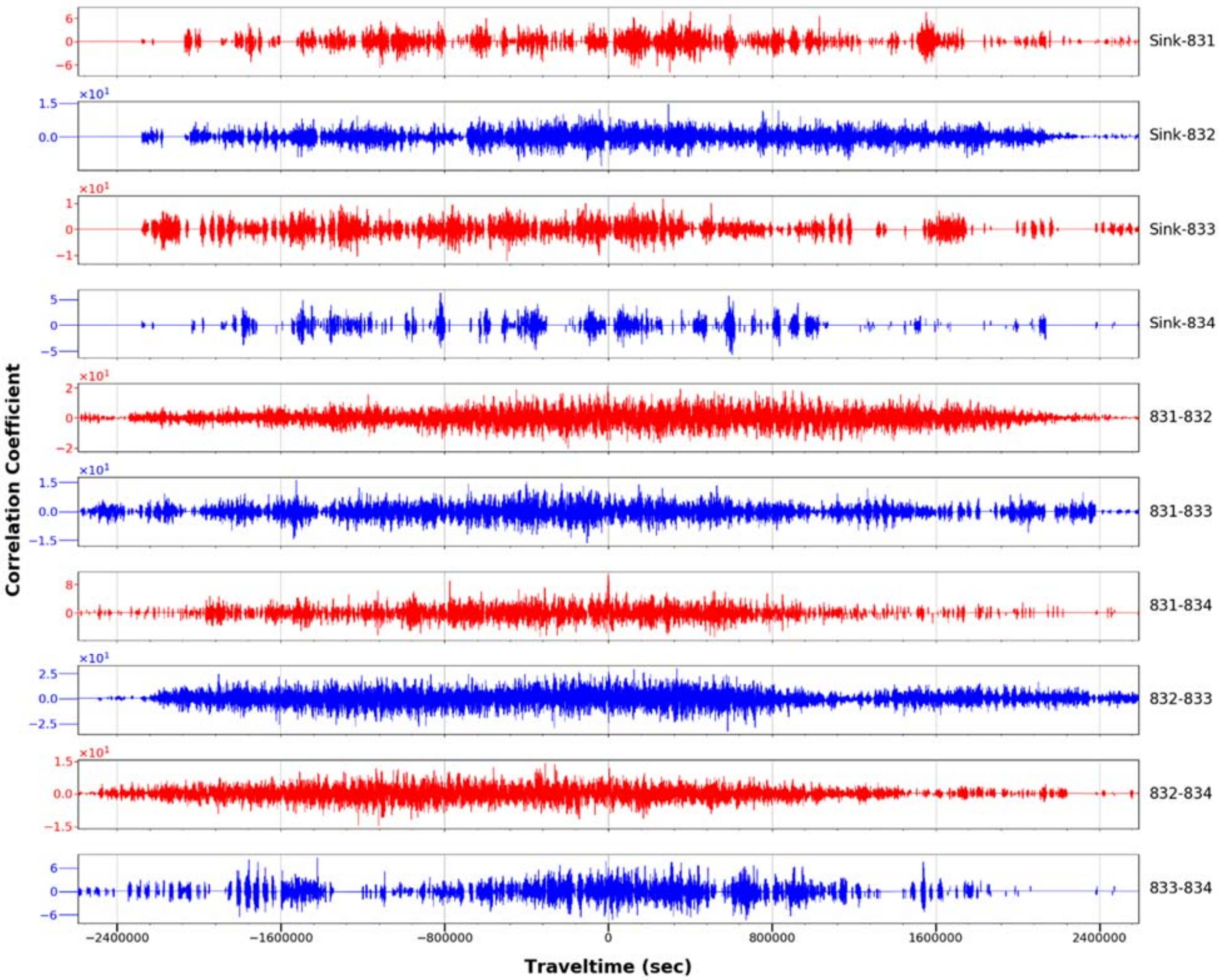

Figure 5. Stacked cross-correlograms from 30-day data segment lengths and normalized water level amplitudes. Each panel displays a single stacked correlogram with the measurement site pair labeled on the righthand side as "site1"-"site2". Traveltime is featured along the x-axis in units of seconds and scaled such that negative and positive time is symmetric about zero seconds. Unitless correlation coefficients are along the y-axis. For y-axis values in scientific notation, the base and exponent is displayed atop the left-side of the panel.

Figure 6 shows cross-correlograms stacked from the 7-day segment length normalized data. The correlograms from measurement pairs that included the Sink showed no discernable pattern. The wavetrain amplitude of these signals generally were high for short and mid-length traveltimes, then tapered toward the ends. In contrast, the correlograms from measurement pairs between the monitoring wells were dominated by a 12-hour period sinusoidal oscillation which tapered toward the end of the records roughly symmetric about zero traveltime. Three pairs (831-832, 831-834, and 832-833) also contained distinct peaks at and near zero traveltime.

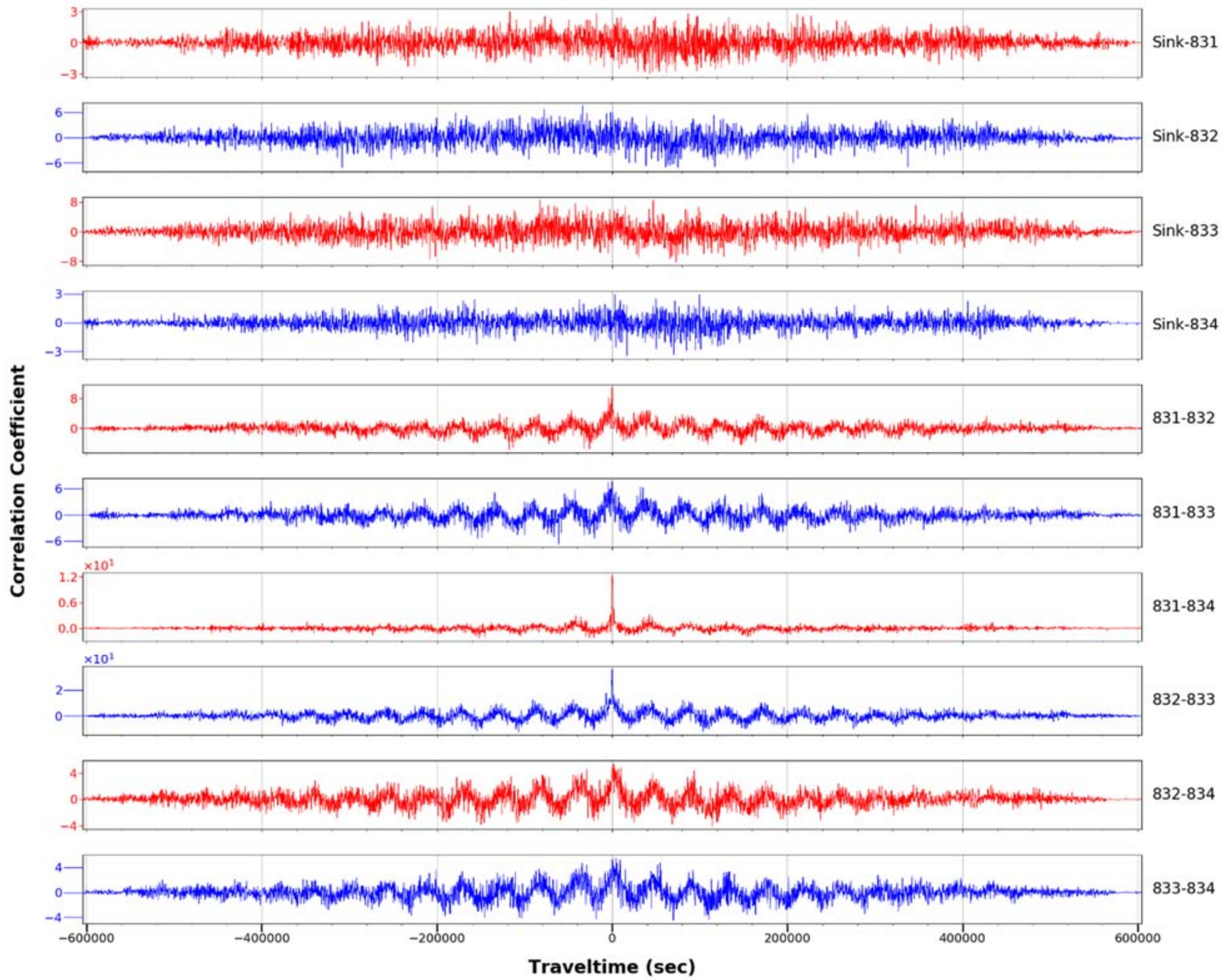

Figure 6. Stacked cross-correlograms from 7-day data segment lengths and normalized water level amplitudes. Each panel displays a single stacked correlogram with the measurement site pair labeled on the righthand side as "site1"-"site2". Traveltime is featured along the x-axis in units of seconds and scaled such that negative and positive time is symmetric about zero seconds. Unitless correlation coefficients are along the y-axis. For y-axis values in scientific notation, the base and exponent is displayed atop the left-side of the panel.

Figure 7 shows cross-correlograms stacked from all the daily segment length normalized data. Similar to the 7-day increment correlogram stacks described above, here too, the stacked correlograms exhibited the 12-hour period oscillation. In this scenario, however, the oscillation was visible for all station pairs. The correlograms from the four measurement pairs that included the Sink were nearly in-phase with each other, though a closer match of long-period signal magnitudes existed between Sink-831 and Sink-834, and between Sink-832 and Sink-833 (All Daily Length Data Segments – Normalized Amplitudes). Notably, the correlograms from the four measurement pairs that included the Sink were not symmetric about zero traveltime, and out of phase with the correlograms between the monitoring wells. Additionally, for the correlograms between the monitoring wells, the long-period oscillations were interrupted by a prominent peak near zero traveltime, especially for 831-834 (Figure A- 77).

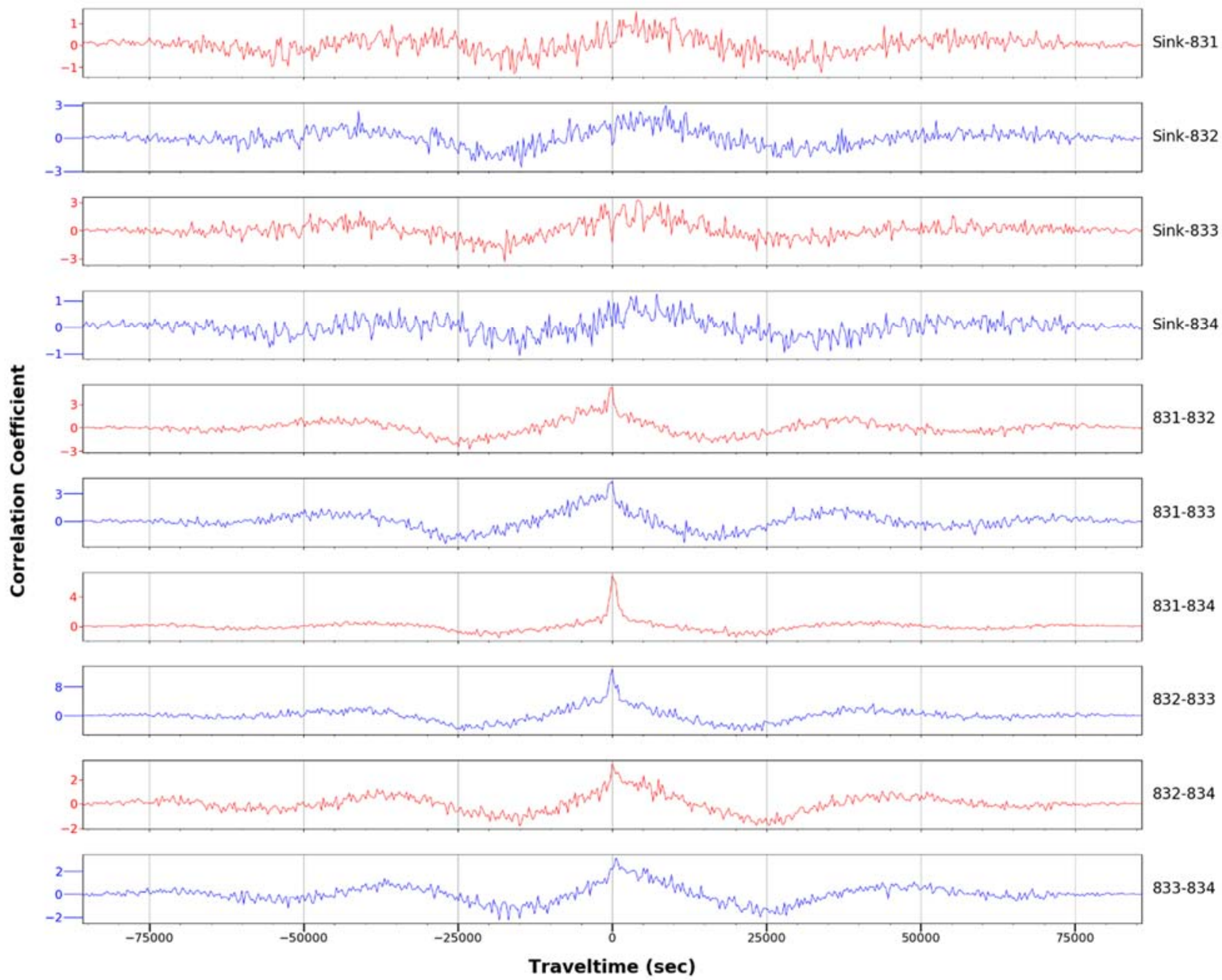

Figure 7. Stacked cross-correlograms from daily data segment lengths and normalized water level amplitudes. Each panel displays a single stacked correlogram with the measurement site pair labeled on the righthand side as "site1"-"site2". Traveltime is featured along the x-axis in units of seconds and scaled such that negative and positive time is symmetric about zero seconds. Unitless correlation coefficients are along the y-axis. For y-axis values in scientific notation, the base and exponent is displayed atop the left-side of the panel.

Figure 8 shows cross-correlograms stacked from the normalized daily data segment lengths which span the pumping period. Here, the 12-hour period oscillation observed in the stack of all daily correlograms appeared muted or was masked by higher amplitude noise for all pairs, but especially for those pairs that included the Sink and 831-834. Likewise, the prominent central peaks previously observed were greatly reduced, or no longer visible for the station pairs: 831-832, 831-833, 832-834, and 833-834. The station pair Sink-831 presented two apparent peaks (Figure A- 83): a prominent peak near zero traveltime, and a spike at ~25000 sec (~7hr). A potential signal at approximately negative 20000 sec for the pair Sink-833 was observed in the correlogram, spectrogram, and filtered correlogram (Figure A- 85 and Figure A- 93, respectively), though not distinct.

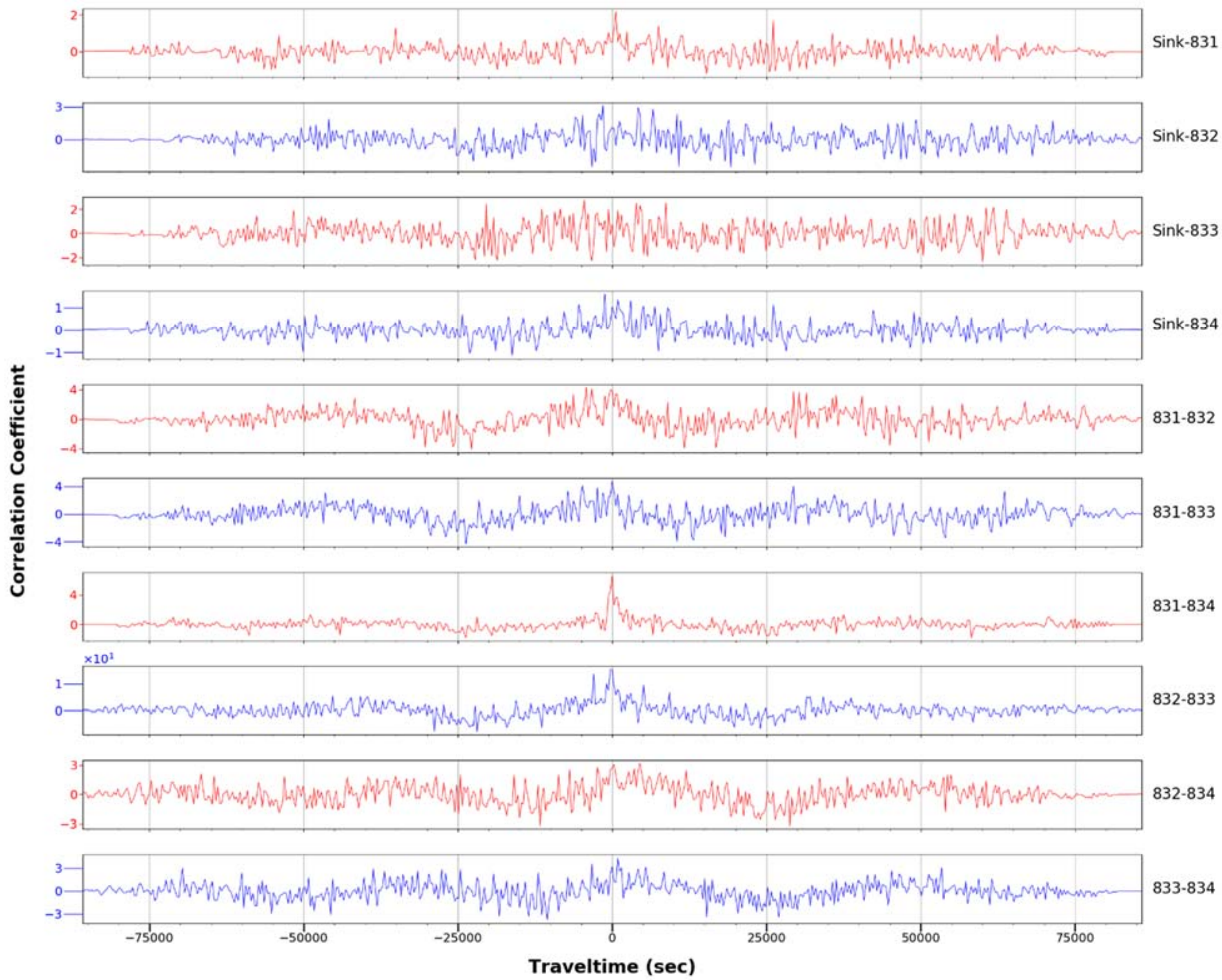

Figure 8. Stacked cross-correlograms from daily data segment lengths and normalized water level amplitudes. Only the segments from the period when water was pumped into the sinkhole were included in the stack. Each panel displays a single stacked correlogram with the measurement site pair labeled on the righthand side as "site1"-"site2". Traveltime is featured along the x-axis in units of seconds and scaled such that negative and positive time is symmetric about zero seconds. Unitless correlation coefficients are along the y-axis. For y-axis values in scientific notation, the base and exponent is displayed atop the left-side of the panel.

CROSS-CORRELOGRAMS FROM PRESERVED AMPLITUDES

This section presents the stacked cross-correlograms produced from data segments whose water level amplitudes were not normalized (amplitudes were preserved) for all four scenarios. They are organized as: the 30-day segment lengths, 7-day lengths, daily, followed by those from the pumping period. Supporting figures are shown in Appendix A Figure A- 95 - Figure A- 140

Figure 9 and Figure 10 show the stacked cross-correlograms of the 30-day and 7-day segment lengths, respectively. In both, a prominent spike (or trough) at or near zero traveltime for nearly all pairs was observed. Likewise, a spike was observed at ~560000 sec (~155 hr) for the following station pairs:

- For the 30-day increment correlograms -- pairs Sink-833, Sink-834, 831-833, 831-834, 832-833, and 832-834
- For the 7-day increment correlograms -- pairs Sink-832, Sink-833, Sink-834, 831-833, 831-834, and 832-834

In both instances, the pairs Sink-831, Sink-832, Sink-833 displayed a visibly higher amplitude noise floor for positive traveltimes compared to the negative traveltimes. In contrast, the correlograms from measurement pairs between the monitoring wells were dominated by a 12-hour period sinusoidal oscillation which tapered toward the end of the records symmetrically about zero traveltime.

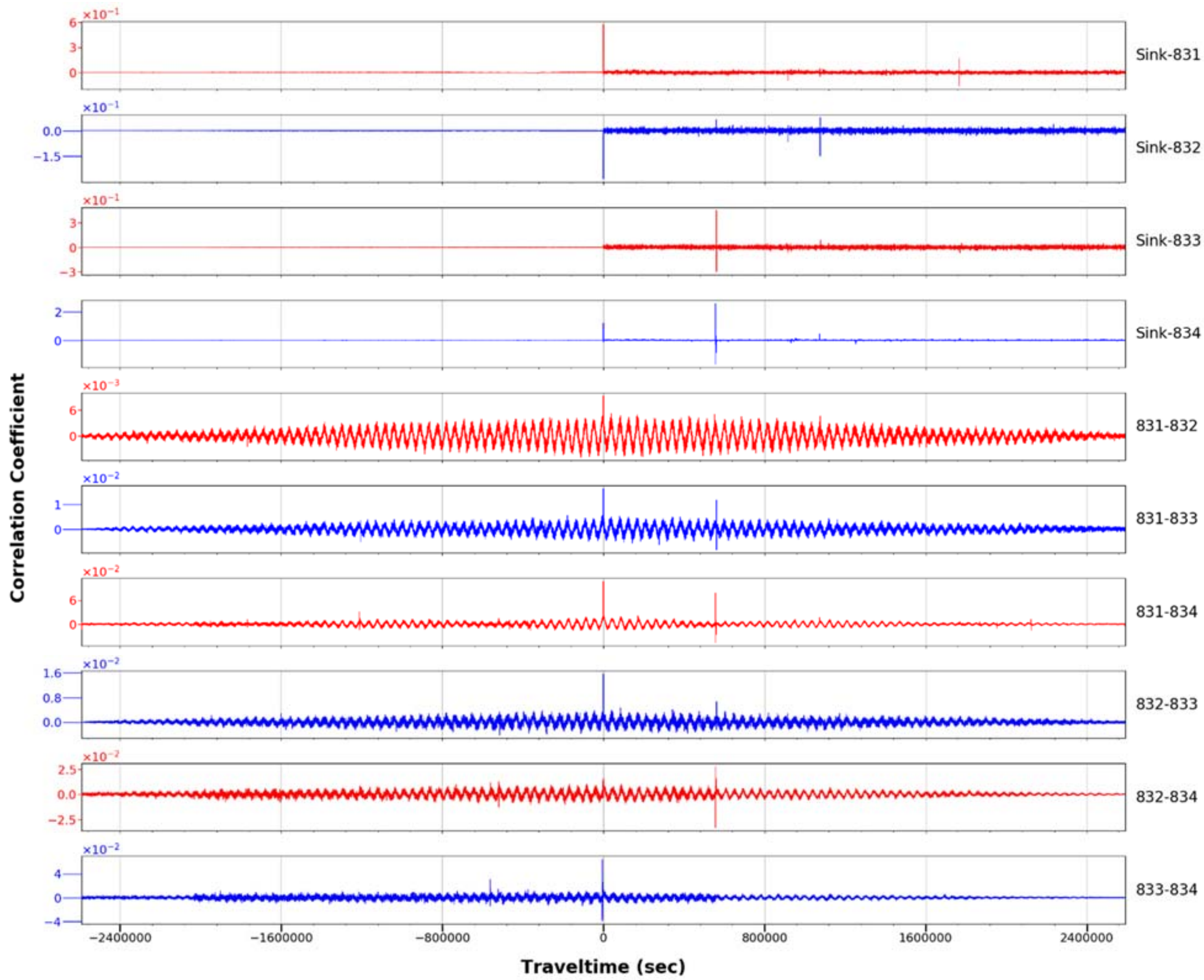

Figure 9. Stacked cross-correlograms from 30-day data segment lengths with preserved water level amplitudes (without normalizing). Each panel displays a single stacked correlogram with the measurement site pair labeled on the righthand side as "site1"-"site2". Traveltime is featured along the x-axis in units of seconds and scaled such that negative and positive time is symmetric about zero seconds. Unitless correlation coefficients are along the y-axis. For y-axis values in scientific notation, the base and exponent is displayed atop the left-side of the panel.

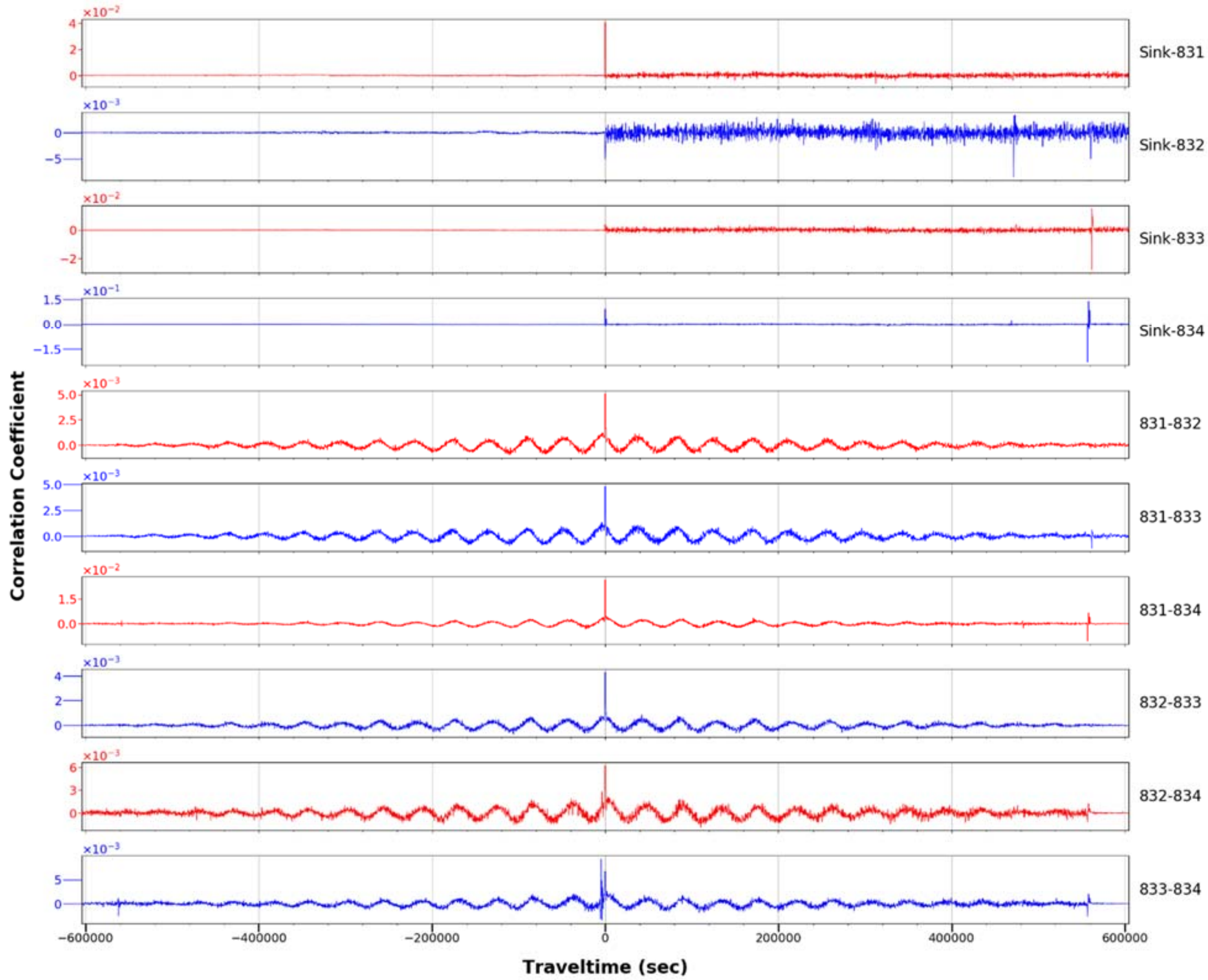

Figure 10. Stacked cross-correlograms from 7-day data segment lengths with preserved water level amplitudes (without normalizing). Each panel displays a single stacked correlogram with the measurement site pair labeled on the righthand side as "site1"-"site2". Traveltime is featured along the x-axis in units of seconds and scaled such that negative and positive time is symmetric about zero seconds. Unitless correlation coefficients are along the y-axis. For y-axis values in scientific notation, the base and exponent is displayed atop the left-side of the panel.

Figure 11 shows cross-correlograms stacked from all the daily segment length data with water level amplitudes preserved. Figure 12 shows those same correlograms low-pass filtered with a corner frequency of 0.00015 Hz. The 12-hour period oscillation previously observed persisted between the monitoring wells, though with smaller relative amplitudes compared to the daily scenario with normalized data (Figure 7), and was also visible, and out of phase with the monitoring wells, for the pairs that included the Sink (Figure 12). As was the case for the 30- and 7-day scenarios, the pairs Sink-831, Sink-832, Sink-833 displayed a higher amplitude noise floor for positive traveltimes relative to the negative traveltimes (Figure A- 119 - Figure A- 121 and Figure A- 129). For nearly all the station pairs, a peak (or trough) at or near zero traveltime was observed. In addition, the following distinct signals were observed in the stacked correlograms, and their high-pass filtered counterparts (Figure A- 129), and the spectrograms (Figure A- 122 - Figure A- 128):

- For Sink-834, peak at ~40,000 sec (just over 11 hours) traveltime
- For the pairs 832-834 and 833-834, a peak at negative 3,000-5,000 sec (between just under 1 hour to 1.5 hours) traveltime

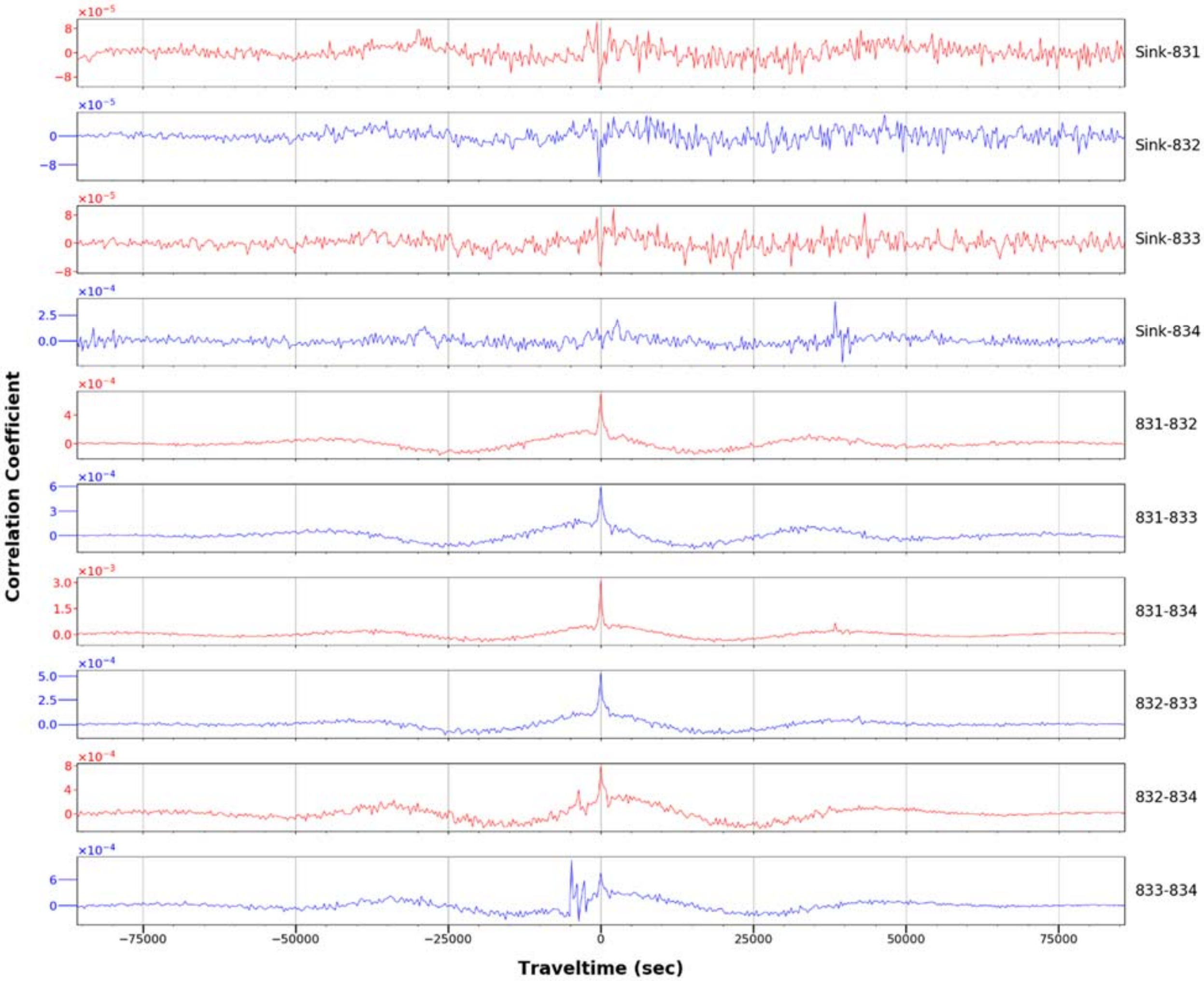

Figure 11. Stacked cross-correlograms from all daily data segment lengths with preserved water level amplitudes (without normalizing). Each panel displays a single stacked correlogram with the measurement site pair labeled on the righthand side as "site1"-"site2". Traveltime is featured along the x-axis in units of seconds and scaled such that negative and positive time is symmetric about zero seconds. Unitless correlation coefficients are along the y-axis. For y-axis values in scientific notation, the base and exponent is displayed atop the left-side of the panel.

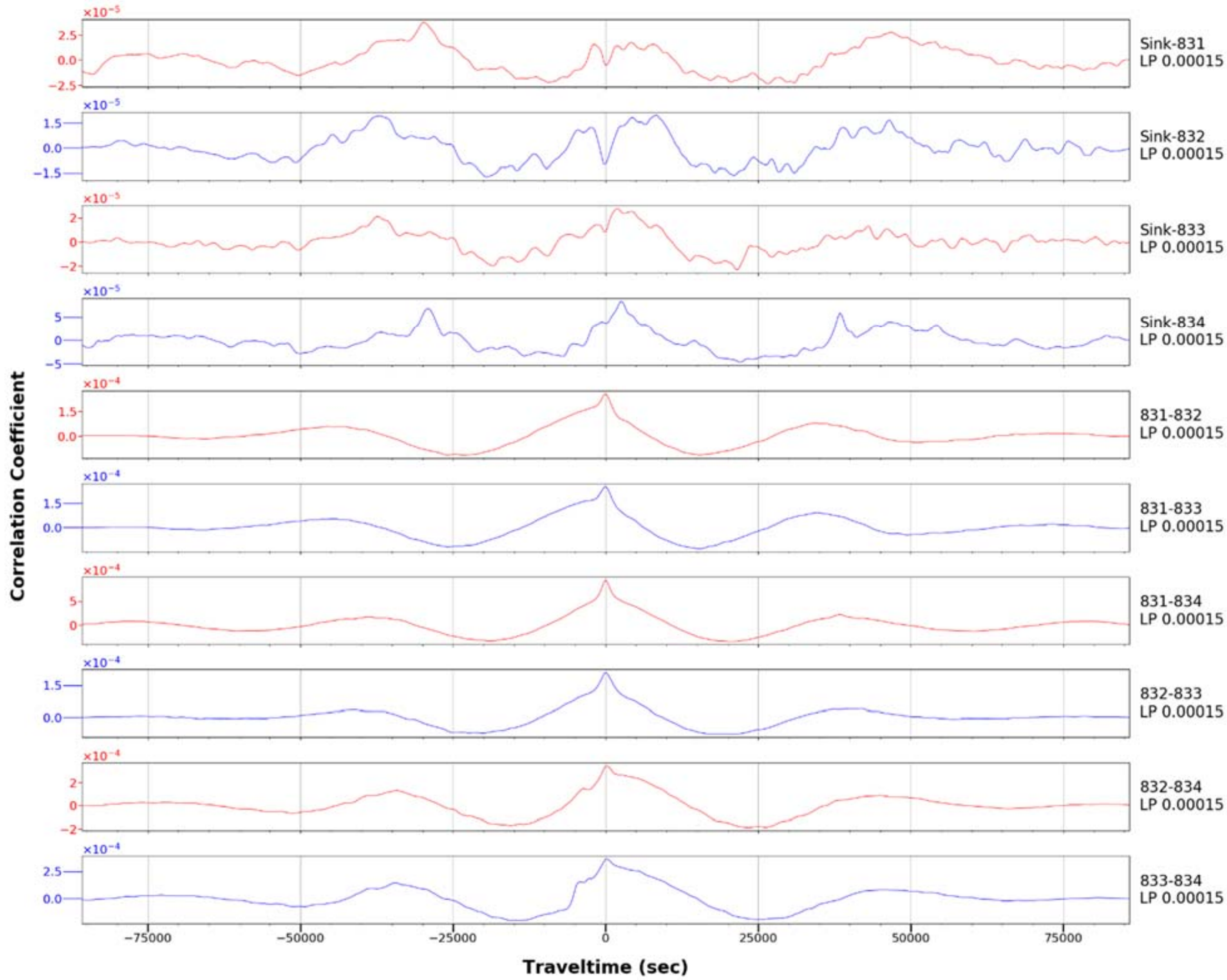

Figure 12. Stacked cross-correlograms from all daily data segment lengths with preserved water level amplitudes (not normalized). Correlograms were low-pass (LP) filtered with a corner frequency of 0.00015 Hz, or a period of just under 2 hours, which is indicated to the right of each panel.

Figure 13 shows cross-correlograms stacked from the daily segment length data which span the pumping period, and where the water level amplitudes were preserved, and Figure 14 shows those same correlograms high-pass filtered with a corner frequency of 0.00015 Hz. As was observed previously, here again the 12-hour period oscillation appeared muted or was masked by higher amplitude noise compared to the stack of all daily correlograms. Again, the station pairs Sink-831, Sink-832, Sink-833 displayed a higher amplitude noise floor for positive traveltimes relative to the negative traveltimes (Figure 14). Compared to the stack of all daily correlograms, both persisted and new signals were observed:

- For Sink-834, a peak persisted at ~40,000 sec (just over 11 hours) traveltime with improved SNR (Figure 13, Figure 14, and Figure A- 133).
- For 831-833, a new peak was observed at ~43000 sec (~12 hours) traveltime (Figure 13, Figure 14, and Figure A- 135).

- For 831-834, a new, strong, peak was observed at ~40000 sec (just over 11 hours) traveltime, and appeared similar to the peak observed in Sink-834 (Figure 13, Figure 14).
- For the pairs 832-834 and 833-834, a peak persisted at negative 3000-5000 sec (between just under 1 hour to 1.5 hours) traveltime with improved SNR (Figure 13, Figure 14, Figure A-138, and Figure A- 139) and a reduced or absent peak at zero traveltime.

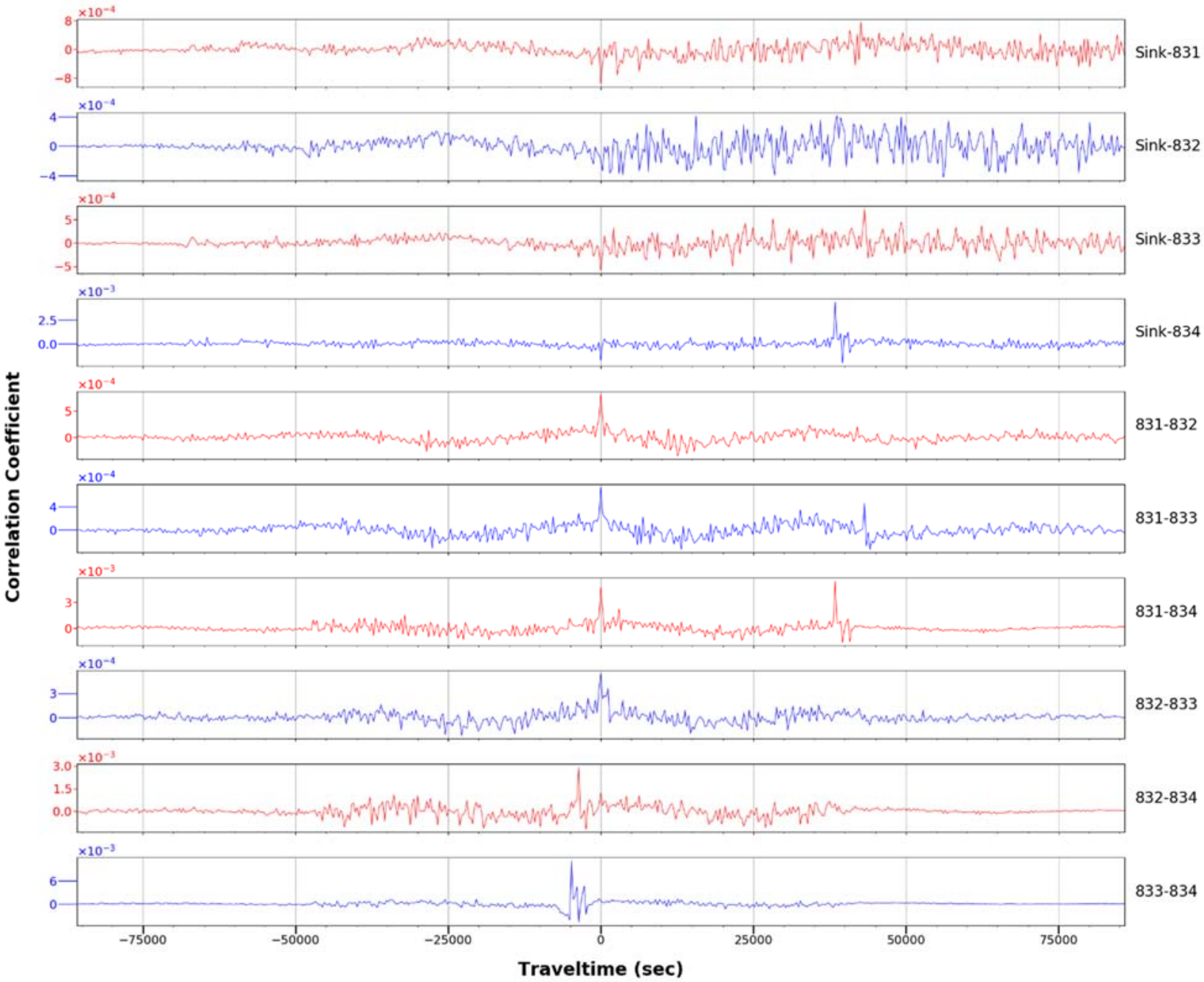

Figure 13. Stacked cross-correlograms from daily data segment with preserved water level amplitudes (without normalizing). Only the segments from the period when water was pumped into the sinkhole were included in the stack. Each panel displays a single stacked correlogram with the measurement site pair labeled on the righthand side as "site1"-"site2". Traveltime is featured along the x-axis in units of seconds and scaled such that negative and positive time is symmetric about zero seconds. Unitless correlation coefficients are along the y-axis. For y-axis values in scientific notation, the base and exponent is displayed atop the left-side of the panel.

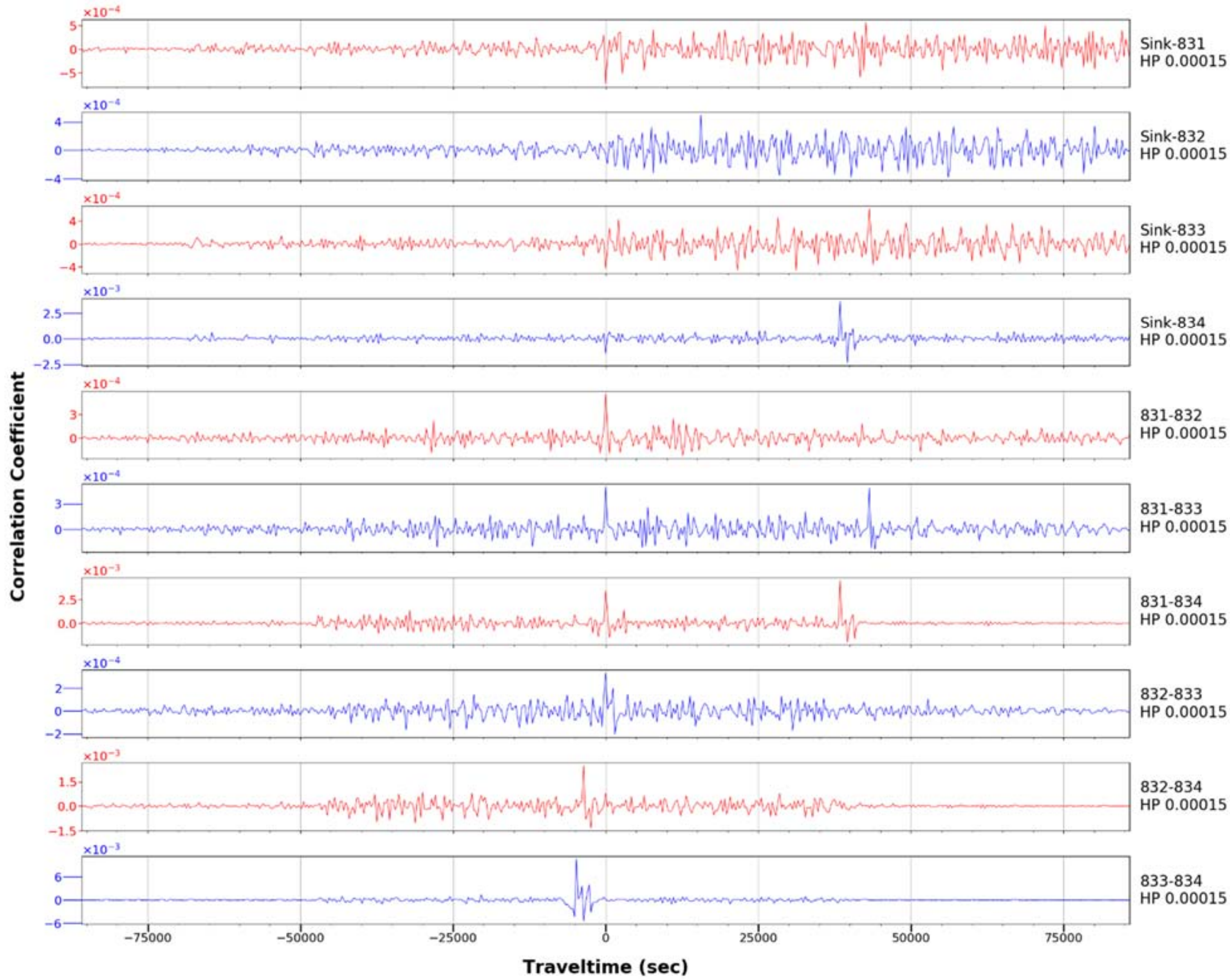

Figure 14. Stacked cross-correlograms from pumping-period-only daily data segment lengths with preserved water level amplitudes (not normalized). Correlograms were high-pass (HP) filtered with a corner frequency of 0.00015 Hz, or a period of just under 2 hours, which is indicated to the right of each panel. Each panel displays a single stacked correlogram with the measurement site pair labeled on the righthand side as "site1"-"site2". Traveltime is featured along the x-axis in units of seconds and scaled such that negative and positive time is symmetric about zero seconds. Unitless correlation coefficients are along the y-axis. For y-axis values in scientific notation, the base and exponent is displayed atop the left-side of the panel.

Chapter 4. DISCUSSION AND INTERPRETATIONS

The previous section described the results of four scenarios tested from two water level amplitude cases. In ambient seismic noise processing, high amplitude/energy events must be accounted for to prevent these events from dominating the correlograms, traditionally through normalizing the record amplitudes prior to cross-correlation (Bensen et al., 2007). In the case of the work outlined in this report, correlating water level data spanning a recharge test, the high amplitude event was the focus of the investigation. The ambient changes originate from far-field and are regional in scope. Thus, local hydraulic distinctions between the measurement sites used for this study arise from the recharge test rather than the regional changes felt by all sites. For the purposes of this study, preserving the water level amplitude (not normalizing the amplitude) appeared necessary to identify hydraulic connection between the measurement sites. Although, it is possible that removing the background, regional-scale, signal would illuminate the same discoveries from the normalized data as those obtained from the data that preserved the water level amplitudes.

Out of the four scenarios, most, but not all, local signals that emerged were most apparent by stacking the daily segmented correlograms. A single signal with high SNR appeared at 155 hr (~6.5 days) for the pairs Sink-832, Sink-833, Sink-834, 831-833, 831-834, and 832-834. At 24-hours long, clearly the daily segment correlograms were unable to capture this signal. However, this signal has not yet been attributed to a physical phenomenon and would require more work to interpret. At the scale of the Sunnyhill study site the daily segments were sufficient to capture all other signals.

Many of the stacked cross-correlograms featured a peak at zero traveltime, despite not being an auto-correlogram. The peaks observed at zero traveltime indicated that the water level at all the measurement locations were responding in similar ways nearly simultaneously. The most likely explanation is that at least one background signal was common to all the monitoring wells and the sinkhole. If true, then removing the background signal would also remove the zero traveltime peaks. More advanced correlation techniques might also account for this, such as wavelet coherence stacking. Potentially, this could also be achieved via cross-correlations with multiple far-field stations, followed by averaging together the resulting stacked correlograms to obtain a regional signal that can be subtracted from correlograms of the measurement sites.

An approximately 12-hour period oscillation was observed for all station pairs, which accounted for at least one of possibly multiple common signals. The signal appeared in both tested cases of water level amplitude (normalized or not) and in all four scenarios, though the most robust (best sampled) were from stacking the full set of daily correlograms due to the larger number of individual correlograms included in the stack (Table 2). The origin of the signal remains uncertain, but bared similarity to solid Earth tides due to the Sun and Moon's gravitational influence. However, regardless of the origin, the correlograms established that the two station records included in a pair possessed the same background signal, but offset ~12 hours from each other. Thus, it is possible to use this information to remove this background signal from each individual correlogram, or potentially even each water level data segment. Furthermore, the observed oscillation at the pairs that included the Sink were out of phase with the monitoring wells pairs, which implied a delay in diffusive water level changes between the sinkhole and the groundwater system. Potentially this delay could be used to determine the transmissivity between the sinkhole and the aquifer system, one of the goals of the Sunnyhill recharge project.

In a limited way, the signals observed in the pumping-period-only scenario overcame the background signal. More concretely, the daily correlogram stacks which isolated the pumping period yielded the most apparent (greatest SNR) signal of propagating local water level changes. Zero second traveltime peaks for some station pairs persisted in this scenario, but others were reduced or absent. This implied that the local changes in water level caused by the water draining from the sinkhole partially or fully masked the regional changes. Before and well after the pumping period the regional signal likely was more prominent than local changes. Up to a point, increasing the number of correlograms from the period of change that are stacked will increase SNR (James et al., 2017), which could be achieved by increasing the number of pumping periods. Removing the background regional signal (as described above) would also aid SNR by reducing the time-series to residual (local) water level changes, which might help illuminate smaller changes.

On their own, correlations of water level changes suggest, but do not prove that water flowed from one place to another. What they show is that water levels in two places changed in similar ways. Hydraulic connection is one explanation for the similar responses to changes. However, other forces may also cause similar responses, such as the expansion and contraction of one aquifer exerting pressure on an adjacent aquifer. However, water which was pumped into the sinkhole drained into the groundwater system and the raw measurements of water levels showed that all the monitoring wells responded in kind (though at different times) to changes in the sinkhole, and combined with the correlograms the following observations and interpretations were made:

1. The water level changes measured at the sinkhole showed poor correlation with any of the monitoring wells except for 834. For the pair Sink-834, a high SNR peak was observed at ~40,000 sec (just over 11 hours) traveltime, and implied that 834 responded to water level changes 11 hours after a similar response at the sinkhole. Apparent noise was observed for the other three pairs (Sink-831, Sink-832, and Sink-833), and the noise was distinctly higher amplitude in positive traveltime (causal branch). This indicated a greater mismatch of changes recorded at the sinkhole and later changes recorded at the three monitoring wells, as compared to the reverse. This pattern was observed in both the pumping-period-only and all daily segment scenarios, implying that increased water draining from the sinkhole was not the cause of the pattern. Well 834 was the only measurement site south of the sinkhole.
2. For 831-834, a similar peak to that observed in Sink-834 was observed at ~40,000 sec (just over 11 hours) traveltime, implying a response to a change in water level at 831 (UFA well) was recorded 11 hours before the same response was recorded to the east at 834. This signal was most apparent in the pumping-period-only scenario. The signal also appeared in the all daily segment scenario, but with low SNR, suggesting that increased water draining from the sinkhole increased the signal amplitude.
3. A negative 3,000-5,000 sec (just under 1 hour to 1.5 hours) traveltime signal appeared for both pairs 832-834 and 833-834, which implied that well 834 responded to a change in water level 1-1.5 hours before the SAS wells 832 (westward) and 833 (northward) responded to a similar change. This correlation was observed in both the pumping-period-only and all daily segment scenarios, which implied correlation was not contingent on the pumped water draining from the sinkhole.
4. A peak was observed at ~43,000 sec (~12 hours) traveltime for the pair 831-833, which indicated that 831 (UFA well) responded to changes 12 hours before 833 (SAS well, northeasterly) responded to similar changes. This correlation only occurred during the pumping-period-only scenario and was not visible when all daily correlograms were included, implying that correlation was contingent on increased water draining from the sinkhole. Interestingly, this signal was not observed for the pair of co-located stations 831-832.
5. The raw time-series of water levels showed that both 831 and 834 records were similar, and that both appeared to respond directly to changes in Sink water levels. Compared to well 831, well 834 recorded greater amplitude changes in response to changes in sinkhole water levels. Conversely, wells 832 and 833, while similar to each other, appeared to have a delayed and stretched response to sinkhole water level changes.

6. The spectrograms and filtered correlograms showed that correlated signals from local changes occupied frequencies above 0.00015 Hz, or a signal period of less than 2 hours (~1.85 hr = 1hr 51 min). Conversely, background signals were visible at frequencies below 0.00015 Hz, though this separation may not be absolute.

This suggests the following:

- Well 834 did not measure the SAS, but potentially measured the UFA or an aquifer that was partially isolated from the SAS and UFA (potentially within the ICU). That well 834 responded so similar to 831 suggested that some hydraulic connection existed between 834 and the UFA. However, well 831 did not correlate with the Sink, as was observed for Sink-834, despite the raw water level measurements showing a clear response to the sinkhole. This could have been the result of signal stretching, similar but less exaggerated than the SAS well responses, which the applied correlation technique would not have been able to correct. Nevertheless, the raw water level data at 831 showed a response from the sinkhole and a correlation was observed for pair 831-834 during the pumping period, which strongly suggests a connection of some sort between 831 and 834 exists.
- The sinkhole did not appear directly connected to the SAS but did appear connected to the aquifer measured by well 834 (potentially UFA or aquifer within ICU) and some connection exists with the portion of the UFA that well 831 measured.
- The SAS appeared buffered from the UFA (via the ICU). However, that buffer was not absolute, perhaps due to thick sandy infill into the sinkhole, as evidenced by the delayed and stretched response of 832 and 833 to sinkhole water level changes, as well as the correlation observed for the pair 831-833.
- Local correlated signals appeared to occupy a different, higher, frequency band than lower frequency background signals.

Chapter 5. RECOMMENDATIONS

The work detailed above was conducted on a dataset that was not collected with cross-correlation in mind. Therefore, to assist with the design of future projects, a series of recommendations were compiled that are intended to improve data collection and expand the capabilities and quality of this method. The recommendations are listed below:

- Increase the sampling rate of water level measurements high enough to record propagating pressure waves. The exact sampling rate is site specific and needs to be determined, but, as an example, a ≥2 Hz sampling rate would be required to measure a pressure wave propagating at 1.5 km/sec (the bulk sound speed in open water at 20 °C, 68 °F) between two sites 1.5 km apart.
- Match the increased sampling rate at more distant wells in order to determine the "reach" of a measurable change in water level or a pressure wave, and to construct a background signal that can be removed (subtraction or deconvolution) from data to reveal local changes. This would be especially beneficial if it also increased azimuthal coverage of a study area.
- Consider adding hydrophones to measure changes in acoustic pressure waves.

- The recharging period was an event that introduced local changes to the system. However, the single pumping event did not yield many correlograms which to include in the stack (Table 2). Future studies should cycle the pumping to invoke multiple, non-uniform, signal periods to correlate and stack. A second consideration would be to use multiple and scheduled bursts from air guns to invoke pressure waves into the aquifer system rather than pumping water into the system. Potentially this technique could be used directly at monitoring wells, also. Although consideration would be needed to determine whether those bursts could damage the well.
- Explore more advanced methods of cross-correlating two time-series. This work used what is known as the "traditional" cross-correlation method in seismology, chosen because the method is well established and accessible. Utilizing more advanced techniques would improve the resolution, quality, and capabilities of the results.

Chapter 6. CONCLUSION

This project demonstrated that cross-correlation techniques regularly applied in seismology also successfully determined a correlation of water level changes between the sinkhole and adjacent wells, and between the adjacent wells. Combined with analysis of the raw water level data, the correlation results verified that the Sunnyhill sinkhole is hydraulically connected to the Floridan Aquifer system (FAS). The results also demonstrated that, with further development of the methodology and utilizing more advanced techniques, other hydraulic properties might be accessible, as well, such as: estimating the leakance and transmissivity between measurement sites, and constructing a background signal that is common to a group of measurement sites which could be removed to reveal local changes in water levels. Thus, the goals of this portion of the Sunnyhill recharge project were met.

Three different data segment lengths were evaluated to determine the length required to capture correlated changes: 24-hour segments (daily), 7-day segments (weekly), and 30-day segments (monthly). Most, but not all, local signals that emerged were most apparent in the stacked daily segmented correlograms, and therefore a 24-hour segment length was sufficient at the scale of the Sunnyhill study site. Likewise, it was unclear whether water level amplitudes should be normalized prior to correlation, as commonly done in seismology. For the purposes of this study, preserving the water level amplitude (not normalizing the amplitude) appeared necessary to identify hydraulic connection between the measurement sites. Furthermore, the period of active pumping (the recharge period) yielded signals with the greatest SNR relative to periods before or well after the sinkhole drained and equalized with the groundwater system.

An approximately 12-hour period oscillation was observed for all station pairs, potentially caused by solid Earth tides from the Sun and Moon's gravitational influence. It is possible to use this information to remove this background signal from each individual correlogram, or potentially even each water level data segment. Furthermore, the observed oscillation at the pairs that included the Sink were out of phase with the monitoring wells pairs, implying a delay in diffusive water level changes between the sinkhole and the groundwater system. Potentially this delay could be used to determine the transmissivity between the sinkhole and the aquifer system, one of the goals of the Sunnyhill recharge project.

From the analysis of the water level time-series data and the results of cross-correlation, the following site characteristics were determined:

Well M-0834 did not measure the SAS, but potentially measured the UFA or an aquifer that was partially isolated from the SAS and UFA (potentially within the ICU). Furthermore, the UFA at well M-0831 appeared to possess some sort of connection, though limited, to the aquifer that M-0834 measures. The sinkhole did not appear directly connected to the SAS but did appear connected to the aquifer measured by well M-0834, as well as some connection to the portion of the UFA that well M-0831 measured. The SAS appeared buffered from the UFA (via the ICU). However, that buffer was not absolute, perhaps due to thick sandy infill into the sinkhole. Finally, local correlated signals appeared to occupy a different, higher, frequency band than lower frequency background signals.

REFERENCES

Bensen, G., Ritzwoller, M., Barmin, M., Levshin, A., Lin, F., Moschetti, M., et al. (2007). Processing seismic ambient noise data to obtain reliable broad-band surface wave dispersion measurements. Geophysical Journal International, 169(3), 1239–1260. https://doi.org/10.1111/j.1365-246x.2007.03374.x

Bremner, P. M., Panning, M. P., Russo, R. M., Mocanu, V., Stanciu, A. C., Torpey, M., Hongsresawat, S., VanDecar, J. C., LaMaskin, T. A., and Foster, D. A. (2019). Crustal shear wave velocity structure of central Idaho and eastern Oregon from ambient seismic noise: Results from the IDOR Project. Journal of Geophysical Research: Solid Earth. https://doi.org/10.1029/2018JB016350

Davis, J. B., Lee, D. J., Jin, W., and Bremner, P. M. (2020). Aquifer recharge potential of a collapse type sinkhole: Sunnyhill Restoration Area, Marion County, Florida. St. Johns River Water Management District Report.

Gallego, A., Russo, R., Comte, D., Mocanu, V., Murdie, R., & Vandecar, J. (2010). Seismic noise tomography in the Chile ridge subductionregion.Geophysical Journal International,182(3), 1478–1492. https://doi.org/10.1111/j.1365-246x.2010.04691.x

Goldstein, P. (2003). Sac2000: Signal processing and analysis tools for seismologists and engineers,The IASPEI International Handbook of Earthquake and Engineering Seismology, chapter 85(pp. 1613–1614). London: Academic Press.

Goldstein, P., & Snoke, A. (2005). SAC availability for the IRIS community.Incorporated Institutions for Seismology Data ManagementCenter Electronic Newsletter. Retrieved from http://www.iris.edu/dms/newsletter/vol7/no1/sac-availability-for-the-iris-community/

James, S. R., Screaton, E. J., Russo, R. M., Panning, M. P., Bremner, P. M., Stanciu, A. C., Torpey, M. E., Hongsresawat, S., and Farrell, M. E. (2017). Hydrostratigraphy characterization of the Floridan aquifer system using ambient seismic noise. Geophysical Journal International, 209(2), 876-889. https://doi.org/10.1093/gji/ggx064

Wiggins, Ralph A. (1976). Interpolation of digitized curves. Bulletin of the Seismological Society of America, 66 (6): 2077–2081. https://pubs.geoscienceworld.org/bssa/article-pdf/66/6/2077/2700429/BSSA0660062077.pdf

APPENDIX A. SUPPORTING FIGURES

All the supporting correlogram and spectrogram figures are presented herein. The figures are organized in two major sections, separating the auto- and cross- correlograms or spectrograms, and each of those contain eight minor sections separating the four data segment length scenarios and both water level amplitude cases. The correlograms and spectrograms follow the same format described in Figure 3 and Figure 4, respectively, in the main text, and is repeated below for convenience.

The stacked correlogram figures consist of as many panels as there are station pairs, one panel per pair. Each panel displays a single stacked correlogram with the measurement site pair labeled on the righthand side as "site1"-"site2". Traveltime is featured along the x-axis in units of seconds and scaled such that negative and positive time is symmetric about zero seconds. Unitless correlation coefficients are along the y-axis. For y-axis values in scientific notation, the base and exponent is displayed atop the left-side of the panel.

The spectrogram figures consist of two panels:

1. The top panel displays the stacked correlogram with traveltime featured along the top-*x*-axis and unitless correlation coefficients marked on the *y*-axis. Horizontal lines reference the estimated signal to noise ratio values 1, 3, or 6 (shown in the legend to the right of the panel). The measurement station pair appears on the top and to the right of the panel.
2. The bottom panel displays the spectrogram of the correlogram featured in the top panel. The spectrogram is aligned along the *x*-axis to the correlogram. Frequency in units of Hertz is marked along the *y*-axis, and the color scales with relative power (scalebar to the right of the panel) where increasing color intensity corresponds to increasing power.

AUTO-CORRELOGRAMS AND ASSOCIATED SPECTROGRAMS

30-Day Length Data Segments – Normalized Amplitudes

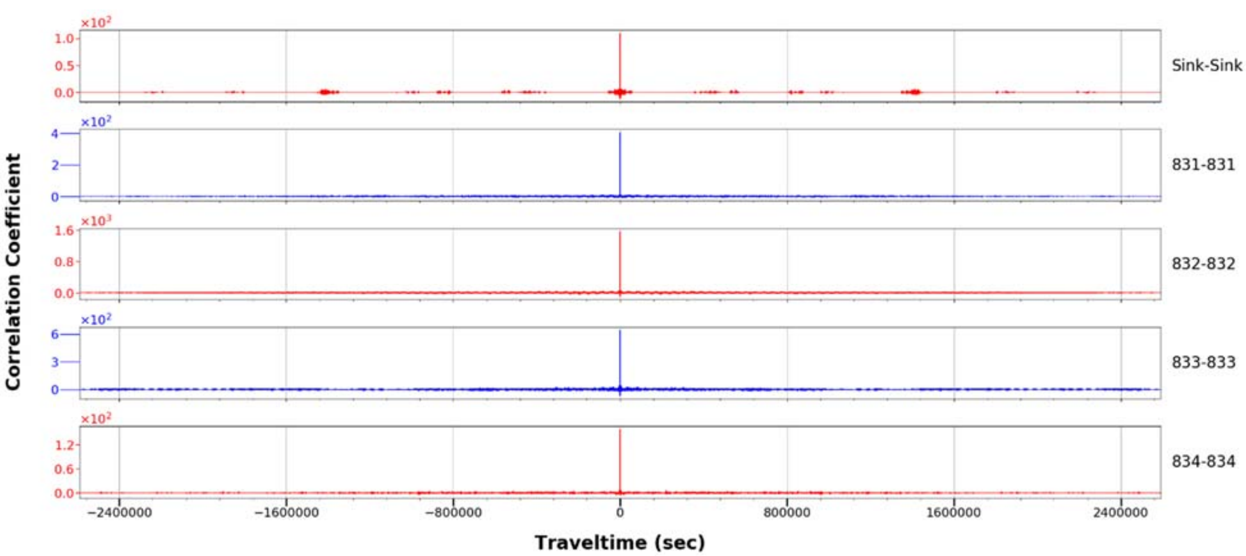

Figure A- 1. Stacked auto-correlograms from normalized 30-day data segments.

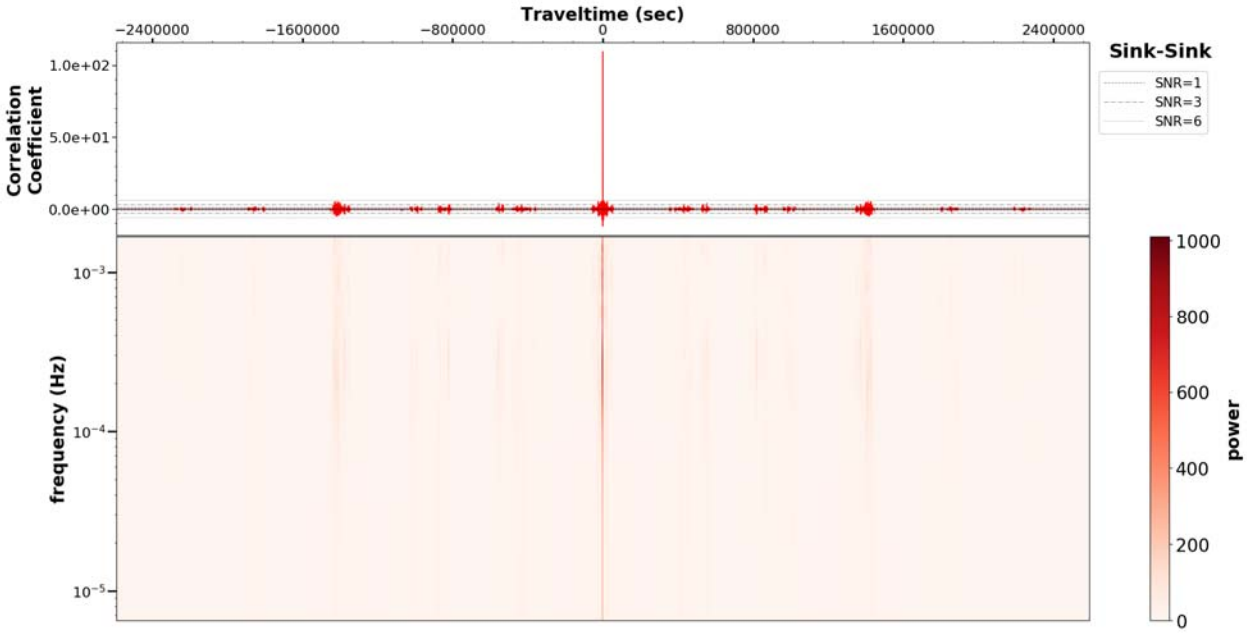

Figure A- 2. Spectrogram from stacked auto-correlated normalized 30-day length data segments. Station pair: Sink-Sink

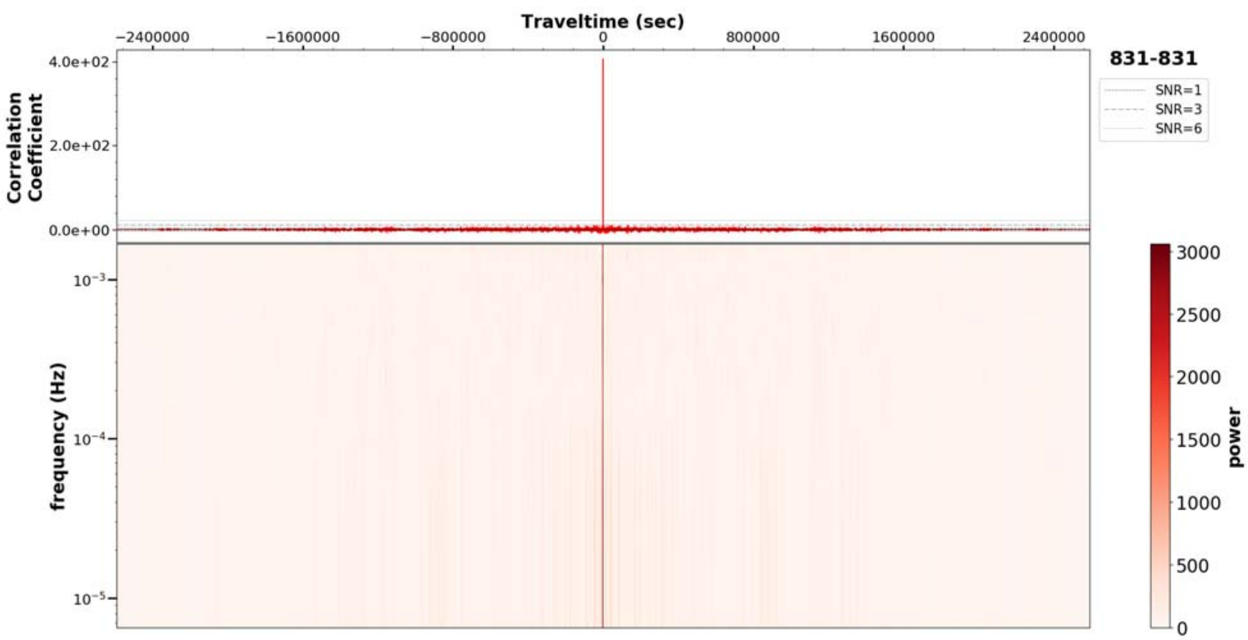

Figure A- 3. Spectrogram from stacked auto-correlated normalized 30-day length data segments. Station pair: 831-831

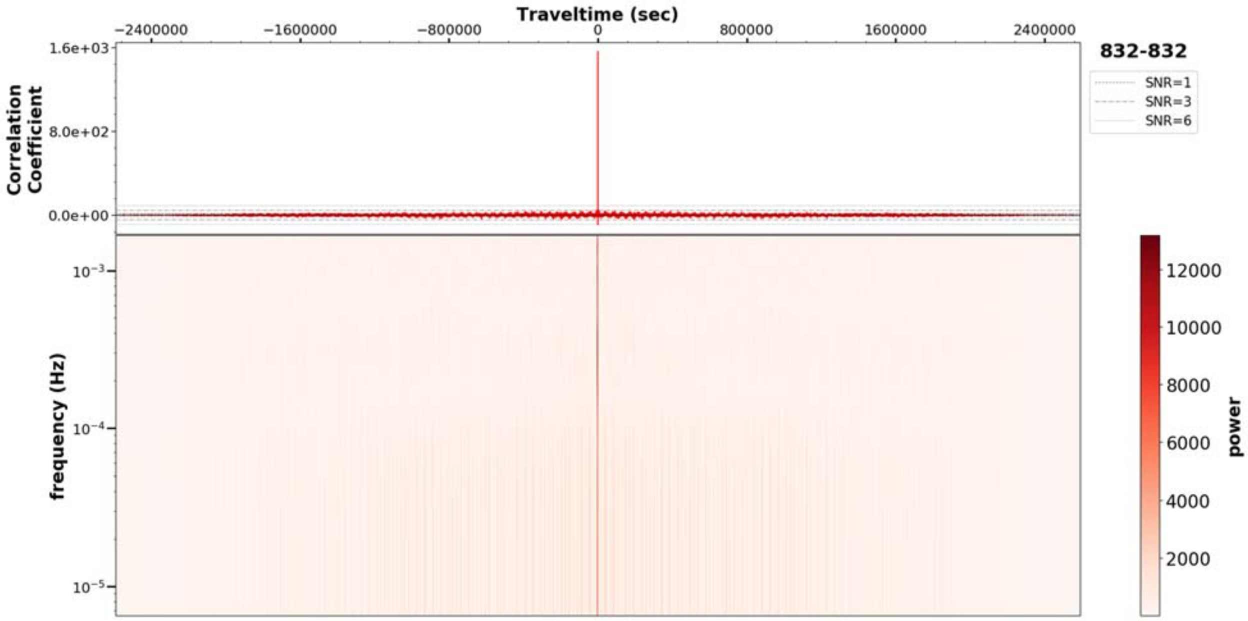

Figure A- 4. Spectrogram from stacked auto-correlated normalized 30-day length data segments. Station pair: 832-832

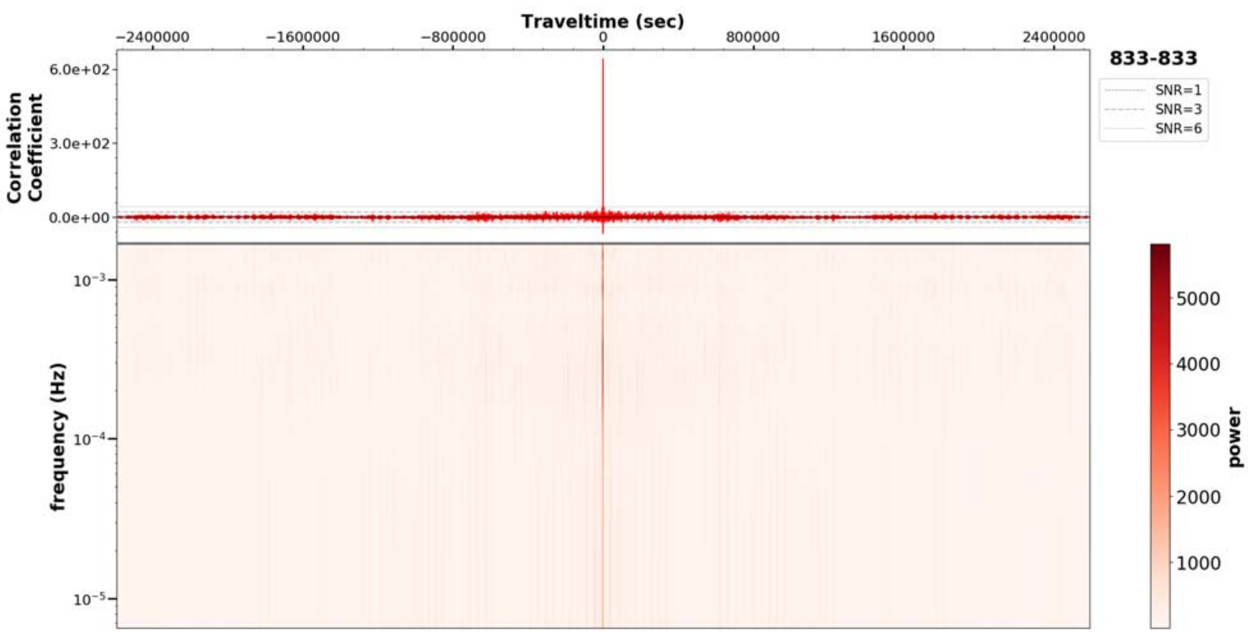

Figure A- 5. Spectrogram from stacked auto-correlated normalized 30-day length data segments. Station pair: 833-833

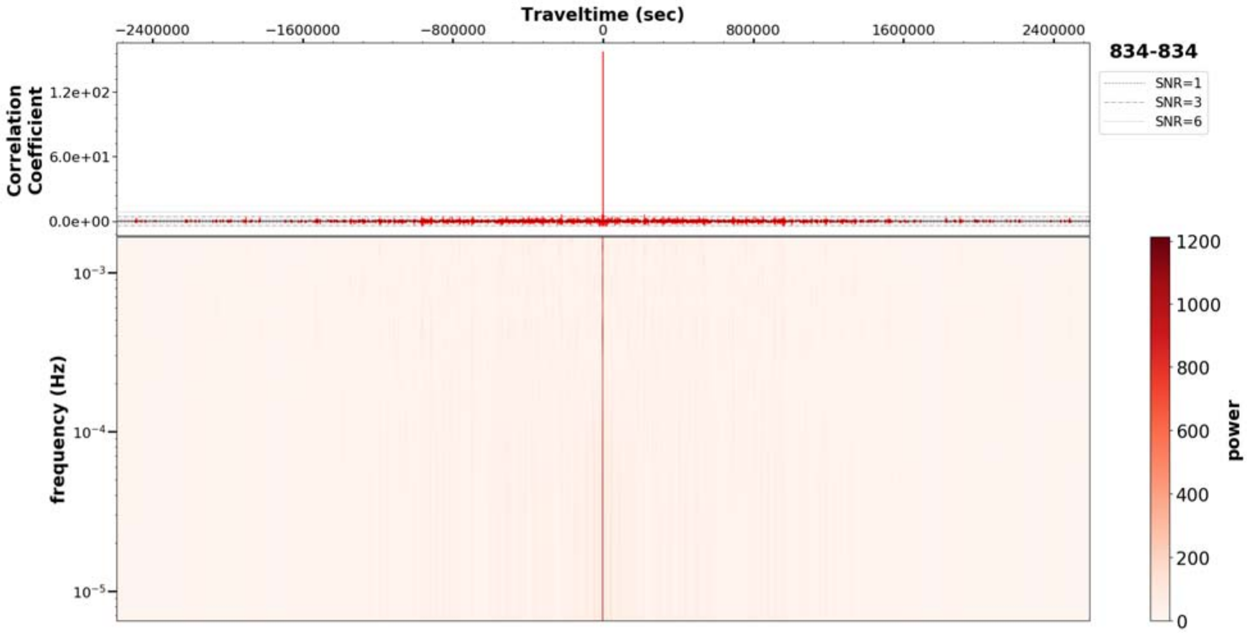

Figure A- 6. Spectrogram from stacked auto-correlated normalized 30-day length data segments. Station pair: 834-834

7-Day Length Data Segments – Normalized Amplitudes

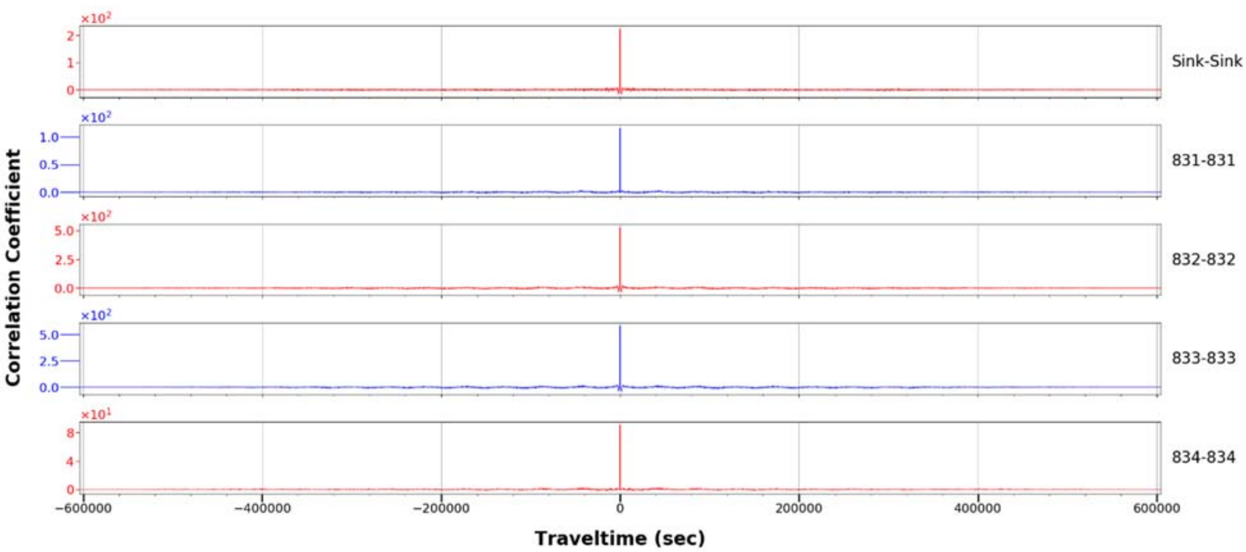

Figure A- 7. Stacked auto-correlograms from normalized 7-day data segments.

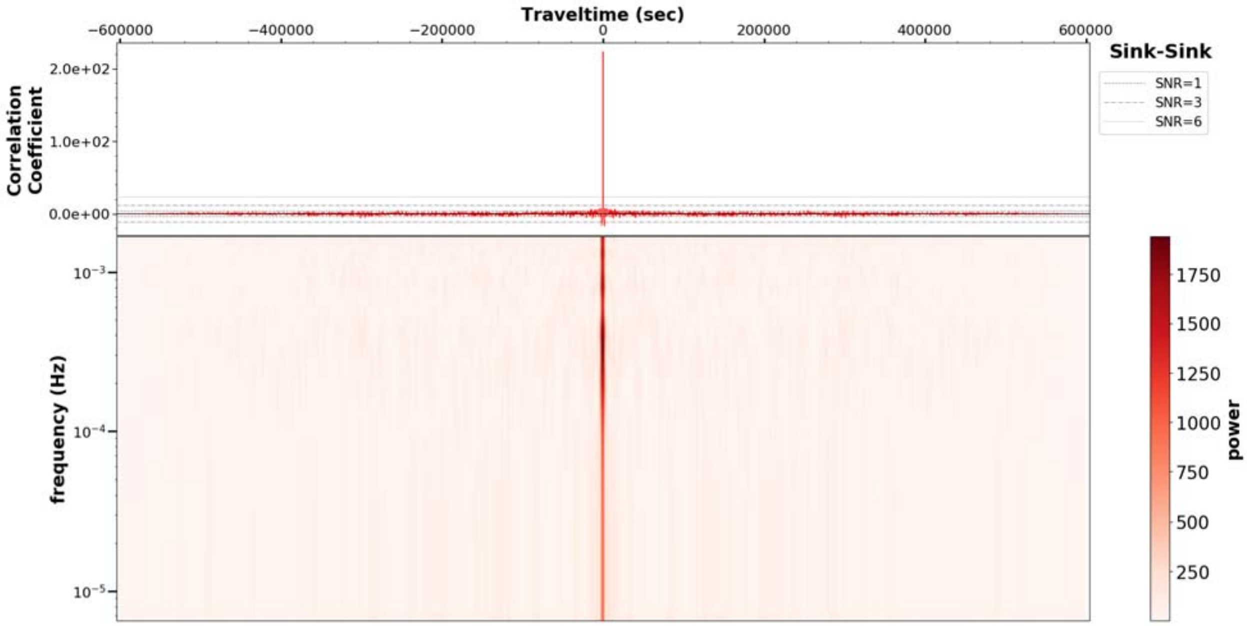

Figure A- 8. Spectrogram from stacked auto-correlated normalized 7-day length data segments. Station pair: Sink-Sink

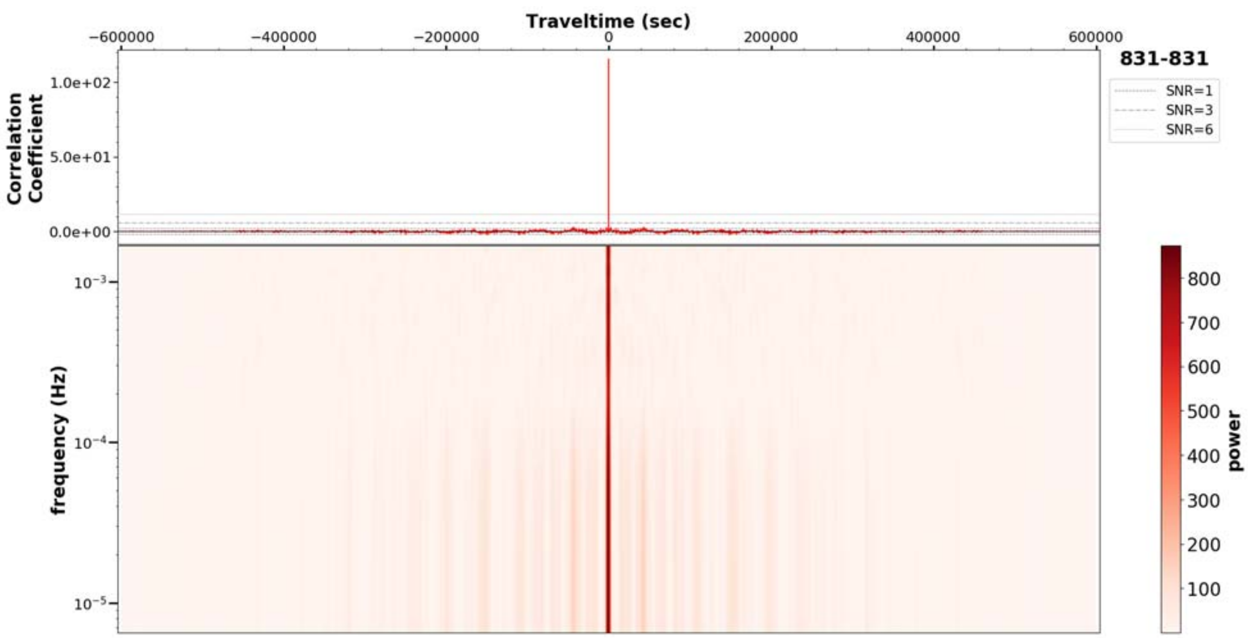

Figure A- 9. Spectrogram from stacked auto-correlated normalized 7-day length data segments. Station pair: 831-831

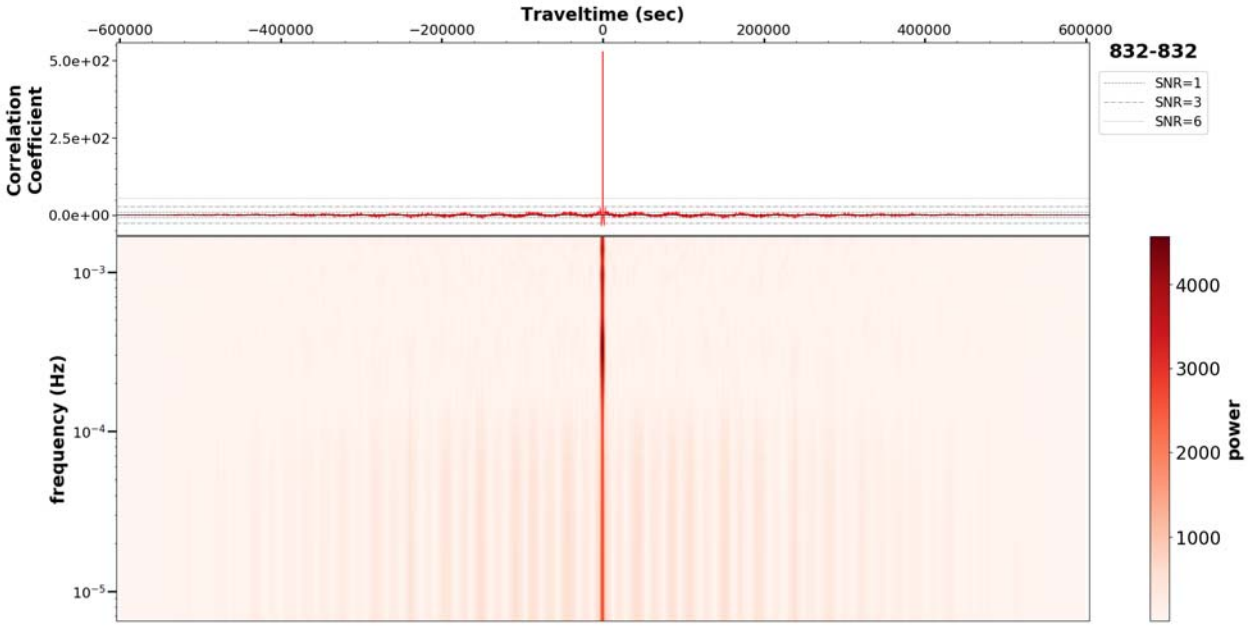

Figure A- 10. Spectrogram from stacked auto-correlated normalized 7-day length data segments. Station pair: 832-832

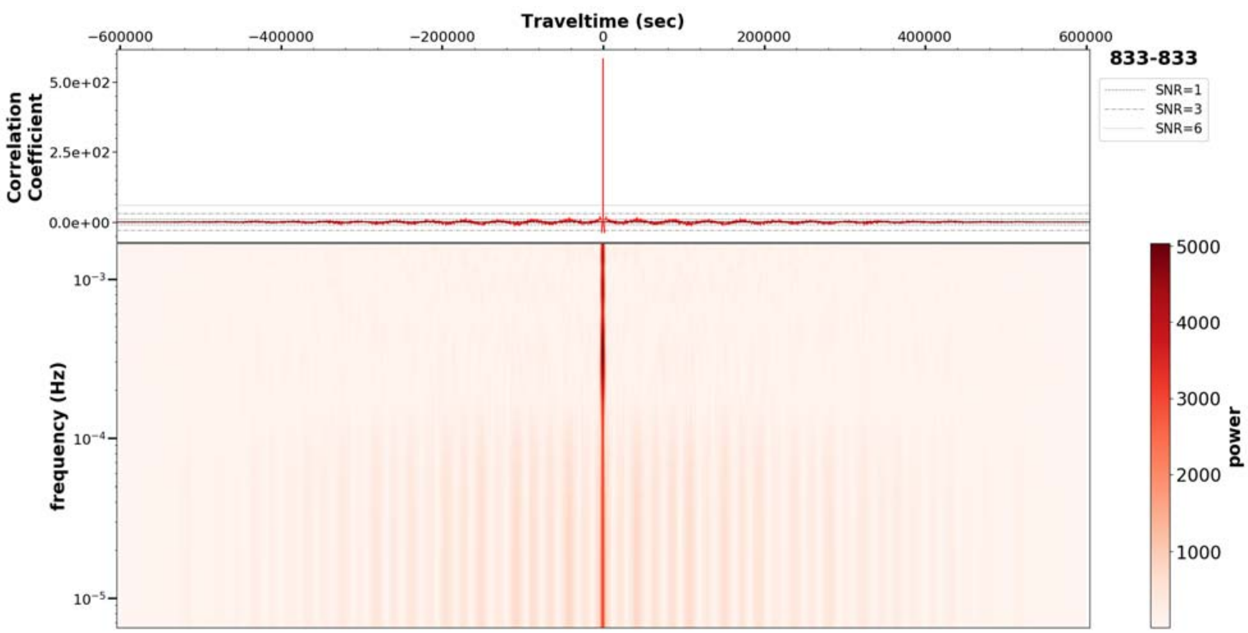

Figure A- 11.Spectrogram from stacked auto-correlated normalized 7-day length data segments. Station pair: 833-833

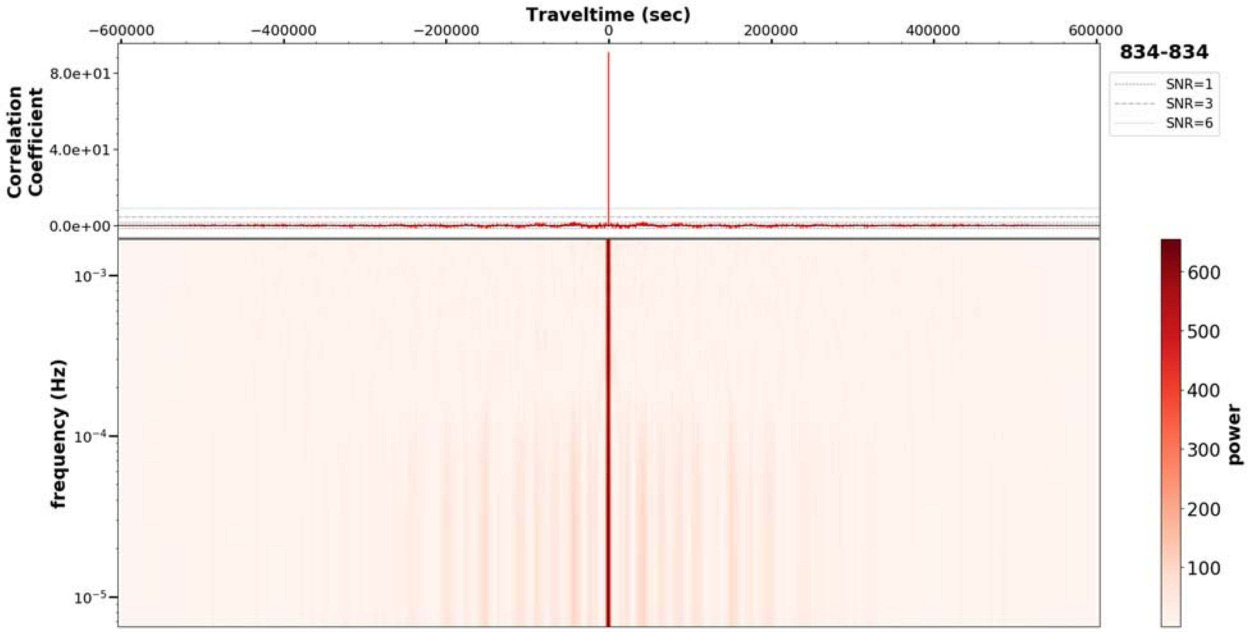

Figure A- 12. Spectrogram from stacked auto-correlated normalized 7-day length data segments. Station pair: 834-834

All Daily Length Data Segments – Normalized Amplitudes

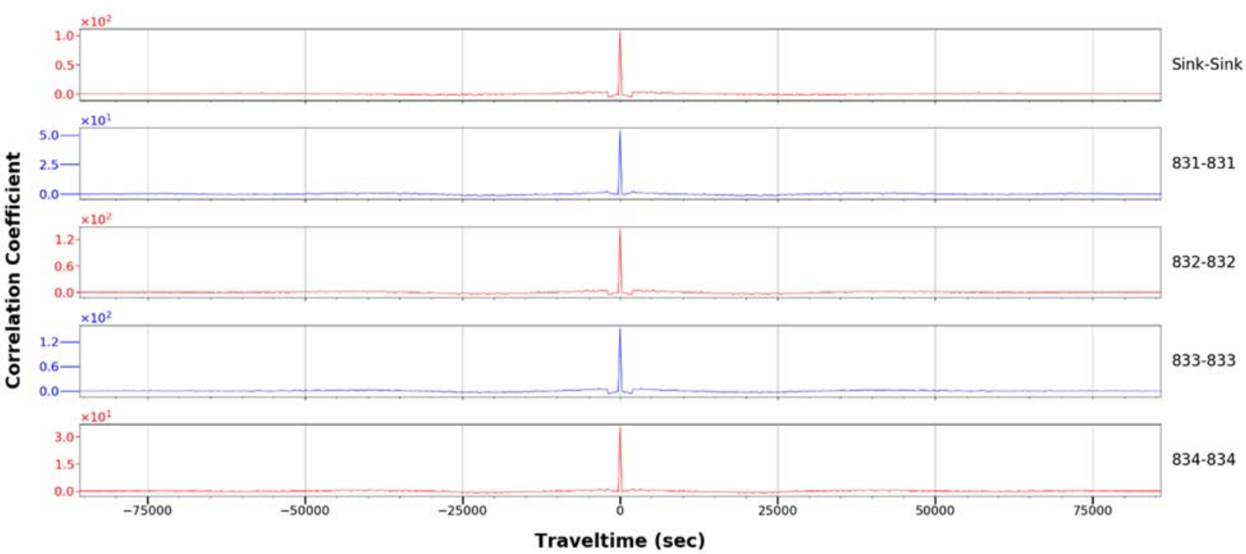

Figure A- 13. Stacked auto-correlograms from all normalized daily data segments.

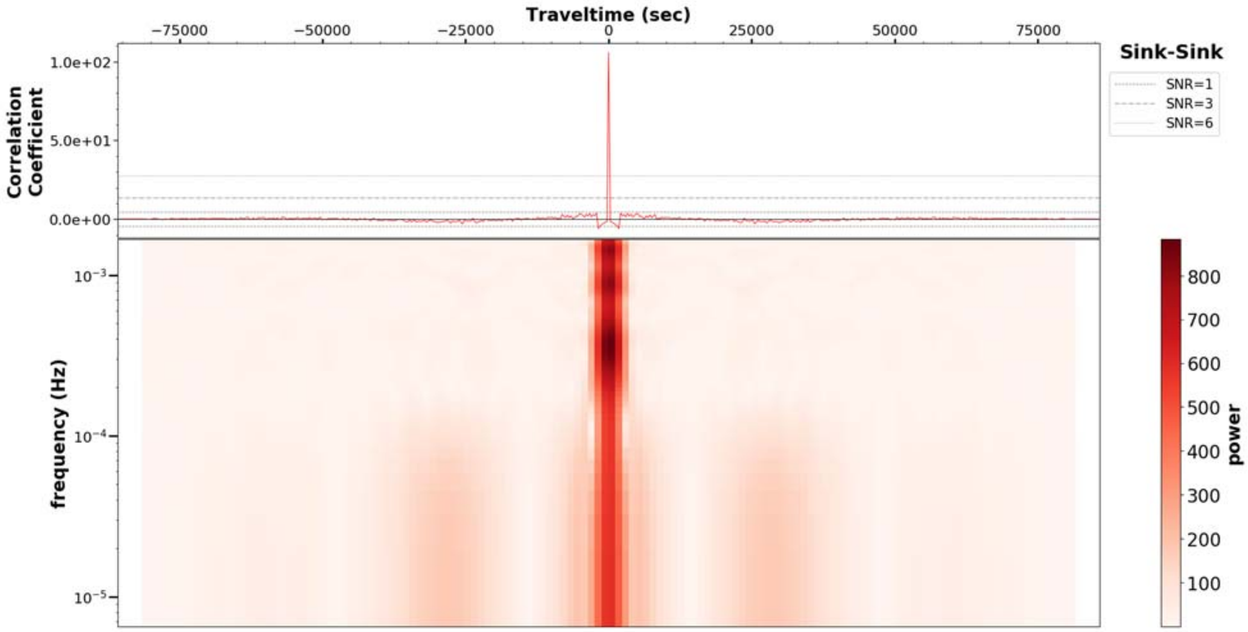

Figure A- 14. Spectrogram from stacked auto-correlated normalized daily length data segments, all segments. Station pair: Sink-Sink

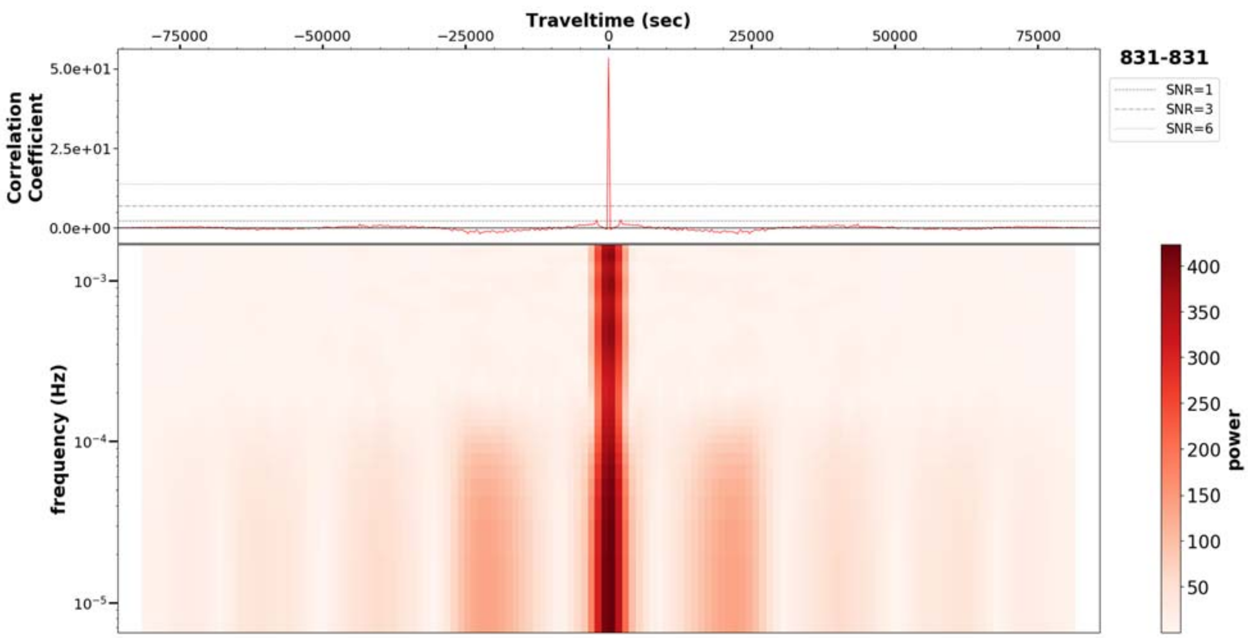

Figure A- 15. Spectrogram from stacked auto-correlated normalized daily length data segments, all segments. Station pair: 831-831

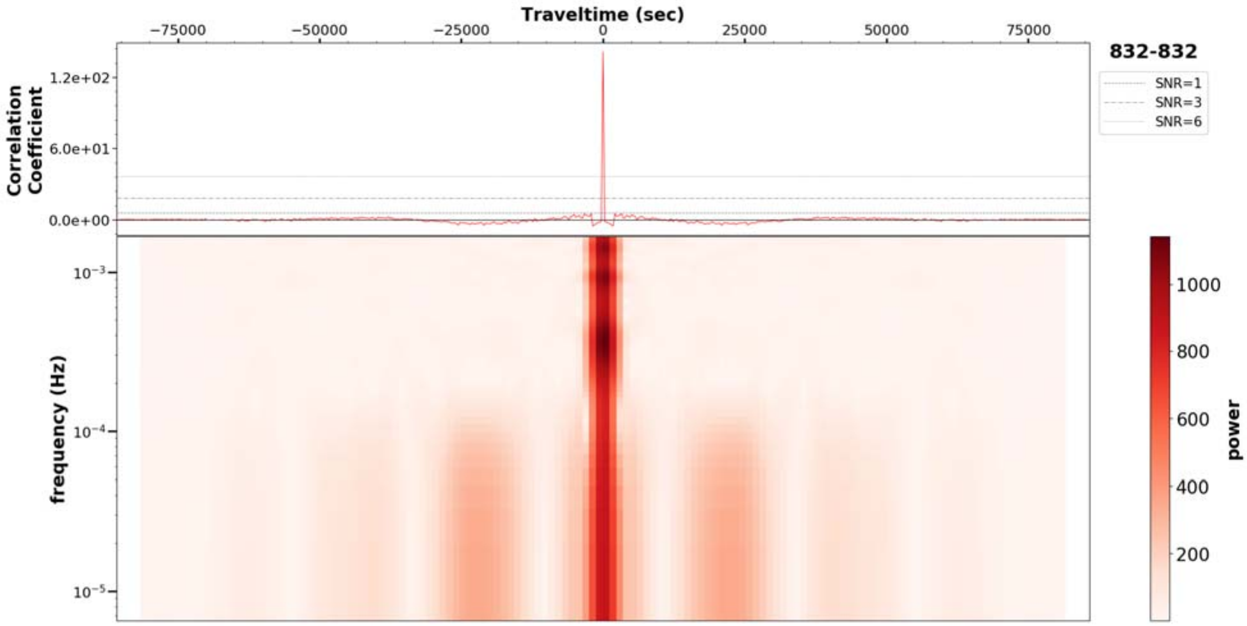

Figure A- 16. Spectrogram from stacked auto-correlated normalized daily length data segments, all segments. Station pair: 832-832

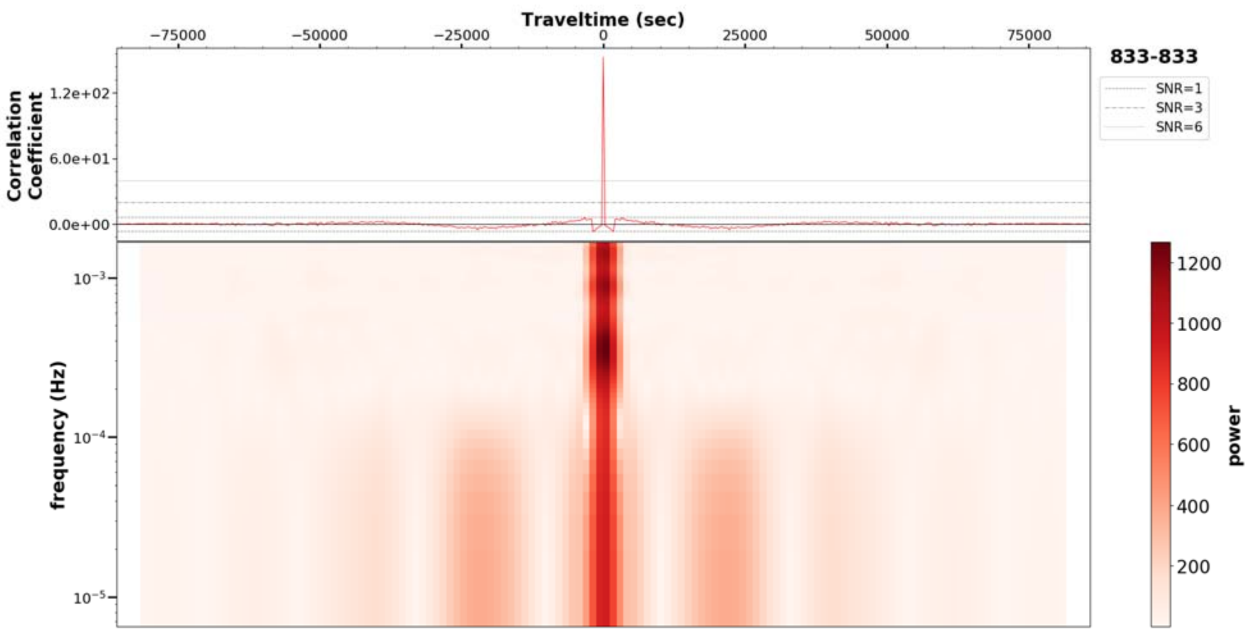

Figure A- 17. Spectrogram from stacked auto-correlated normalized daily length data segments, all segments. Station pair: 833-833

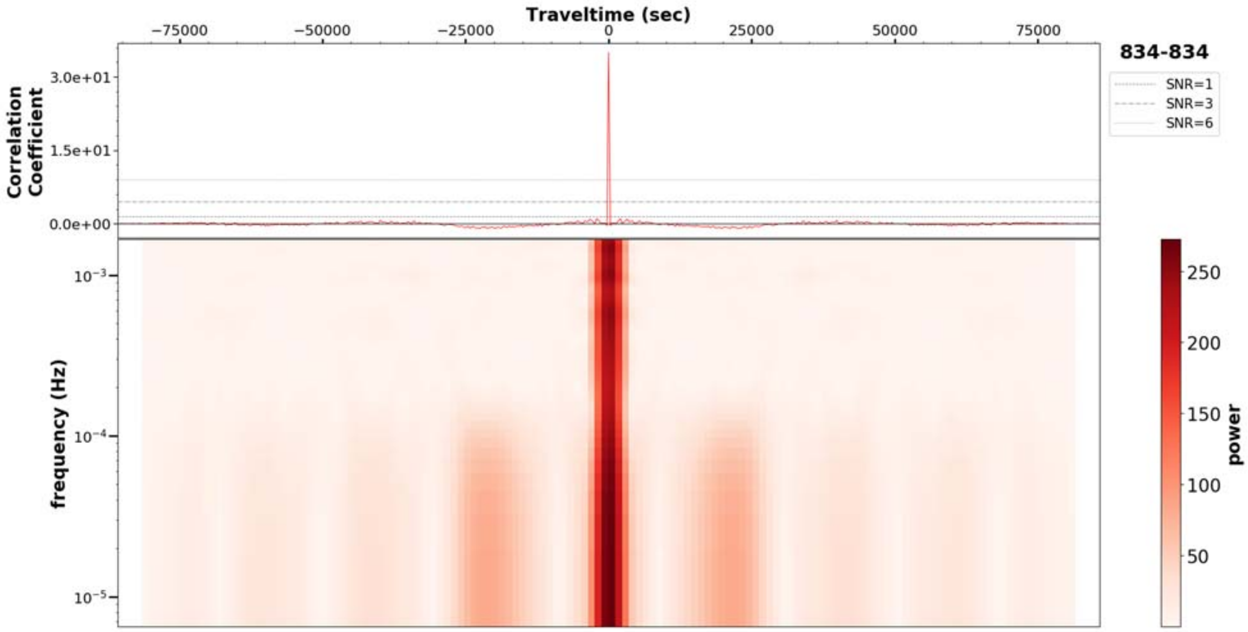

Figure A- 18. Spectrogram from stacked auto-correlated normalized daily length data segments, all segments. Station pair: 834-834

Pumping-Period-Only Daily Length Data Segments – Normalized Amplitudes

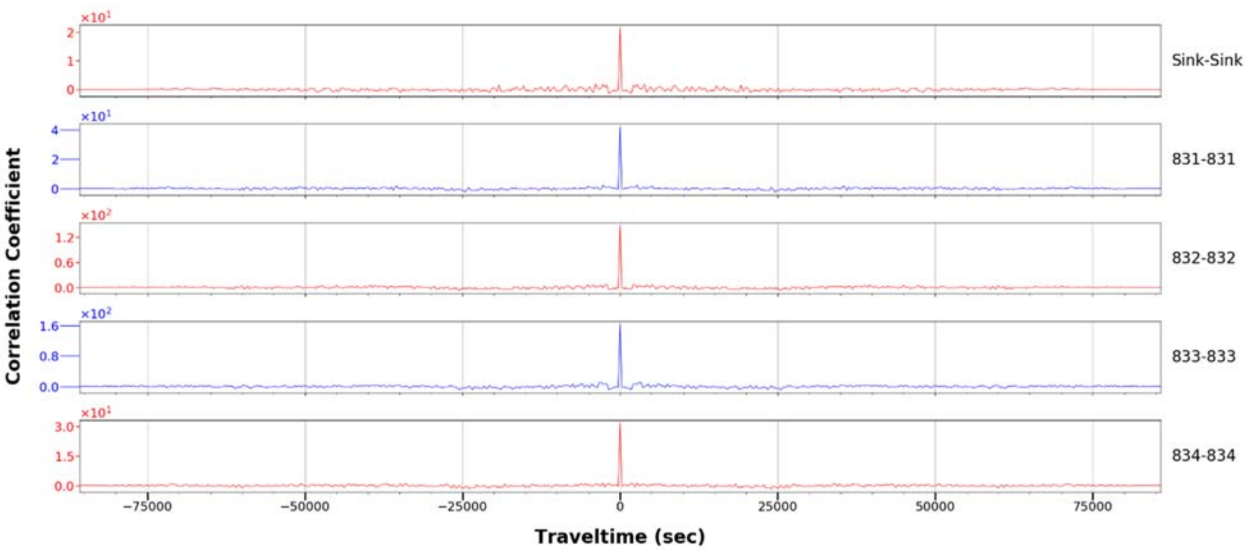

Figure A- 19. Stacked auto-correlograms from pumping-period-only normalized daily data segments.

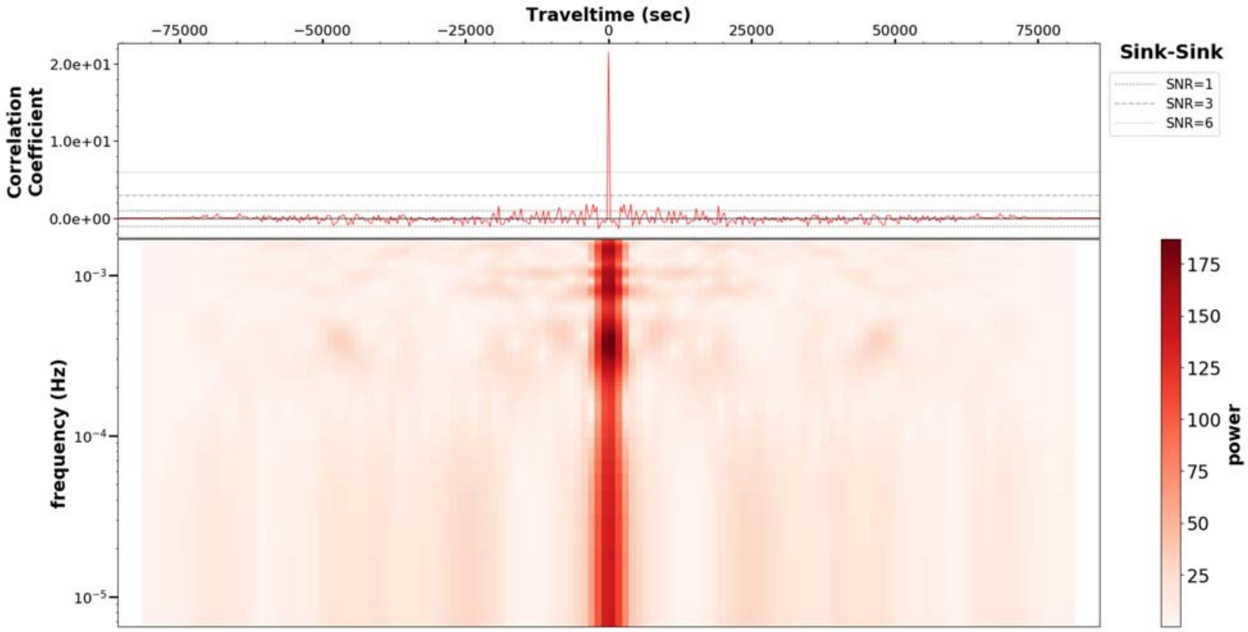

Figure A- 20. Spectrogram from stacked auto-correlated normalized daily length data segments, pumping-period-only segments. Station pair: Sink-Sink

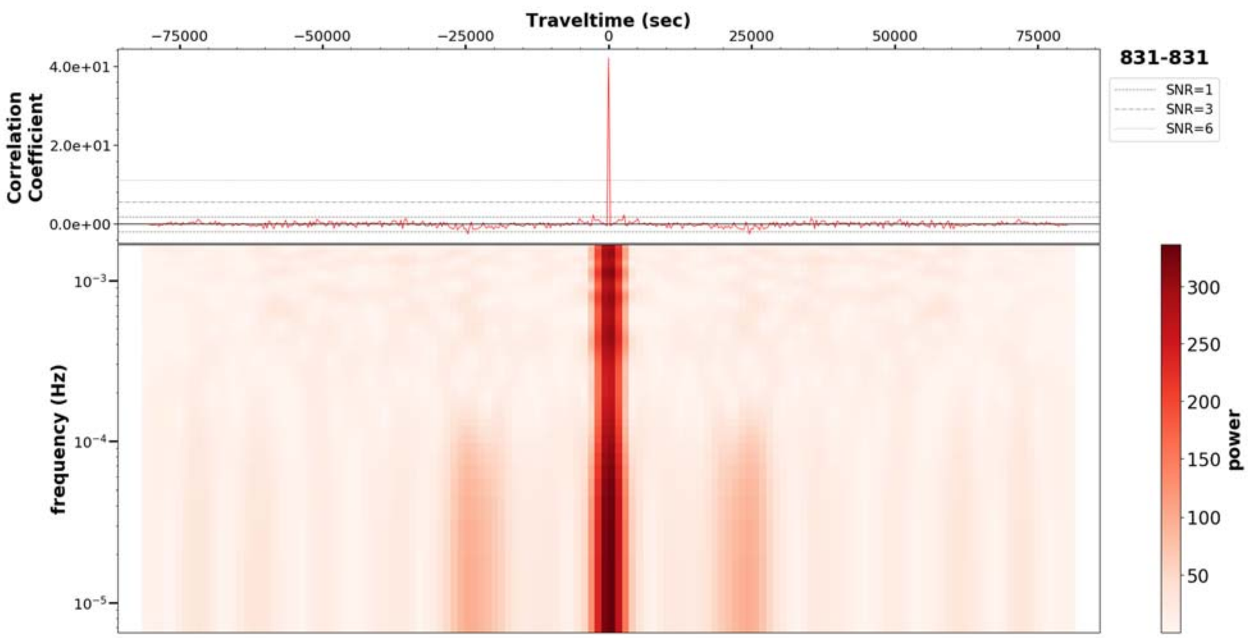

Figure A- 21. Spectrogram from stacked auto-correlated normalized daily length data segments, pumping-period-only segments. Station pair: 831-831

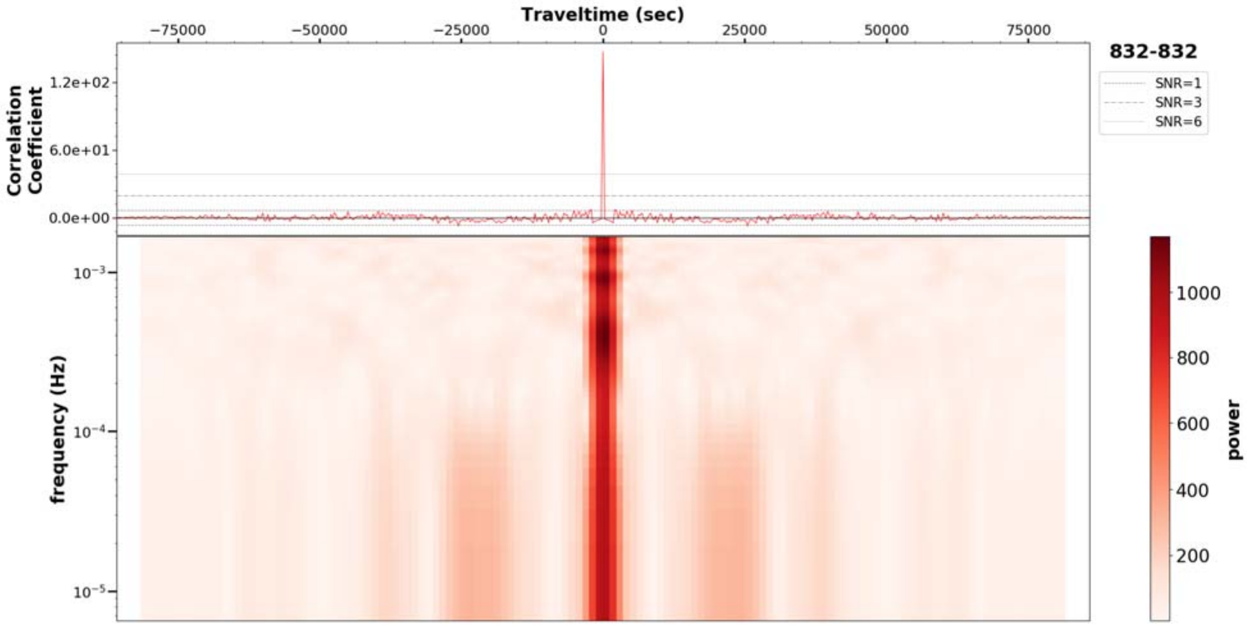

Figure A- 22. Spectrogram from stacked auto-correlated normalized daily length data segments, pumping-period-only segments. Station pair: 832-832

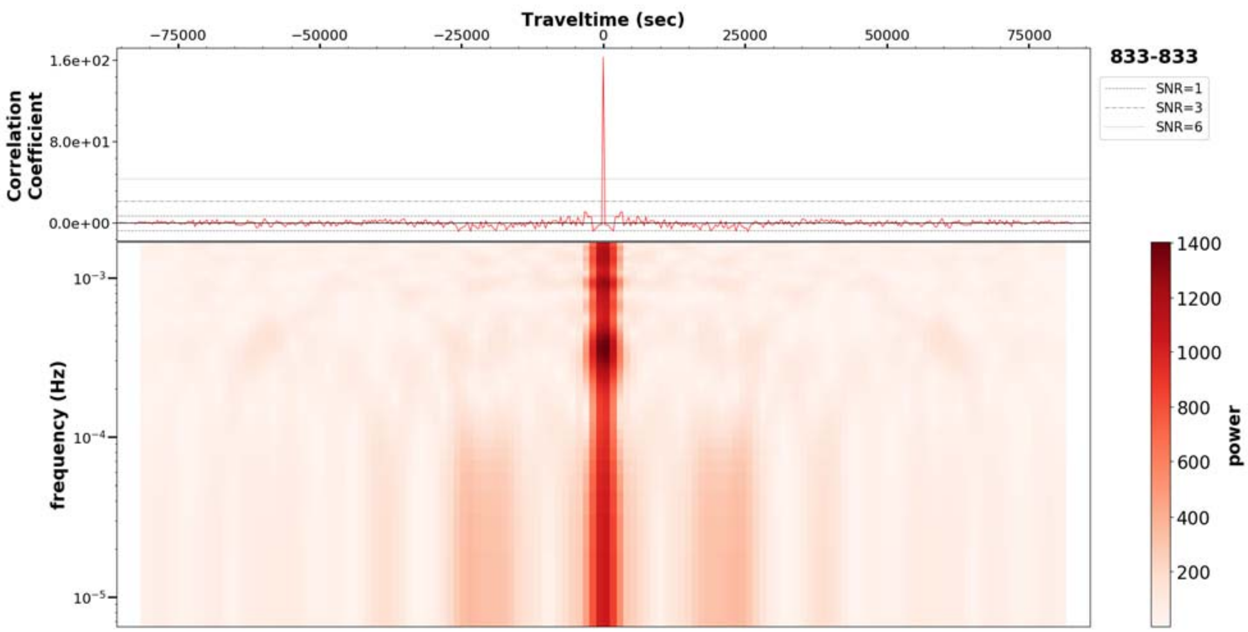

Figure A- 23. Spectrogram from stacked auto-correlated normalized daily length data segments, pumping-period-only segments. Station pair: 833-833

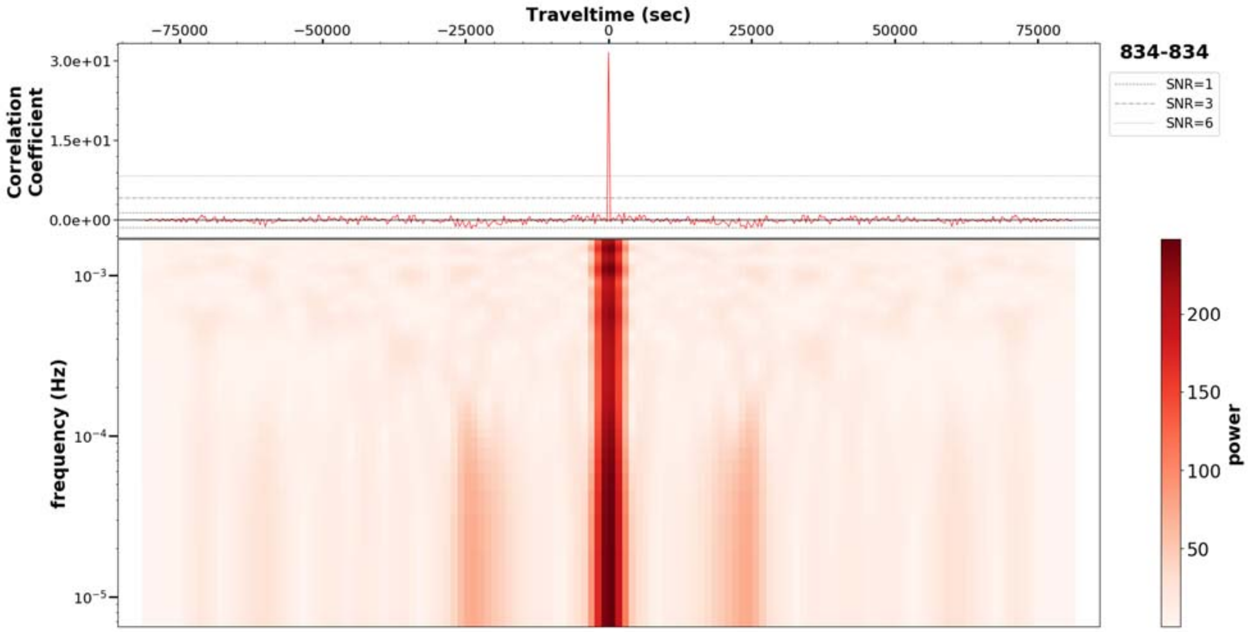

Figure A- 24. Spectrogram from stacked auto-correlated normalized daily length data segments, pumping-period-only segments. Station pair: 834-834

30-Day Length Data Segments – Preserved Amplitudes

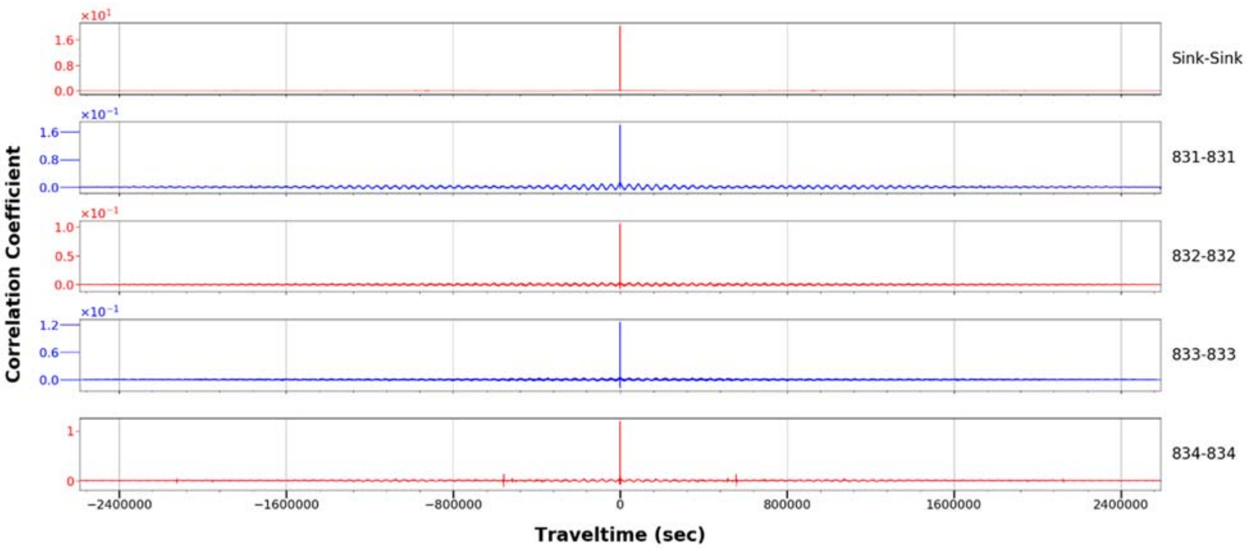

Figure A- 25. Stacked auto-correlograms from 30-day data segments with preserved amplitudes (not normalized).

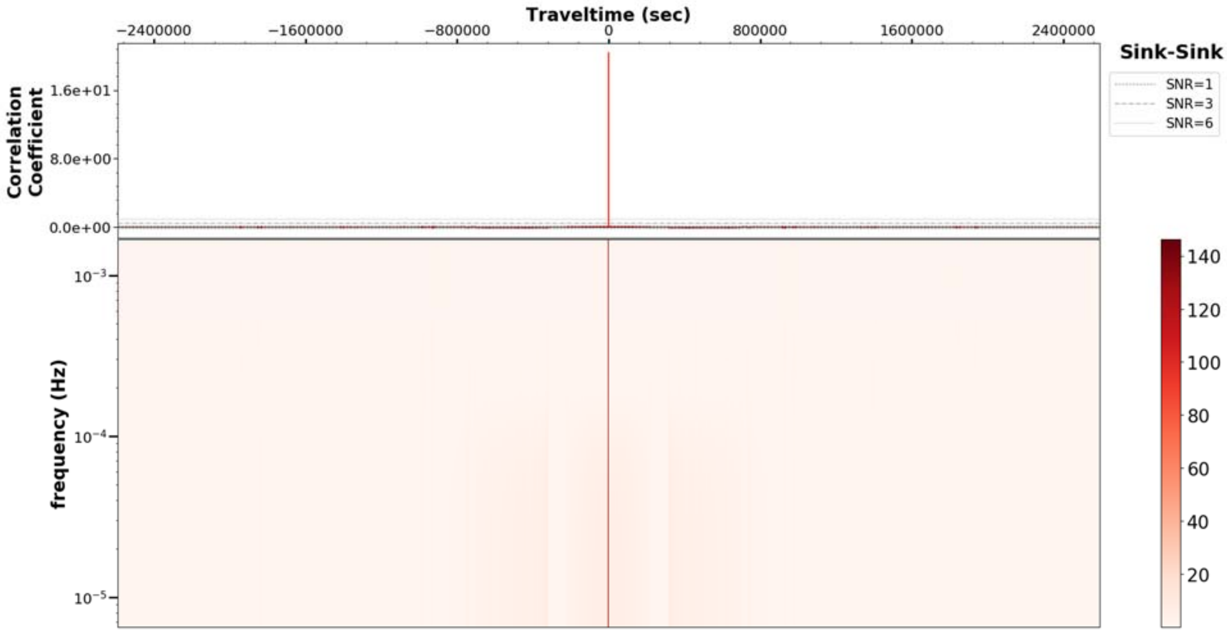

Figure A- 26. Spectrogram from stacked auto-correlated 30-day length data segments with preserved amplitudes (not normalized). Station pair: Sink-Sink

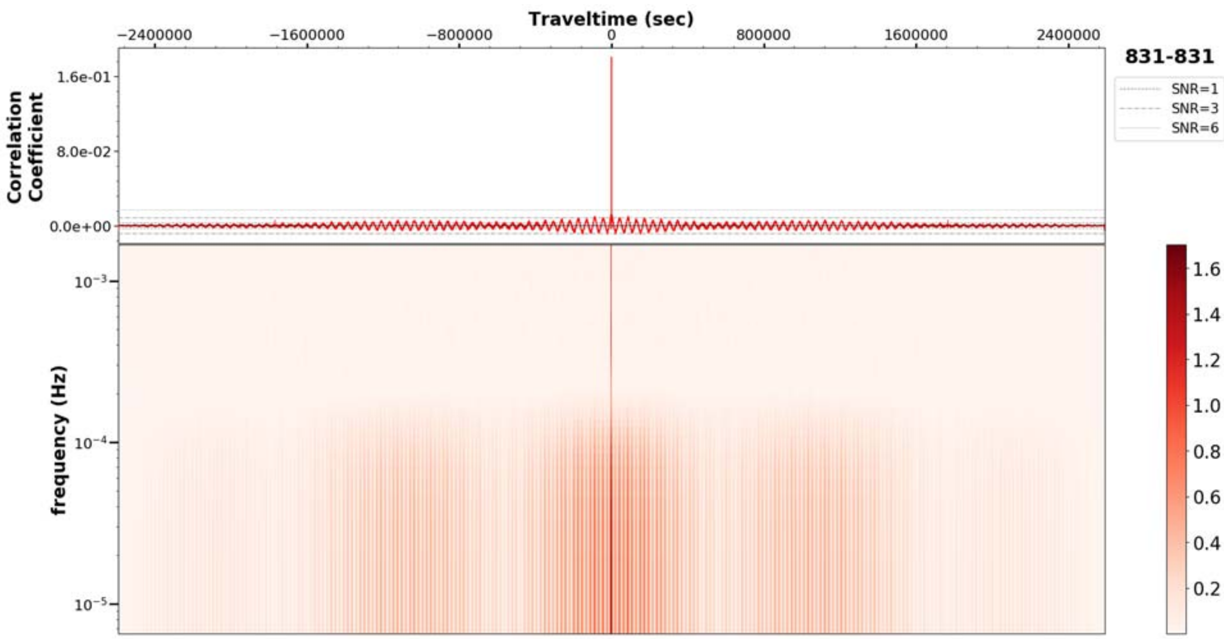

Figure A- 27. Spectrogram from stacked auto-correlated 30-day length data segments with preserved amplitudes (not normalized). Station pair: 831-831

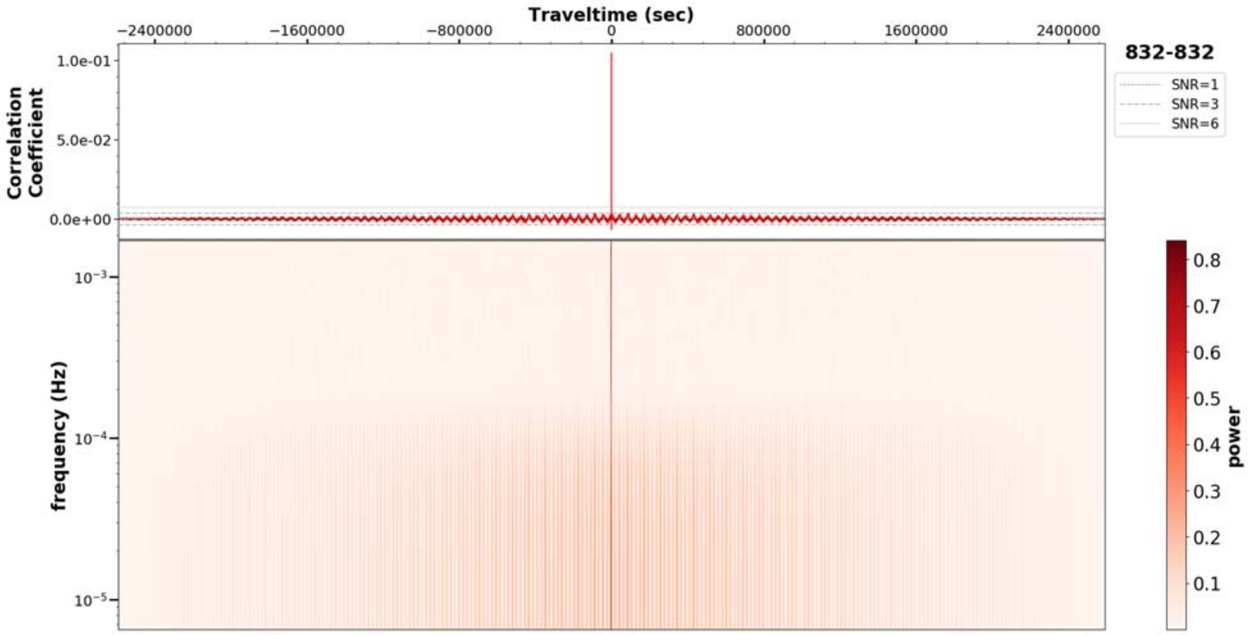

Figure A- 28. Spectrogram from stacked auto-correlated 30-day length data segments with preserved amplitudes (not normalized). Station pair: 832-832

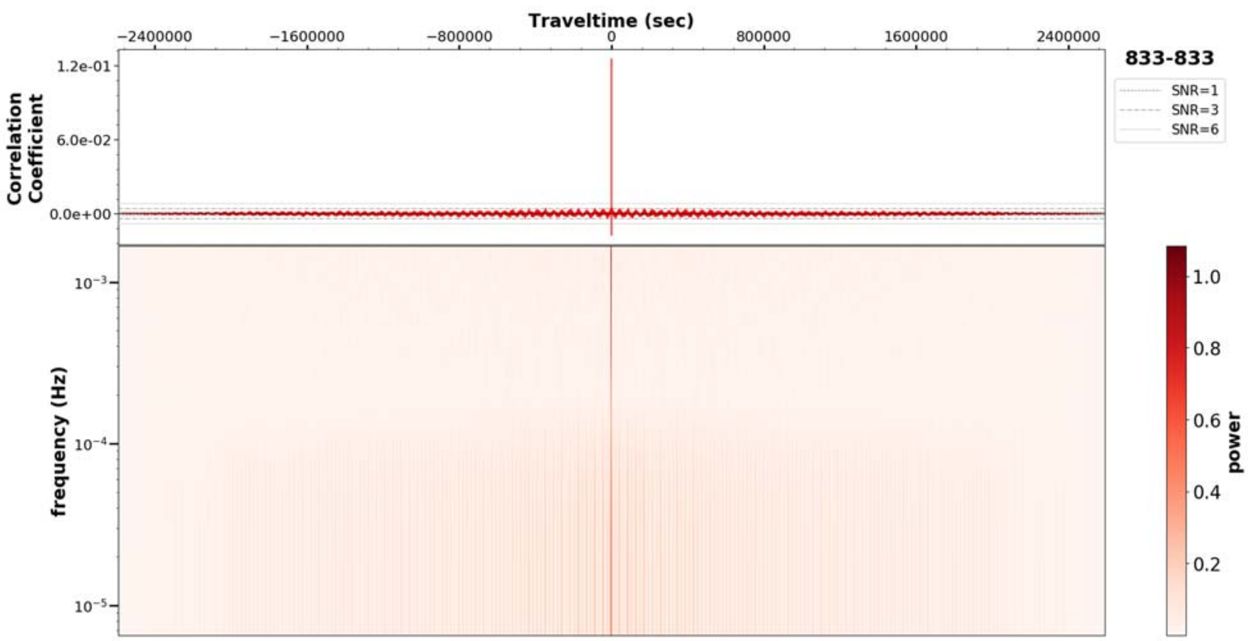

Figure A- 29. Spectrogram from stacked auto-correlated 30-day length data segments with preserved amplitudes (not normalized). Station pair: 833-833

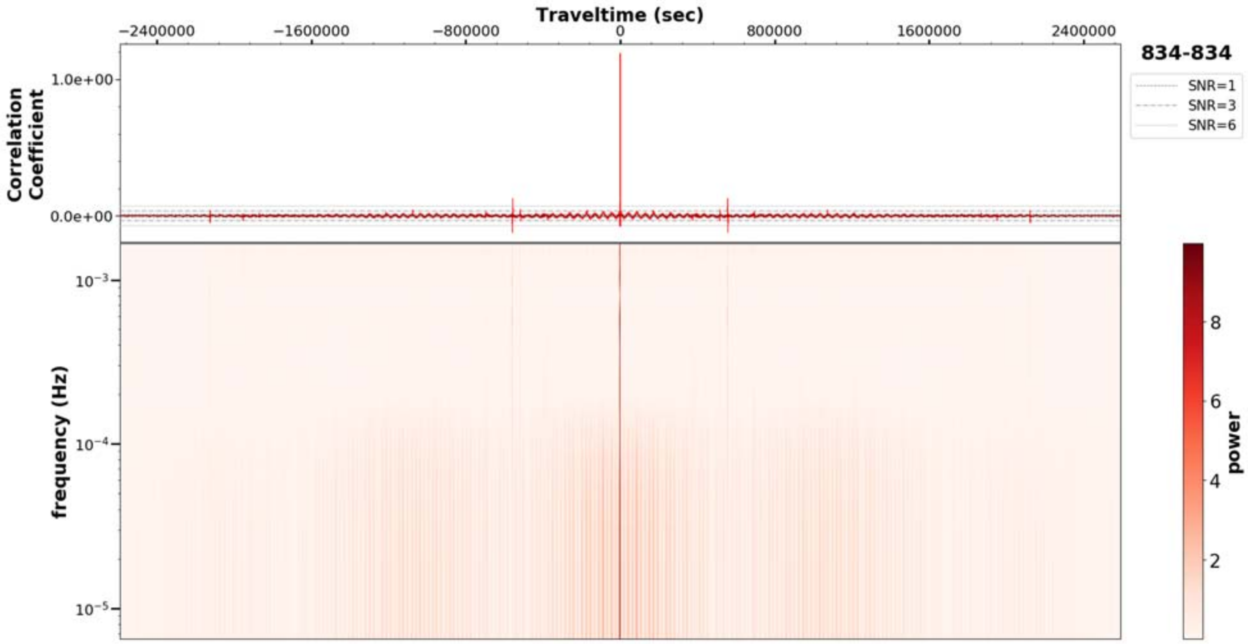

Figure A- 30. Spectrogram from stacked auto-correlated 30-day length data segments with preserved amplitudes (not normalized). Station pair: 834-834

7-Day Length Data Segments – Preserved Amplitudes

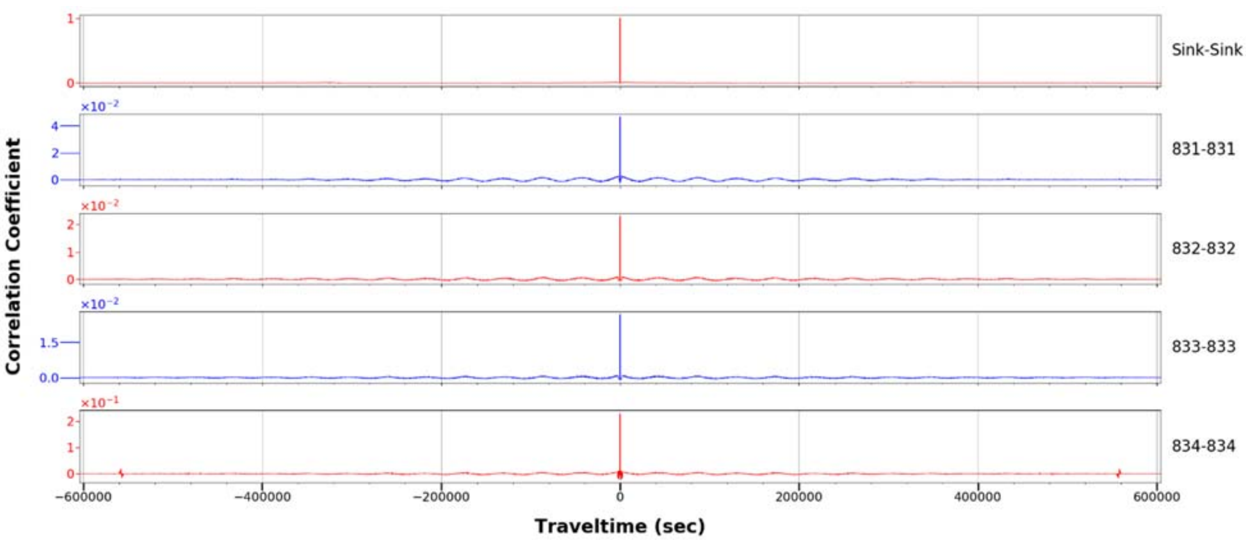

Figure A- 31. Stacked auto-correlograms from 7-day data segments with preserved amplitudes (not normalized).

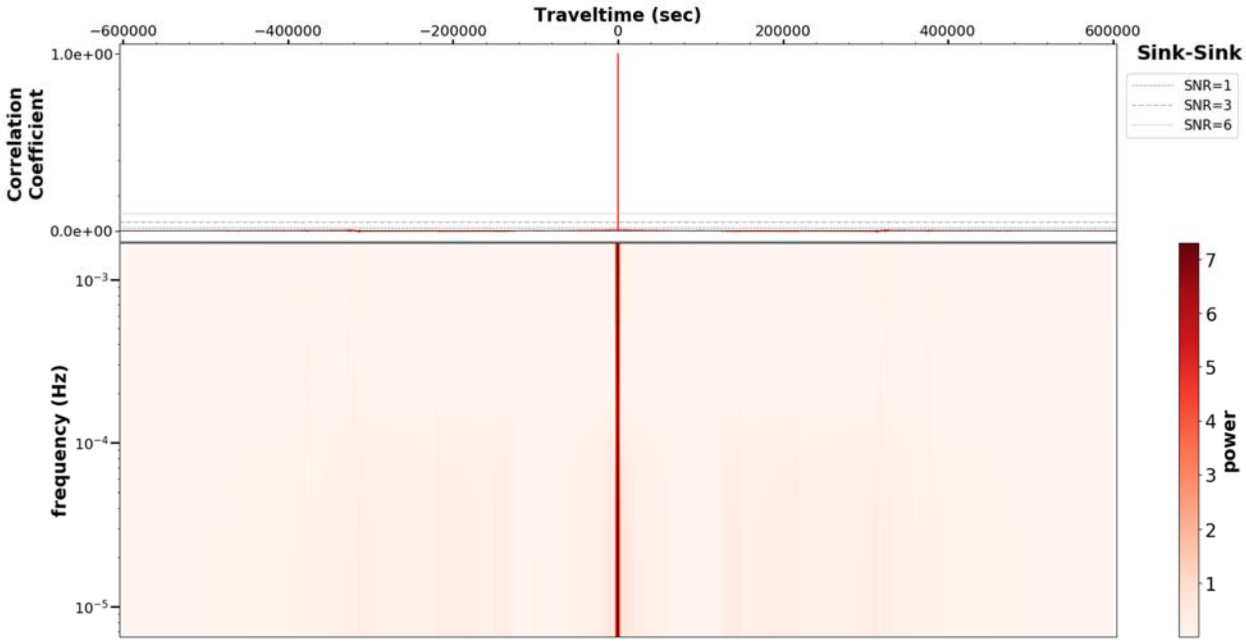

Figure A- 32. Spectrogram from stacked auto-correlated 7-day length data segments with preserved amplitudes (not normalized). Station pair: Sink-Sink

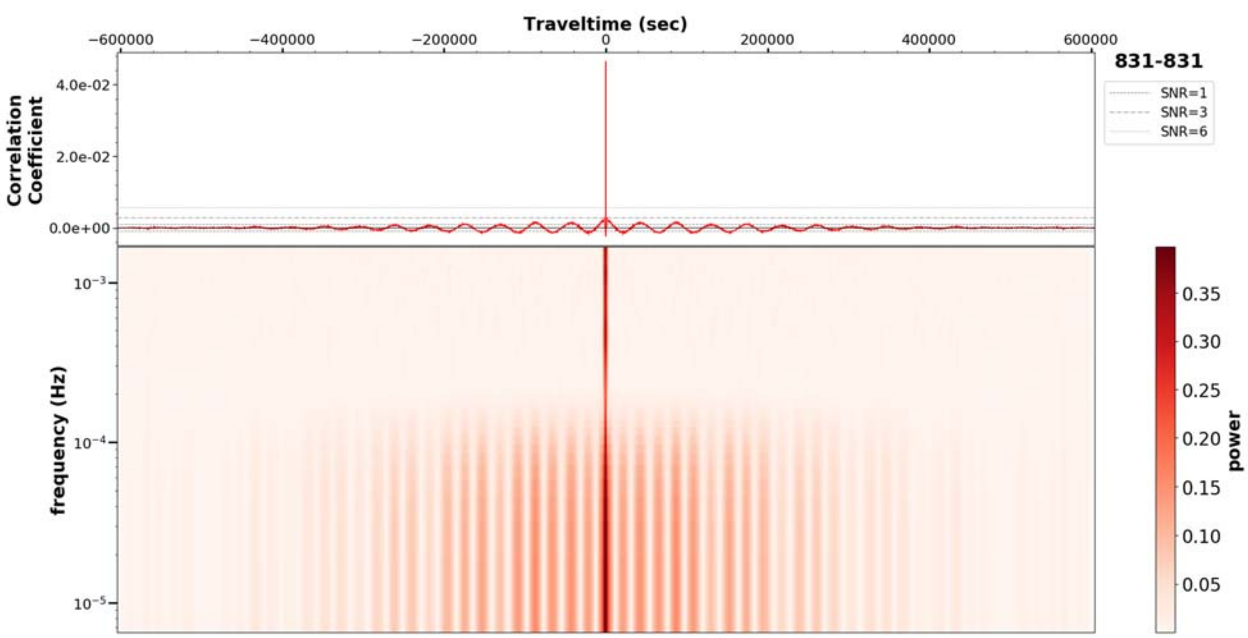

Figure A- 33. Spectrogram from stacked auto-correlated 7-day length data segments with preserved amplitudes (not normalized). Station pair: 831-831

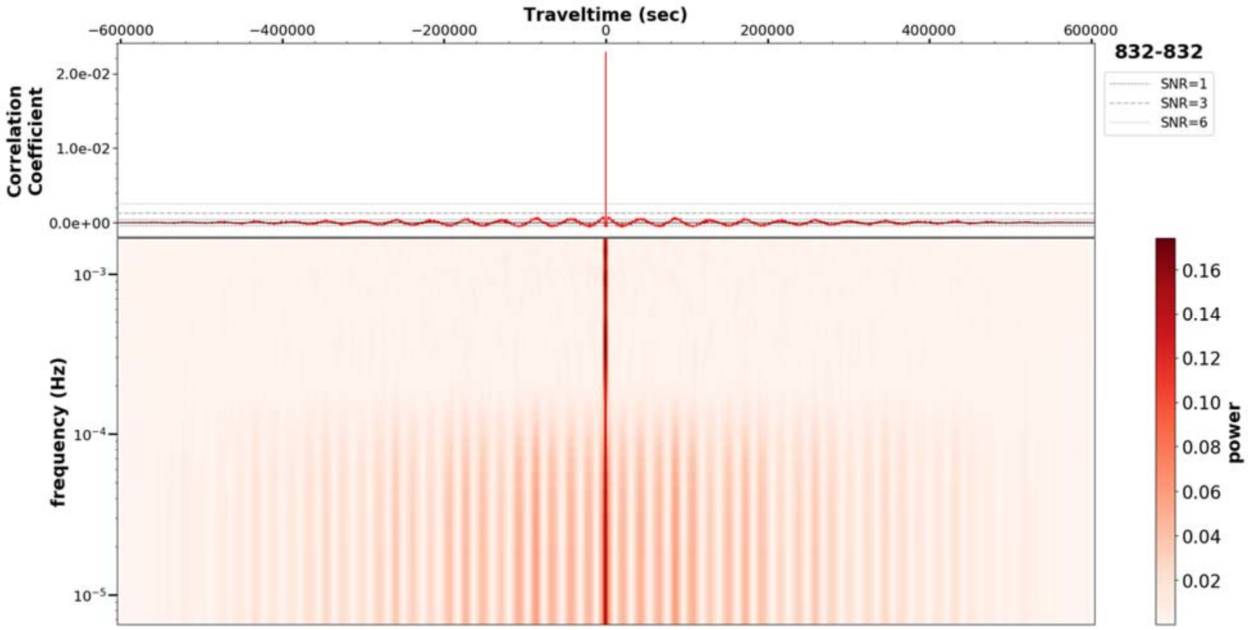

Figure A- 34. Spectrogram from stacked auto-correlated 7-day length data segments with preserved amplitudes (not normalized). Station pair: 832-832

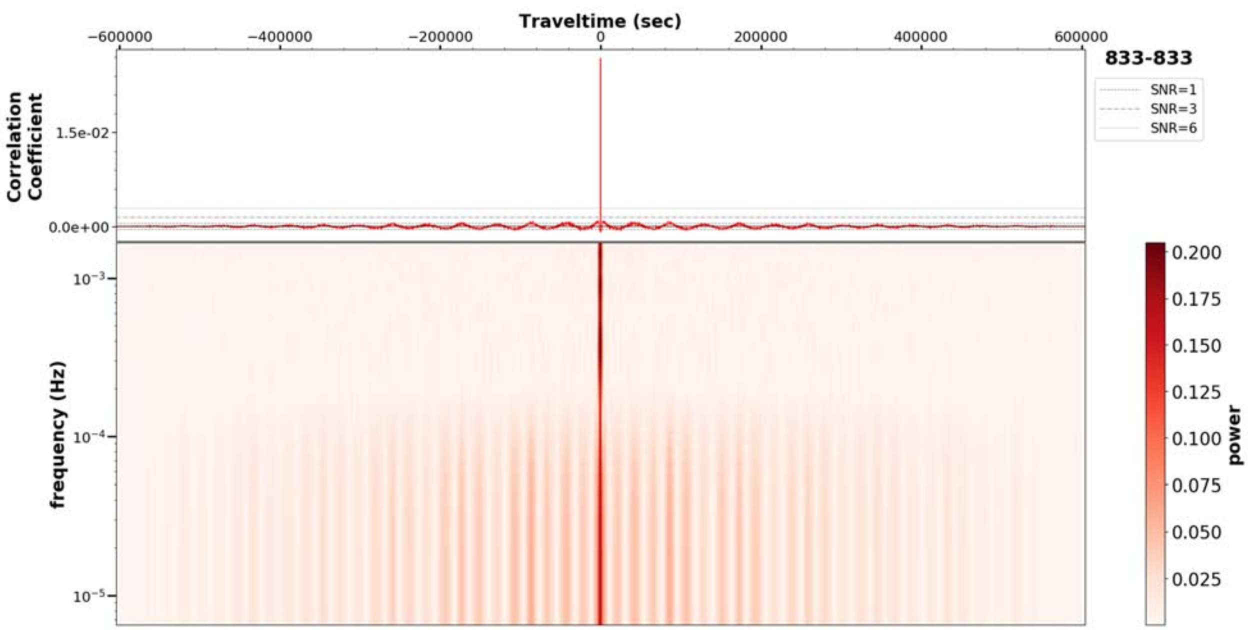

Figure A- 35. Spectrogram from stacked auto-correlated 7-day length data segments with preserved amplitudes (not normalized). Station pair: 833-833

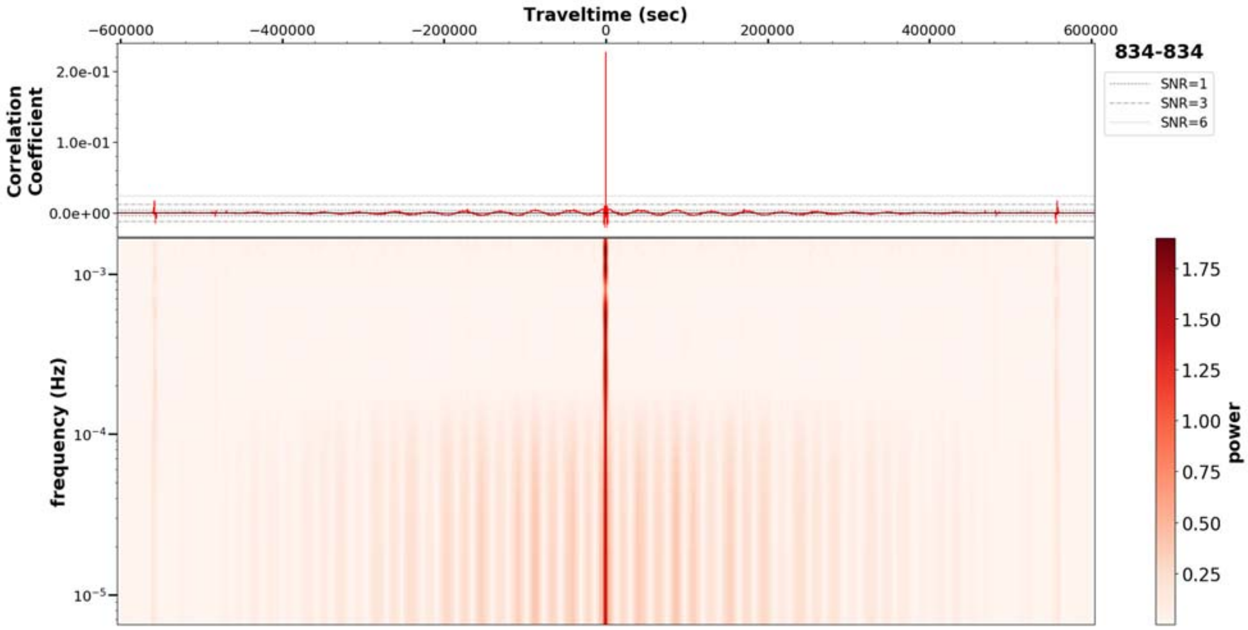

Figure A- 36. Spectrogram from stacked auto-correlated 7-day length data segments with preserved amplitudes (not normalized). Station pair: 834-834

All Daily Length Data Segments – Preserved Amplitudes

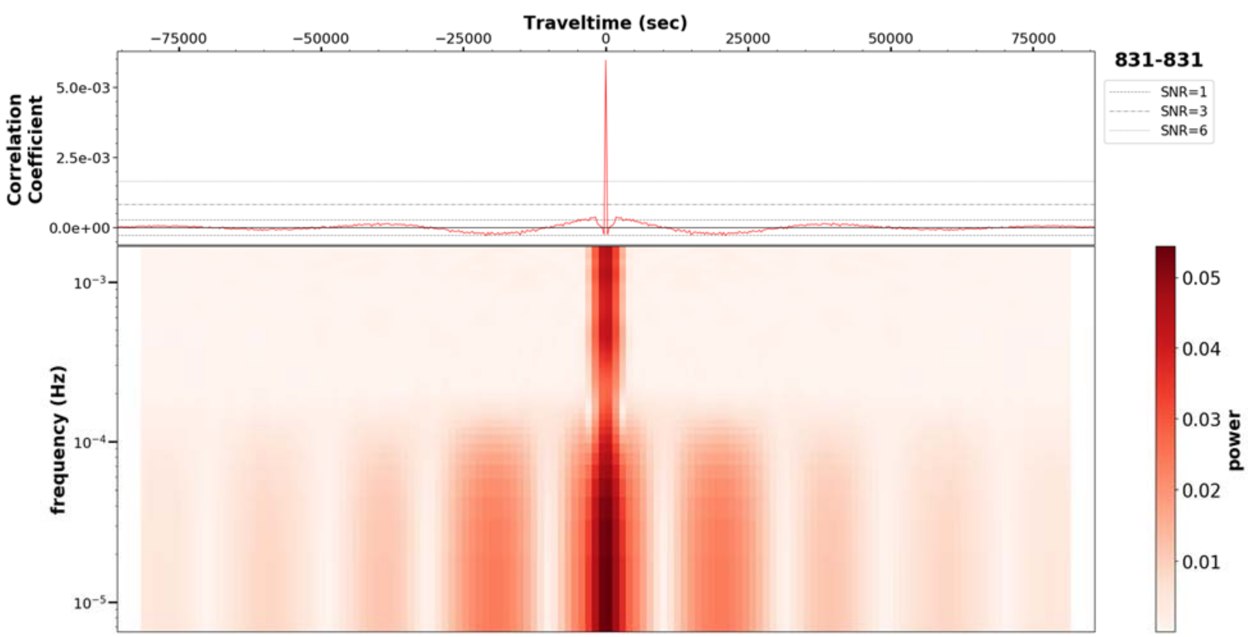

Figure A- 37. Spectrogram from stacked auto-correlated daily length data segments with preserved amplitudes (not normalized), all segments. Station pair: 831-831

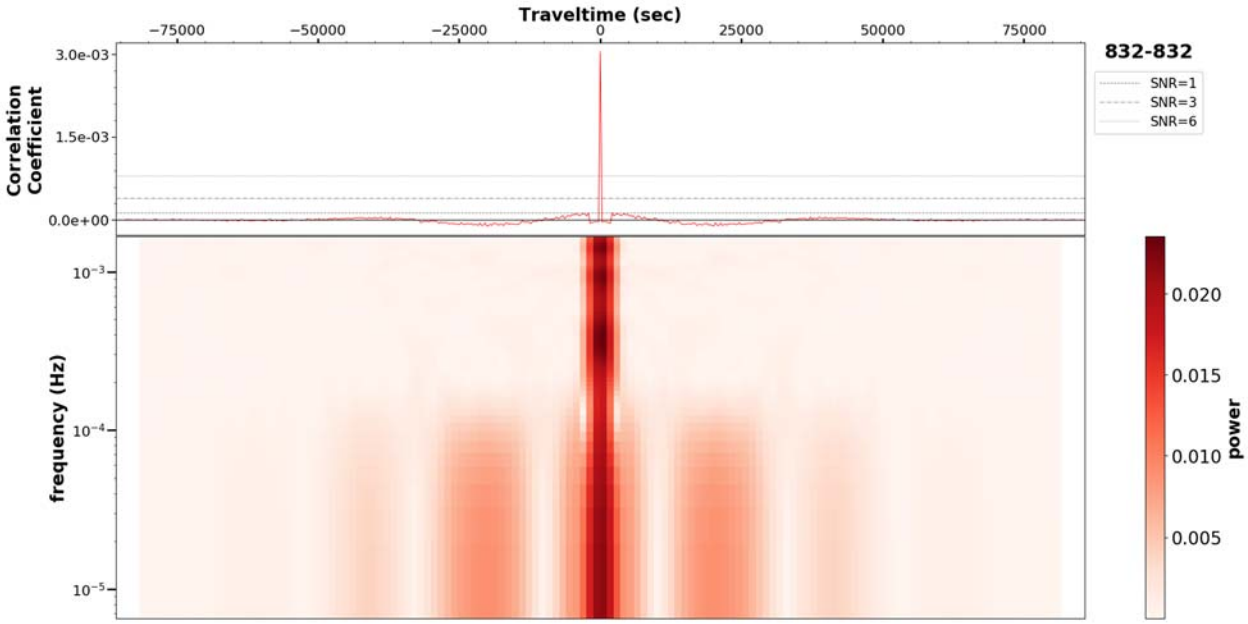

Figure A- 38. Spectrogram from stacked auto-correlated daily length data segments with preserved amplitudes (not normalized), all segments. Station pair: 832-832

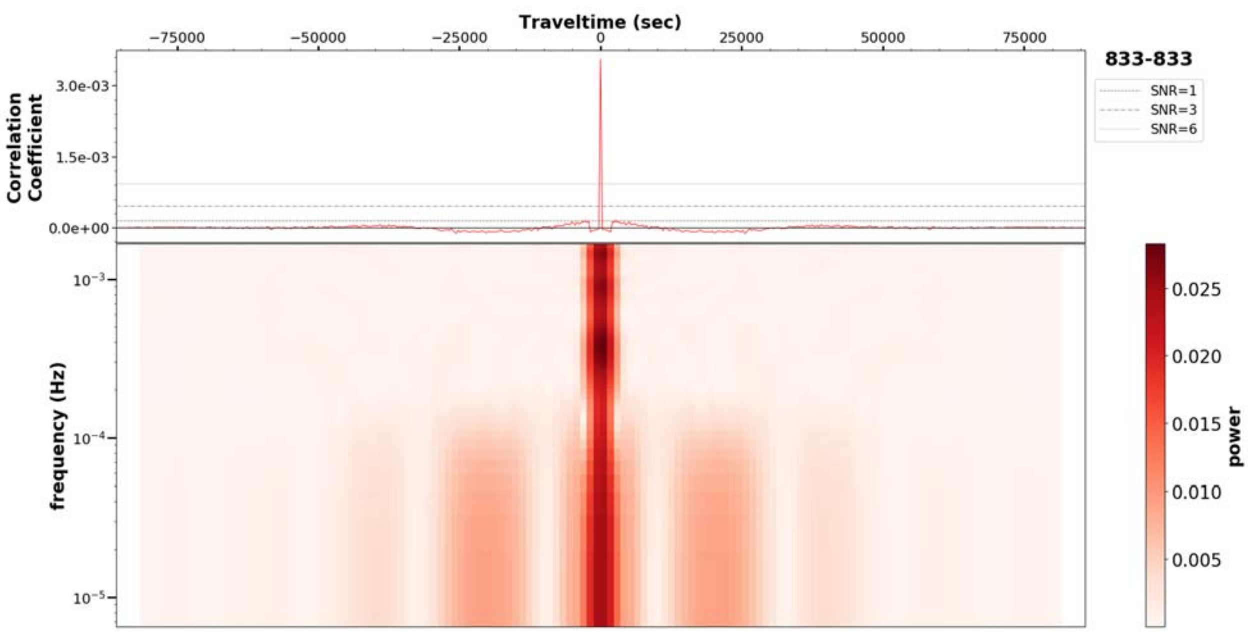

Figure A- 39. Spectrogram from stacked auto-correlated daily length data segments with preserved amplitudes (not normalized), all segments. Station pair: 833-833

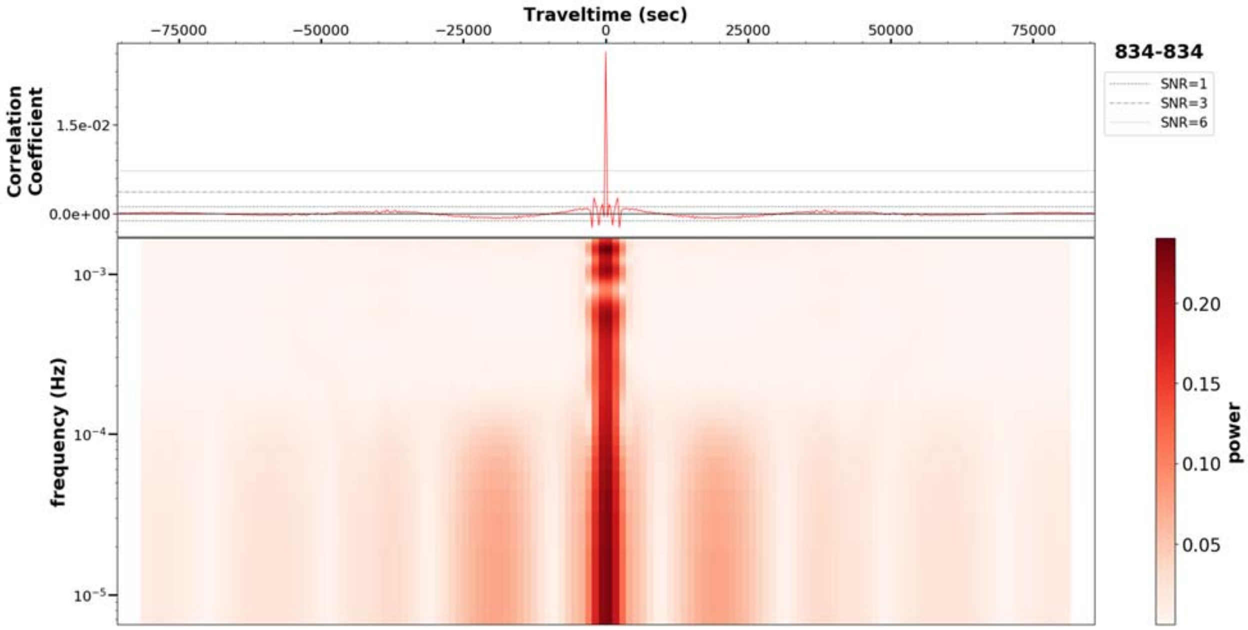

Figure A- 40. Spectrogram from stacked auto-correlated daily length data segments with preserved amplitudes (not normalized), all segments. Station pair: 834-834

Pumping-Period-Only Daily Length Data Segments – Preserved Amplitudes

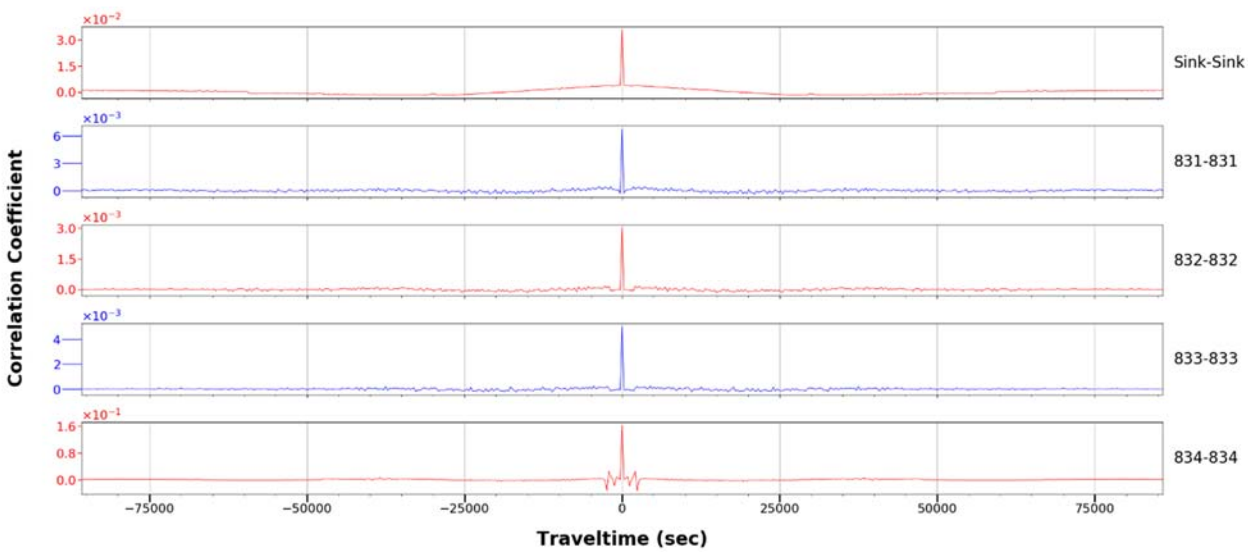

Figure A- 41. Stacked auto-correlograms from pumping-period-only daily data segments with preserved amplitudes (not normalized).

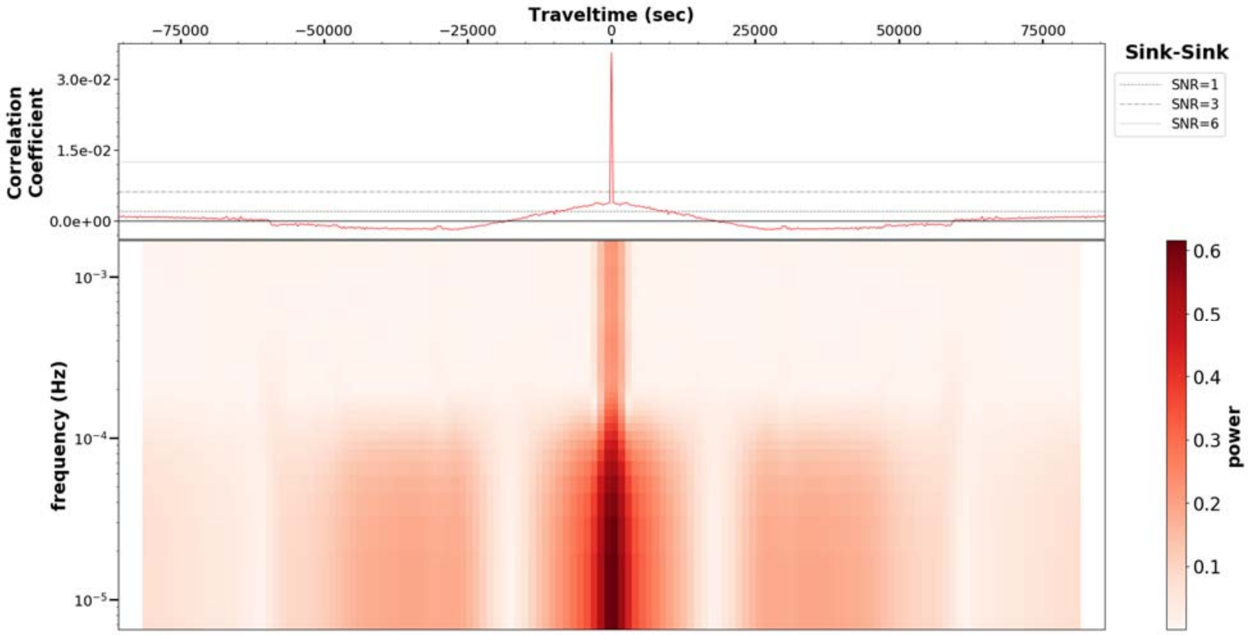

Figure A- 42. Spectrogram from stacked auto-correlated daily length data segments with preserved amplitudes (not normalized), pumping-period-only segments. Station pair: Sink-Sink

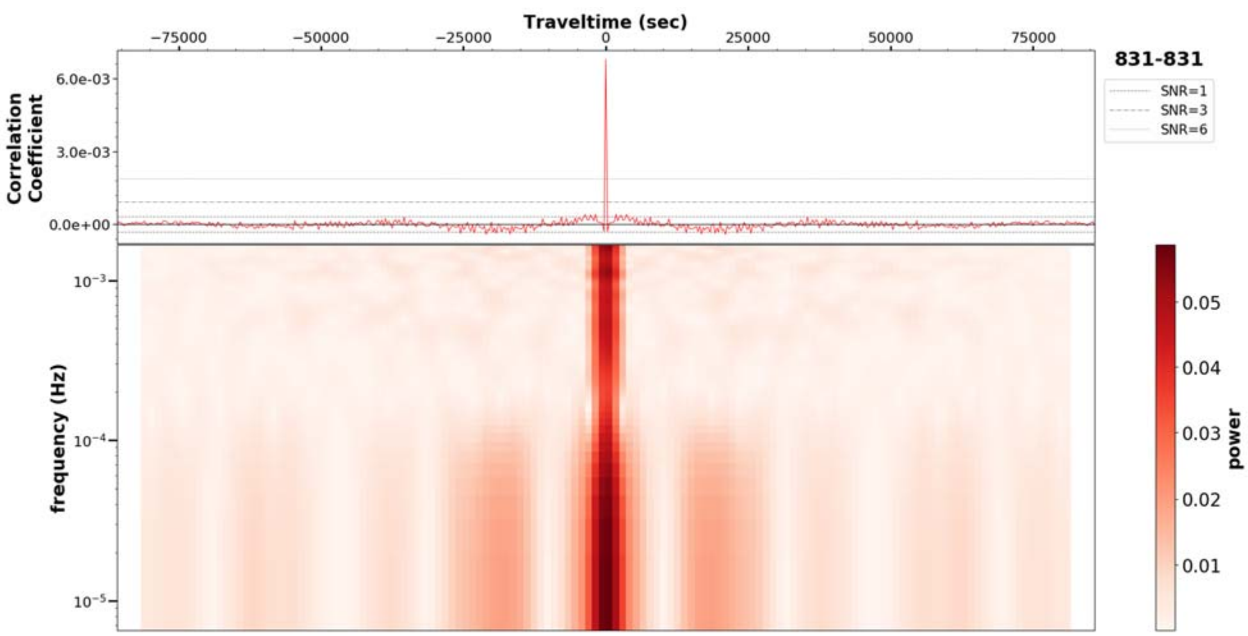

Figure A- 43. Spectrogram from stacked auto-correlated daily length data segments with preserved amplitudes (not normalized), pumping-period-only segments. Station pair: 831-831

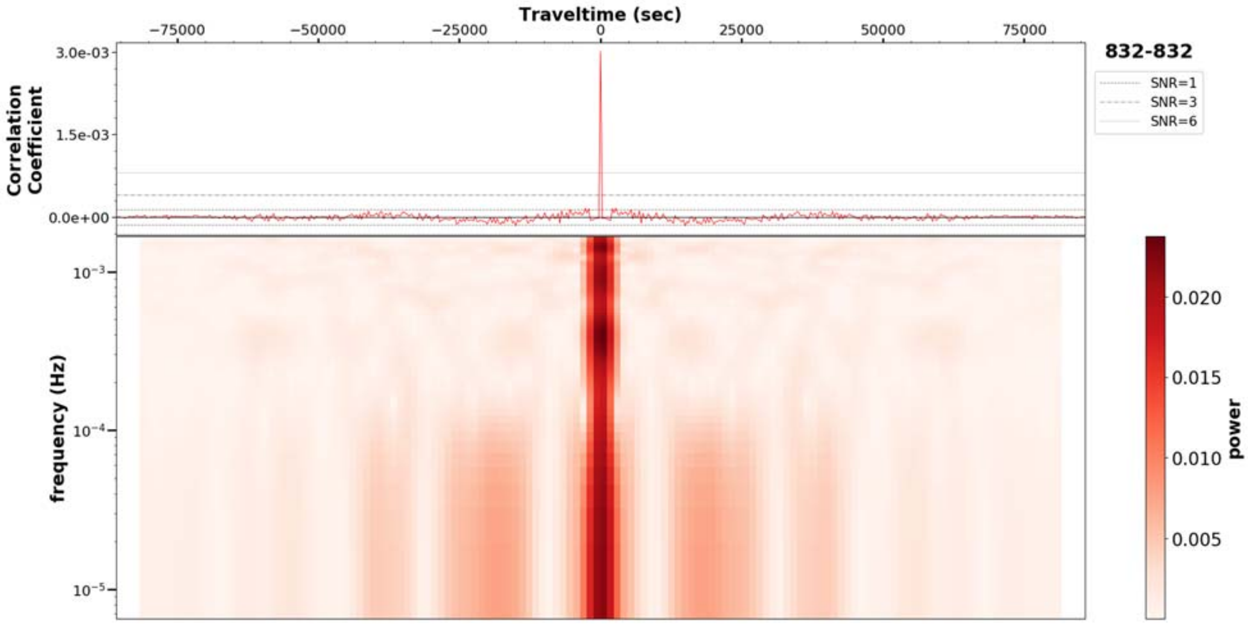

Figure A- 44. Spectrogram from stacked auto-correlated daily length data segments with preserved amplitudes (not normalized), pumping-period-only segments. Station pair: 832-832

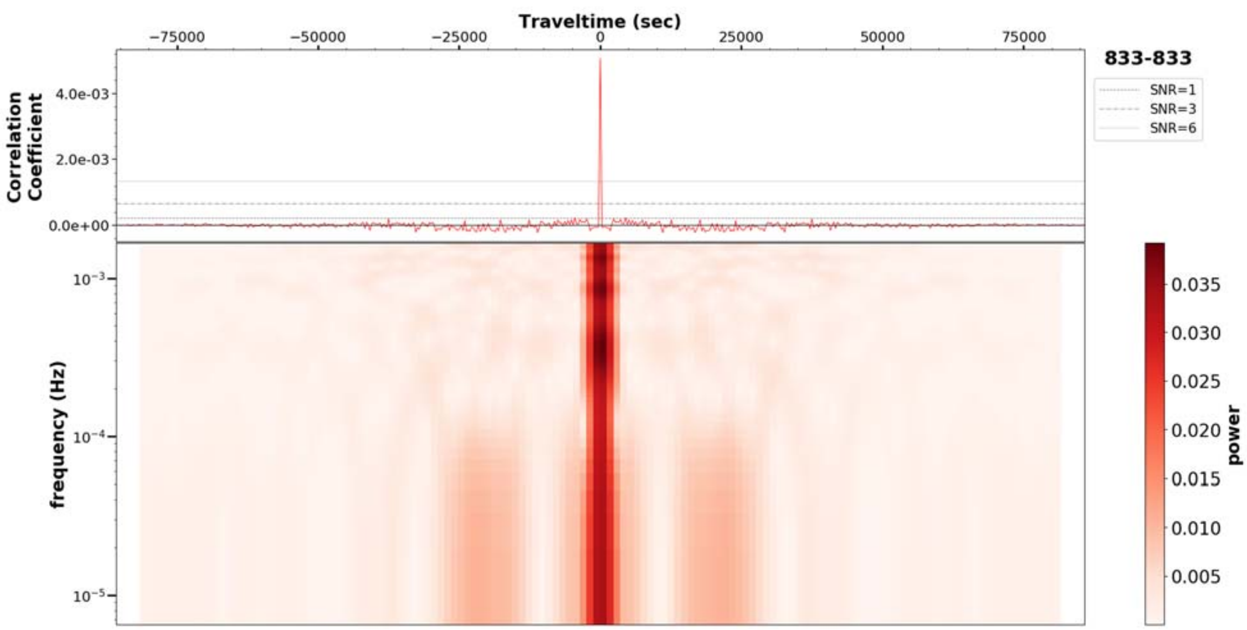

Figure A- 45. Spectrogram from stacked auto-correlated daily length data segments with preserved amplitudes (not normalized), pumping-period-only segments. Station pair: 833-833

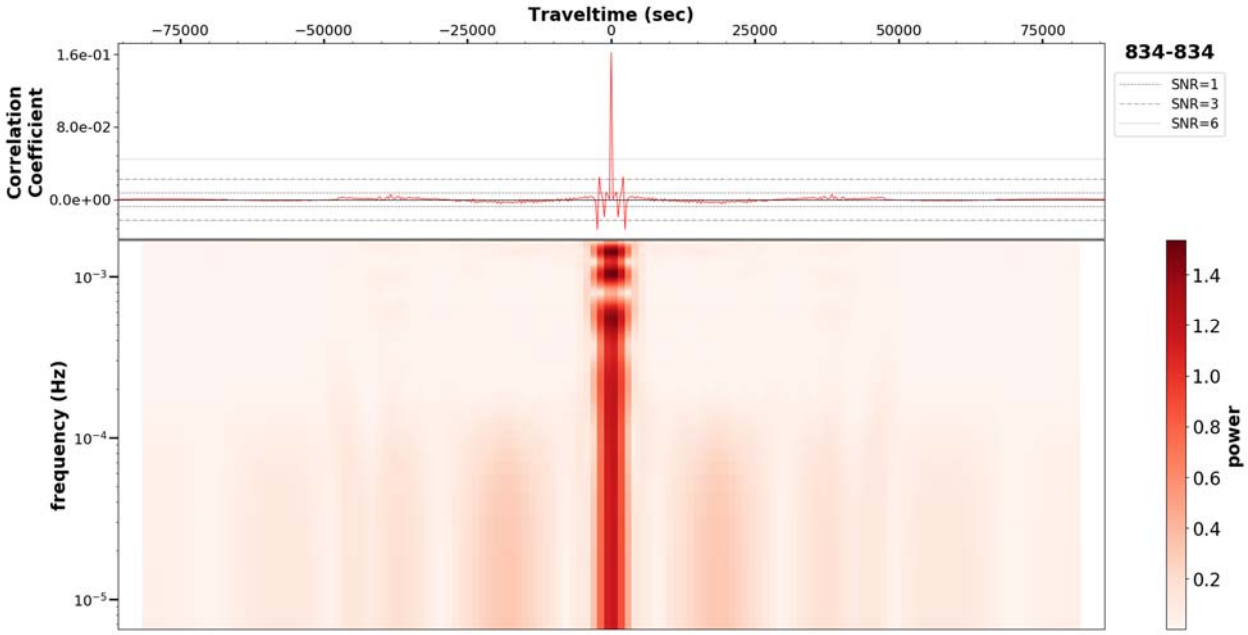

Figure A- 46. Spectrogram from stacked auto-correlated daily length data segments with preserved amplitudes (not normalized), pumping-period-only segments. Station pair: 834-834

Spectrograms and Filtered Correlograms from Cross-Correlograms

30-Day Length Data Segments – Normalized Amplitudes

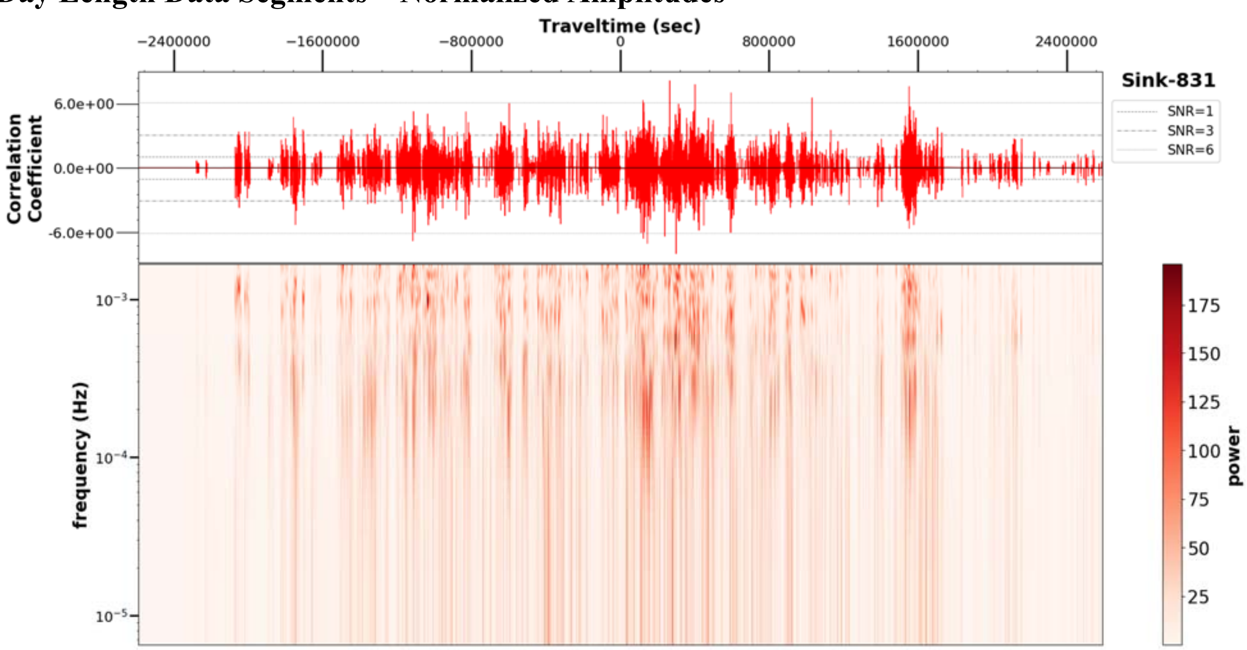

Figure A- 47. Spectrogram from stacked cross-correlated normalized 30-day length data segments. Station pair: Sink-831

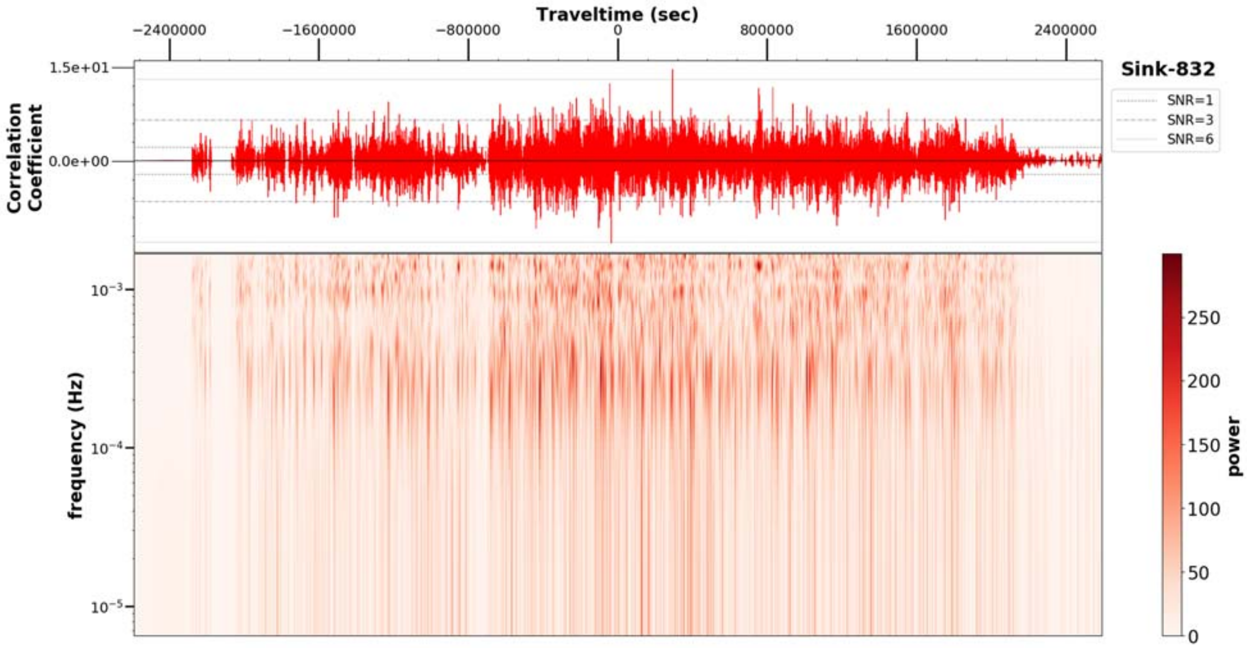

Figure A- 48. Spectrogram from stacked cross-correlated normalized 30-day length data segments. Station pair: Sink-832

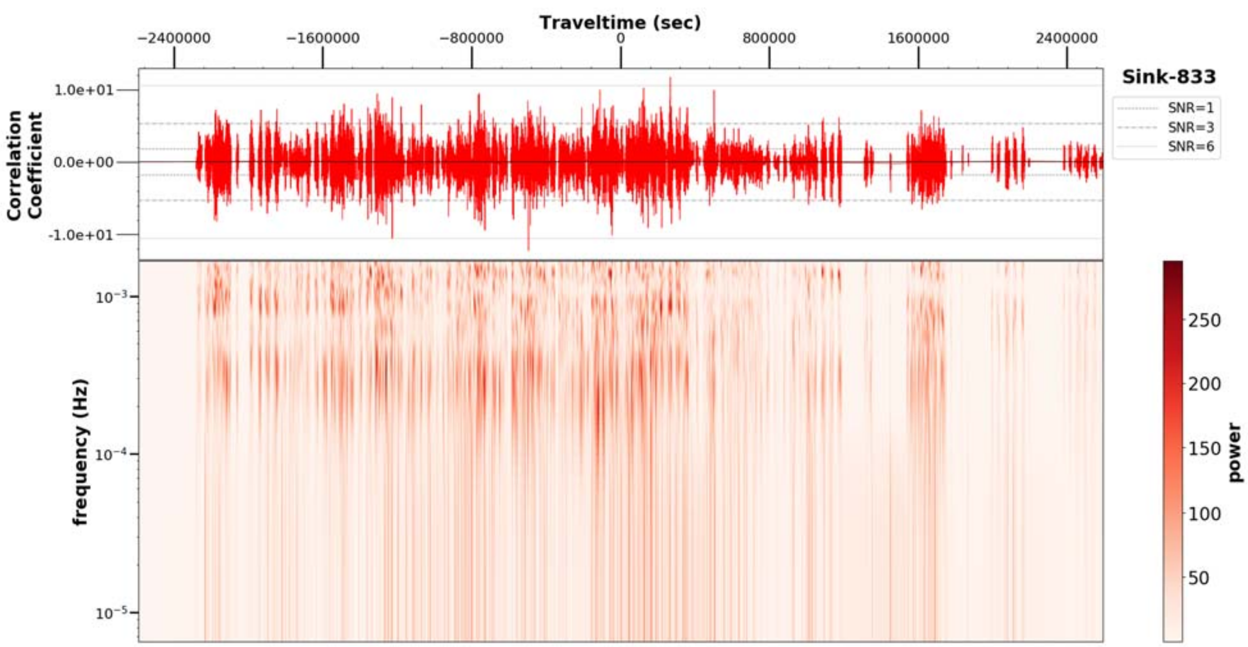

Figure A- 49. Spectrogram from stacked cross-correlated normalized 30-day length data segments. Station pair: Sink-833

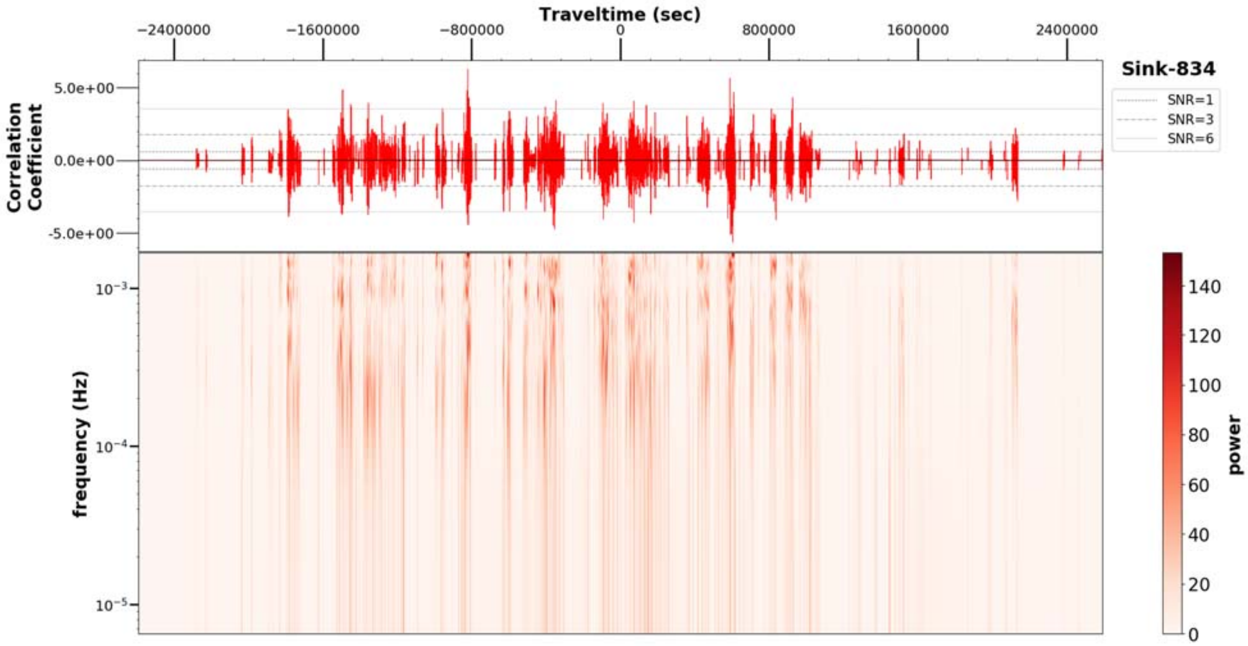

Figure A- 50. Spectrogram from stacked cross-correlated normalized 30-day length data segments. Station pair: Sink-834

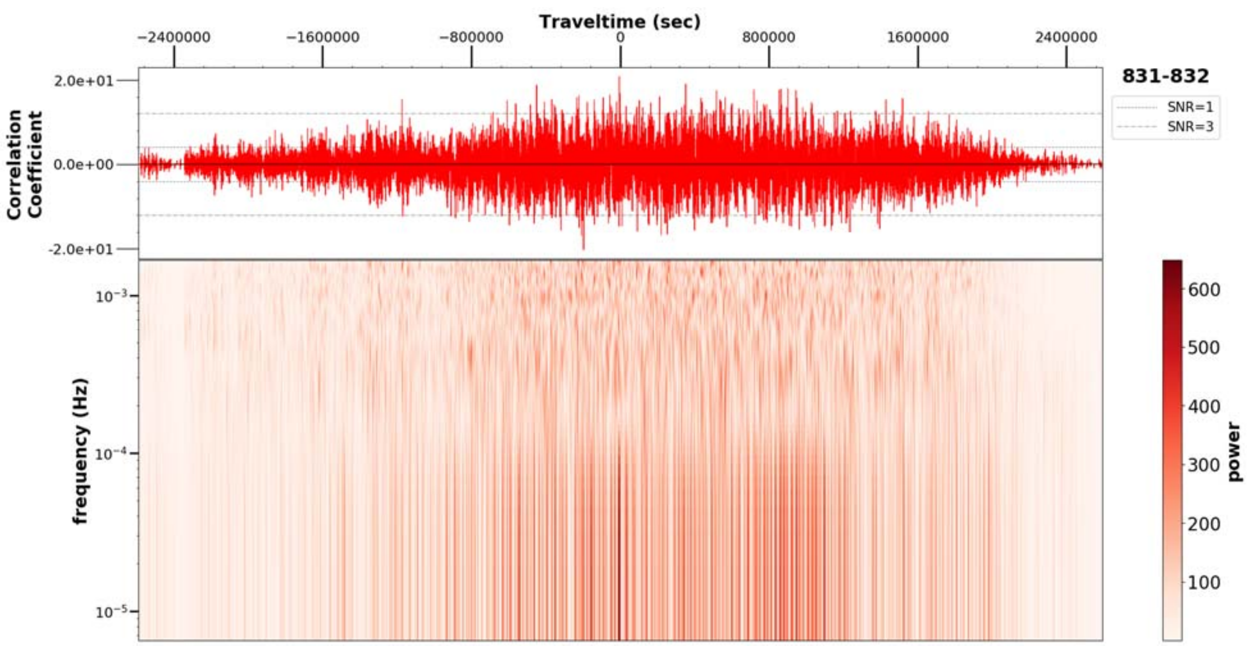

Figure A- 51. Spectrogram from stacked cross-correlated normalized 30-day length data segments. Station pair: 831-832

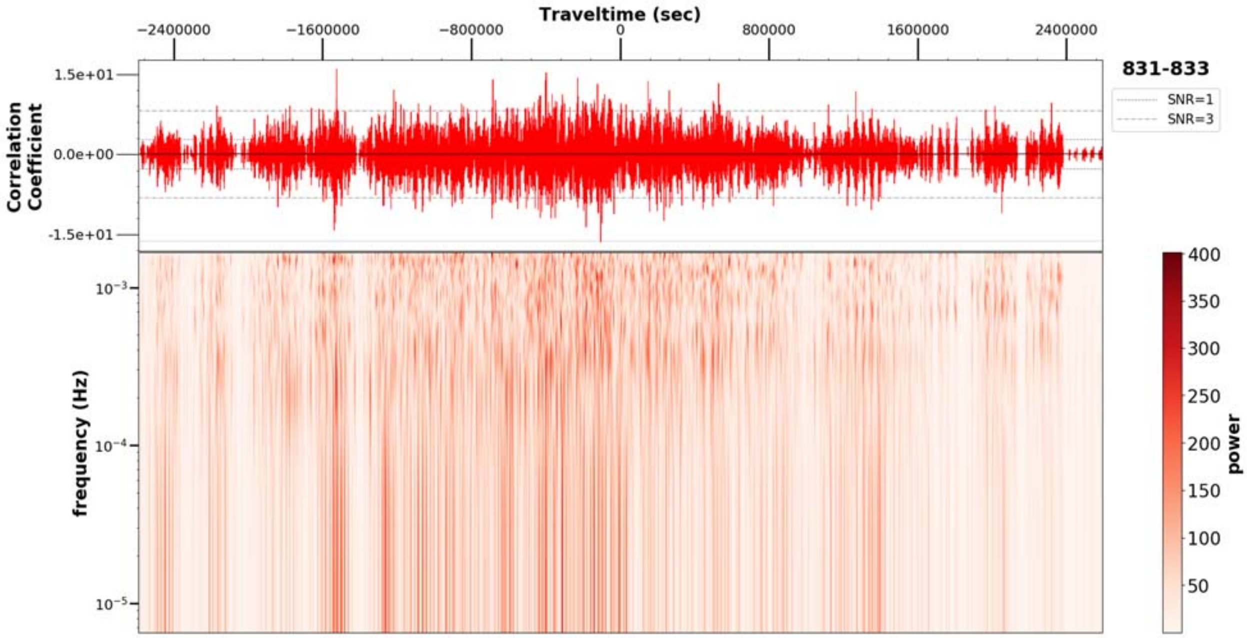

Figure A- 52. Spectrogram from stacked cross-correlated normalized 30-day length data segments. Station pair: 831-833

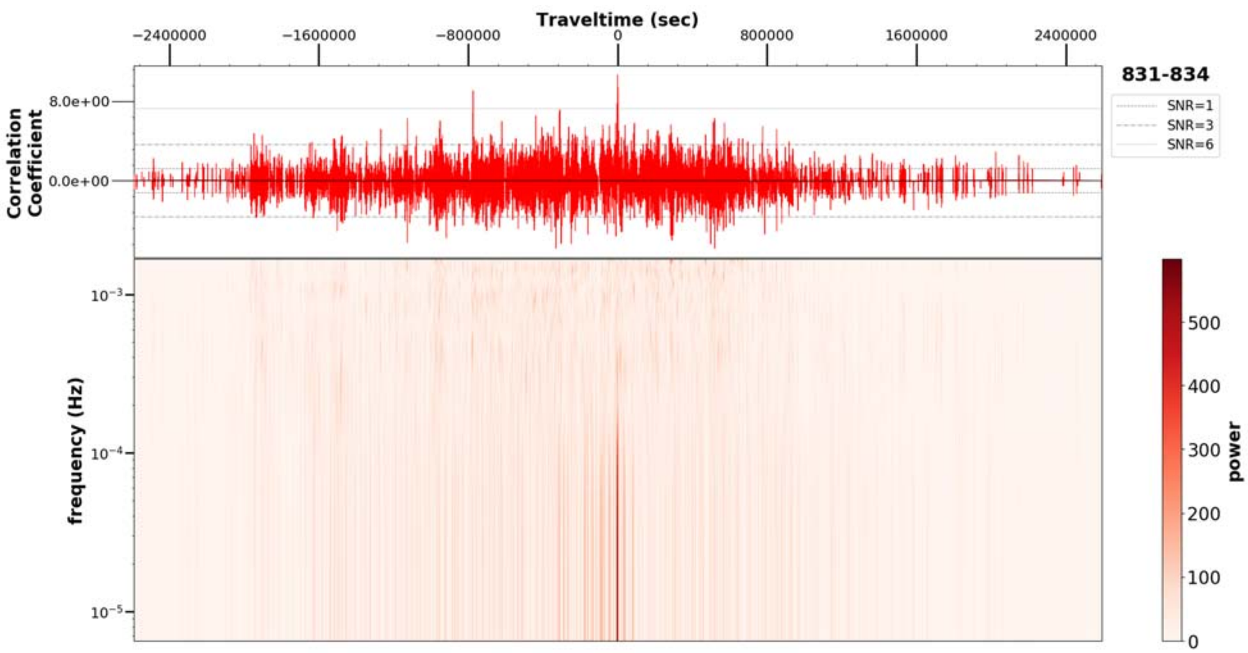

Figure A- 53. Spectrogram from stacked cross-correlated normalized 30-day length data segments. Station pair: 831-834

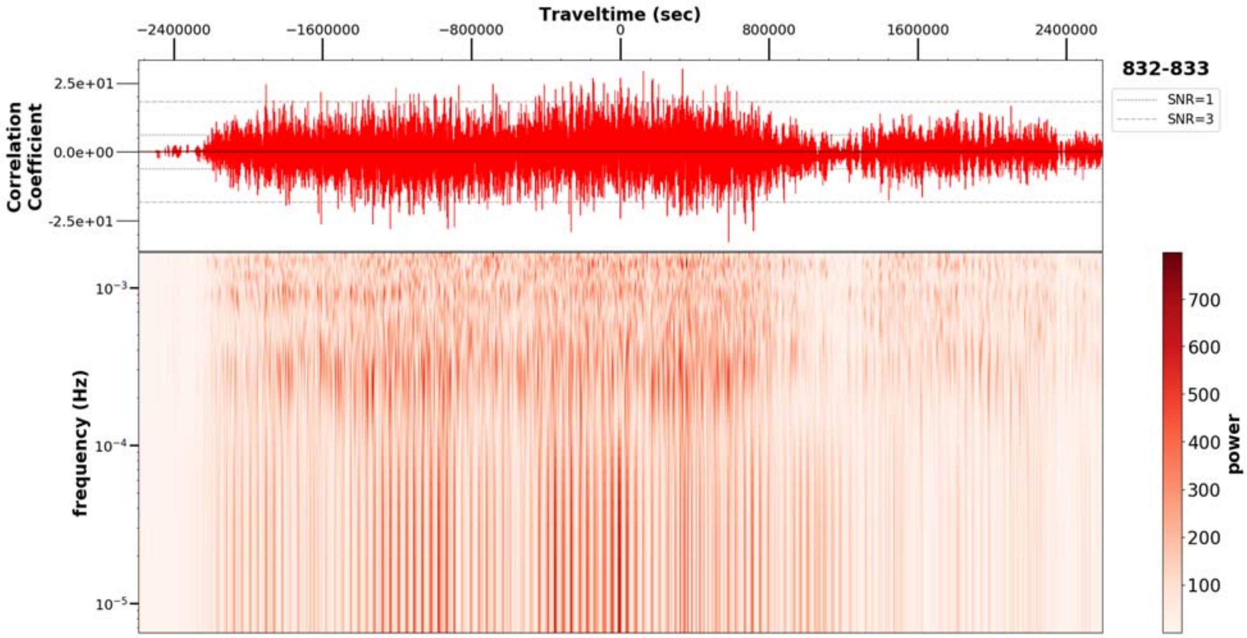

Figure A- 54. Spectrogram from stacked cross-correlated normalized 30-day length data segments. Station pair: 832-833

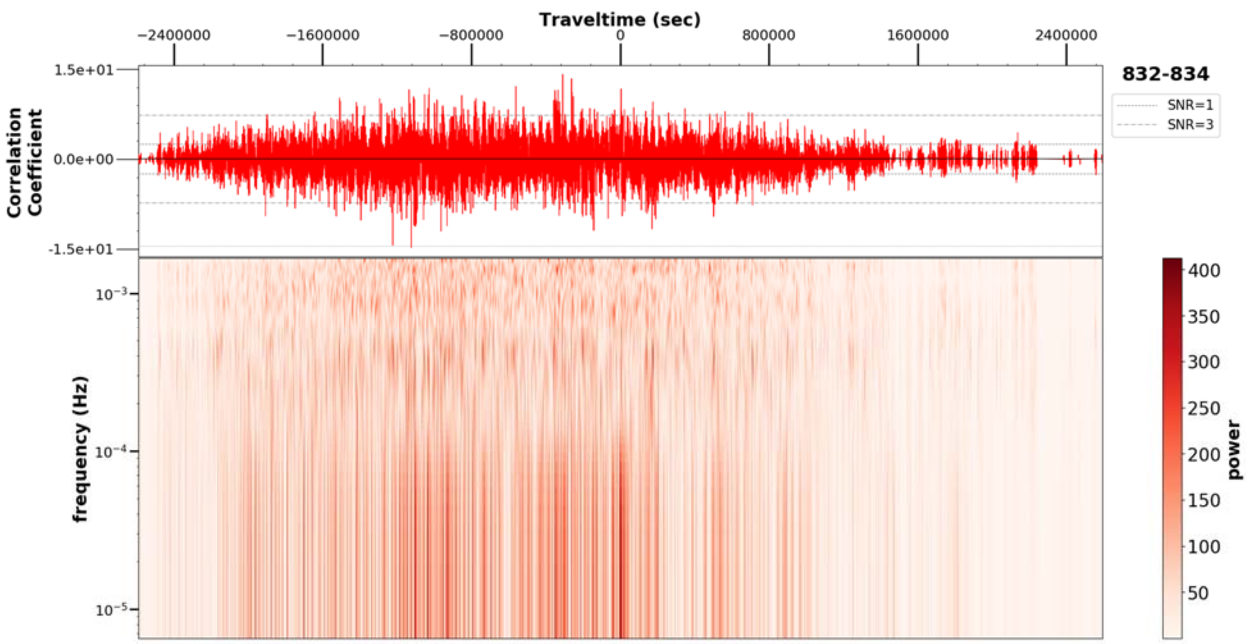

Figure A- 55. Spectrogram from stacked cross-correlated normalized 30-day length data segments. Station pair: 832-834

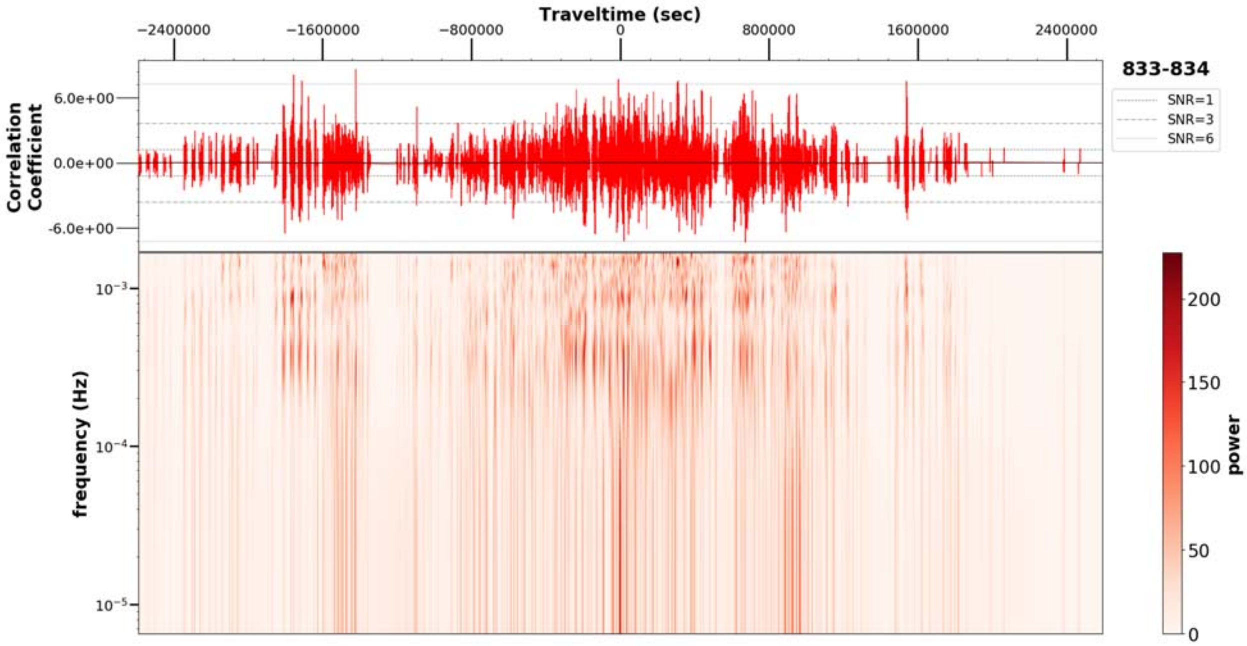

Figure A- 56. Spectrogram from stacked cross-correlated normalized 30-day length data segments. Station pair: 833-834

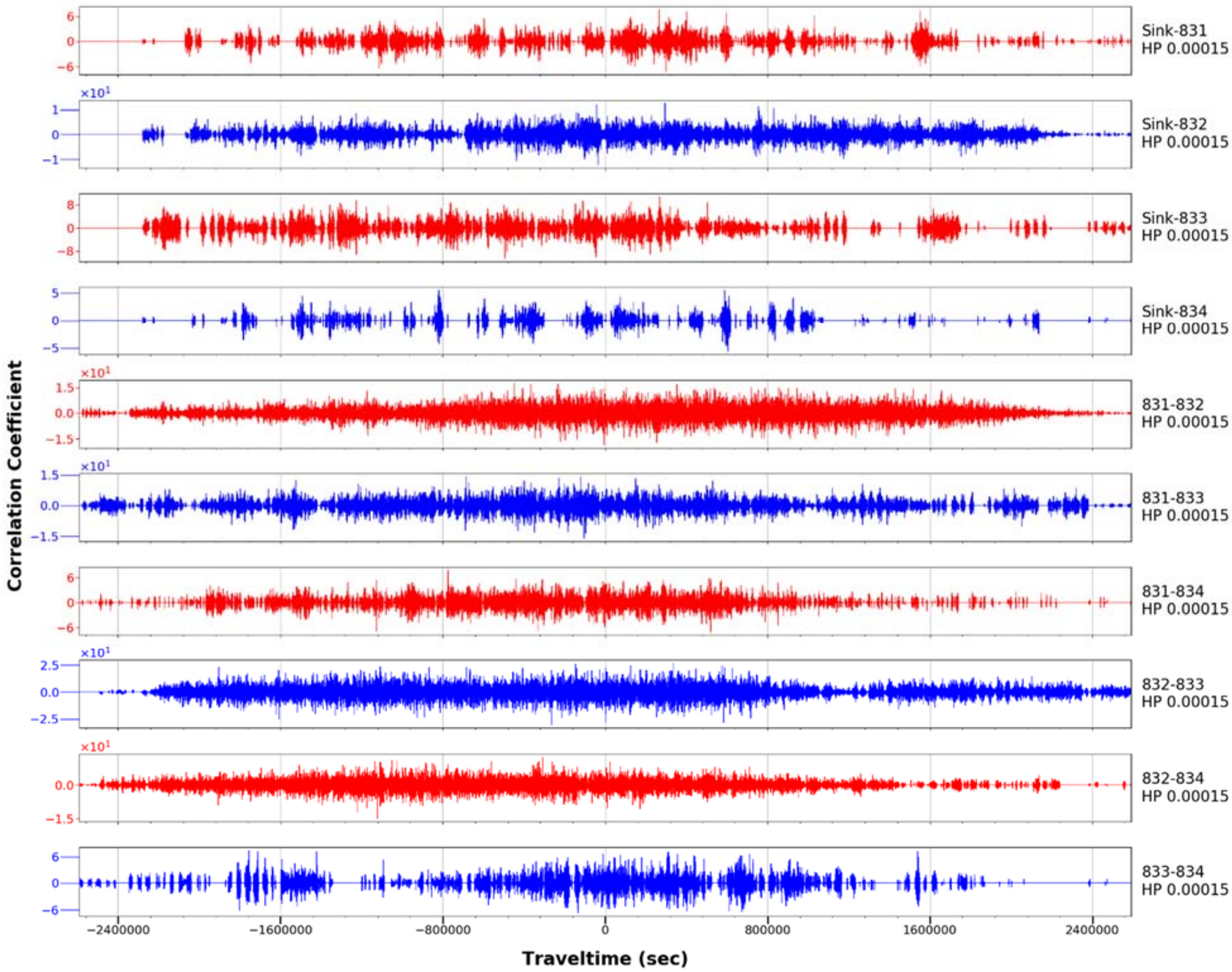

Figure A- 57. Stacked cross-correlograms from 30-day data segment lengths and normalized water level amplitudes. Correlograms were high-pass (HP) filtered with a corner frequency of 0.00015 Hz, or a period of just under 2 hours, which is indicated to the right of each panel.

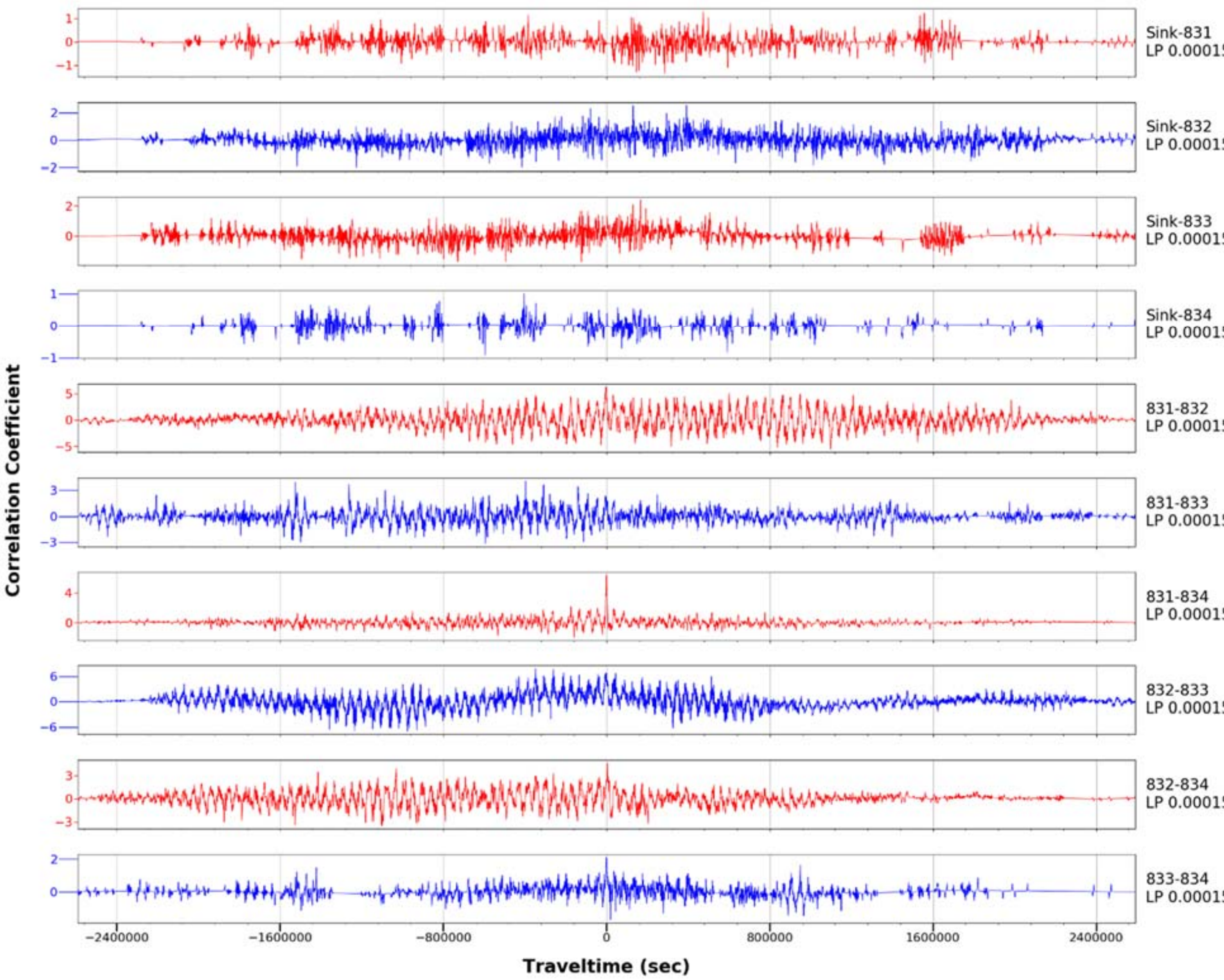

Figure A- 58. Stacked cross-correlograms from 30-day data segment lengths and normalized water level amplitudes. Correlograms were low-pass (LP) filtered with a corner frequency of 0.00015 Hz, or a period of just under 2 hours, which is indicated to the right of each panel.

7-Day Length Data Segments – Normalized Amplitudes

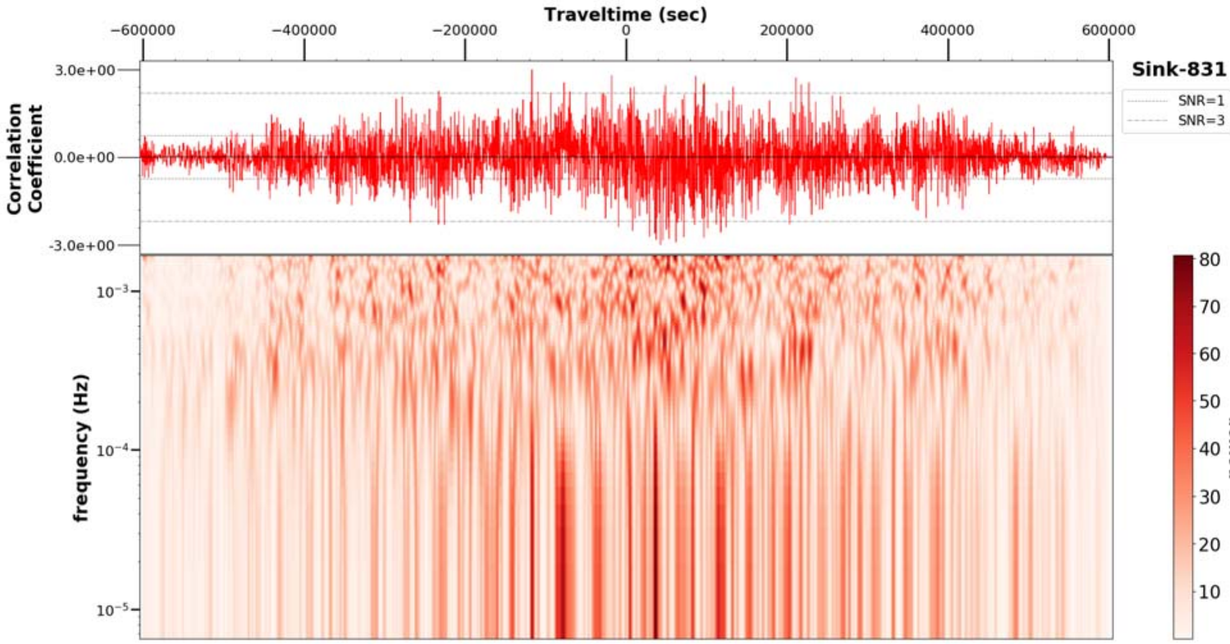

Figure A- 59. Spectrogram from stacked cross-correlated normalized 7-day length data segments. Station pair: Sink-831

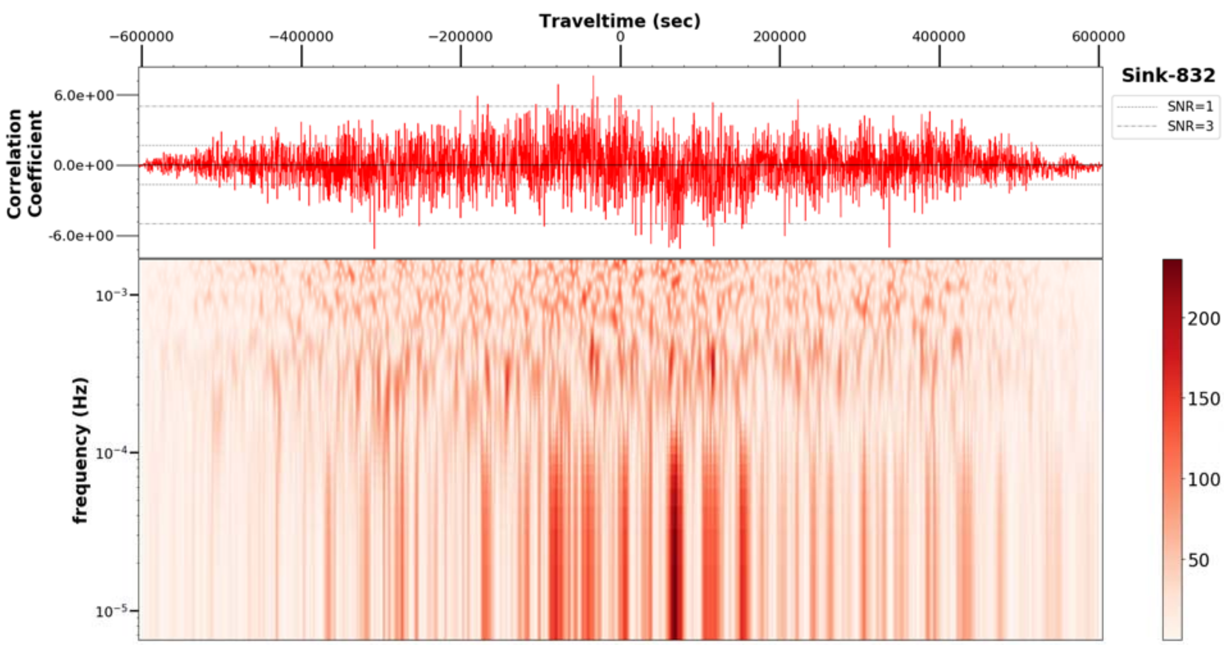

Figure A- 60. Spectrogram from stacked cross-correlated normalized 7-day length data segments. Station pair: Sink-832

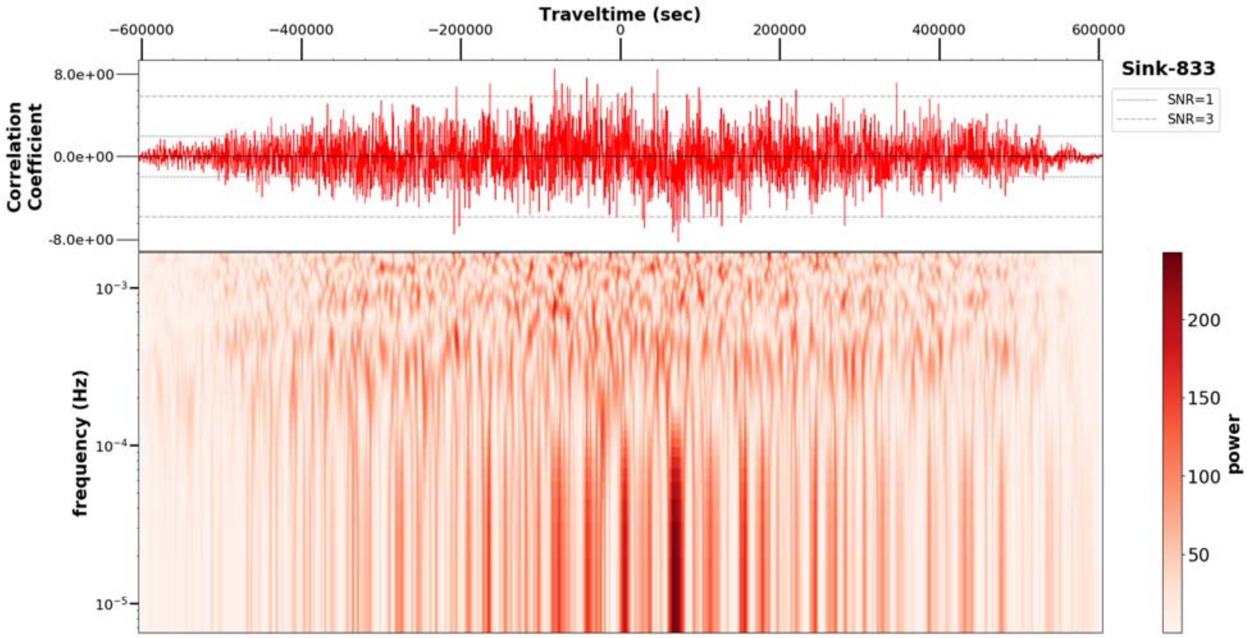

Figure A- 61. Spectrogram from stacked cross-correlated normalized 7-day length data segments. Station pair: Sink-833

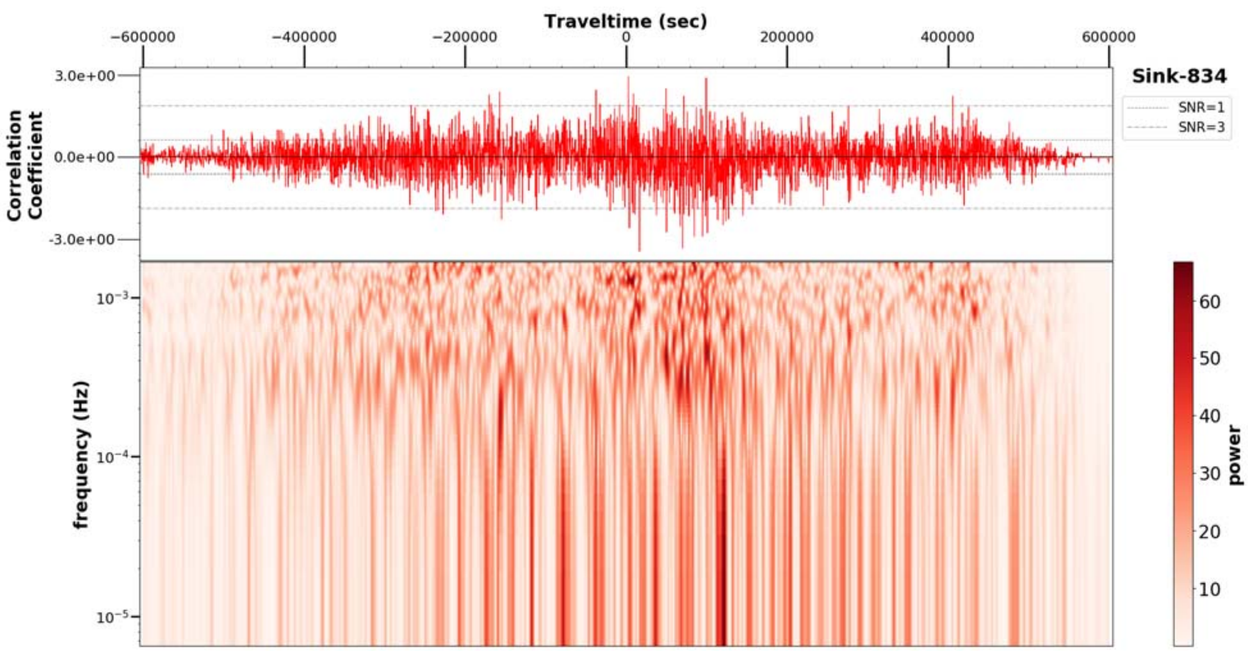

Figure A- 62. Spectrogram from stacked cross-correlated normalized 7-day length data segments. Station pair: Sink-834

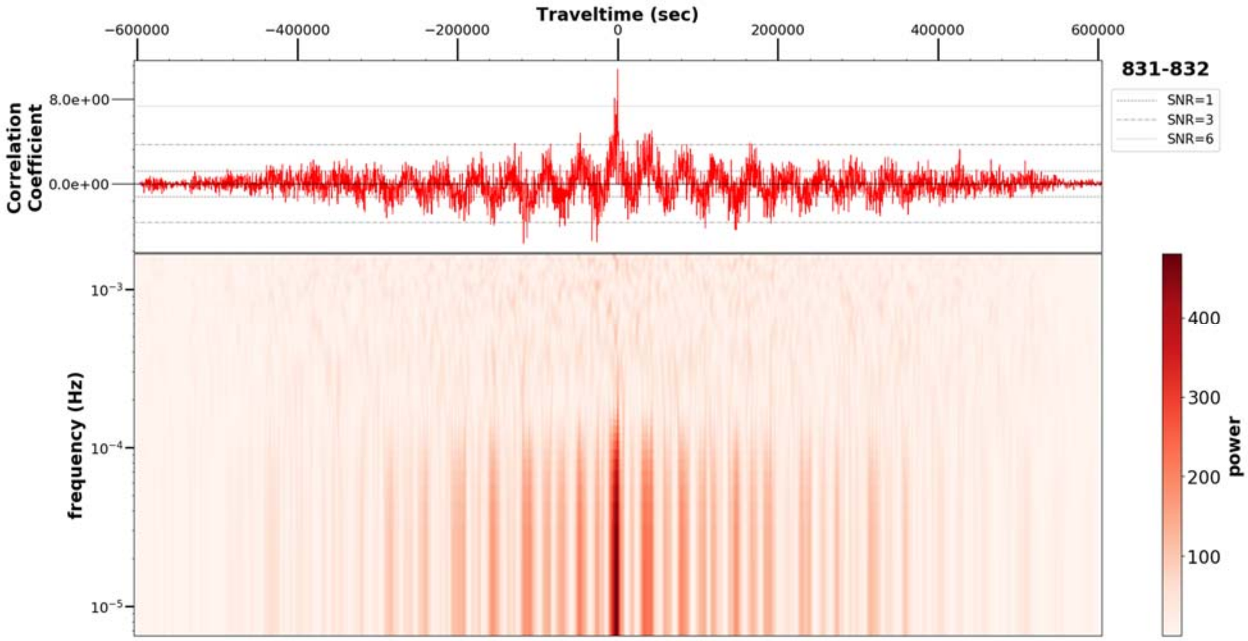

Figure A- 63. Spectrogram from stacked cross-correlated normalized 7-day length data segments. Station pair: 831-832

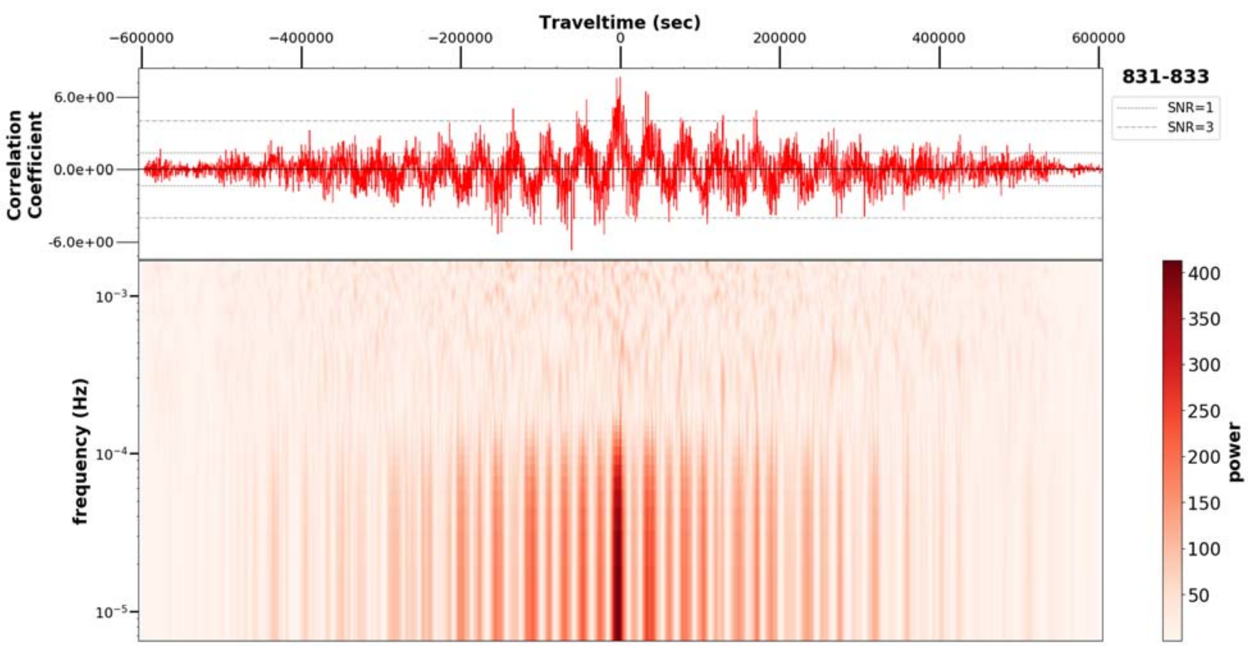

Figure A- 64. Spectrogram from stacked cross-correlated normalized 7-day length data segments. Station pair: 831-833

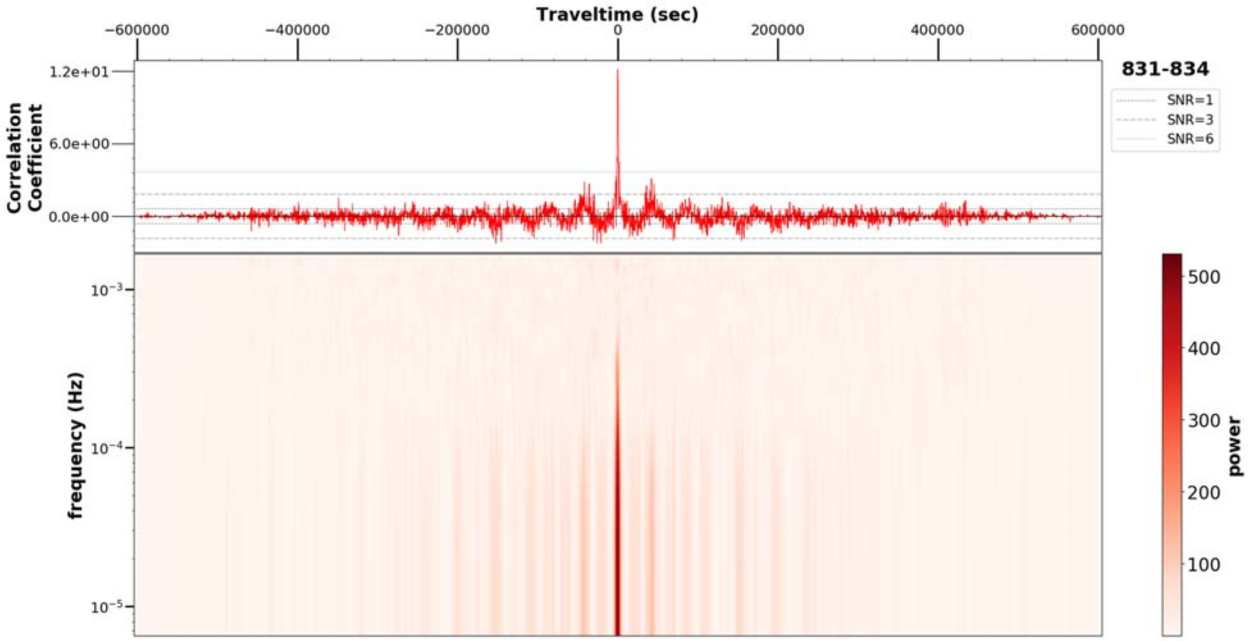

Figure A- 65. Spectrogram from stacked cross-correlated normalized 7-day length data segments. Station pair: 831-834

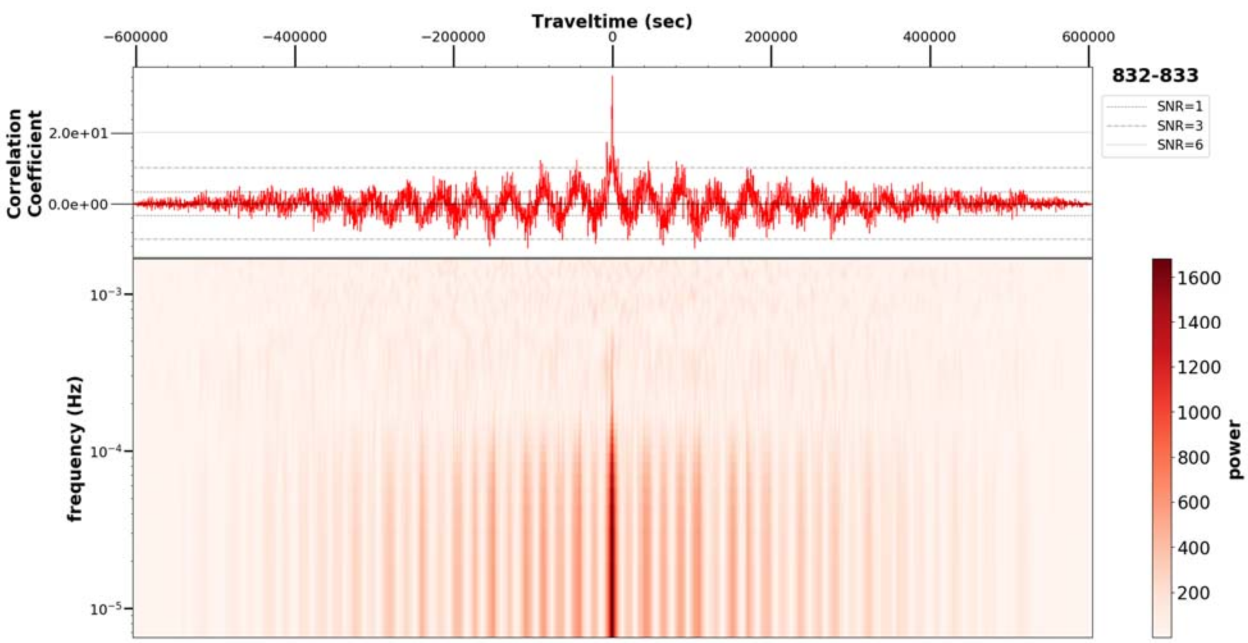

Figure A- 66. Spectrogram from stacked cross-correlated normalized 7-day length data segments. Station pair: 832-833

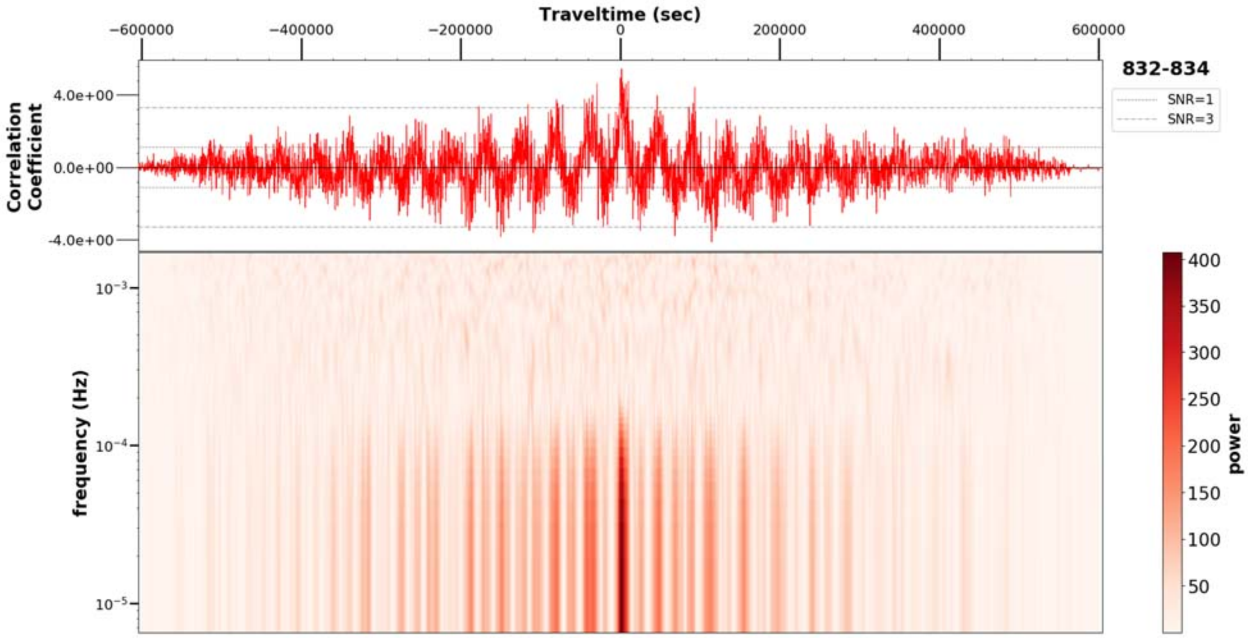

Figure A- 67. Spectrogram from stacked cross-correlated normalized 7-day length data segments. Station pair: 832-834

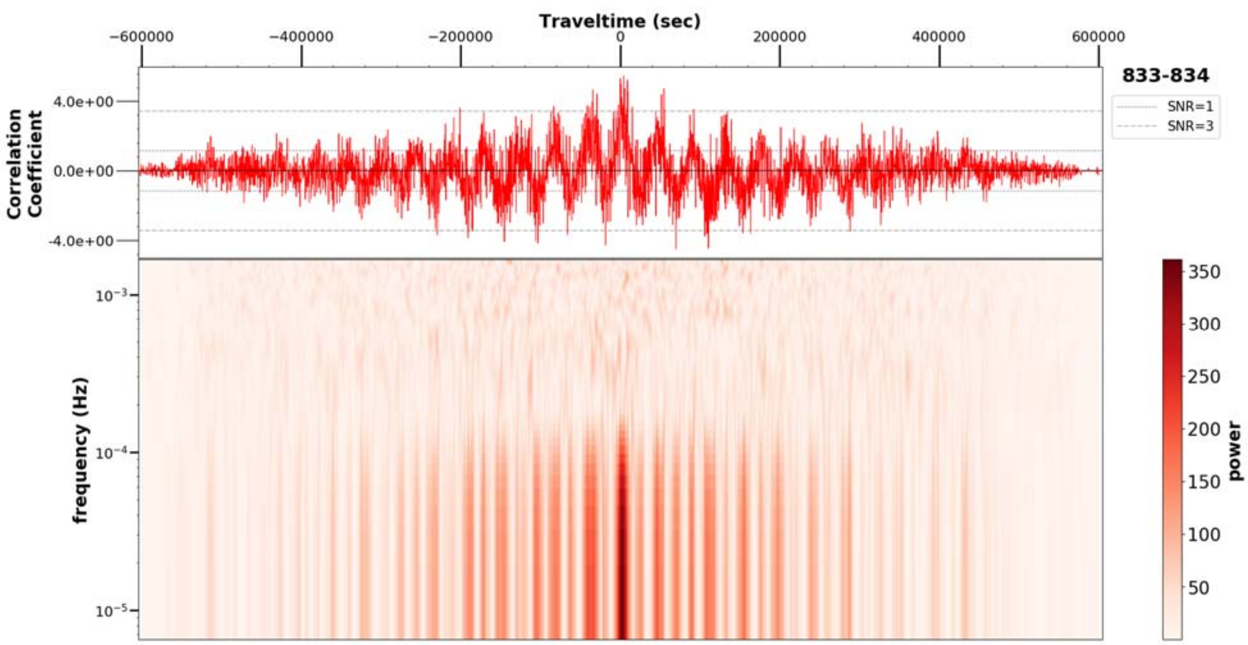

Figure A- 68. Spectrogram from stacked cross-correlated normalized 7-day length data segments. Station pair: 833-834

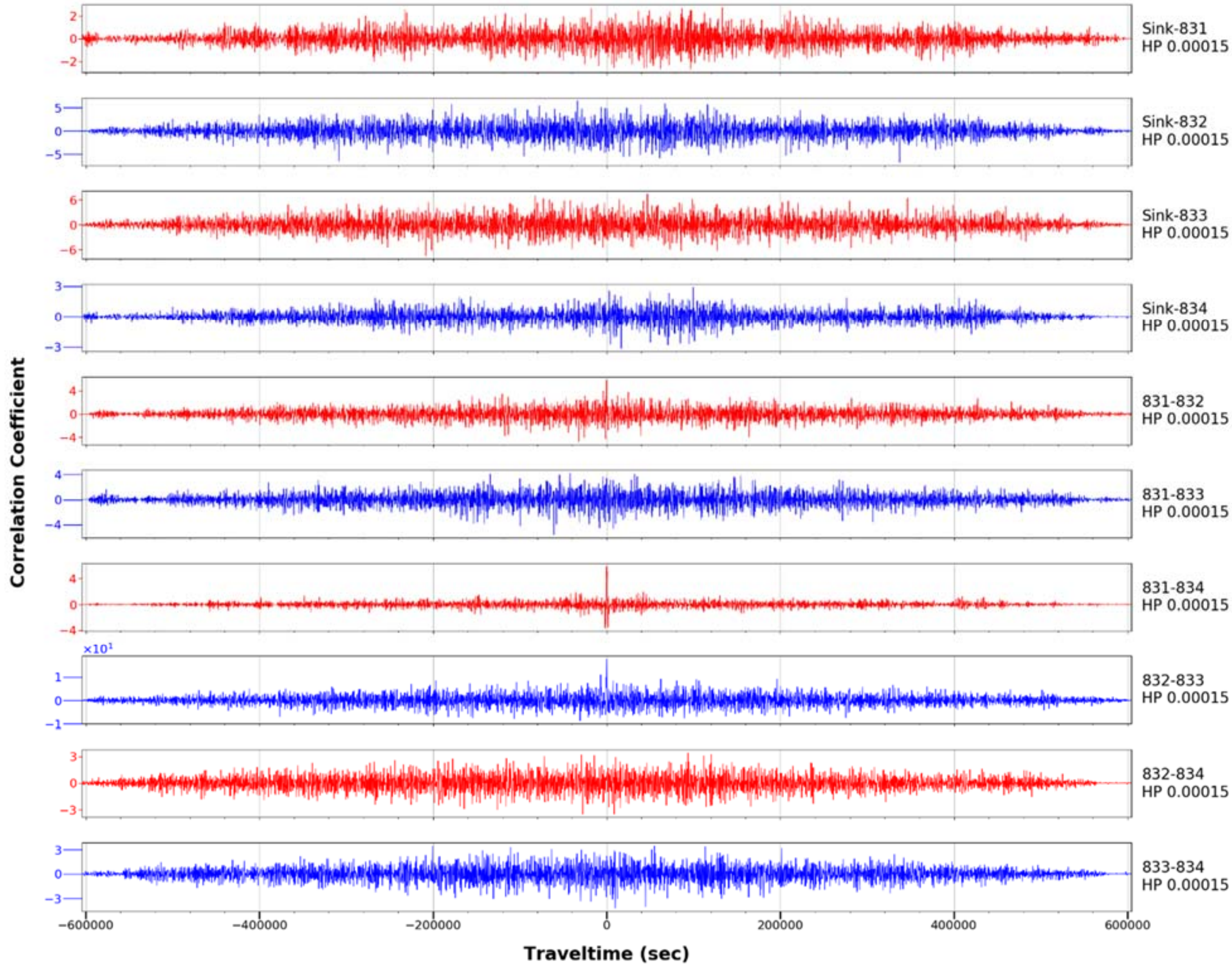

Figure A- 69. Stacked cross-correlograms from 7-day data segment lengths and normalized water level amplitudes. Correlograms were high-pass (HP) filtered with a corner frequency of 0.00015 Hz, or a period of just under 2 hours, which is indicated to the right of each panel.

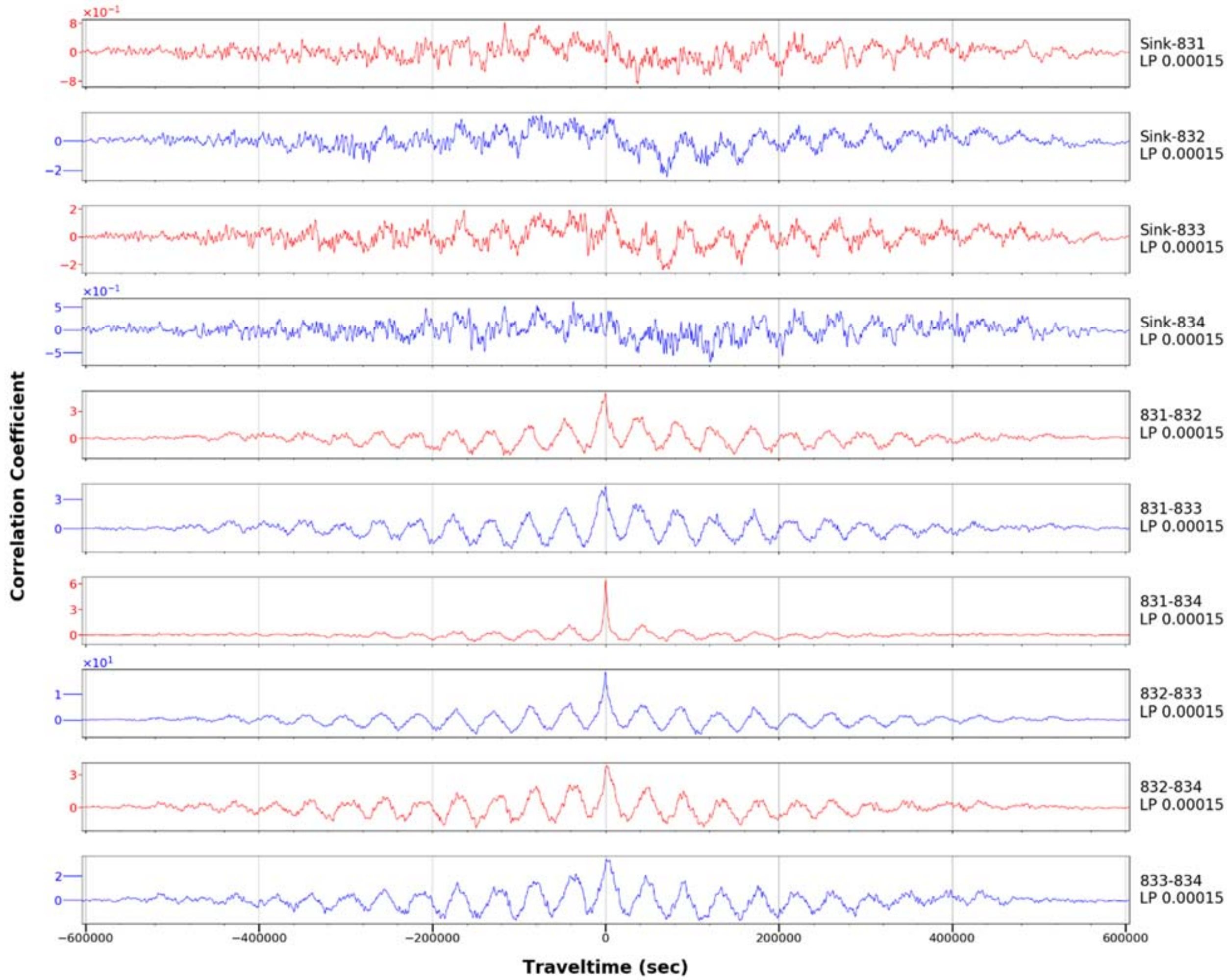

Figure A- 70. Stacked cross-correlograms from 7-day data segment lengths and normalized water level amplitudes. Correlograms were low-pass (LP) filtered with a corner frequency of 0.00015 Hz, or a period of just under 2 hours, which is indicated to the right of each panel.

All Daily Length Data Segments – Normalized Amplitudes

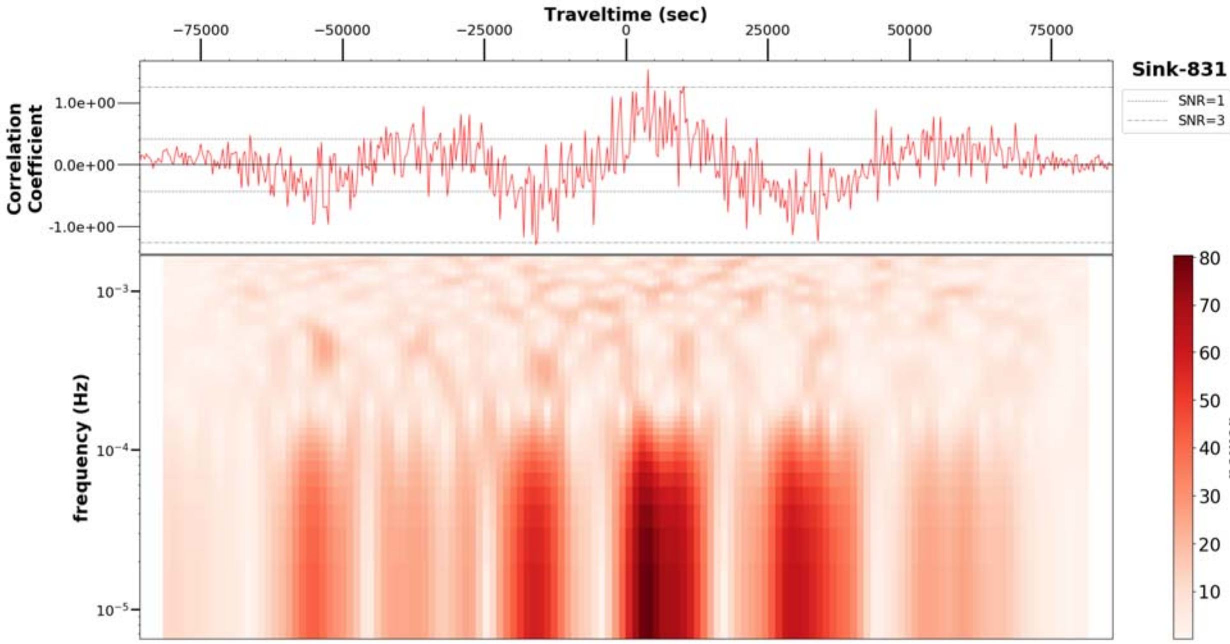

Figure A- 71. Spectrogram from stacked cross-correlated normalized daily length data segments, all segments. Station pair: Sink-831

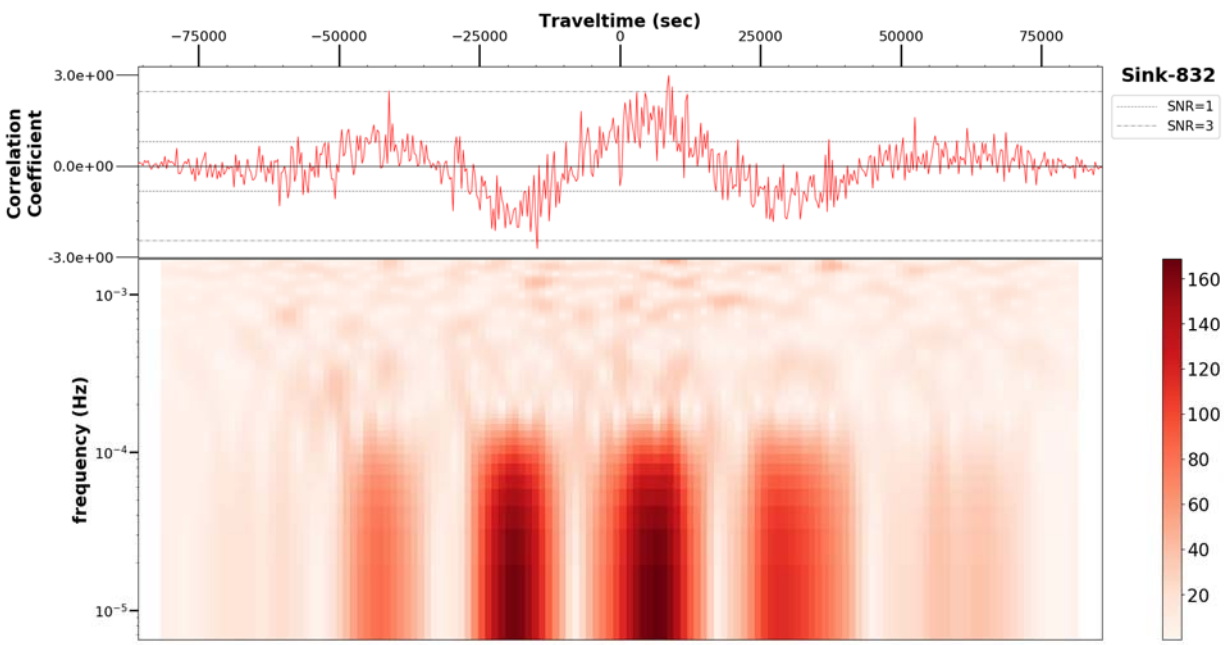

Figure A- 72. Spectrogram from stacked cross-correlated normalized daily length data segments, all segments. Station pair: Sink-832

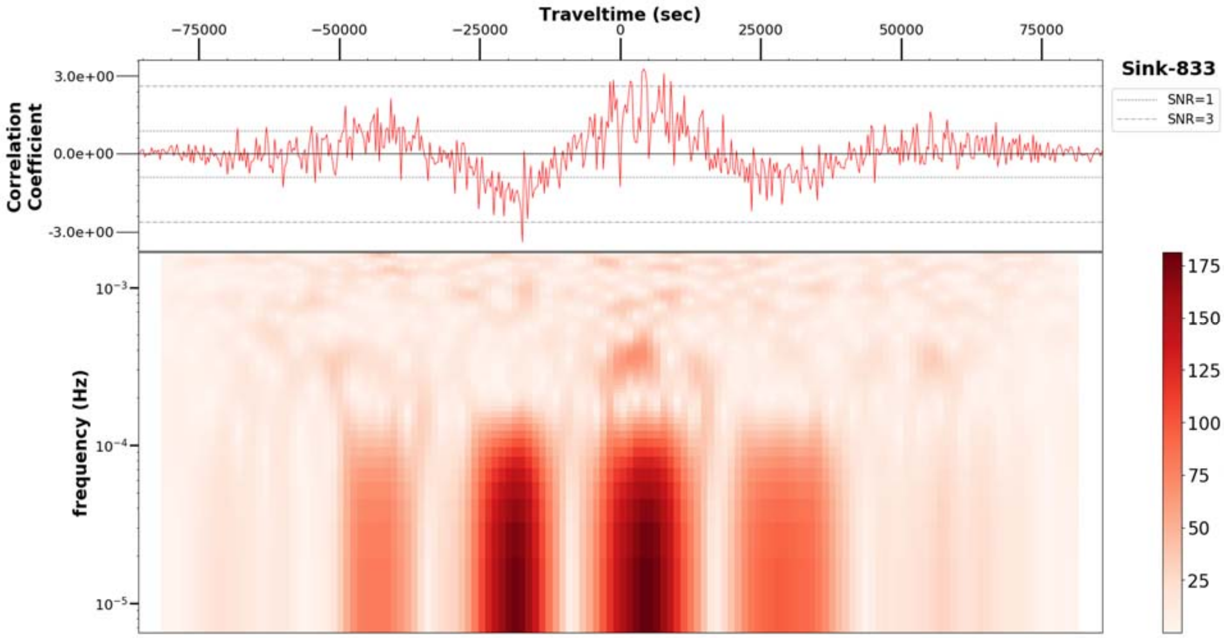

Figure A- 73. Spectrogram from stacked cross-correlated normalized daily length data segments, all segments. Station pair: Sink-833

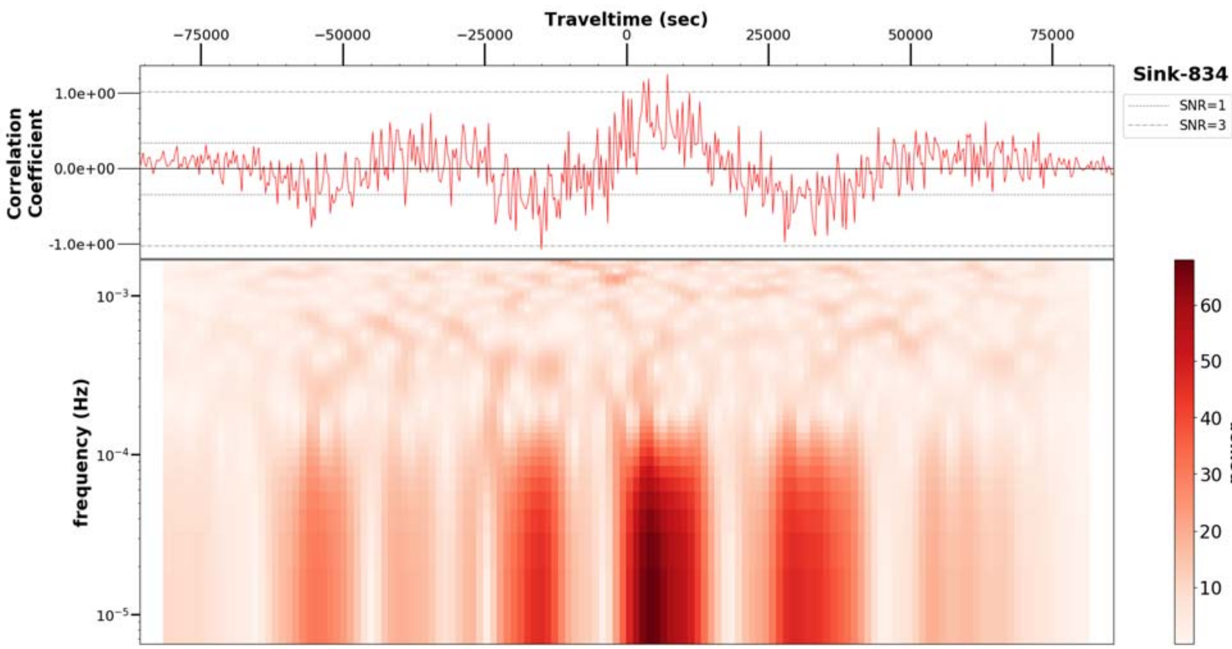

Figure A- 74. Spectrogram from stacked cross-correlated normalized daily length data segments, all segments. Station pair: Sink-834

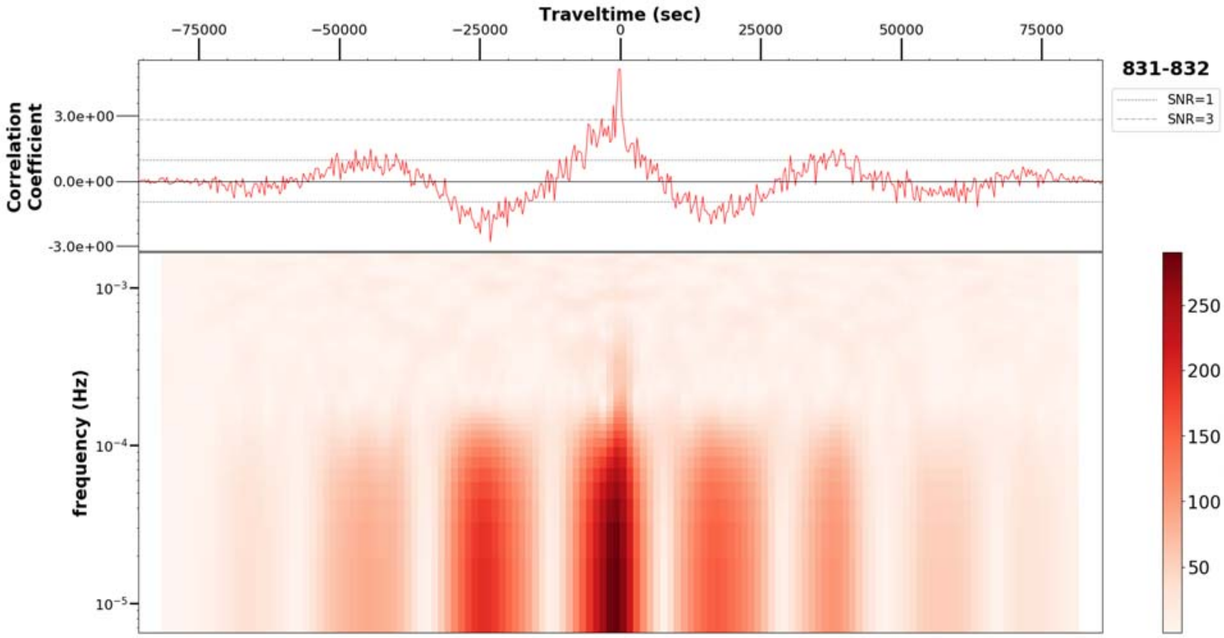

Figure A- 75. Spectrogram from stacked cross-correlated normalized daily length data segments, all segments. Station pair: 831-832

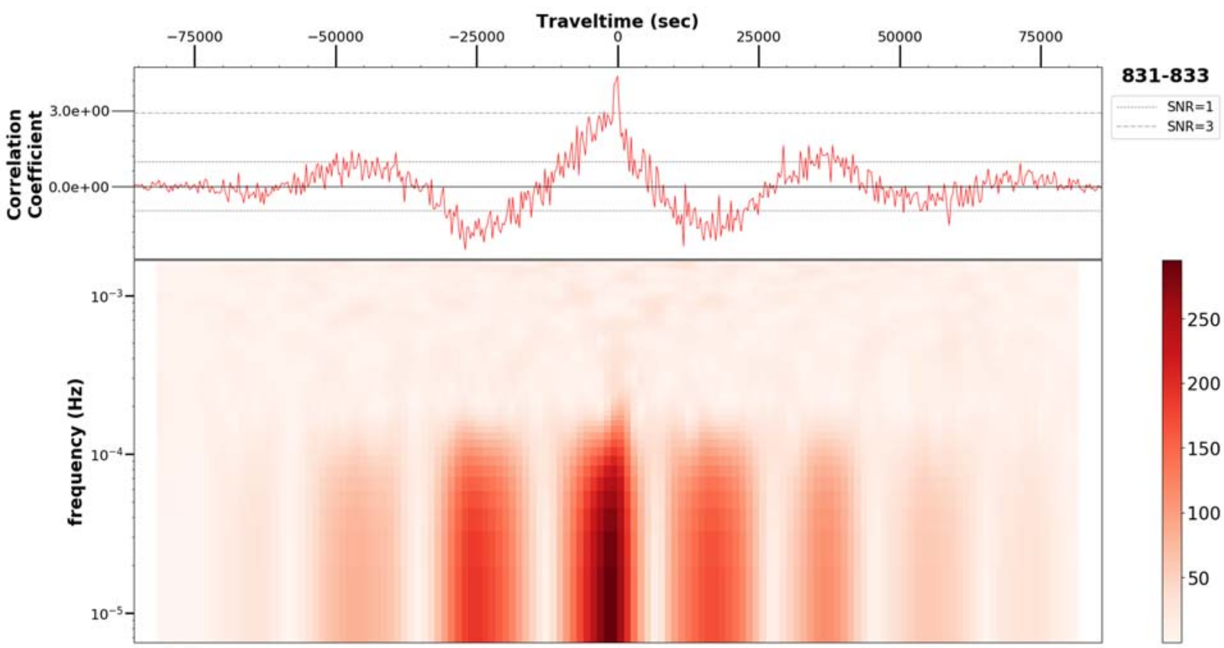

Figure A- 76. Spectrogram from stacked cross-correlated normalized daily length data segments, all segments. Station pair: 831-833

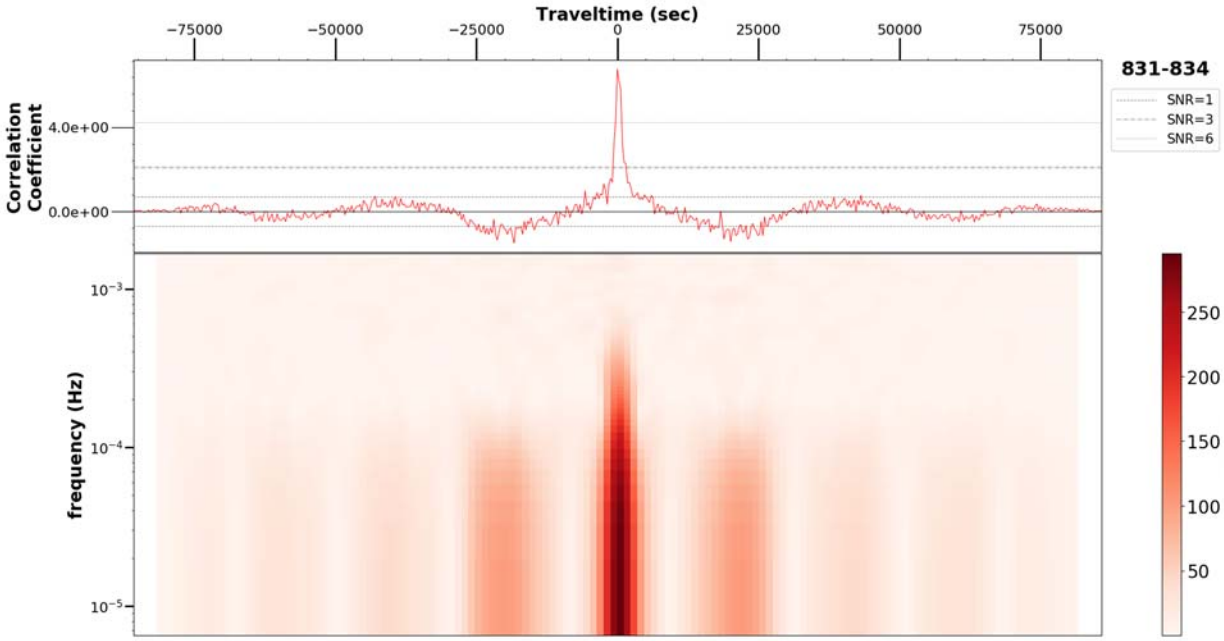

Figure A- 77. Spectrogram from stacked cross-correlated normalized daily length data segments, all segments. Station pair: 831-834

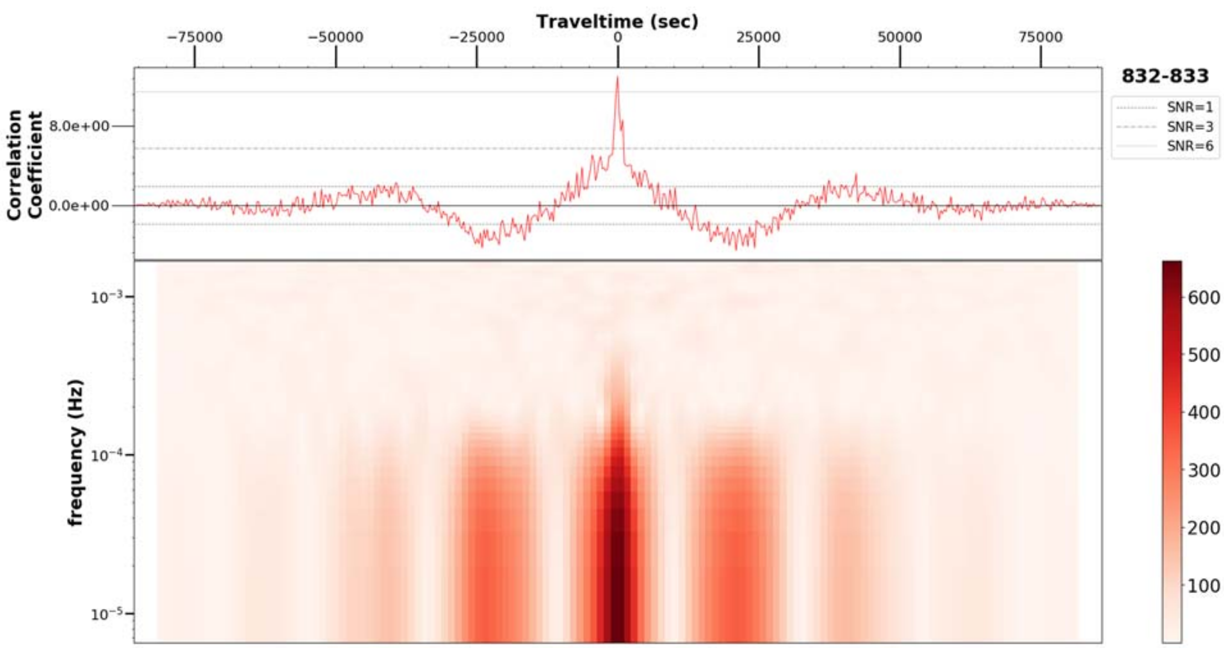

Figure A- 78. Spectrogram from stacked cross-correlated normalized daily length data segments, all segments. Station pair: 832-833

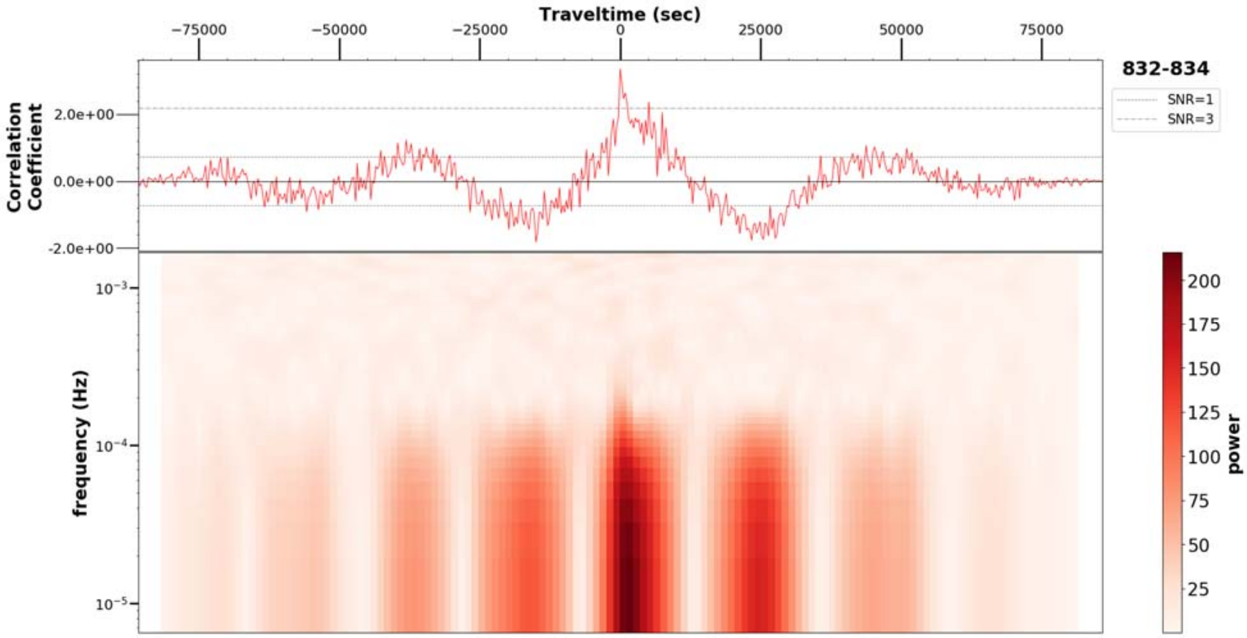

Figure A- 79. Spectrogram from stacked cross-correlated normalized daily length data segments, all segments. Station pair: 832-834

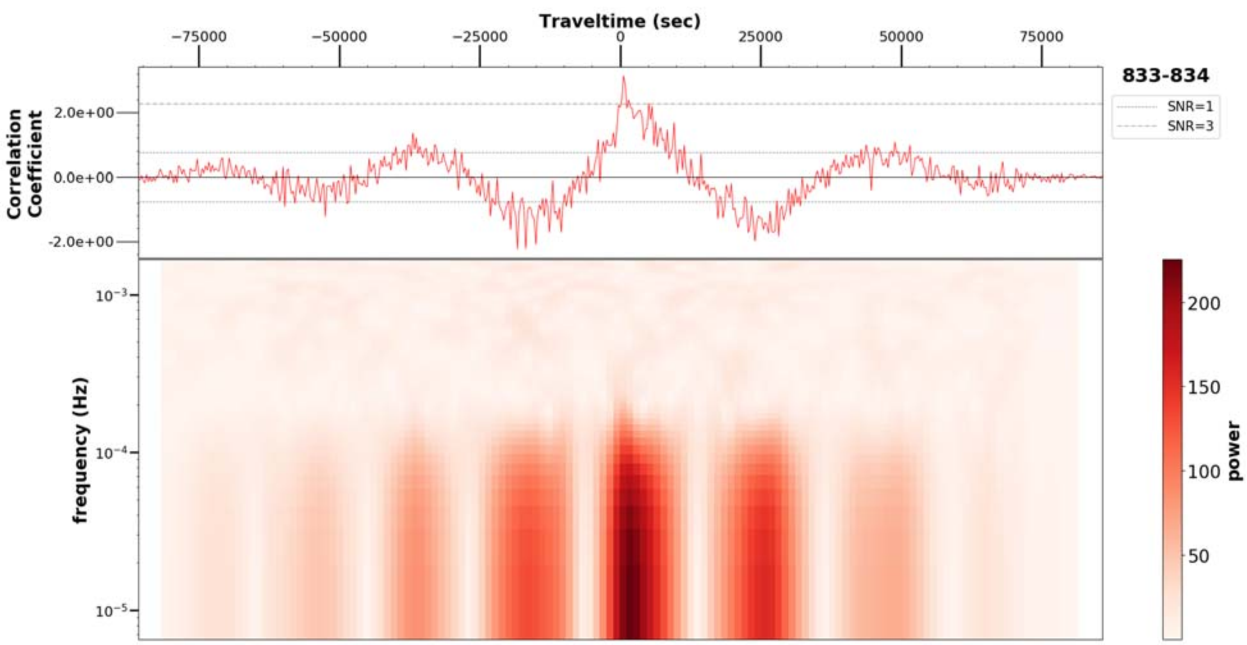

Figure A- 80. Spectrogram from stacked cross-correlated normalized daily length data segments, all segments. Station pair: 833-834

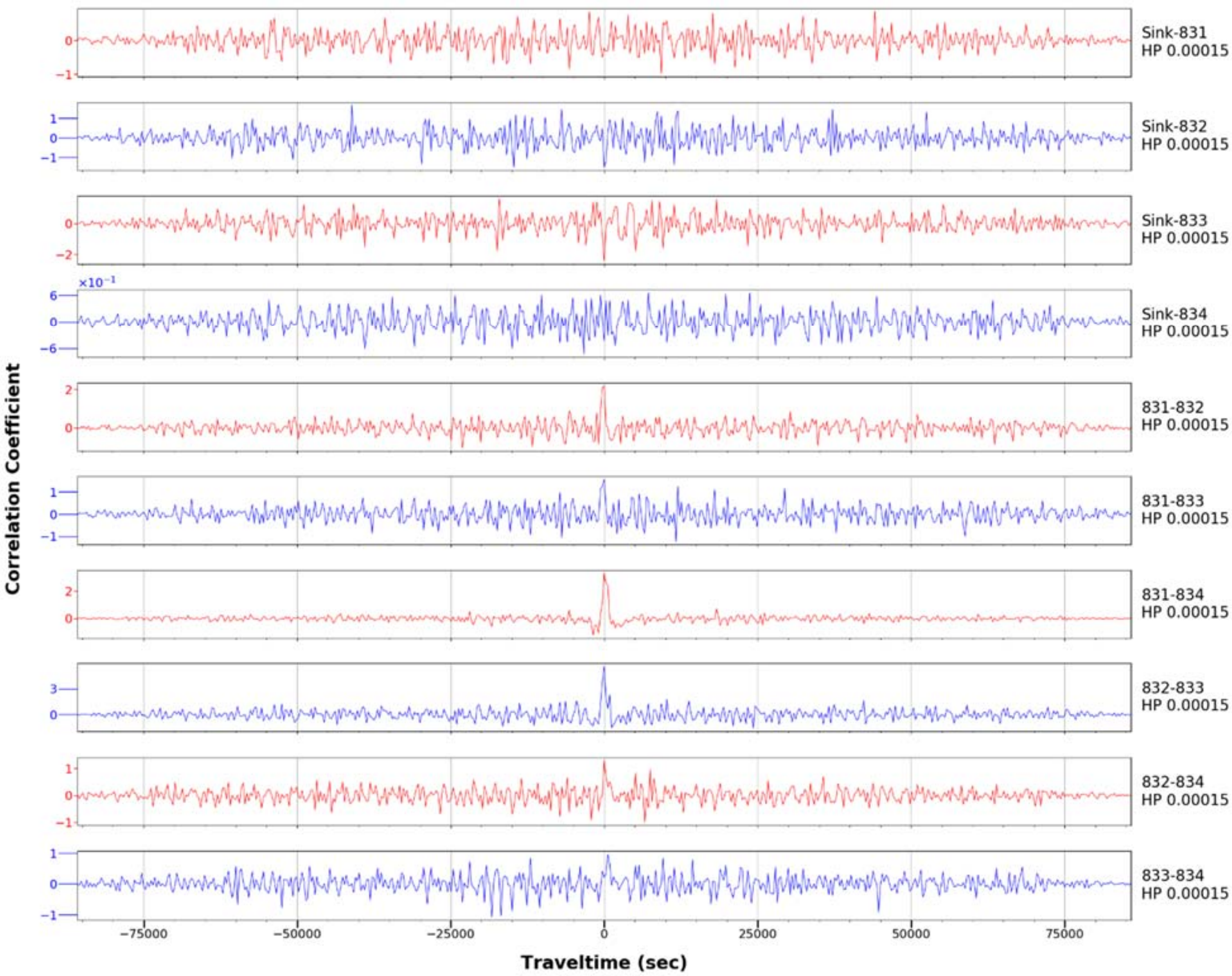

Figure A- 81. Stacked cross-correlograms from all daily data segment lengths and normalized water level amplitudes. Correlograms were high-pass (HP) filtered with a corner frequency of 0.00015 Hz, or a period of just under 2 hours, which is indicated to the right of each panel.

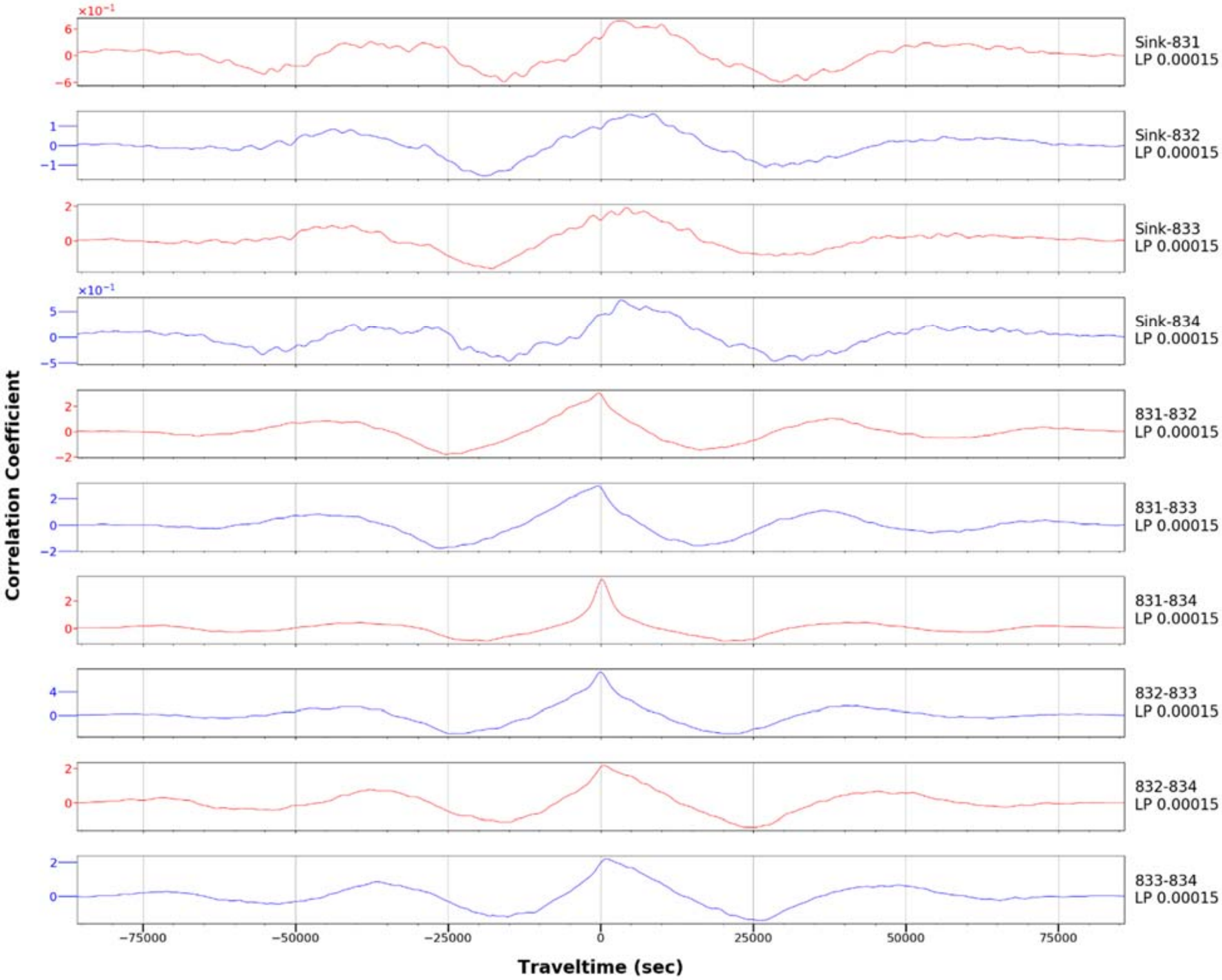

Figure A- 82. Stacked cross-correlograms from all daily data segment lengths and normalized water level amplitudes. Correlograms were low-pass (LP) filtered with a corner frequency of 0.00015 Hz, or a period of just under 2 hours, which is indicated to the right of each panel.

Pumping-Period-Only Daily Length Data Segments – Normalized Amplitudes

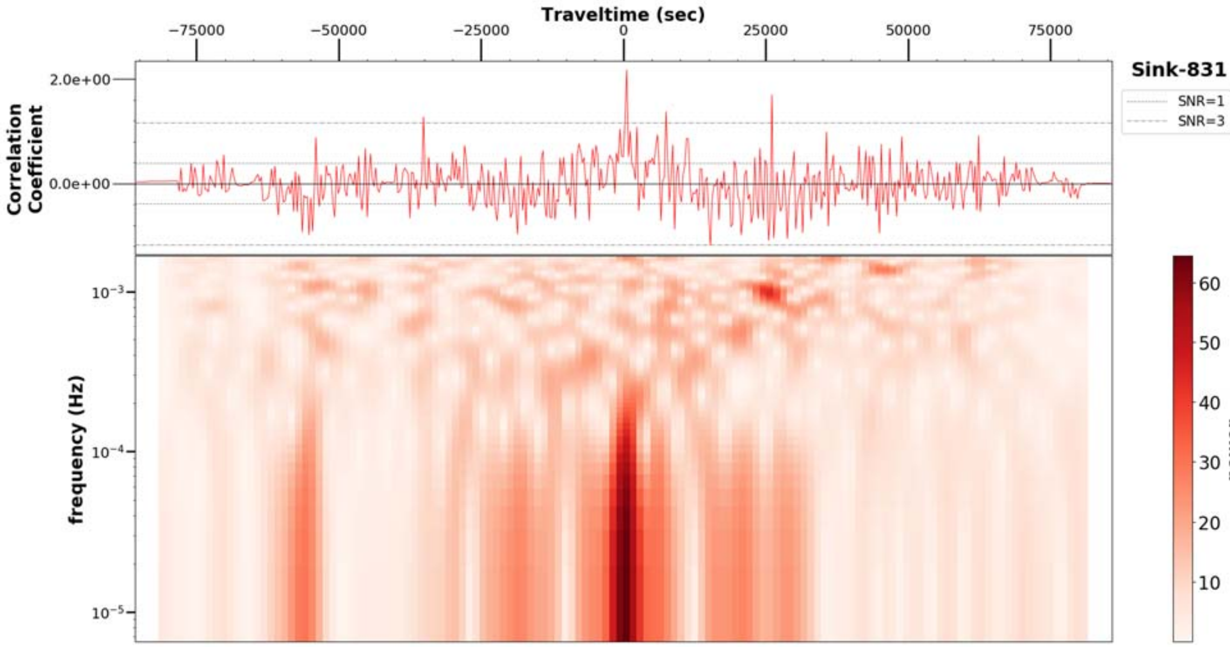

Figure A- 83. Spectrogram from stacked cross-correlated normalized daily length data segments, pumping-period-only segments. Station pair: Sink-831

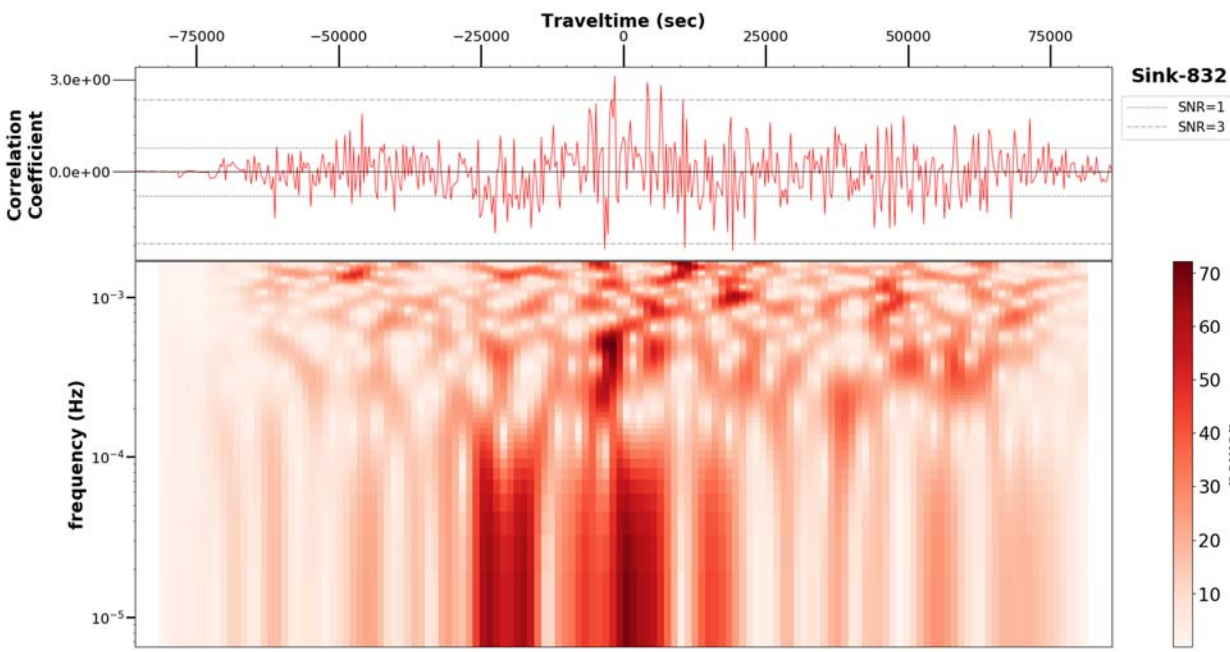

Figure A- 84. Spectrogram from stacked cross-correlated normalized daily length data segments, pumping-period-only segments. Station pair: Sink-832

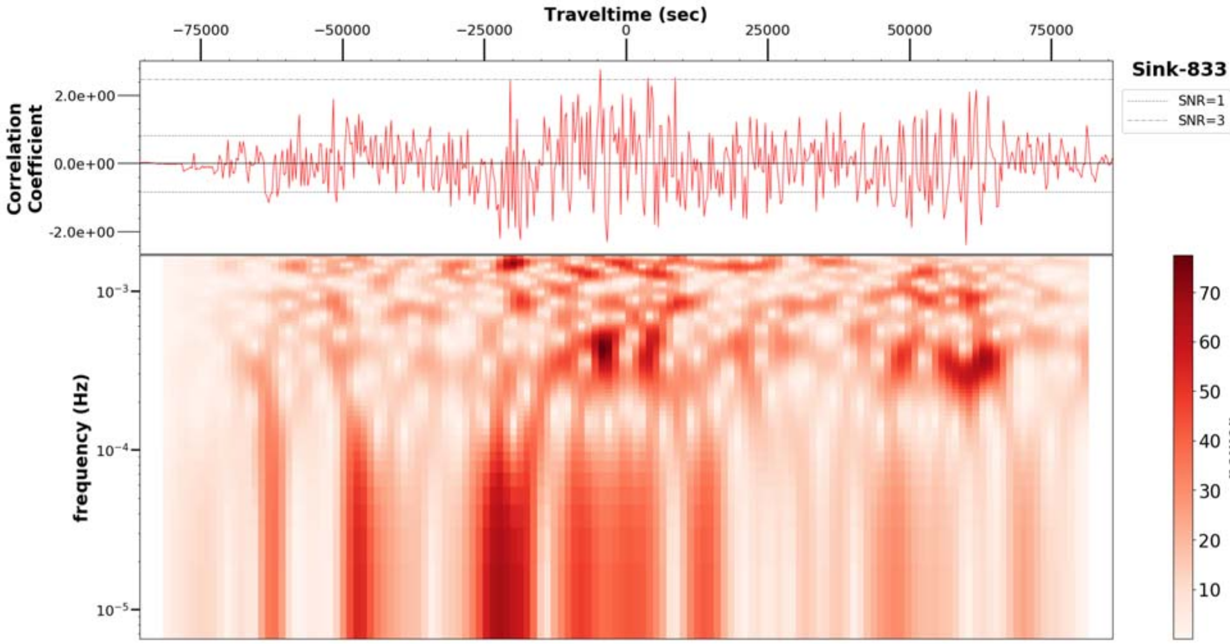

Figure A- 85. Spectrogram from stacked cross-correlated normalized daily length data segments, pumping-period-only segments. Station pair: Sink-833

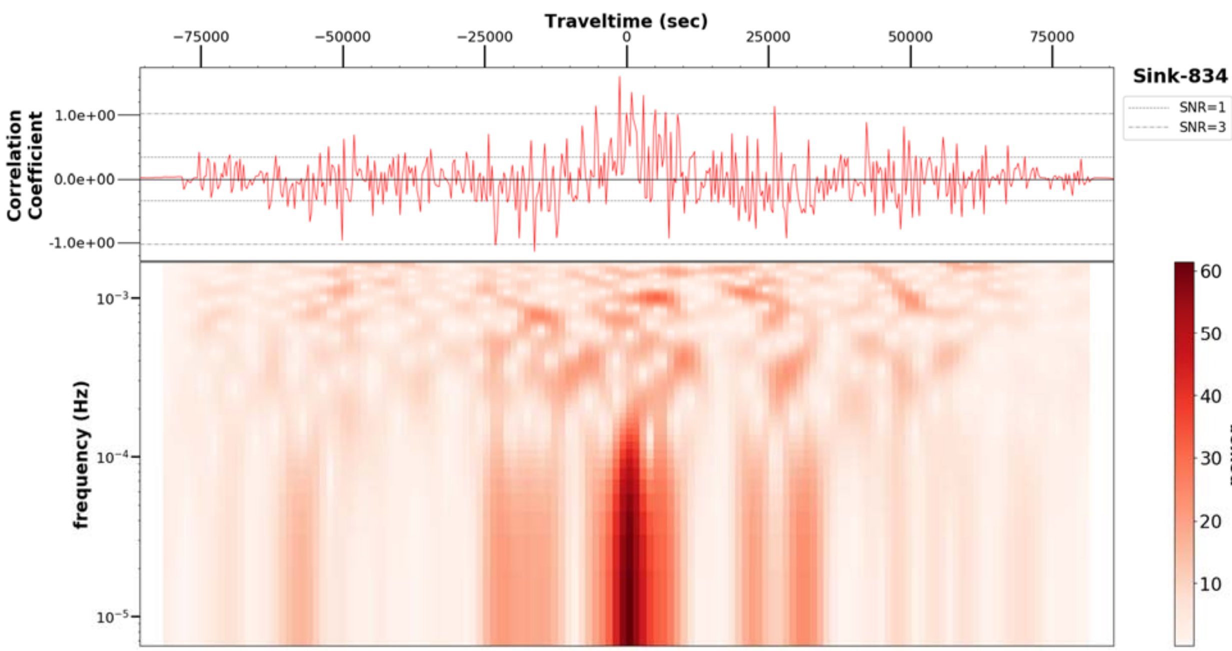

Figure A- 86. Spectrogram from stacked cross-correlated normalized daily length data segments, pumping-period-only segments. Station pair: Sink-834

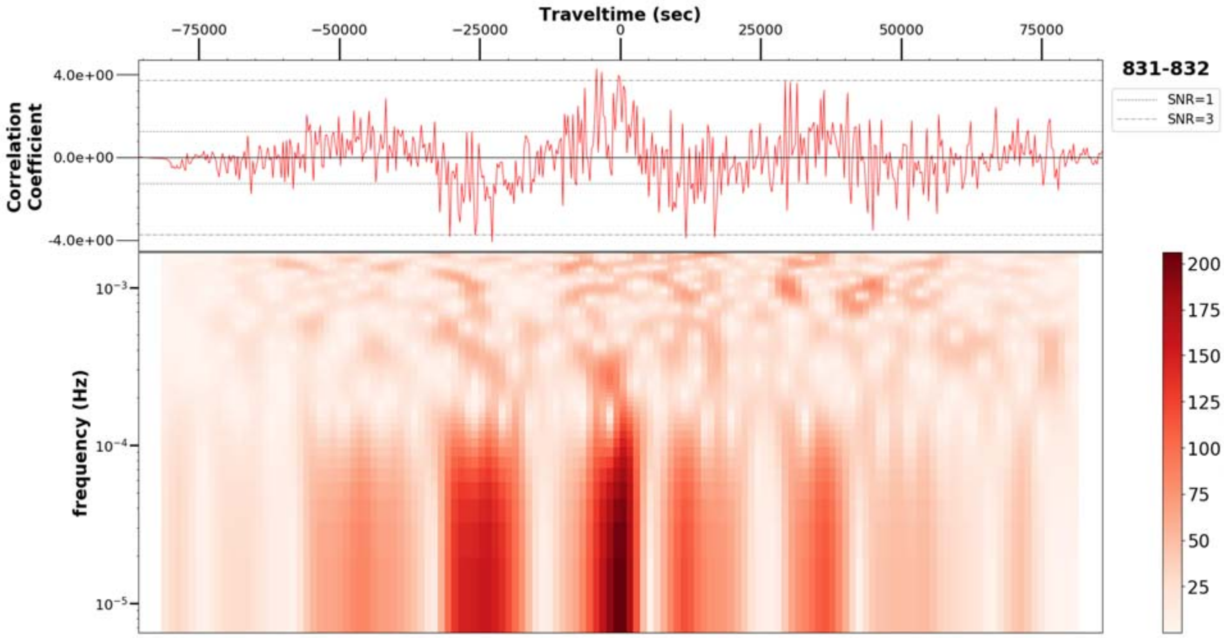

Figure A- 87. Spectrogram from stacked cross-correlated normalized daily length data segments, pumping-period-only segments. Station pair: 831-832

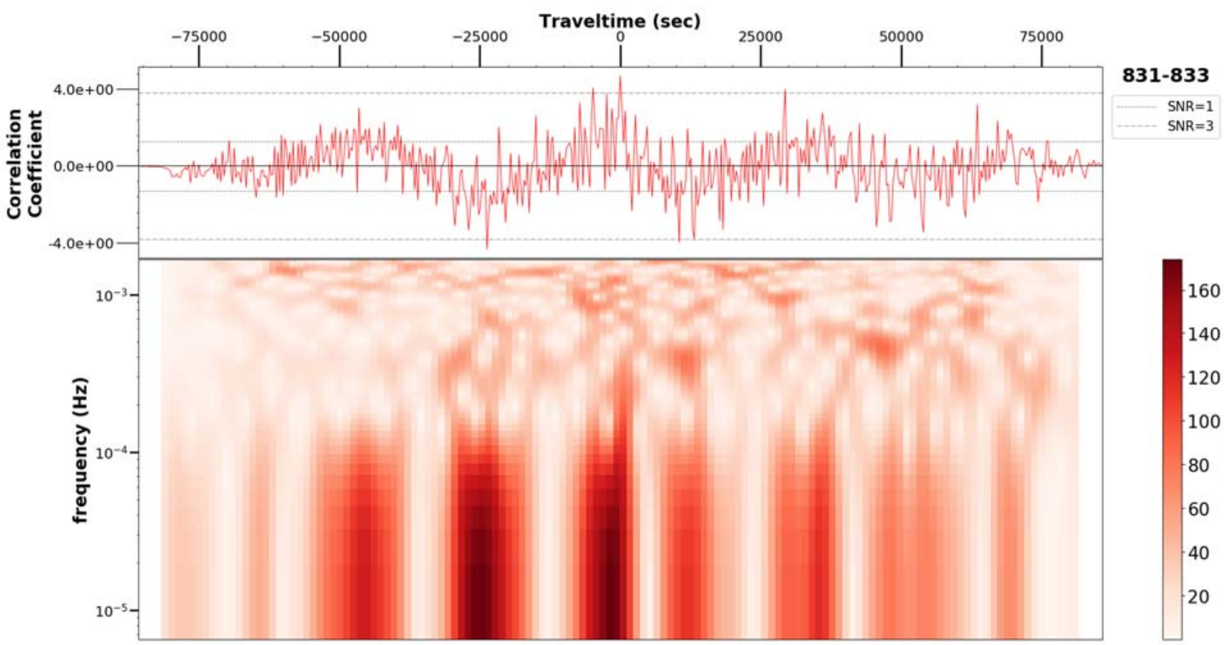

Figure A- 88. Spectrogram from stacked cross-correlated normalized daily length data segments, pumping-period-only segments. Station pair: 831-833

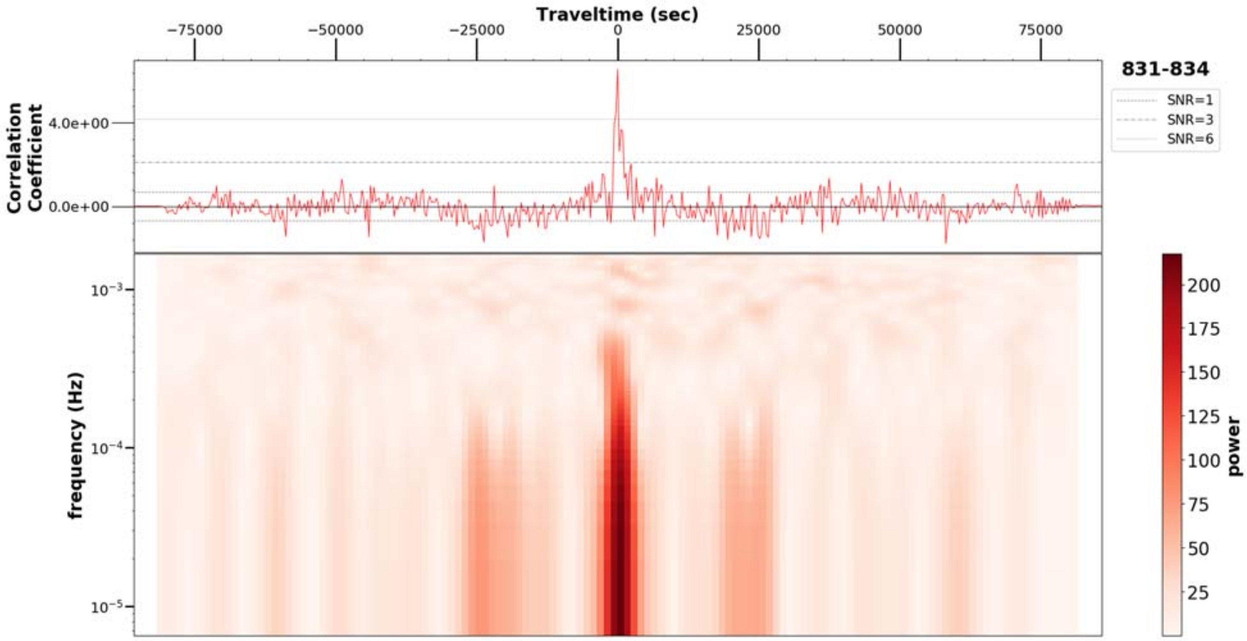

Figure A- 89. Spectrogram from stacked cross-correlated normalized daily length data segments, pumping-period-only segments. Station pair: 831-834

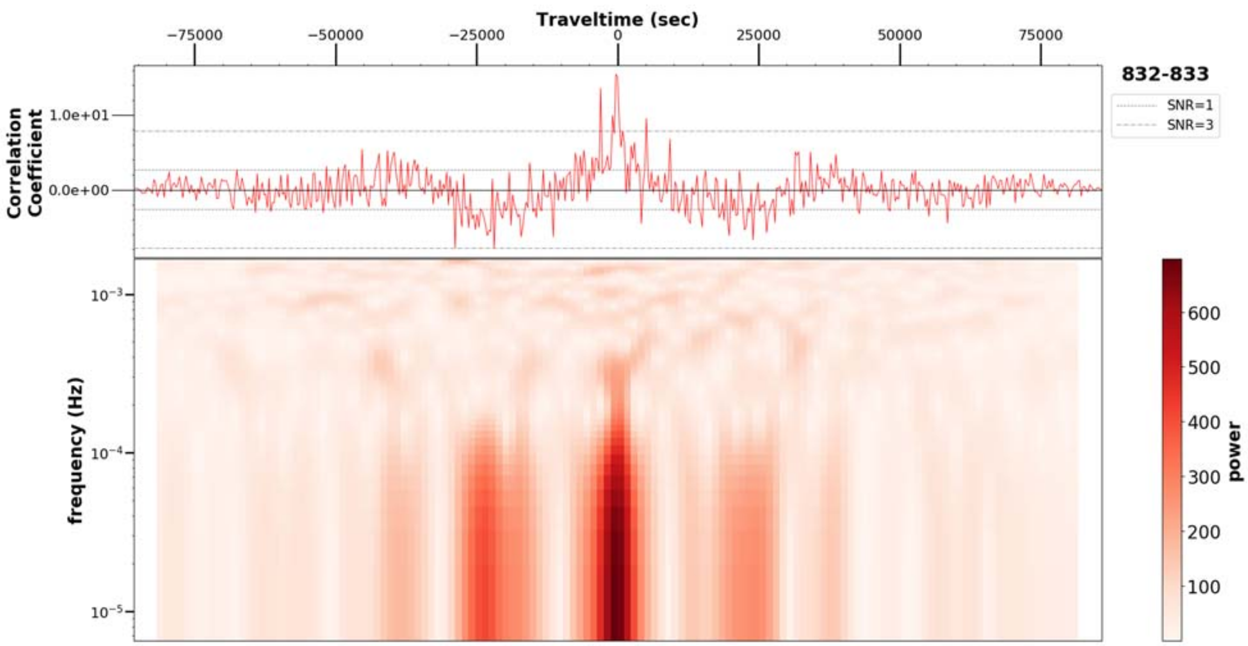

Figure A- 90. Spectrogram from stacked cross-correlated normalized daily length data segments, pumping-period-only segments. Station pair: 832-833

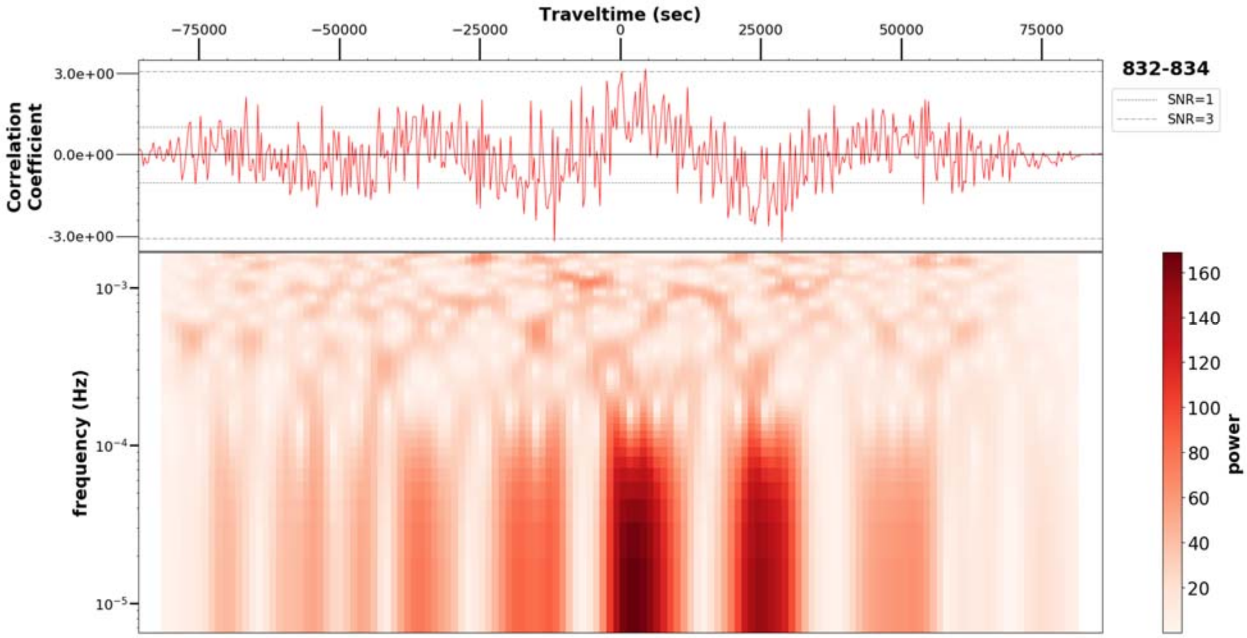

Figure A- 91. Spectrogram from stacked cross-correlated normalized daily length data segments, pumping-period-only segments. Station pair: 832-834

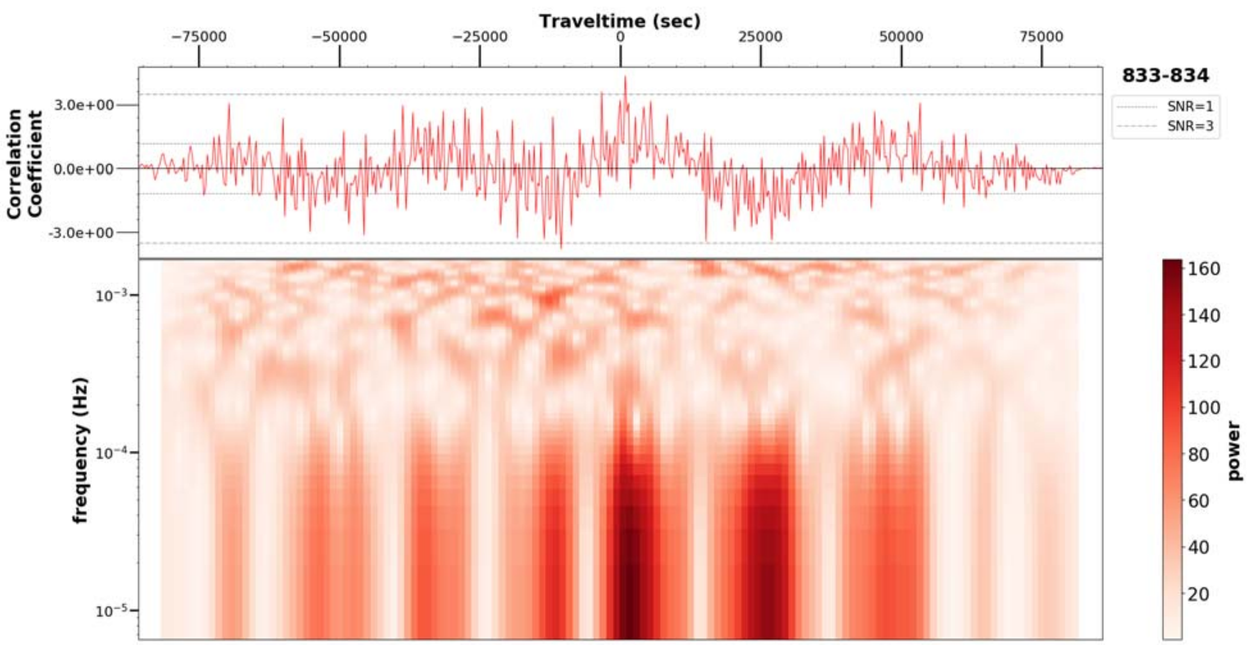

Figure A- 92. Spectrogram from stacked cross-correlated normalized daily length data segments, pumping-period-only segments. Station pair: 833-834

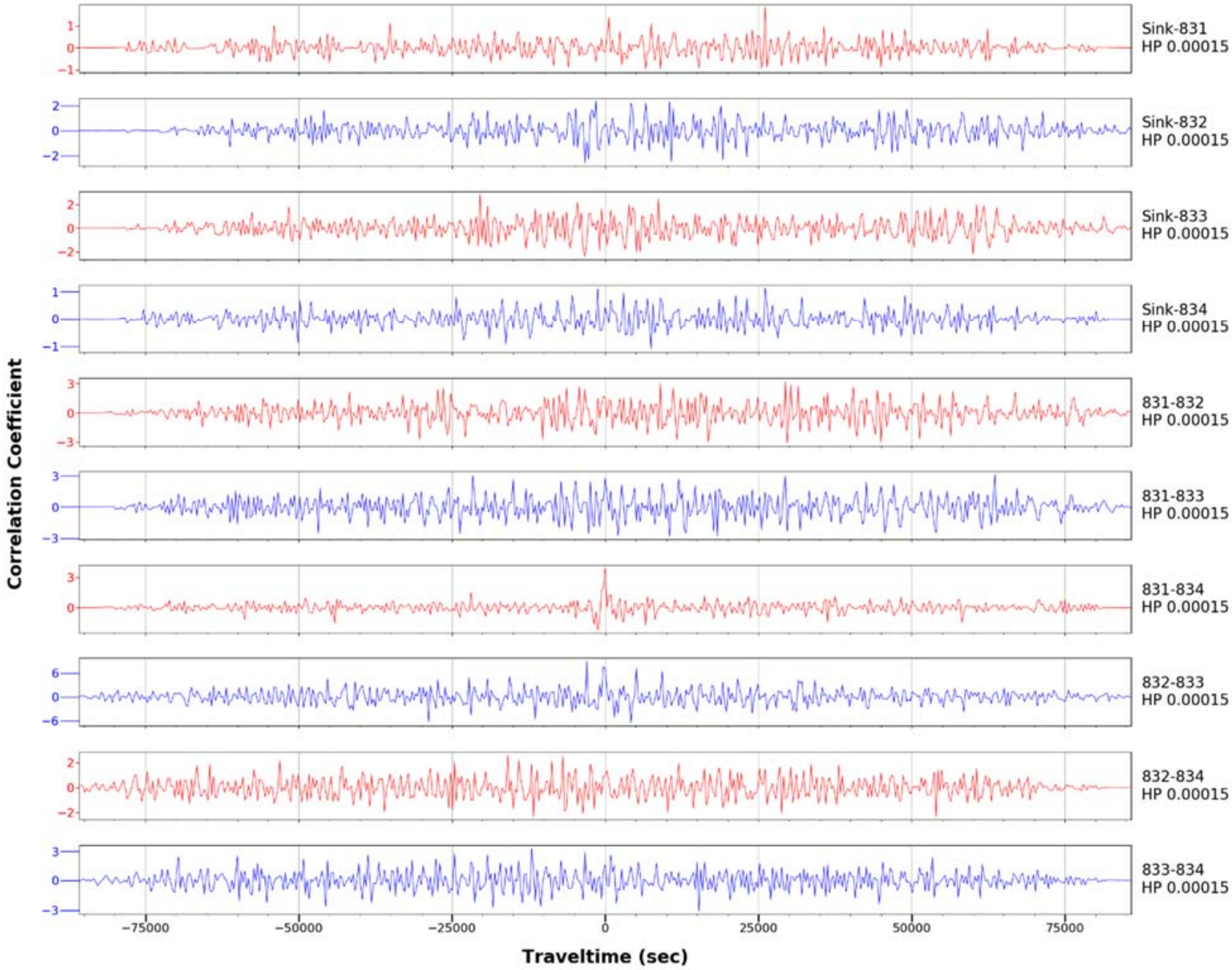

Figure A- 93. Stacked cross-correlograms from pumping-period-only daily data segment lengths and normalized water level amplitudes. Correlograms were high-pass (HP) filtered with a corner frequency of 0.00015 Hz, or a period of just under 2 hours, which is indicated to the right of each panel.

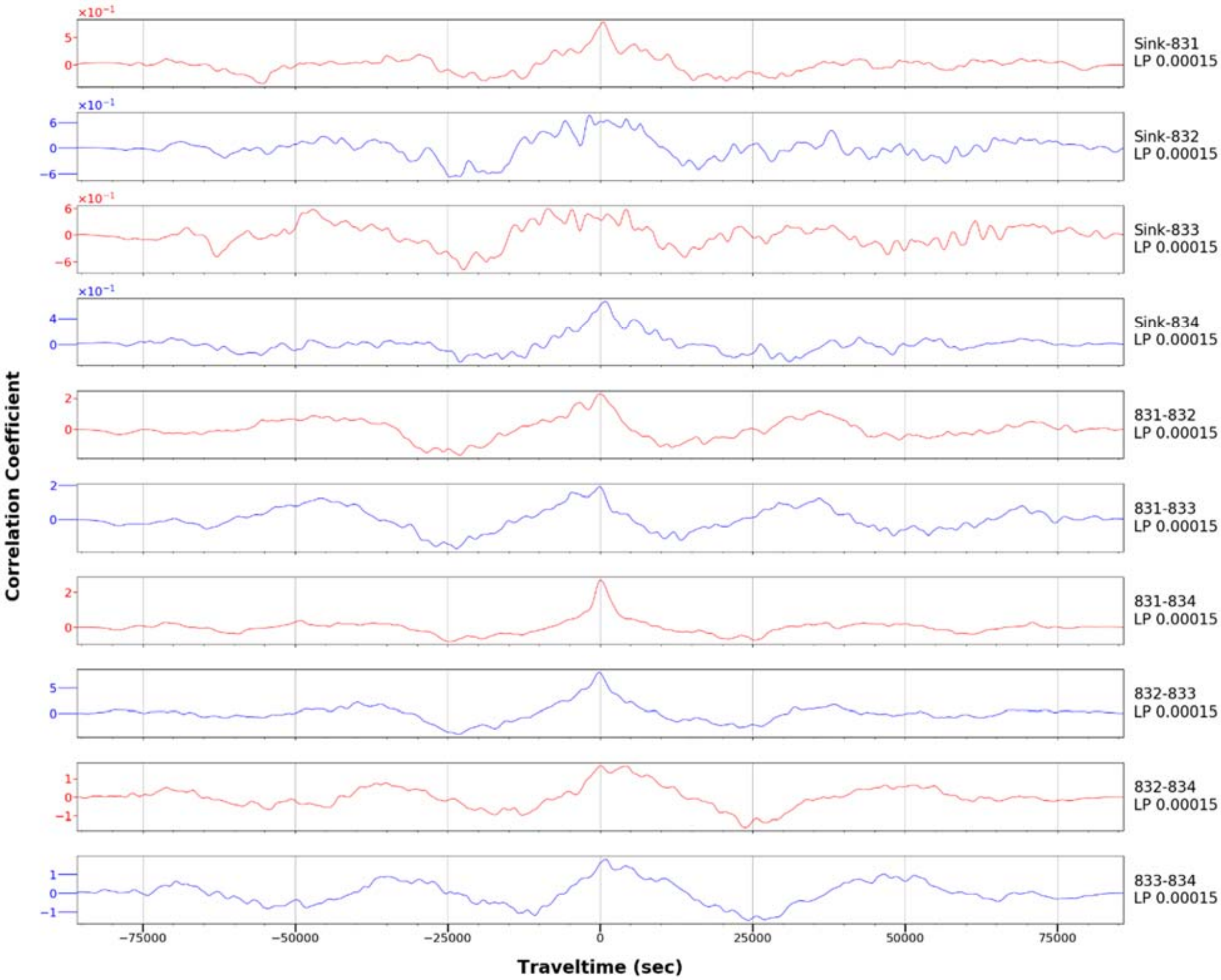

Figure A- 94. Stacked cross-correlograms from pumping-period-only daily data segment lengths and normalized water level amplitudes. Correlograms were low-pass (LP) filtered with a corner frequency of 0.00015 Hz, or a period of just under 2 hours, which is indicated to the right of each panel.

30-Day Length Data Segments – Preserved Amplitudes

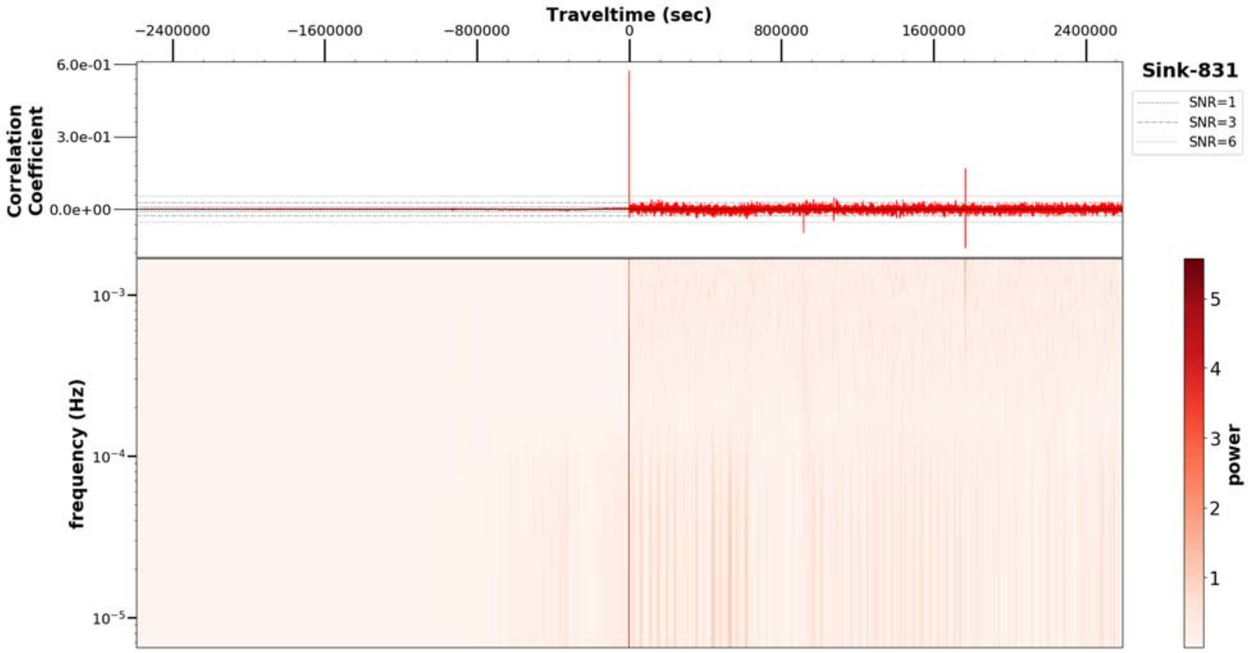

Figure A- 95. Spectrogram from stacked cross-correlated 30-day length data segments with preserved amplitudes (not normalized). Station pair: Sink-831

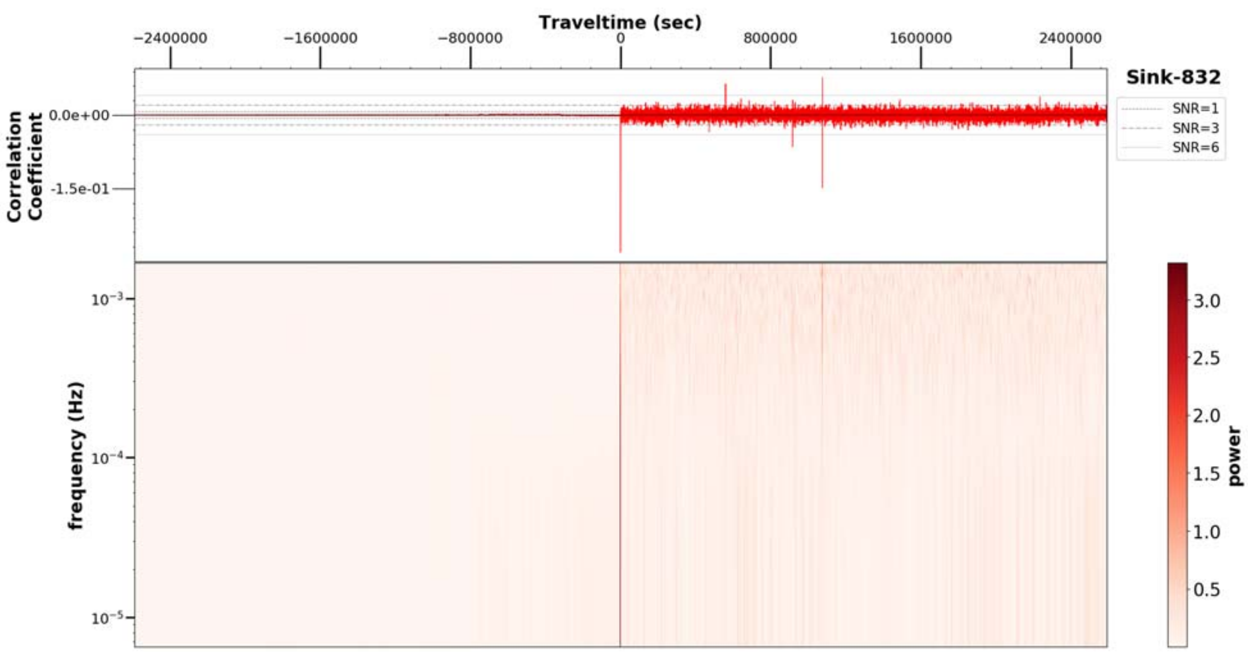

Figure A- 96. Spectrogram from stacked cross-correlated 30-day length data segments with preserved amplitudes (not normalized). Station pair: Sink-832

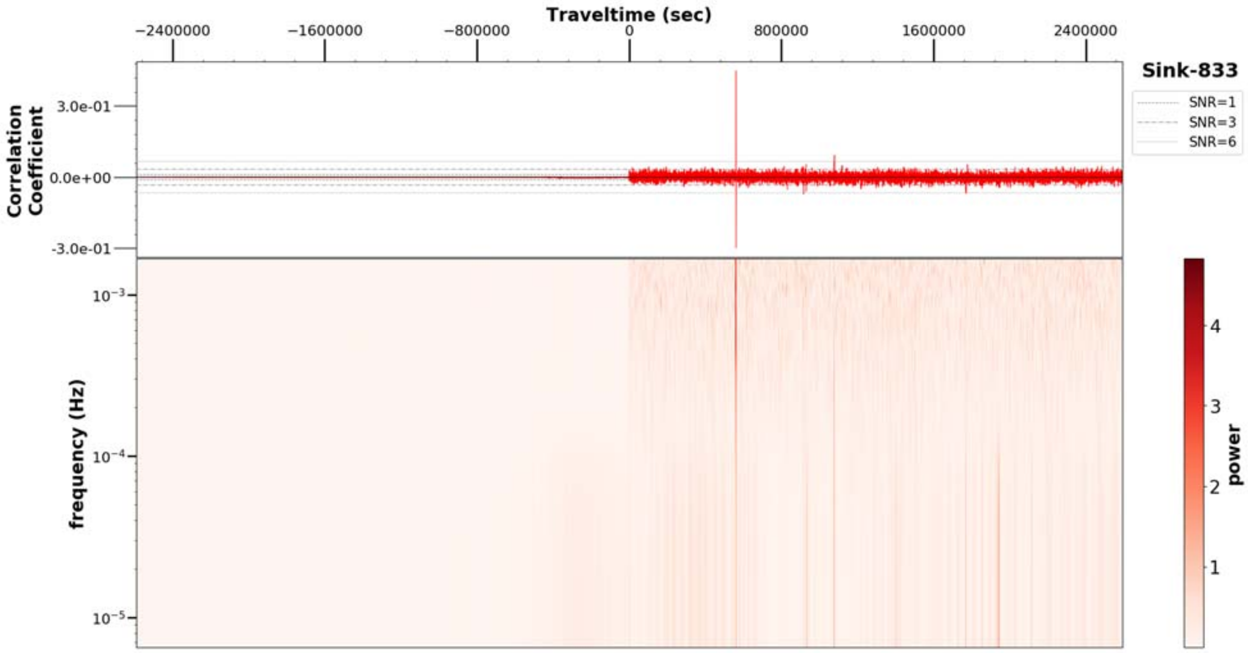

Figure A- 97. Spectrogram from stacked cross-correlated 30-day length data segments with preserved amplitudes (not normalized). Station pair: Sink-833

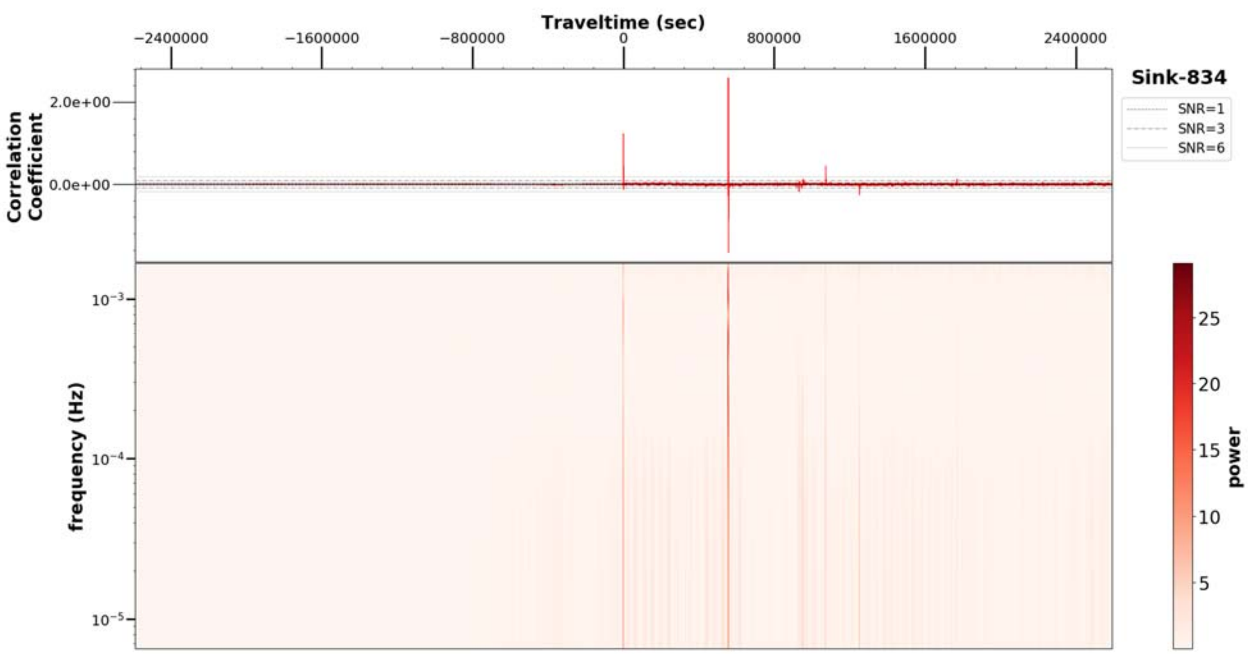

Figure A- 98. Spectrogram from stacked cross-correlated 30-day length data segments with preserved amplitudes (not normalized). Station pair: Sink-834

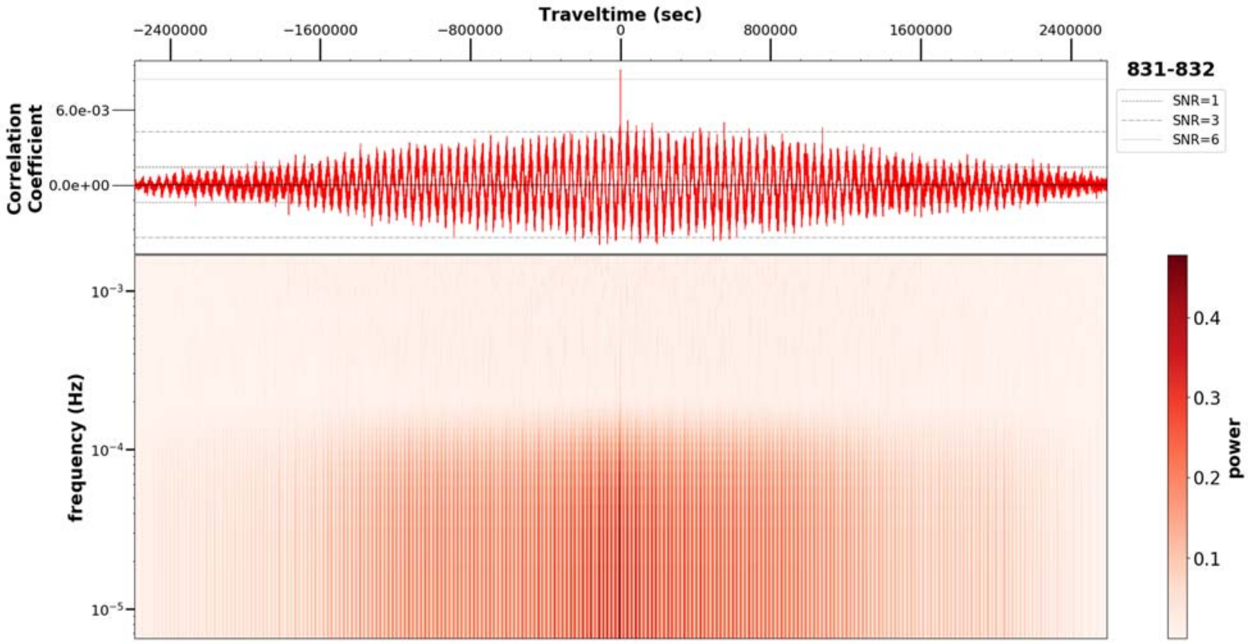

Figure A- 99. Spectrogram from stacked cross-correlated 30-day length data segments with preserved amplitudes (not normalized). Station pair: 831-832

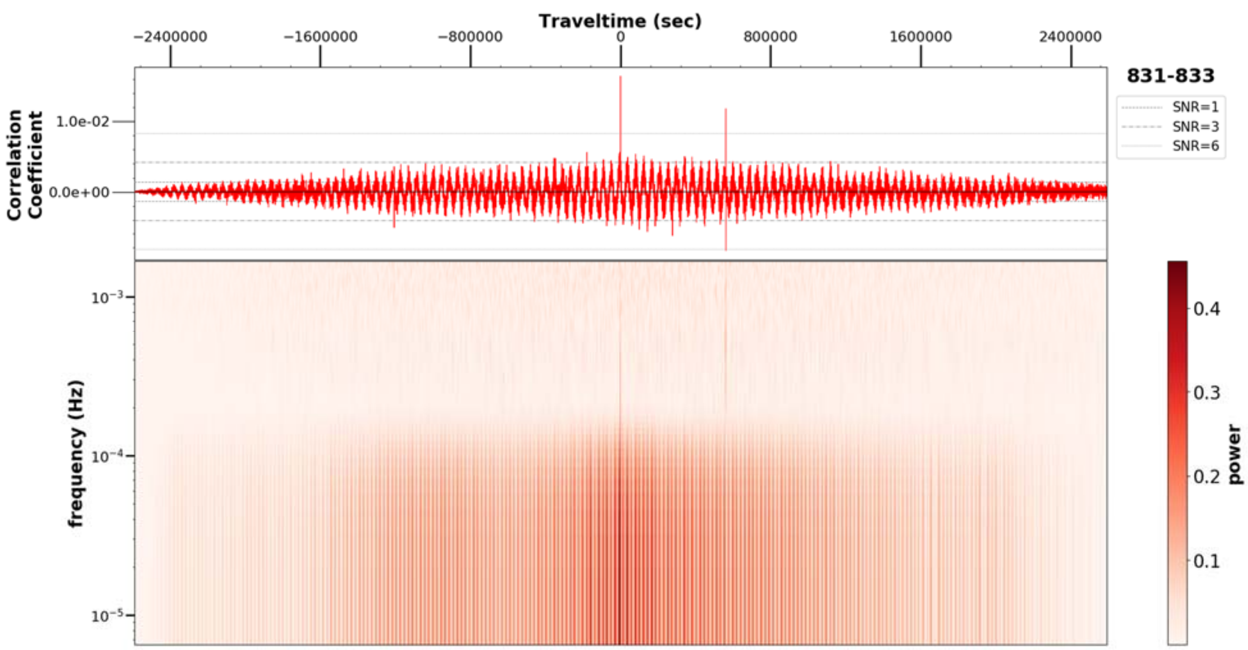

Figure A- 100. Spectrogram from stacked cross-correlated 30-day length data segments with preserved amplitudes (not normalized). Station pair: 831-833

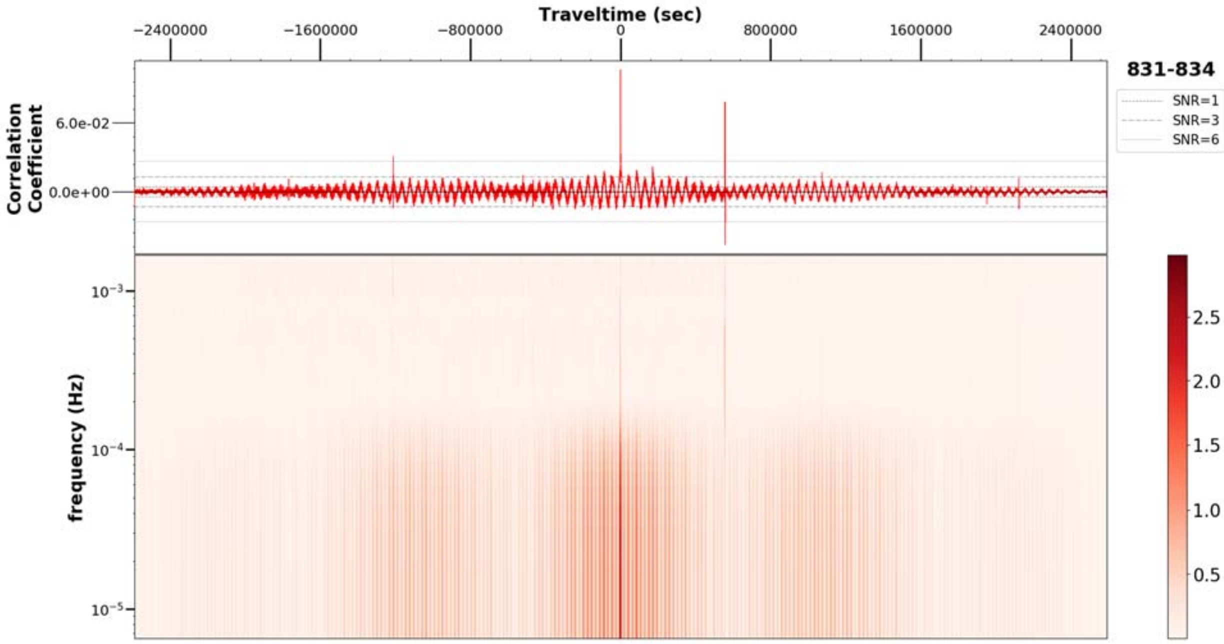

Figure A- 101. Spectrogram from stacked cross-correlated 30-day length data segments with preserved amplitudes (not normalized). Station pair: 831-834

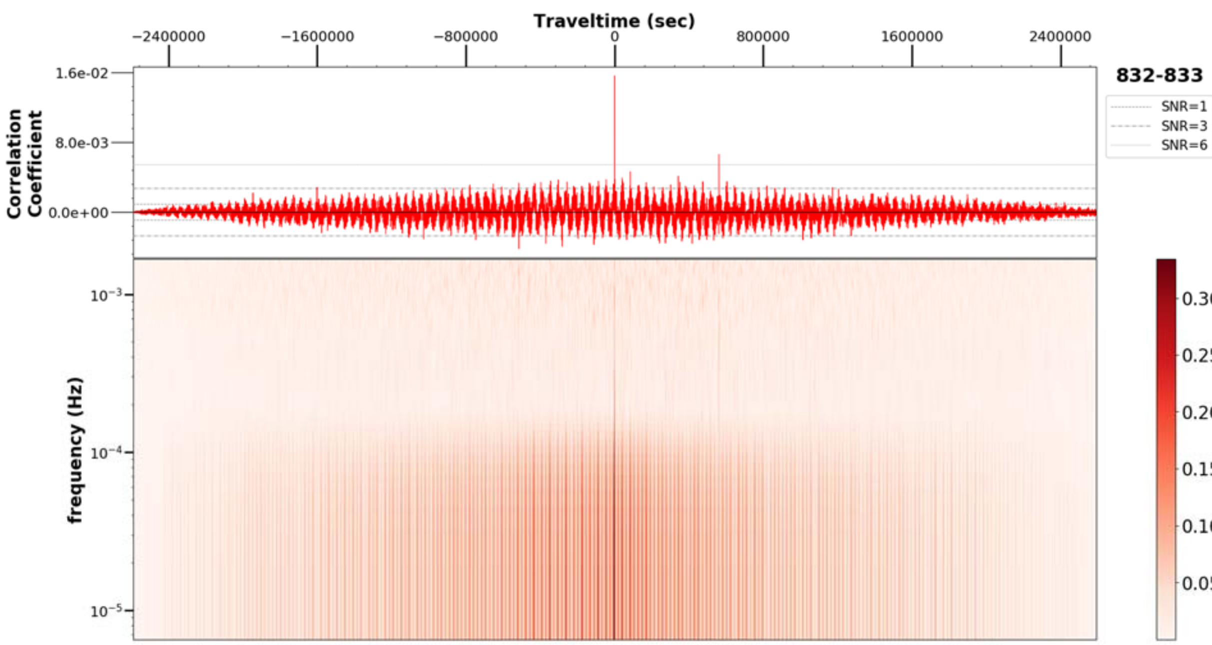

Figure A- 102. Spectrogram from stacked cross-correlated 30-day length data segments with preserved amplitudes (not normalized). Station pair: 832-833

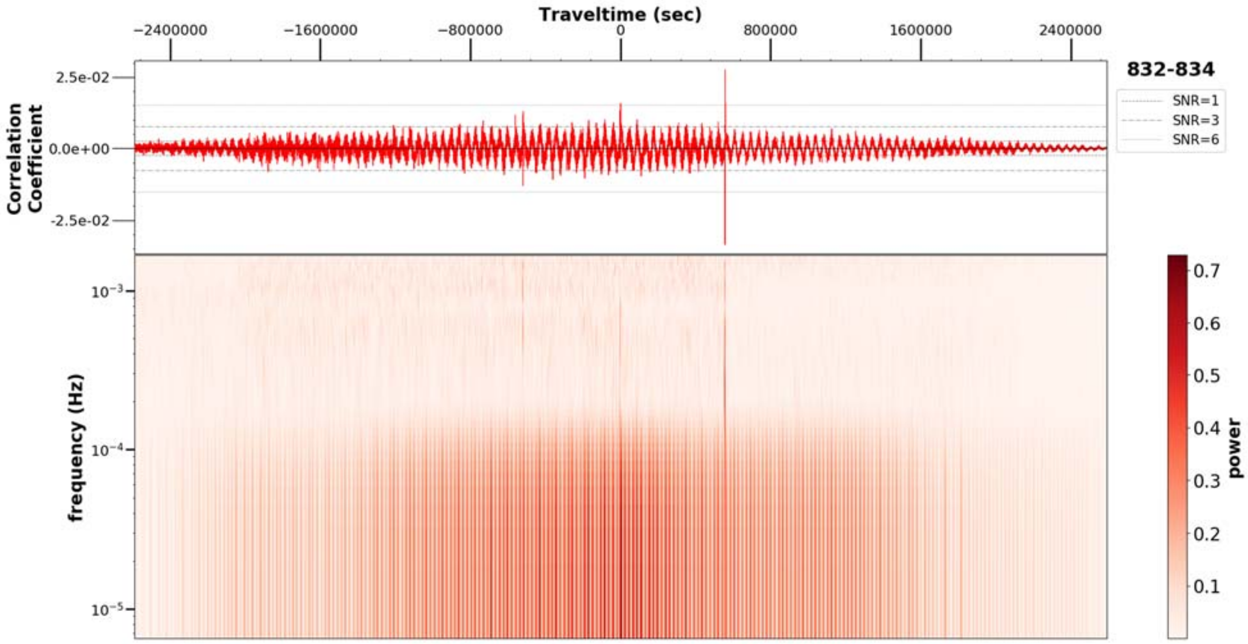

Figure A- 103. Spectrogram from stacked cross-correlated 30-day length data segments with preserved amplitudes (not normalized). Station pair: 832-834

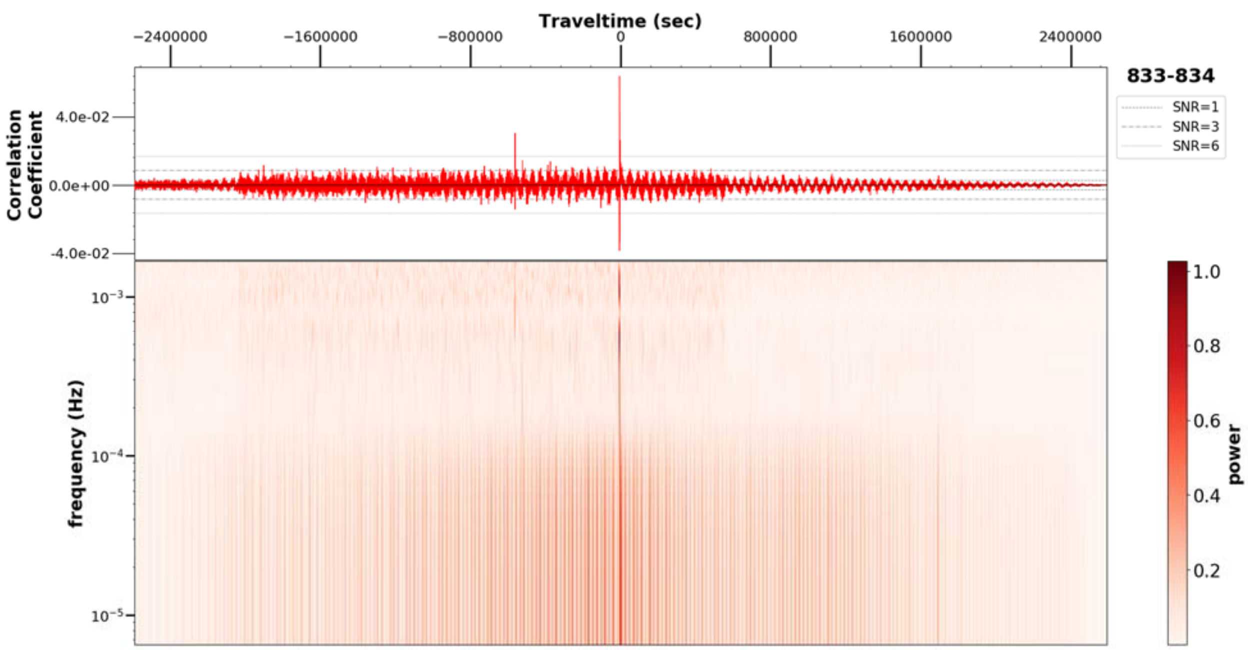

Figure A- 104. Spectrogram from stacked cross-correlated 30-day length data segments with preserved amplitudes (not normalized). Station pair: 833-834

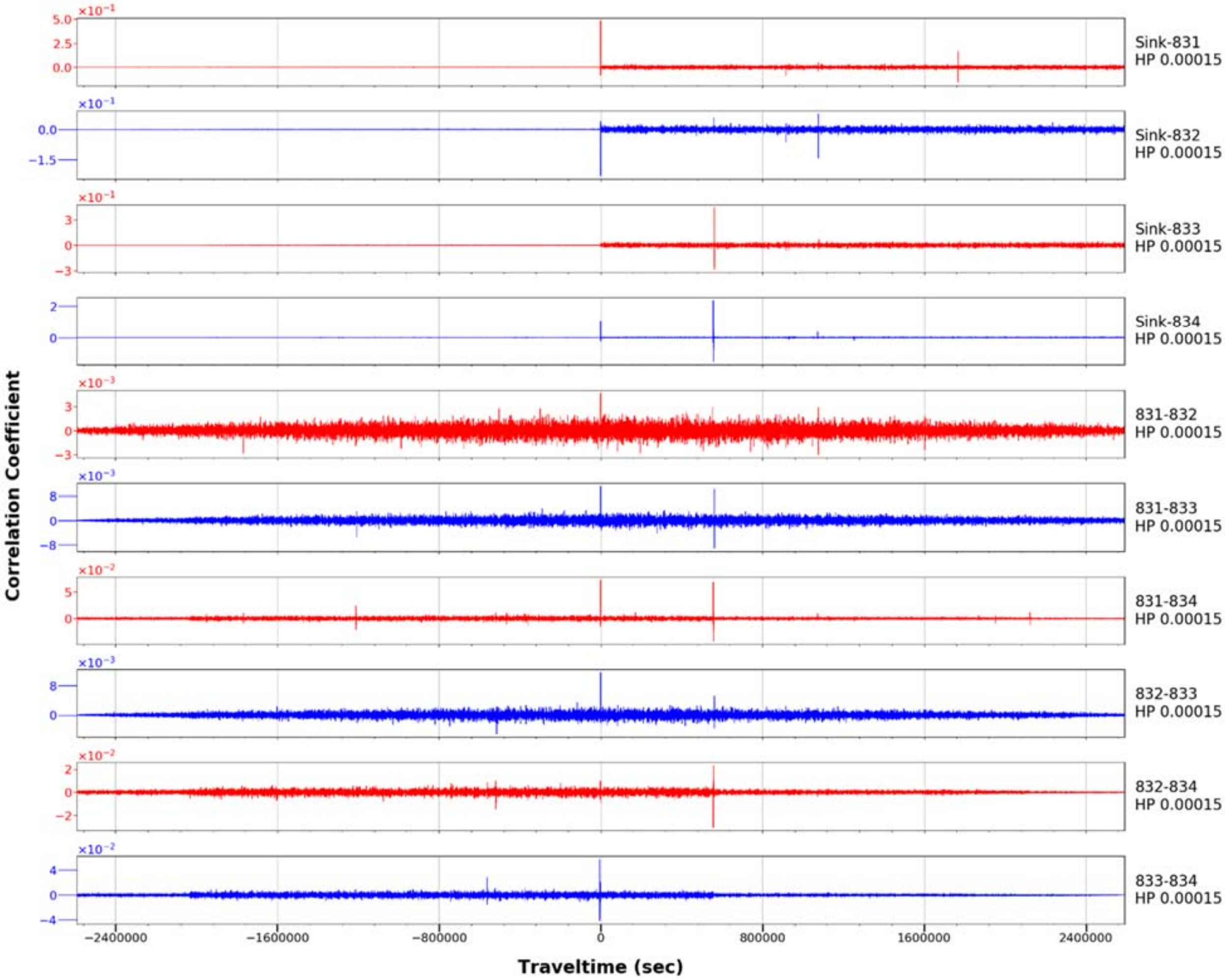

Figure A- 105. Stacked cross-correlograms from 30-day data segment lengths with preserved water level amplitudes (not normalized). Correlograms were high-pass (HP) filtered with a corner frequency of 0.00015 Hz, or a period of just under 2 hours, which is indicated to the right of each panel.

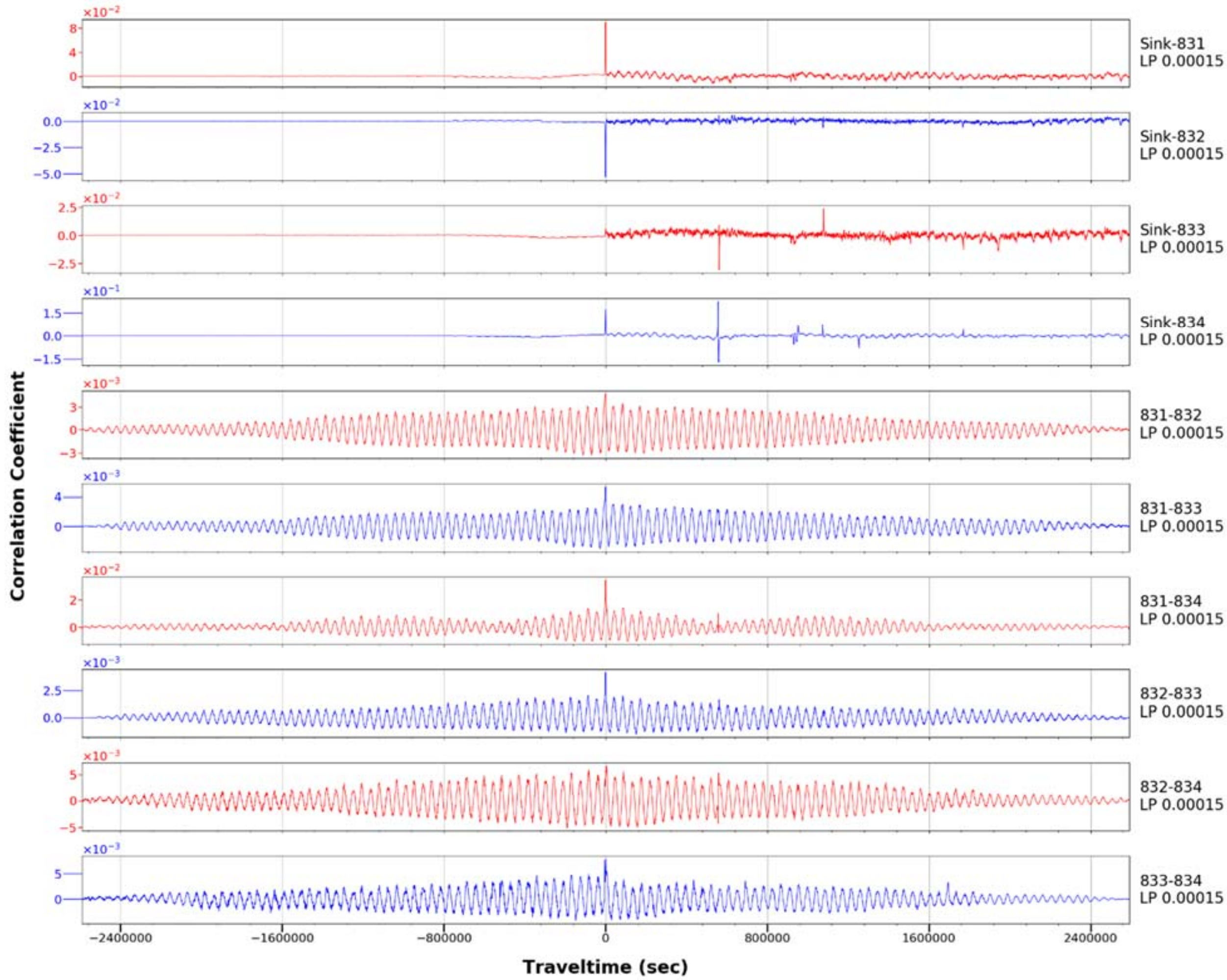

Figure A- 106. Stacked cross-correlograms from 30-day data segment lengths with preserved water level amplitudes (not normalized). Correlograms were low-pass (LP) filtered with a corner frequency of 0.00015 Hz, or a period of just under 2 hours, which is indicated to the right of each panel.

7-Day Length Data Segments – Preserved Amplitudes

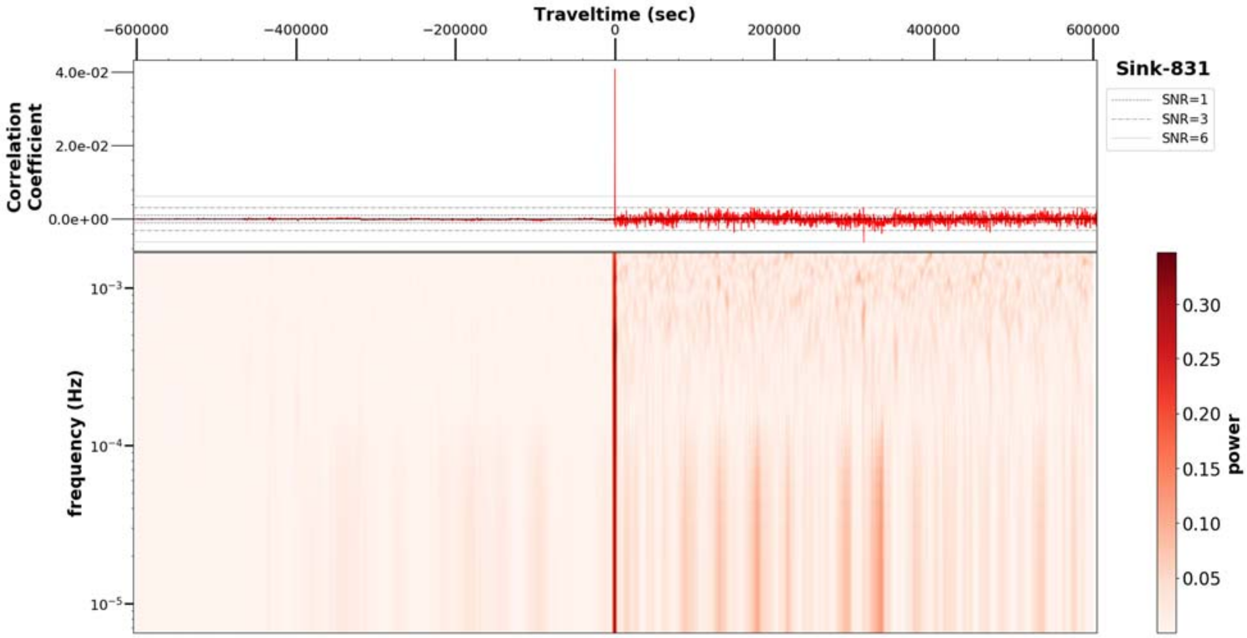

Figure A- 107. Spectrogram from stacked cross-correlated 7-day length data segments with preserved amplitudes (not normalized). Station pair: Sink-831

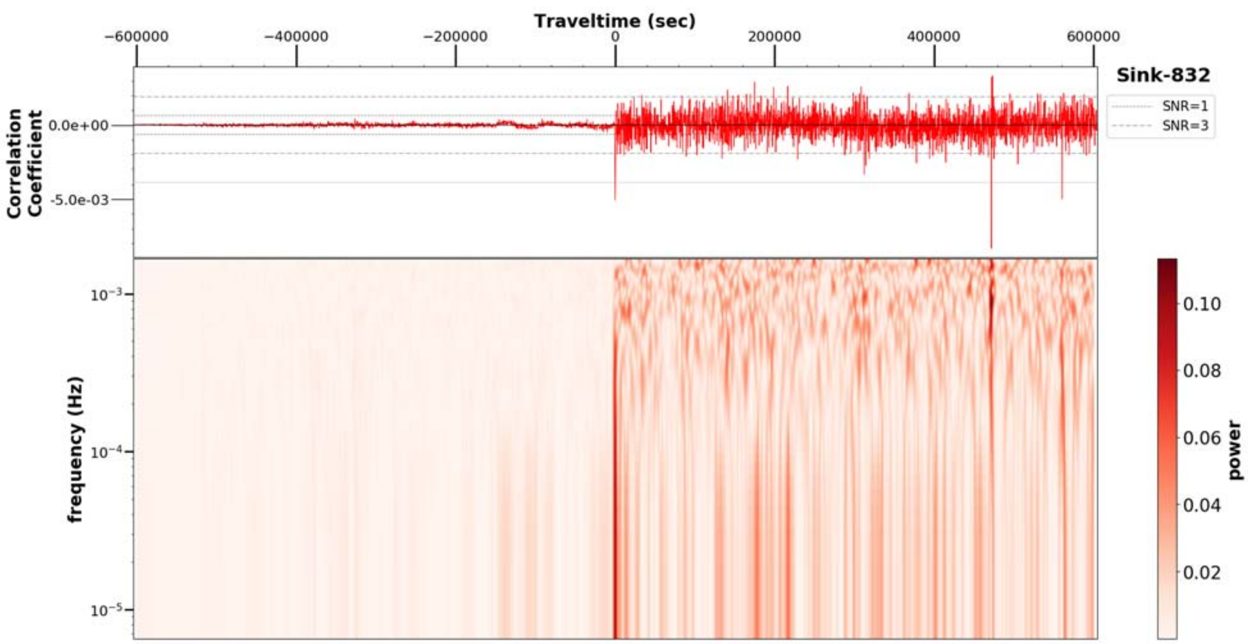

Figure A- 108. Spectrogram from stacked cross-correlated 7-day length data segments with preserved amplitudes (not normalized). Station pair: Sink-832

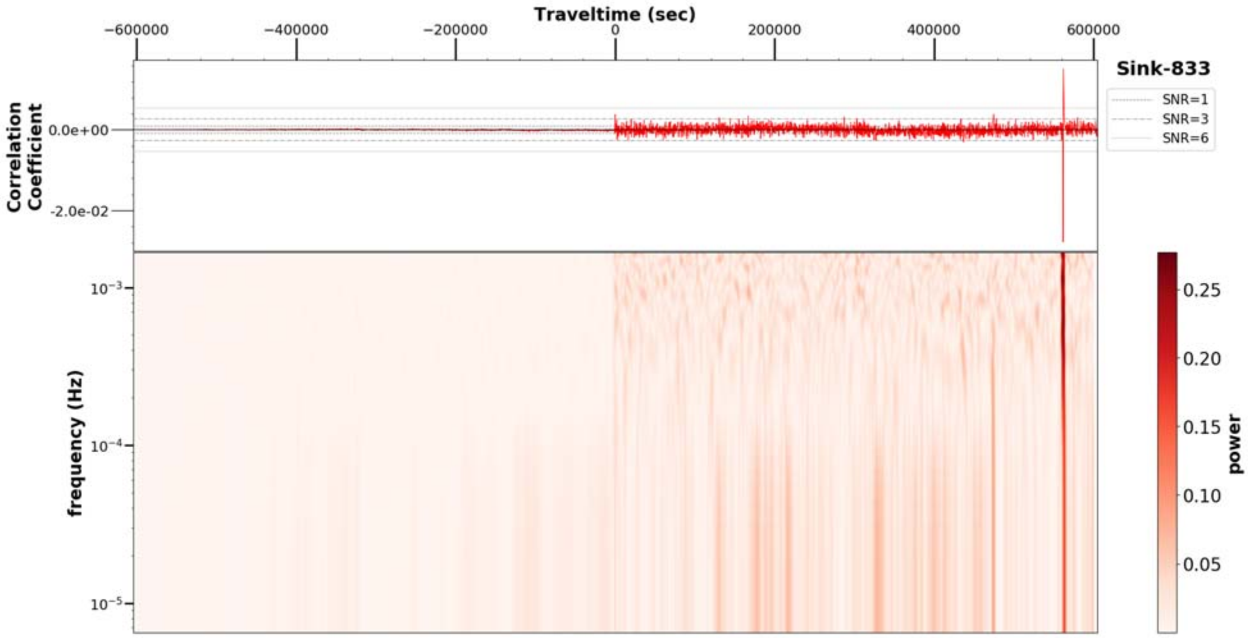

Figure A- 109. Spectrogram from stacked cross-correlated 7-day length data segments with preserved amplitudes (not normalized). Station pair: Sink-833

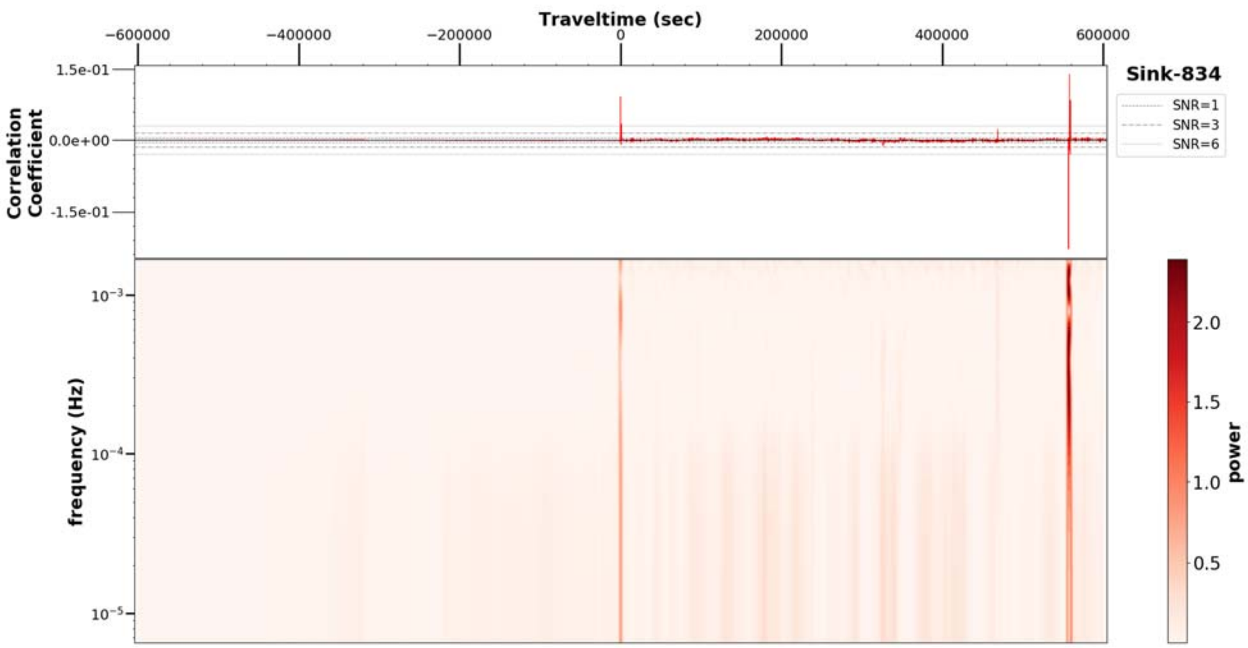

Figure A- 110. Spectrogram from stacked cross-correlated 7-day length data segments with preserved amplitudes (not normalized). Station pair: Sink-834

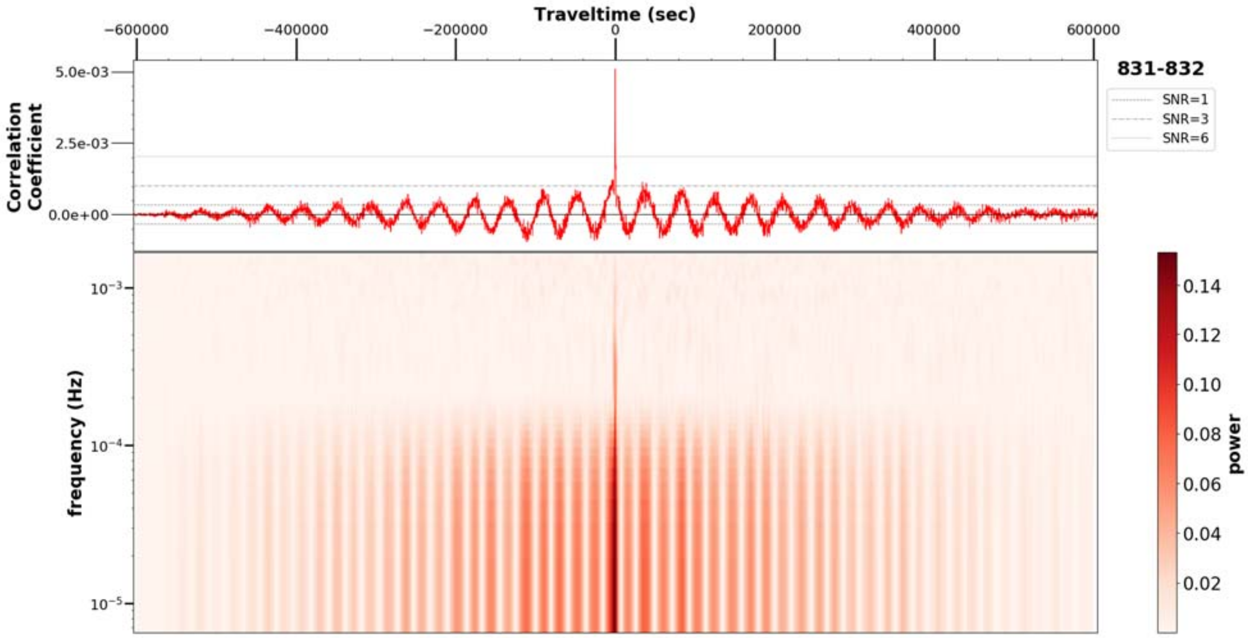

Figure A- 111. Spectrogram from stacked cross-correlated 7-day length data segments with preserved amplitudes (not normalized). Station pair: 831-832

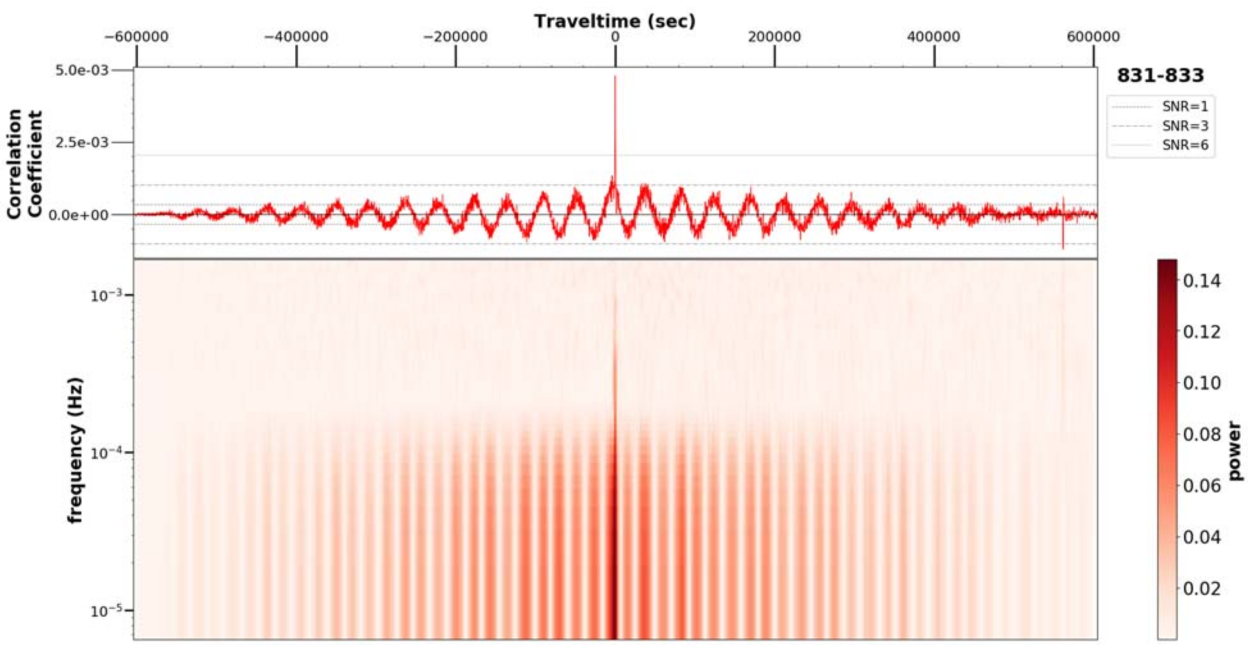

Figure A- 112. Spectrogram from stacked cross-correlated 7-day length data segments with preserved amplitudes (not normalized). Station pair: 831-833

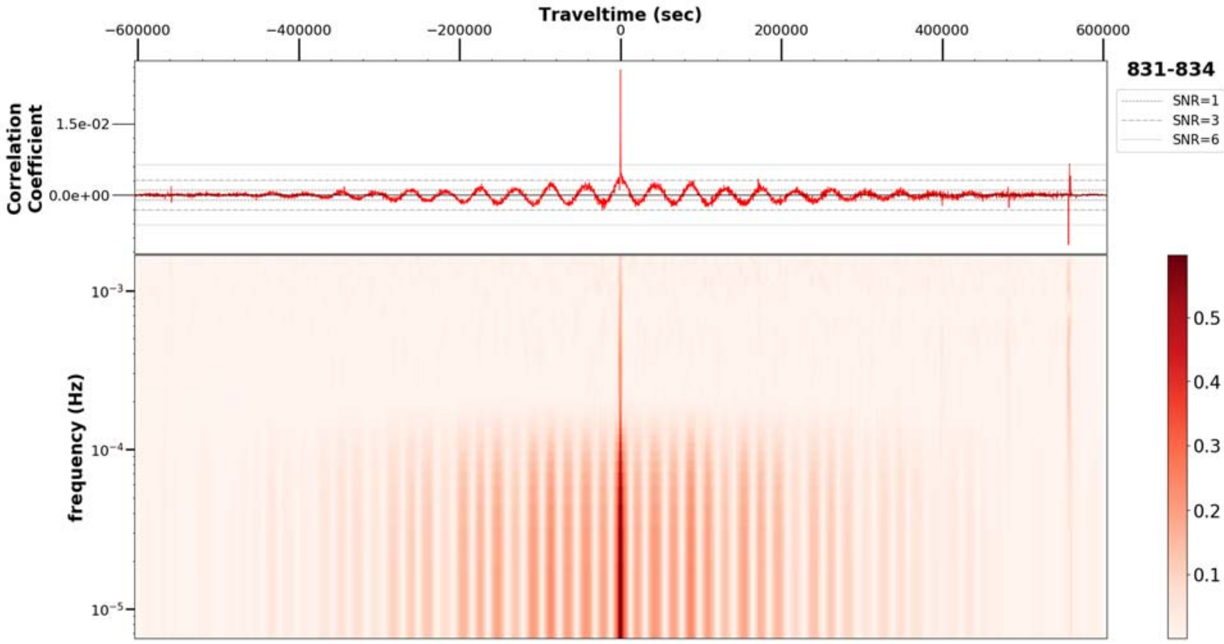

Figure A- 113. Spectrogram from stacked cross-correlated 7-day length data segments with preserved amplitudes (not normalized). Station pair: 831-834

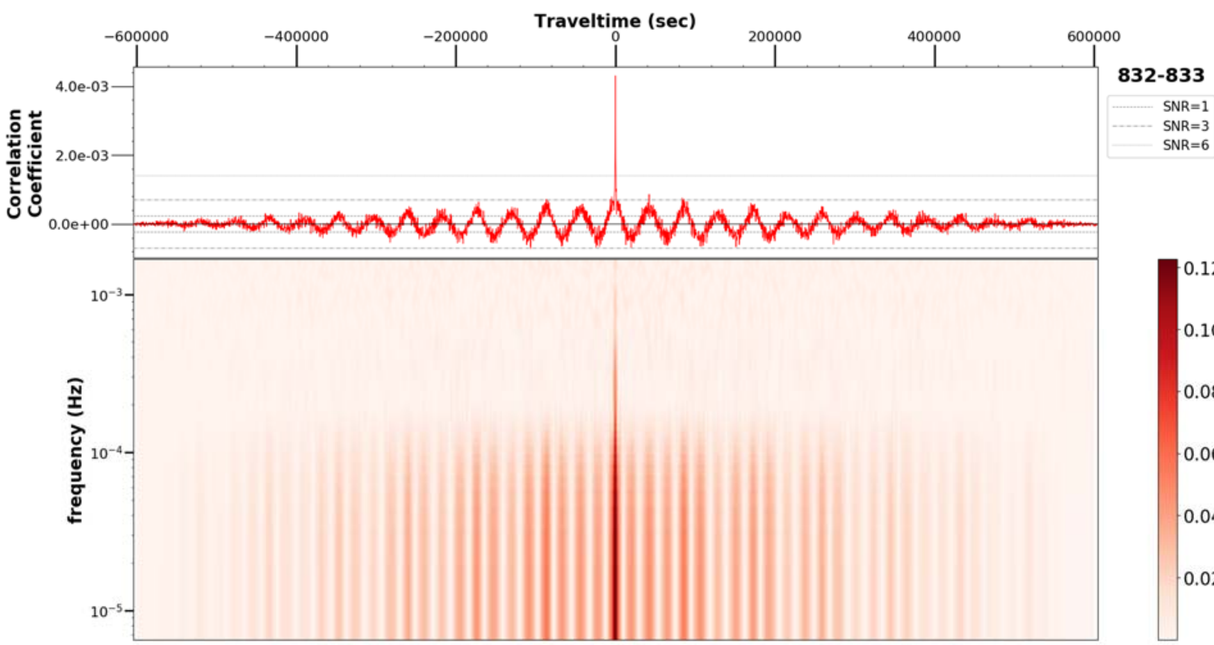

Figure A- 114. Spectrogram from stacked cross-correlated 7-day length data segments with preserved amplitudes (not normalized). Station pair: 832-833

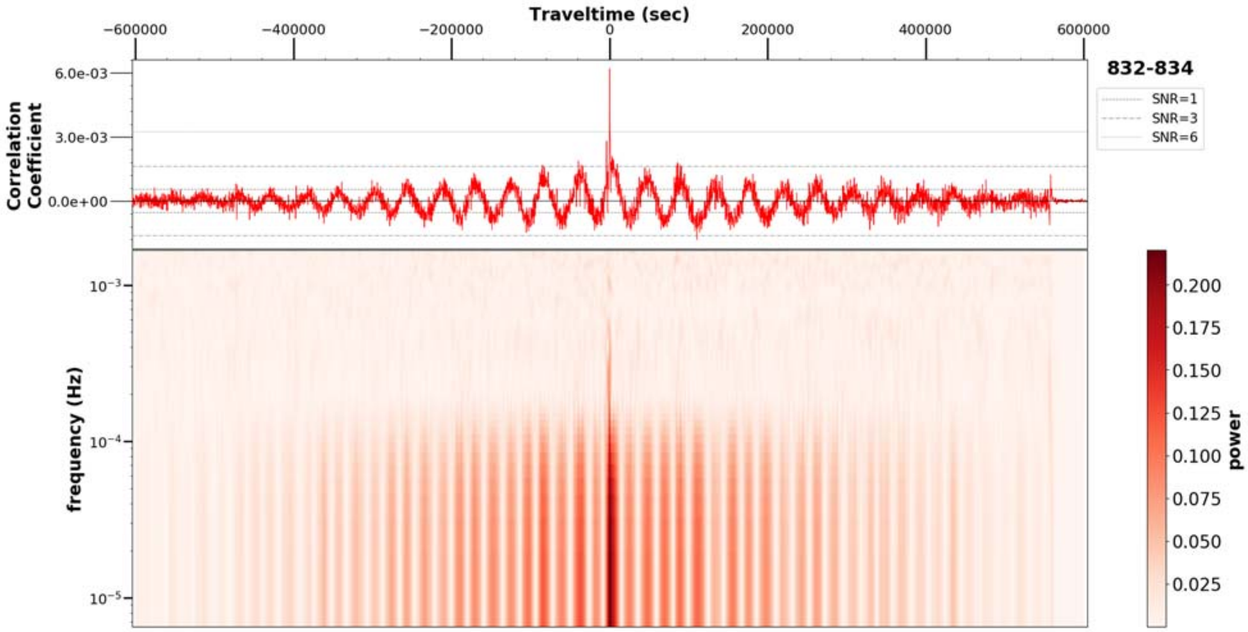

Figure A- 115. Spectrogram from stacked cross-correlated 7-day length data segments with preserved amplitudes (not normalized). Station pair: 832-834

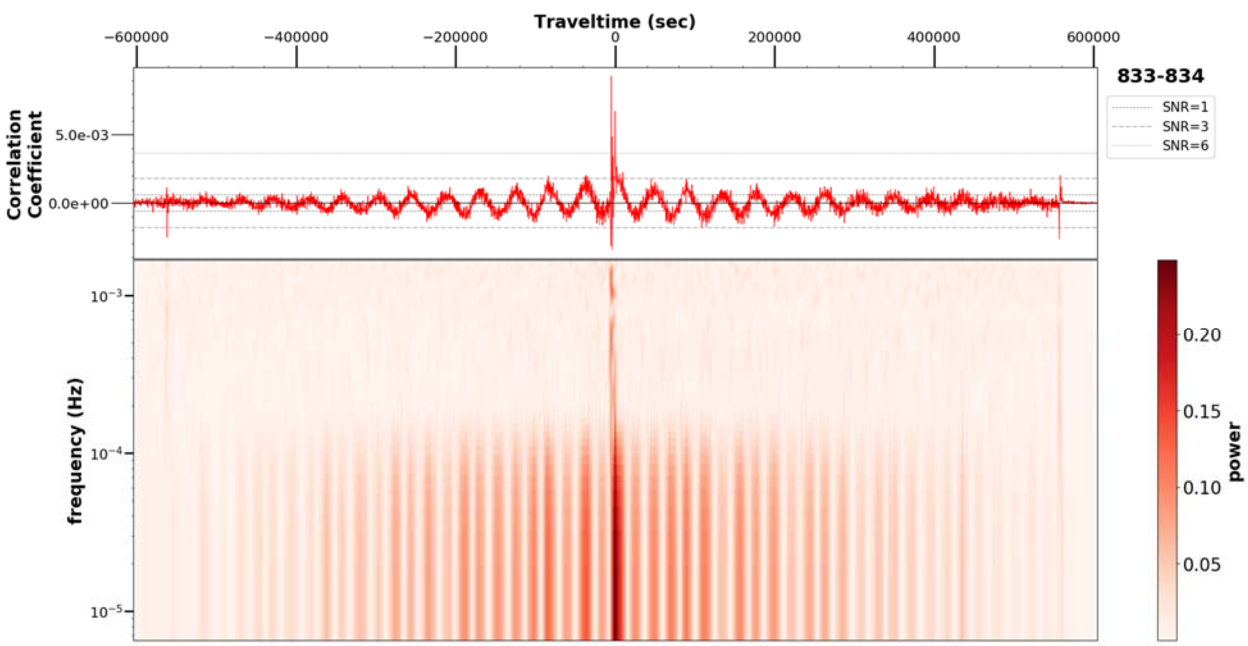

Figure A- 116. Spectrogram from stacked cross-correlated 7-day length data segments with preserved amplitudes (not normalized). Station pair: 833-834

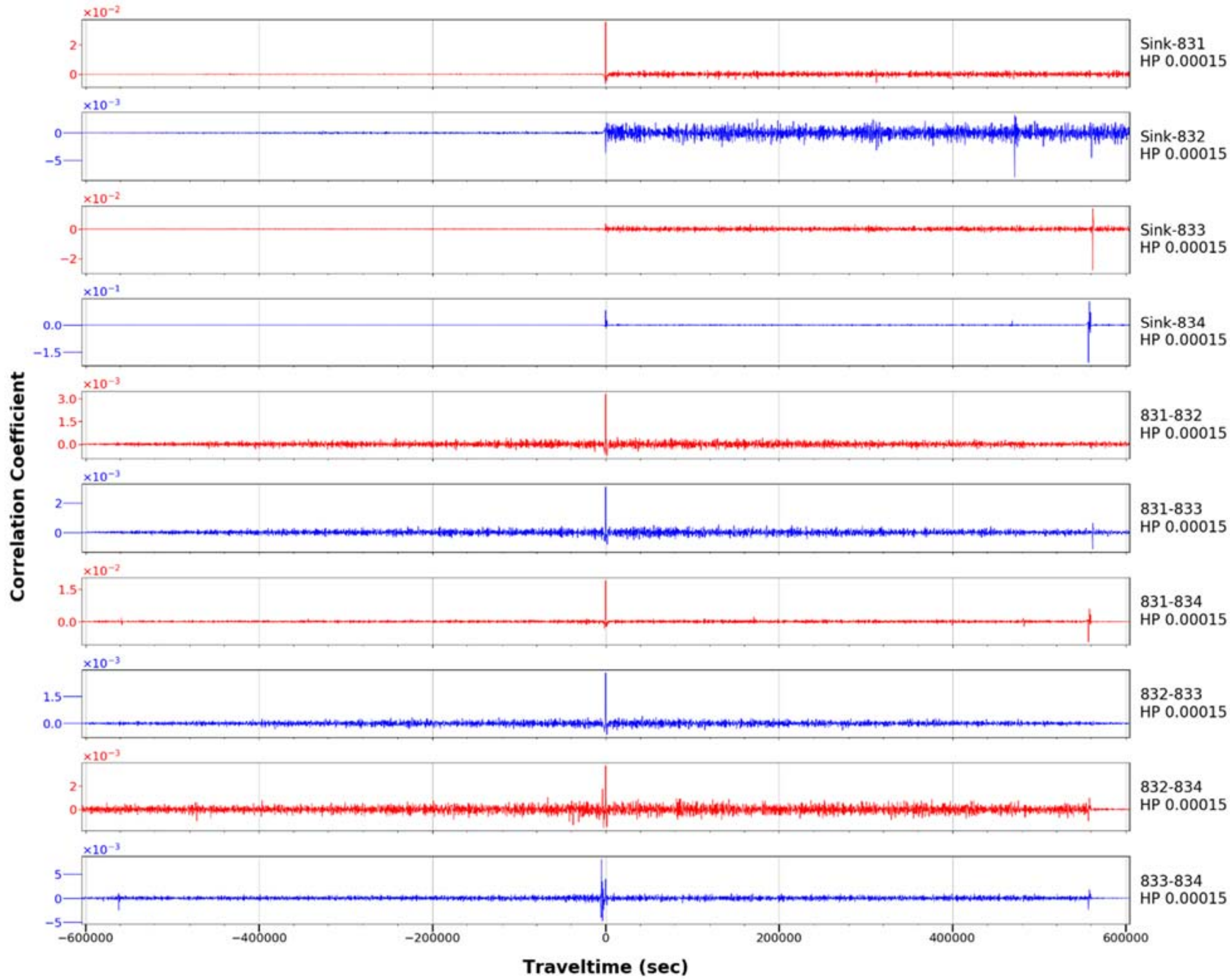

Figure A- 117. Stacked cross-correlograms from 7-day data segment lengths with preserved water level amplitudes (not normalized). Correlograms were high-pass (HP) filtered with a corner frequency of 0.00015 Hz, or a period of just under 2 hours, which is indicated to the right of each panel.

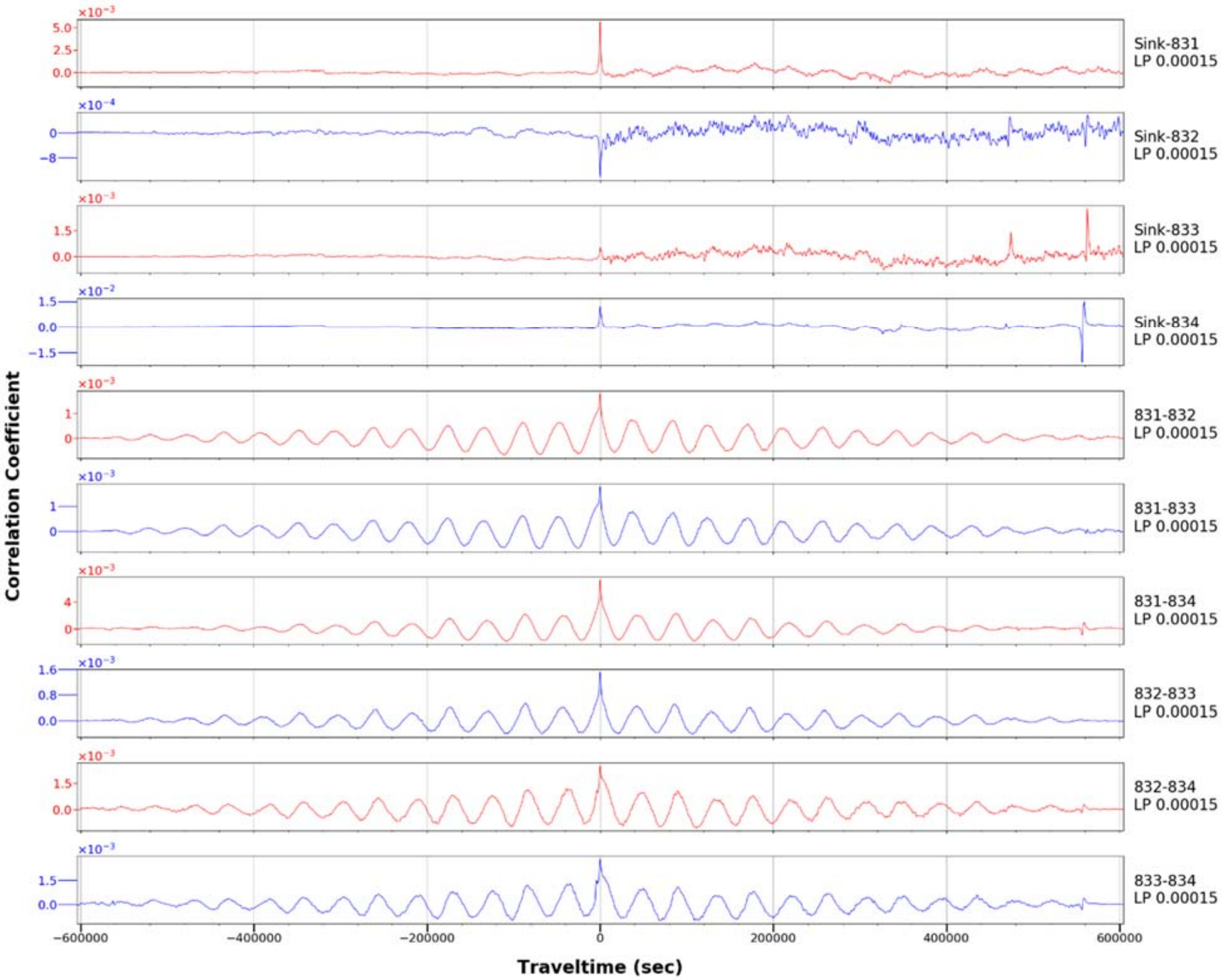

Figure A- 118. Stacked cross-correlograms from 7-day data segment lengths with preserved water level amplitudes (not normalized). Correlograms were low-pass (LP) filtered with a corner frequency of 0.00015 Hz, or a period of just under 2 hours, which is indicated to the right of each panel.

All Daily Length Data Segments – Preserved Amplitudes

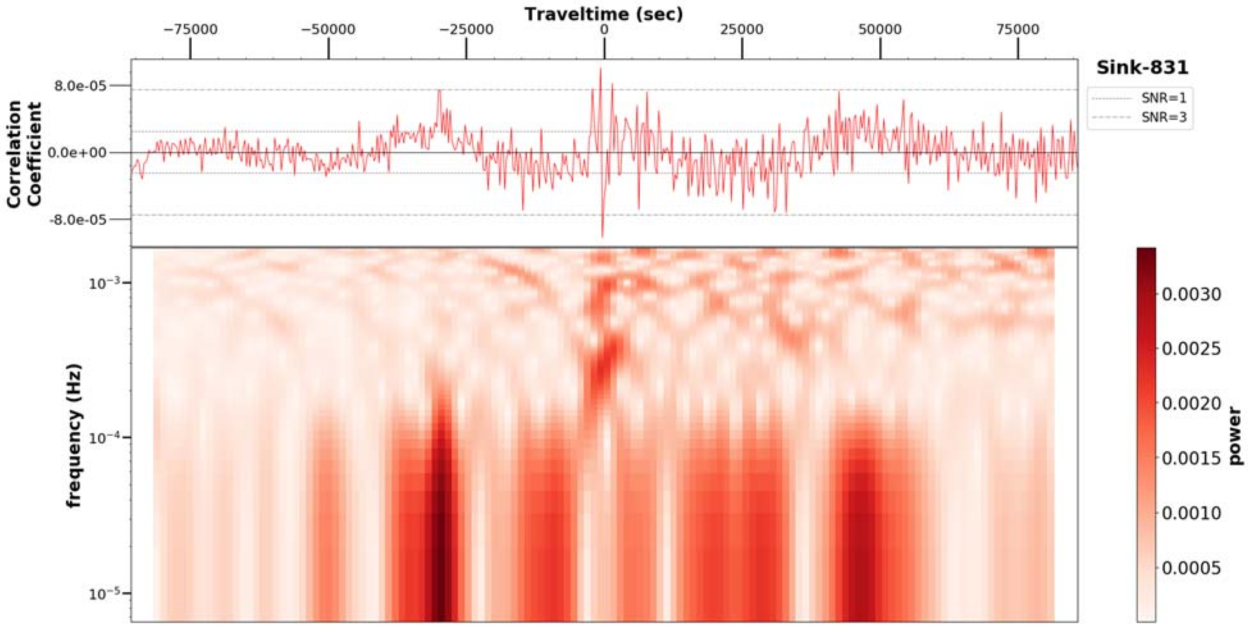

Figure A- 119. Spectrogram from stacked cross-correlated daily length data segments with preserved amplitudes (not normalized), all segments. Station pair: Sink-831

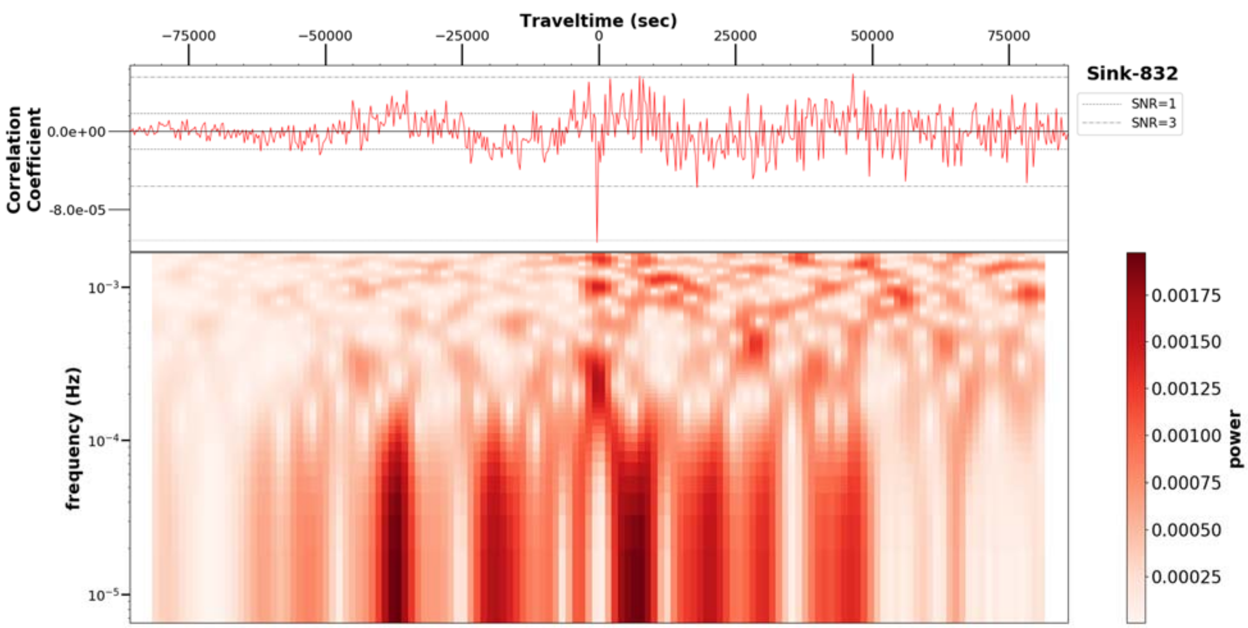

Figure A- 120. Spectrogram from stacked cross-correlated daily length data segments with preserved amplitudes (not normalized), all segments. Station pair: Sink-832

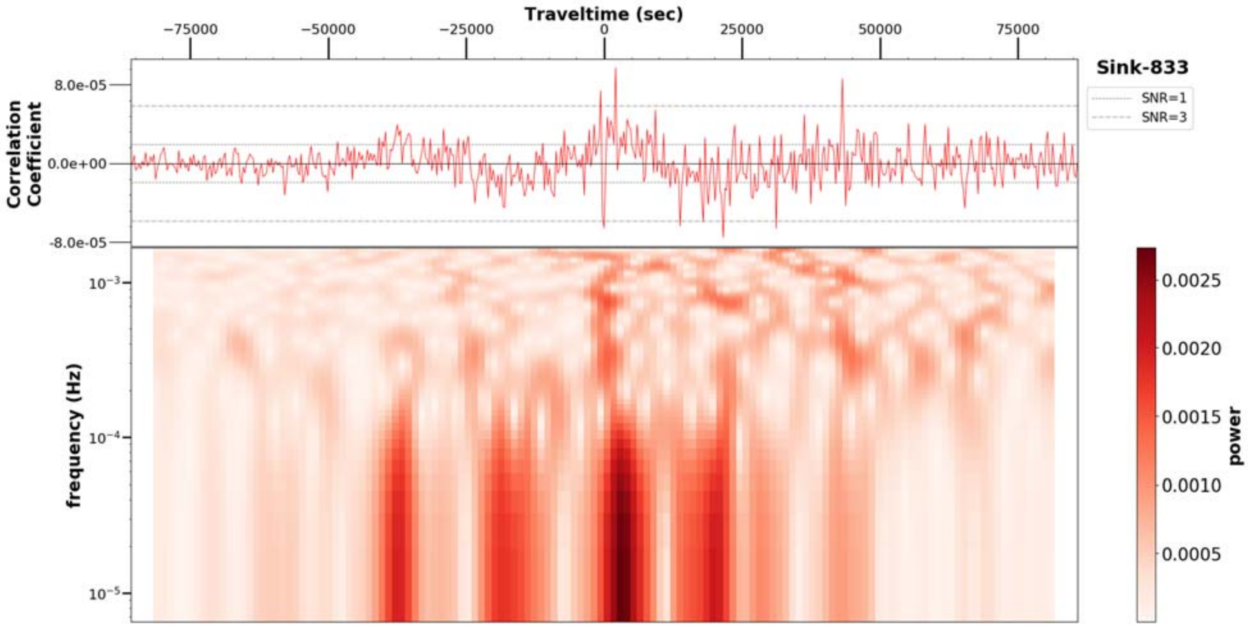

Figure A- 121. Spectrogram from stacked cross-correlated daily length data segments with preserved amplitudes (not normalized), all segments. Station pair: Sink-833

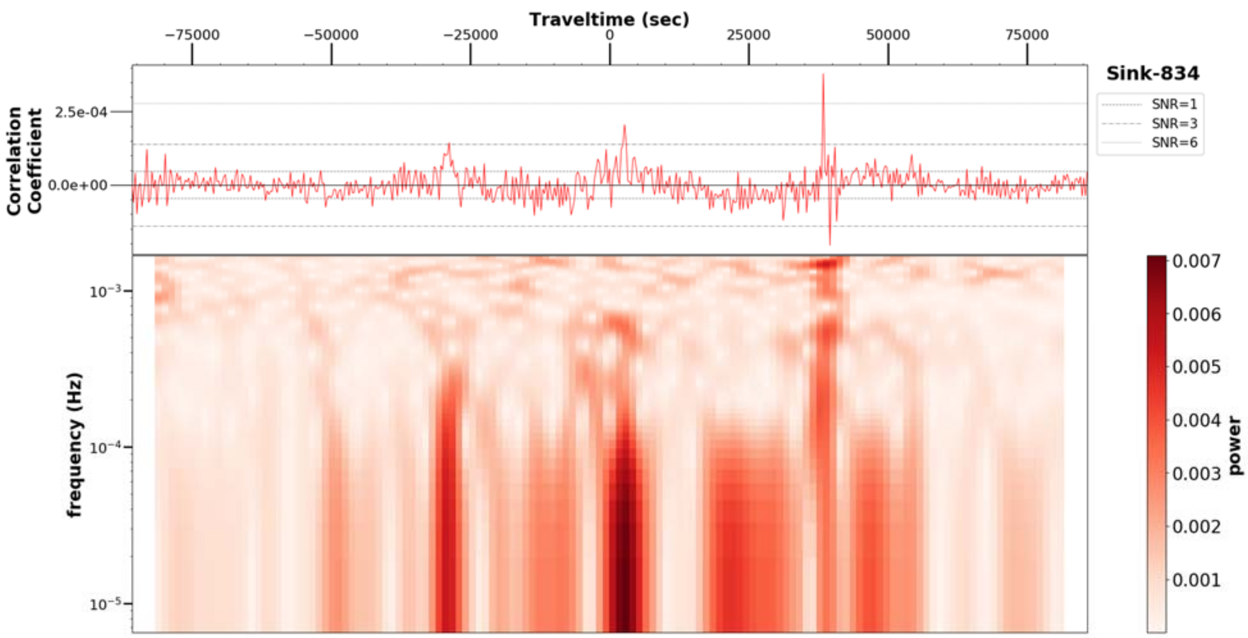

Figure A- 122. Spectrogram from stacked cross-correlated daily length data segments with preserved amplitudes (not normalized), all segments. Station pair: Sink-834

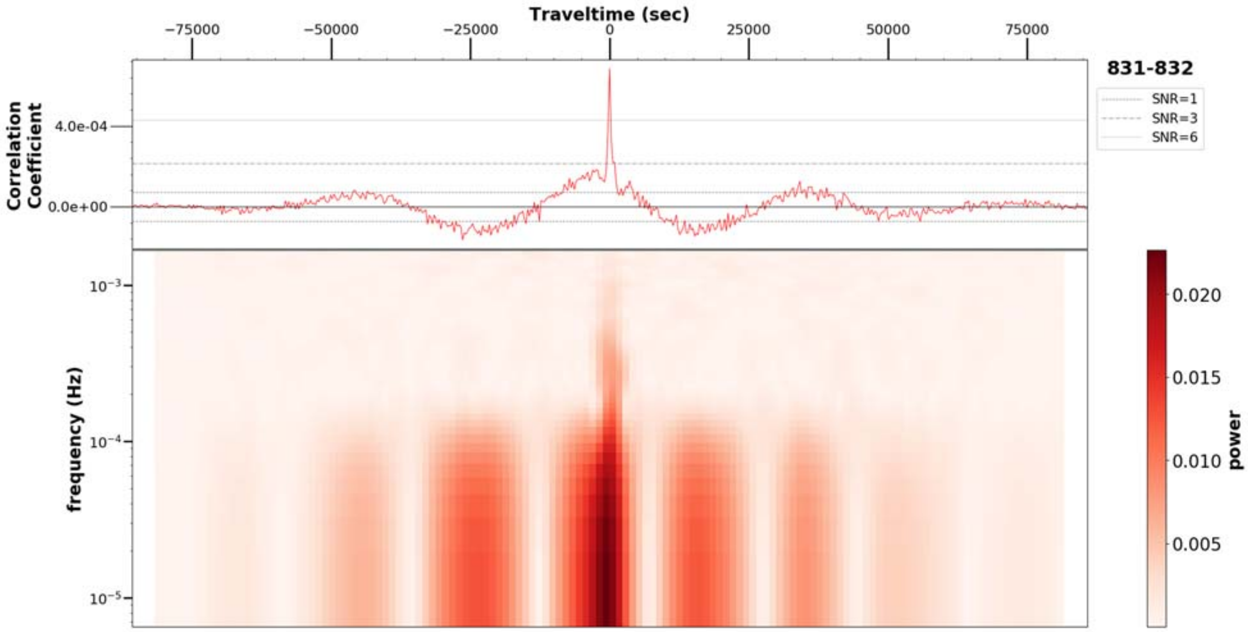

Figure A- 123. Spectrogram from stacked cross-correlated daily length data segments with preserved amplitudes (not normalized), all segments. Station pair: 831-832

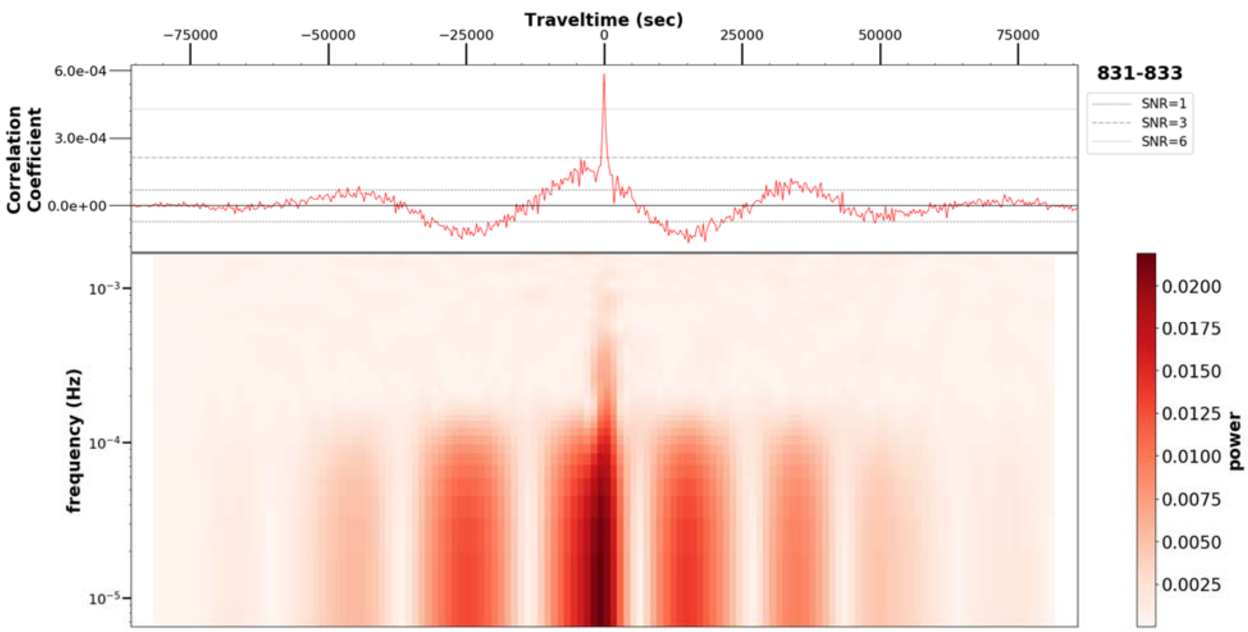

Figure A- 124. Spectrogram from stacked cross-correlated daily length data segments with preserved amplitudes (not normalized), all segments. Station pair: 831-833

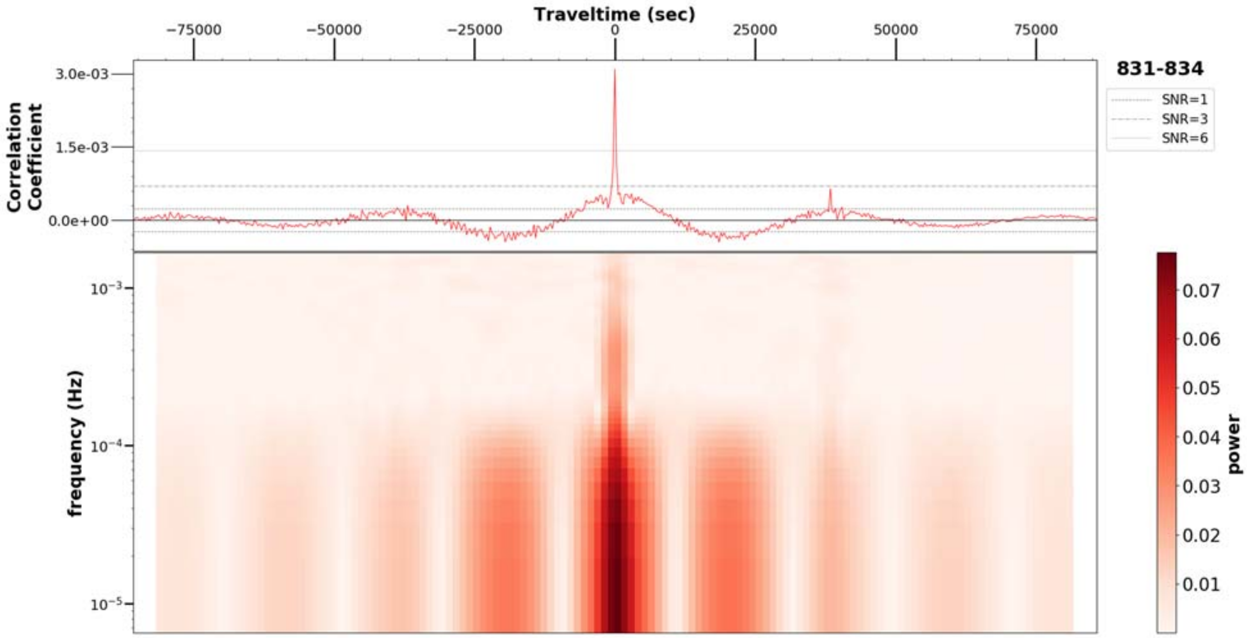

Figure A- 125. Spectrogram from stacked cross-correlated daily length data segments with preserved amplitudes (not normalized), all segments. Station pair: 831-834

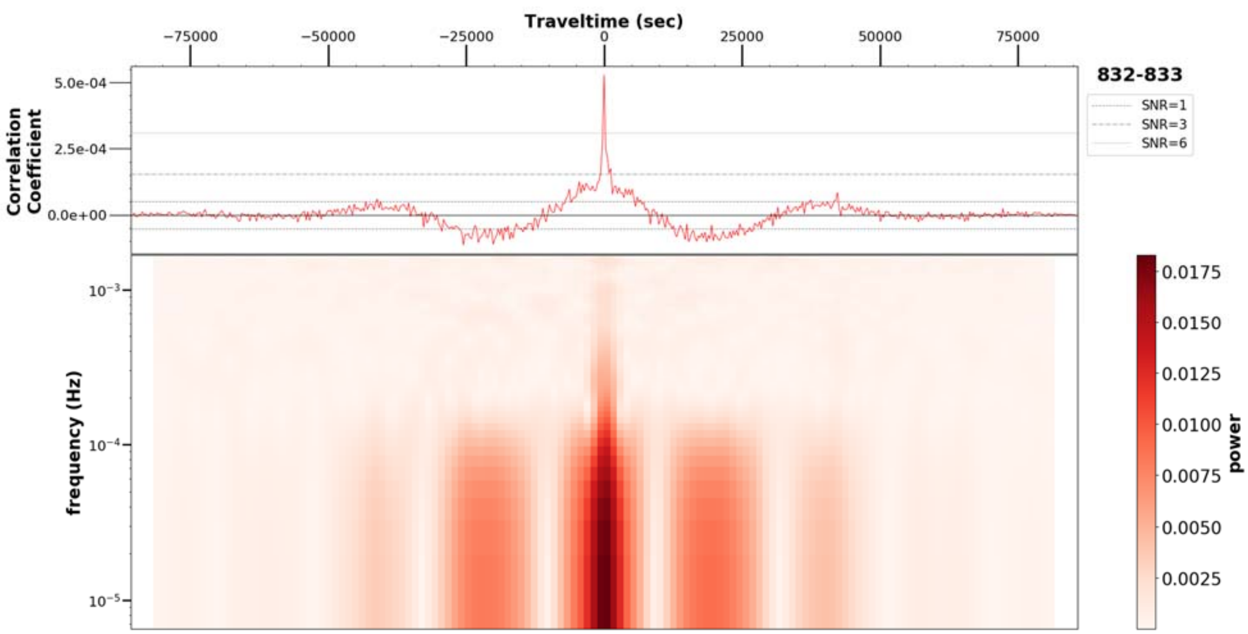

Figure A- 126. Spectrogram from stacked cross-correlated daily length data segments with preserved amplitudes (not normalized), all segments. Station pair: 832-833

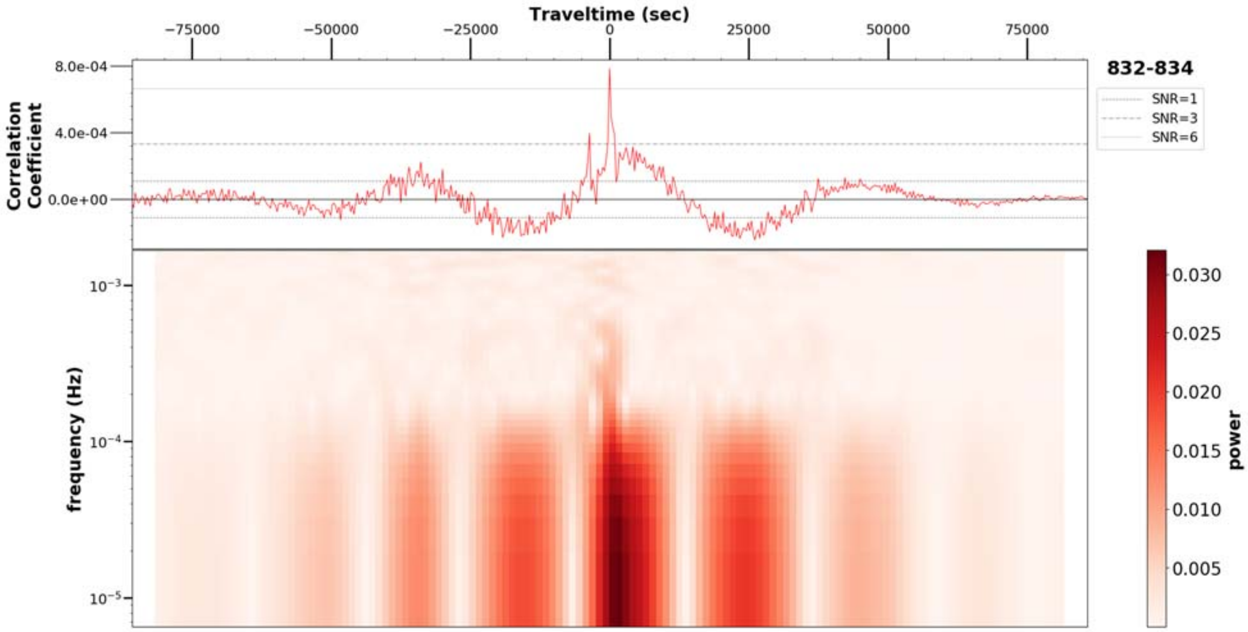

Figure A- 127. Spectrogram from stacked cross-correlated daily length data segments with preserved amplitudes (not normalized), all segments. Station pair: 832-834

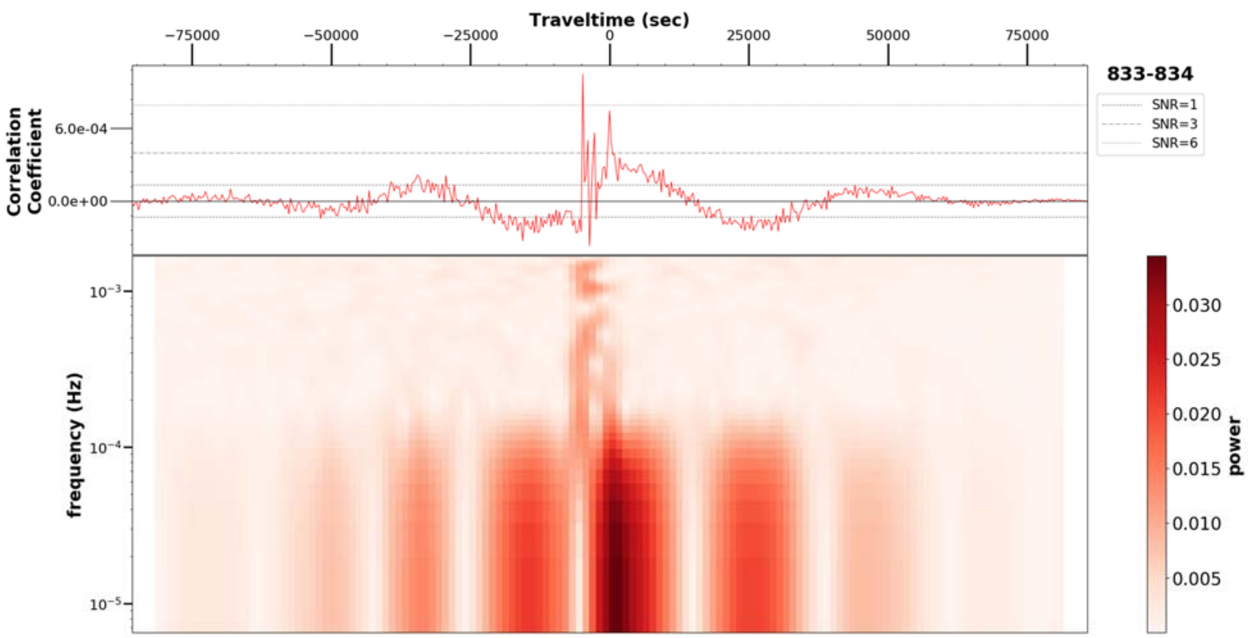

Figure A- 128. Spectrogram from stacked cross-correlated daily length data segments with preserved amplitudes (not normalized), all segments. Station pair: 833-834

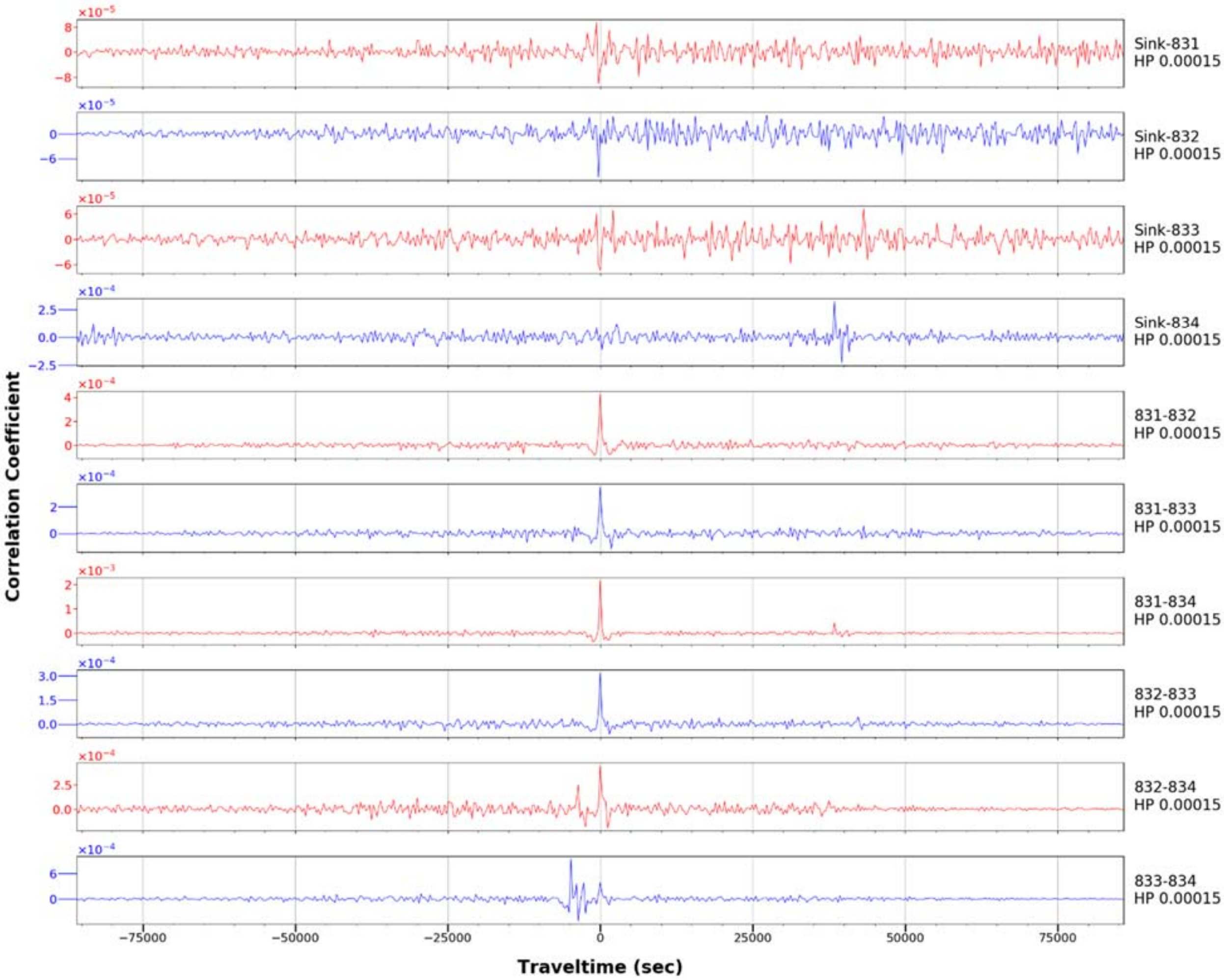

Figure A- 129. Stacked cross-correlograms from all daily data segment lengths with preserved water level amplitudes (not normalized). Correlograms were high-pass (HP) filtered with a corner frequency of 0.00015 Hz, or a period of just under 2 hours, which is indicated to the right of each panel.

Pumping-Period-Only Daily Length Data Segments – Preserved Amplitudes

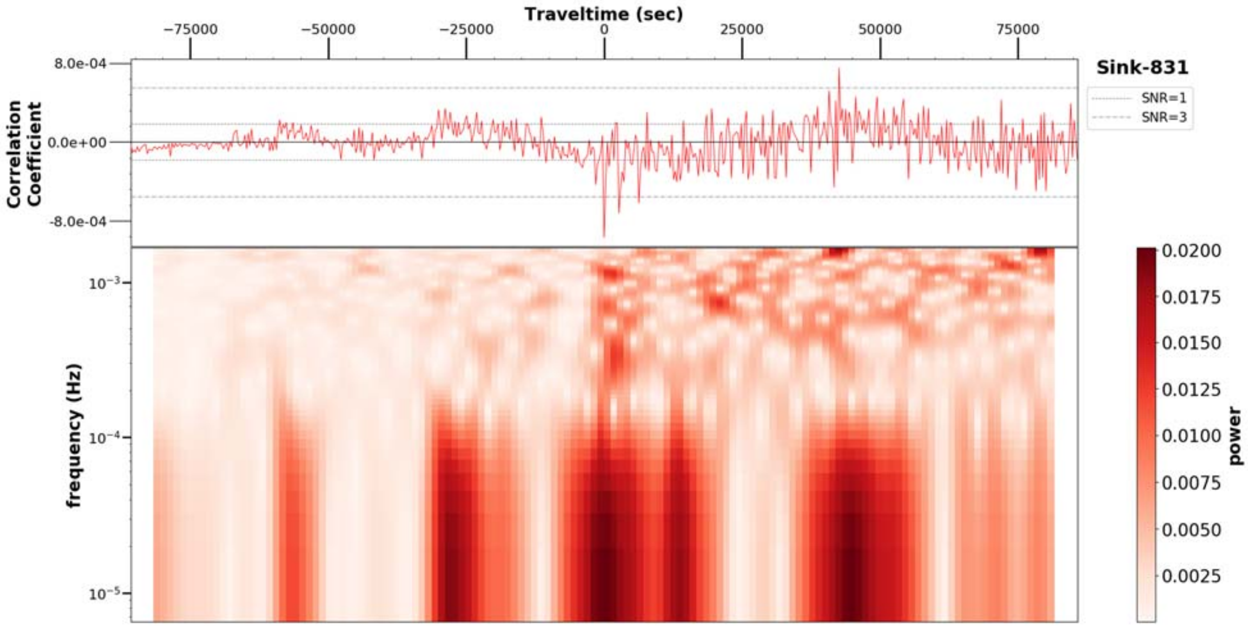

Figure A- 130. Spectrogram from stacked cross-correlated daily length data segments with preserved amplitudes (not normalized), pumping-period-only segments. Station pair: Sink-831

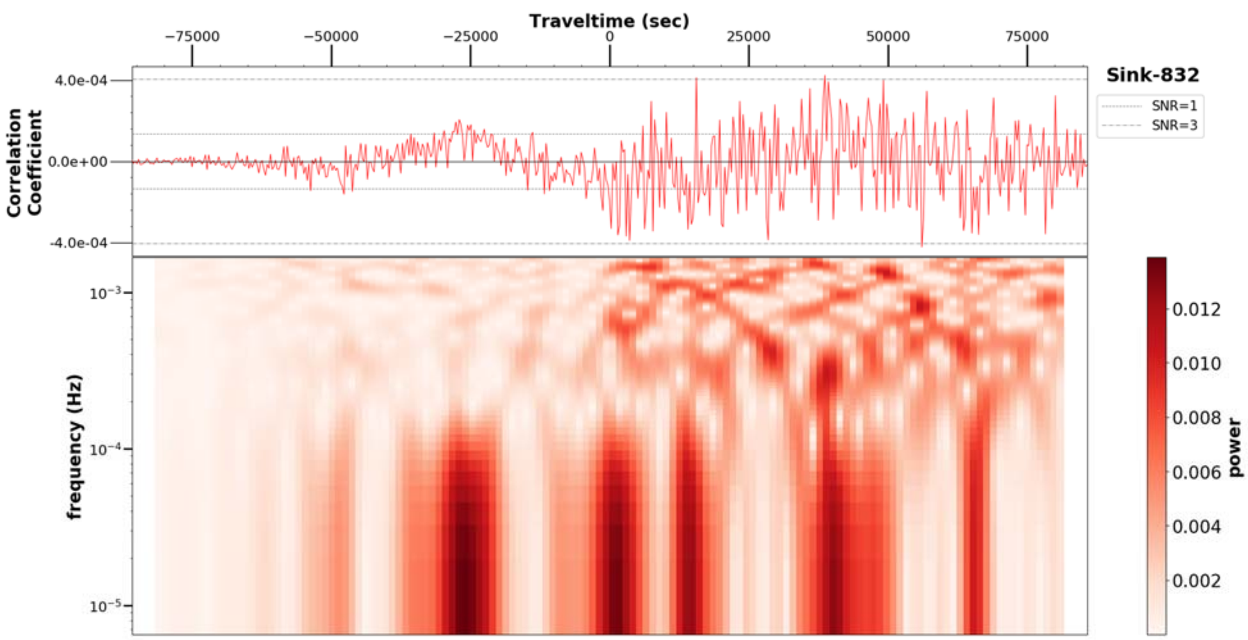

Figure A- 131. Spectrogram from stacked cross-correlated daily length data segments with preserved amplitudes (not normalized), pumping-period-only segments. Station pair: Sink-832

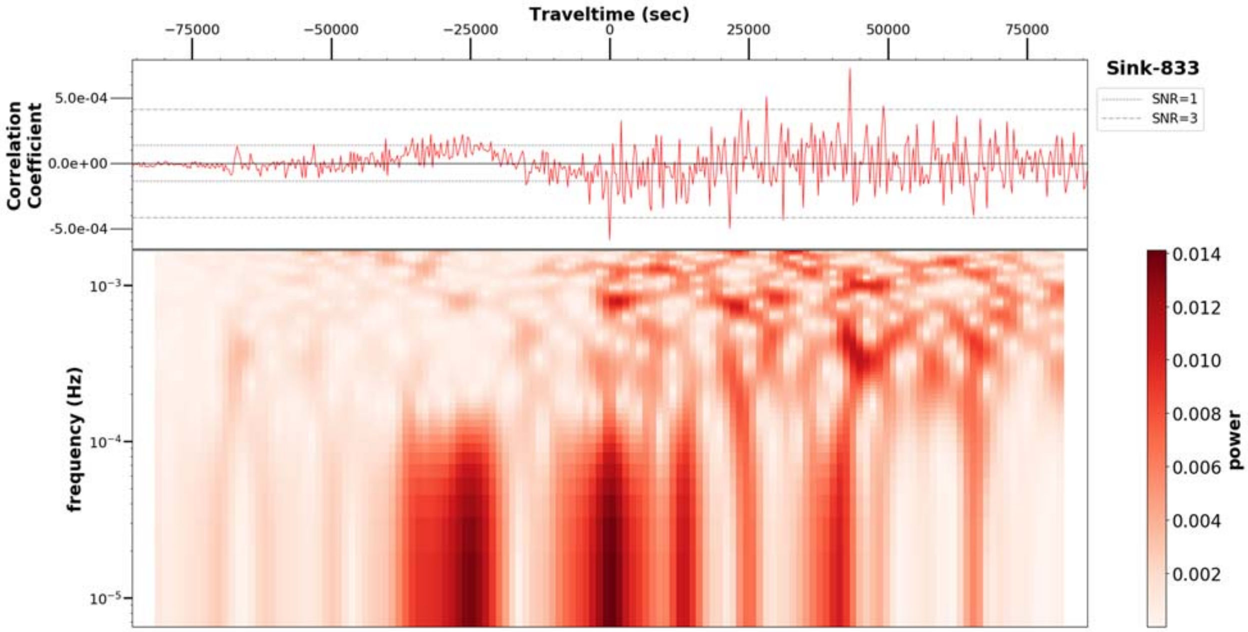

Figure A- 132. Spectrogram from stacked cross-correlated daily length data segments with preserved amplitudes (not normalized), pumping-period-only segments. Station pair: Sink-833

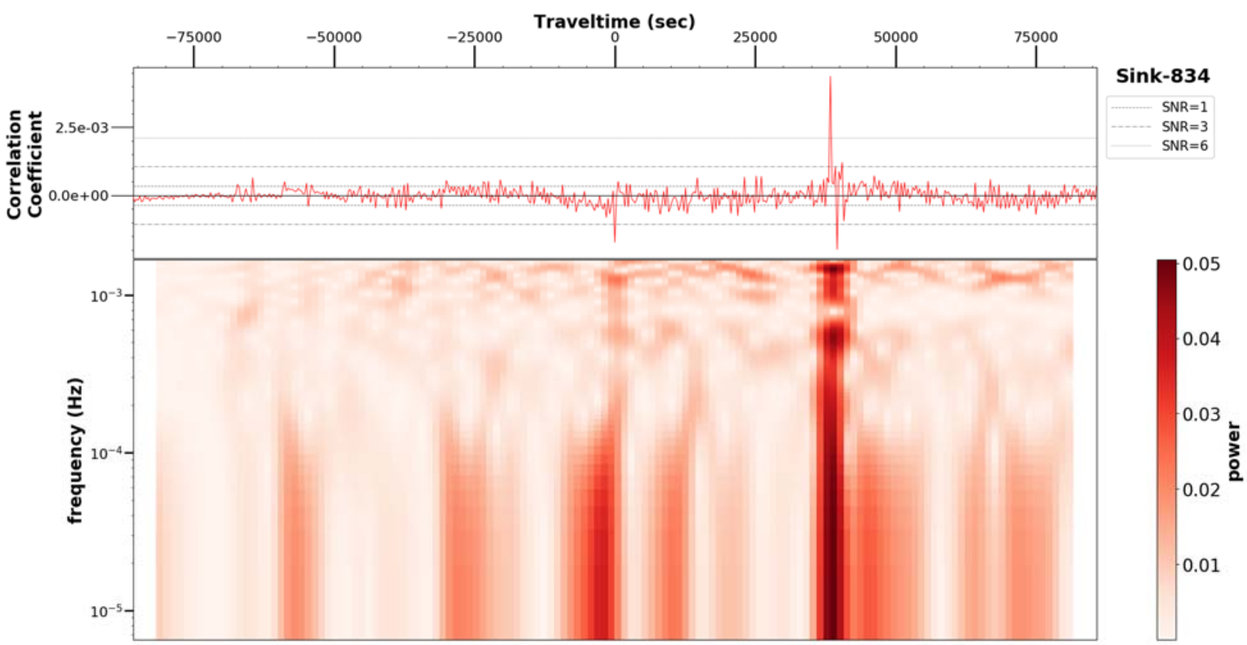

Figure A- 133. Spectrogram from stacked cross-correlated daily length data segments with preserved amplitudes (not normalized), pumping-period-only segments. Station pair: Sink-834

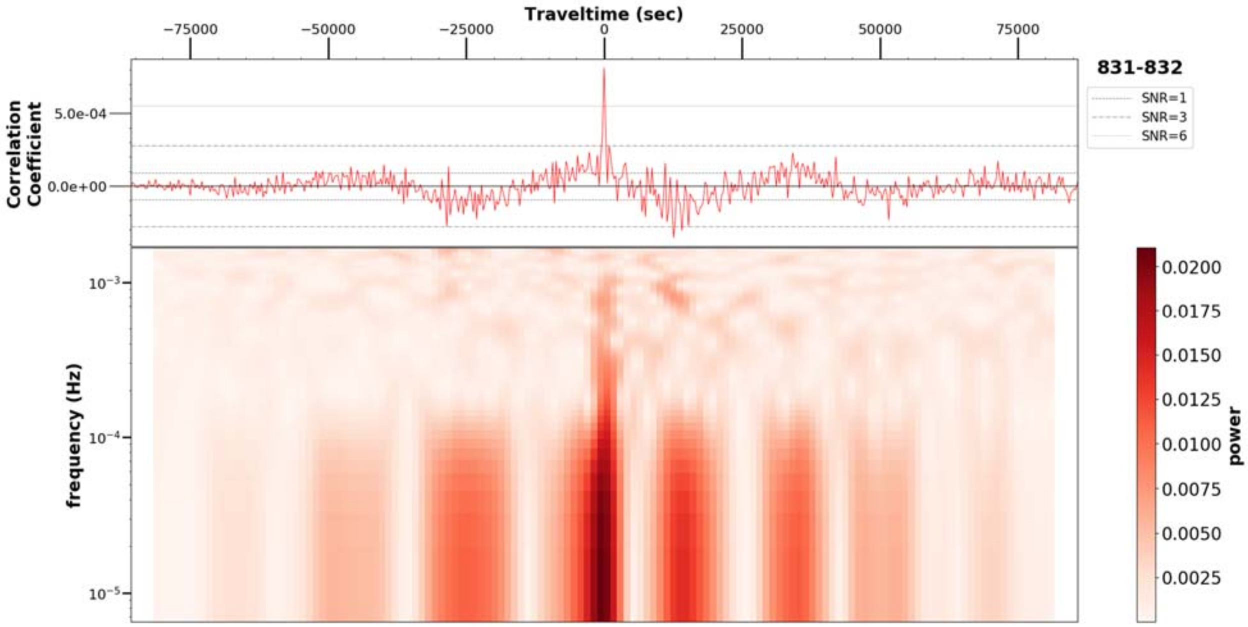

Figure A- 134. Spectrogram from stacked cross-correlated daily length data segments with preserved amplitudes (not normalized), pumping-period-only segments. Station pair: 831-832

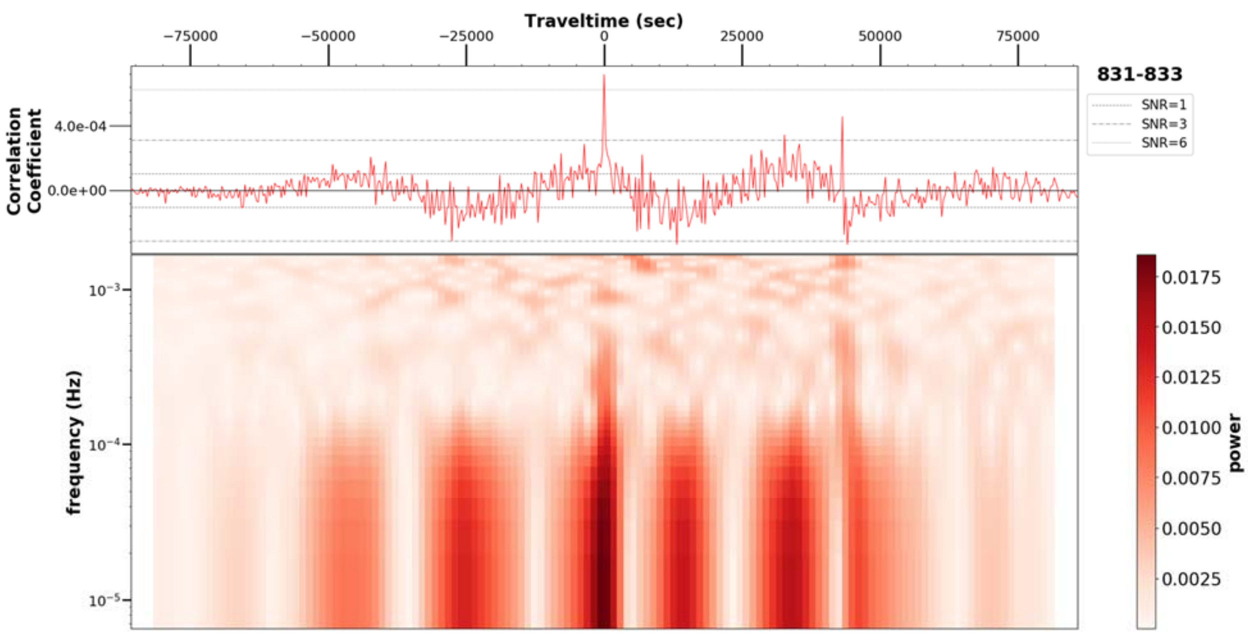

Figure A- 135. Spectrogram from stacked cross-correlated daily length data segments with preserved amplitudes (not normalized), pumping-period-only segments. Station pair: 831-833

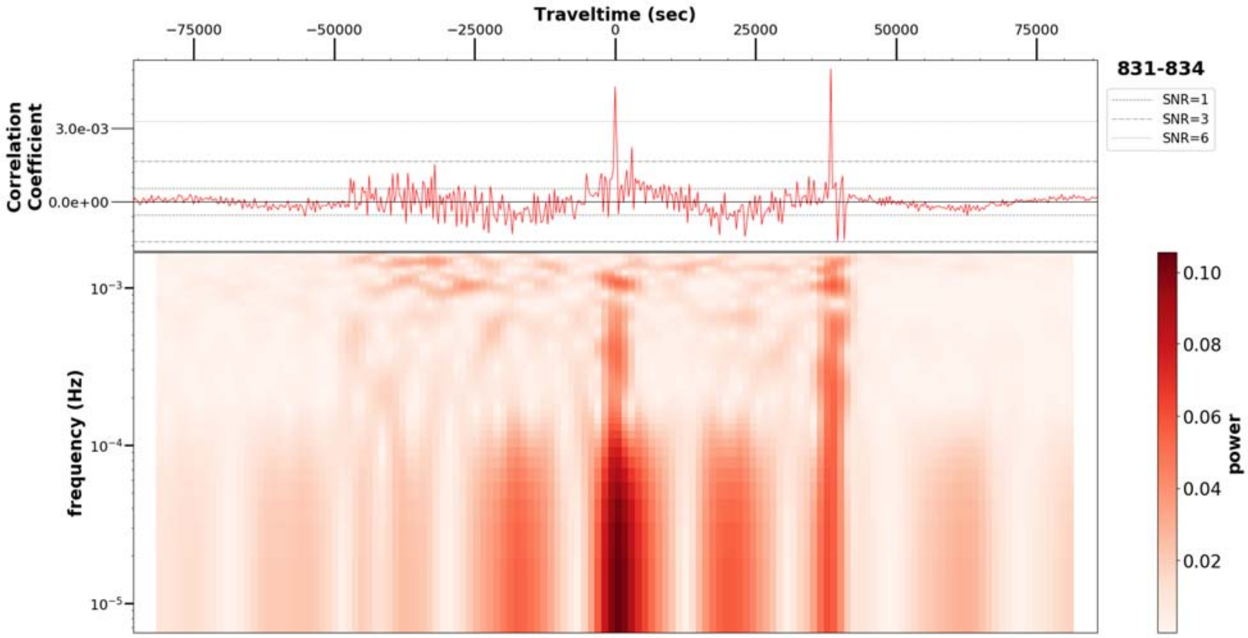

Figure A- 136. Spectrogram from stacked cross-correlated daily length data segments with preserved amplitudes (not normalized), pumping-period-only segments. Station pair: 831-834

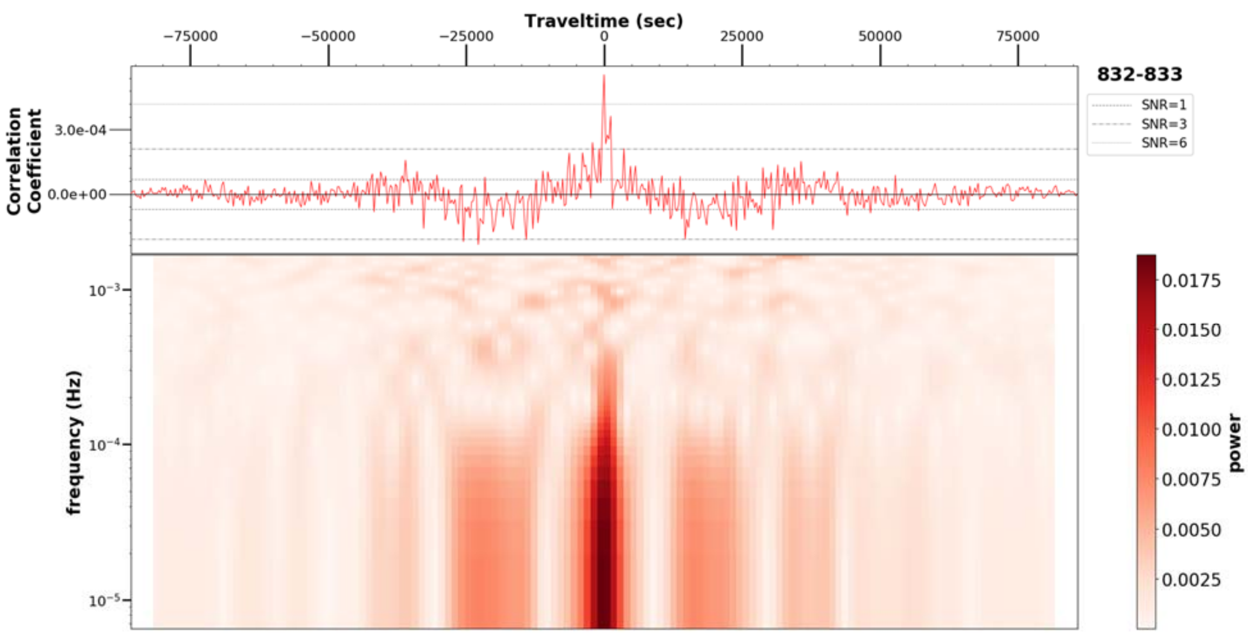

Figure A- 137. Spectrogram from stacked cross-correlated daily length data segments with preserved amplitudes (not normalized), pumping-period-only segments. Station pair: 832-833

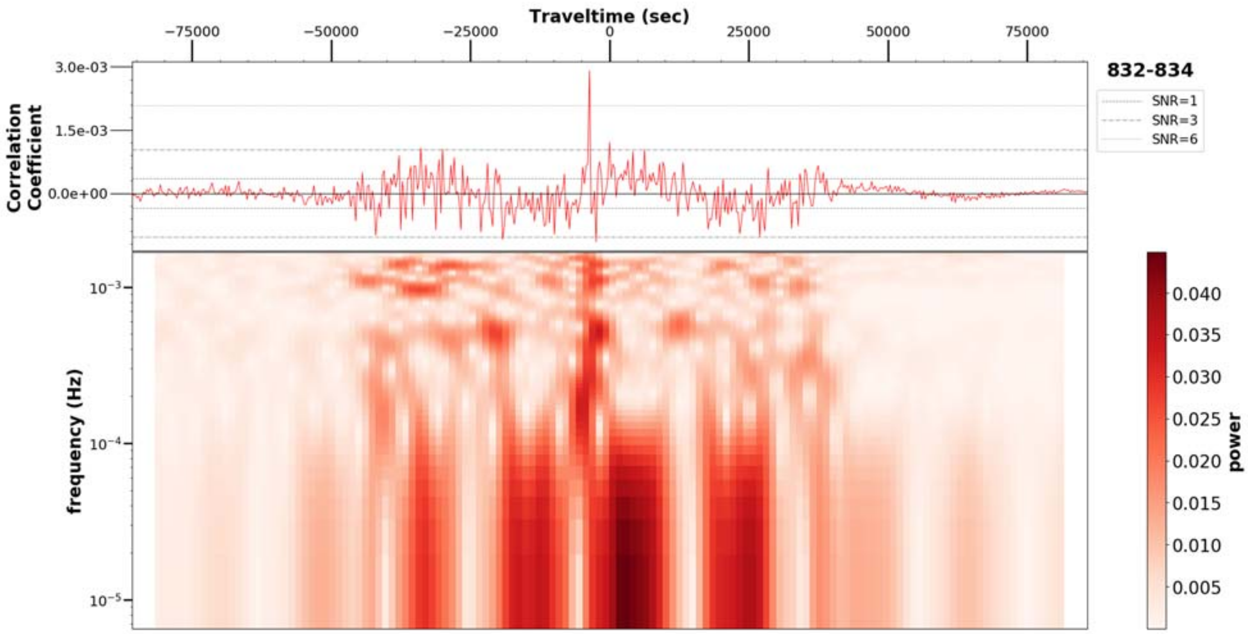

Figure A- 138. Spectrogram from stacked cross-correlated daily length data segments with preserved amplitudes (not normalized), pumping-period-only segments. Station pair: 832-834

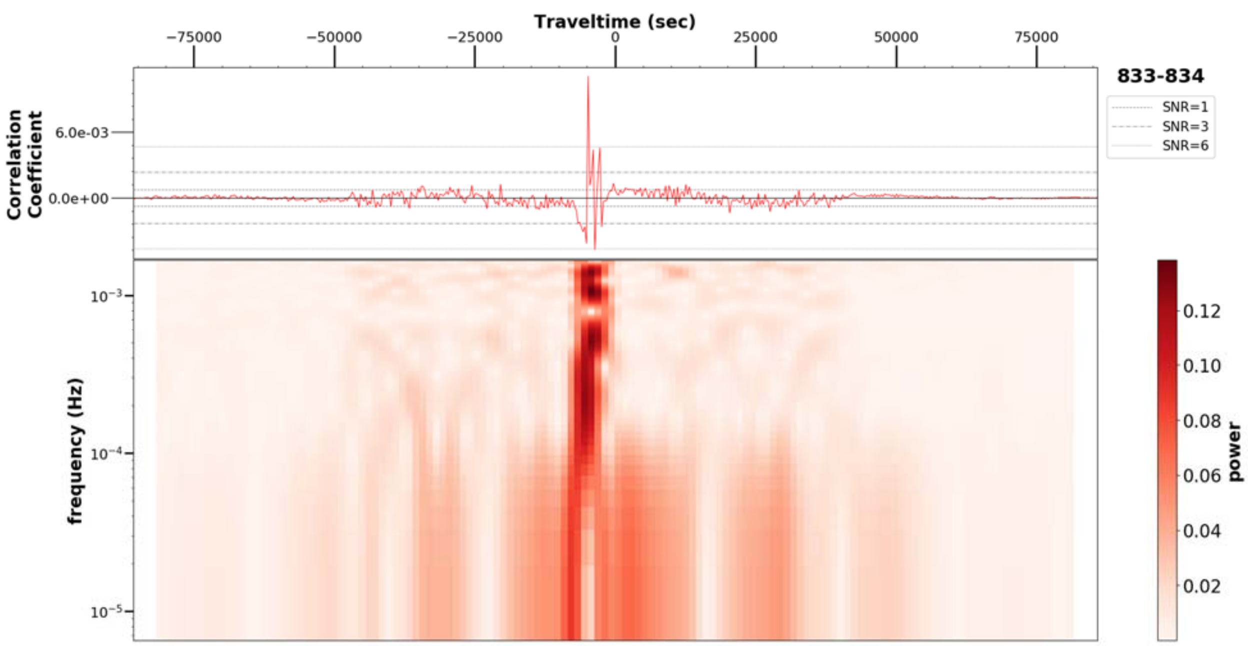

Figure A- 139. Spectrogram from stacked cross-correlated daily length data segments with preserved amplitudes (not normalized), pumping-period-only segments. Station pair: 833-834

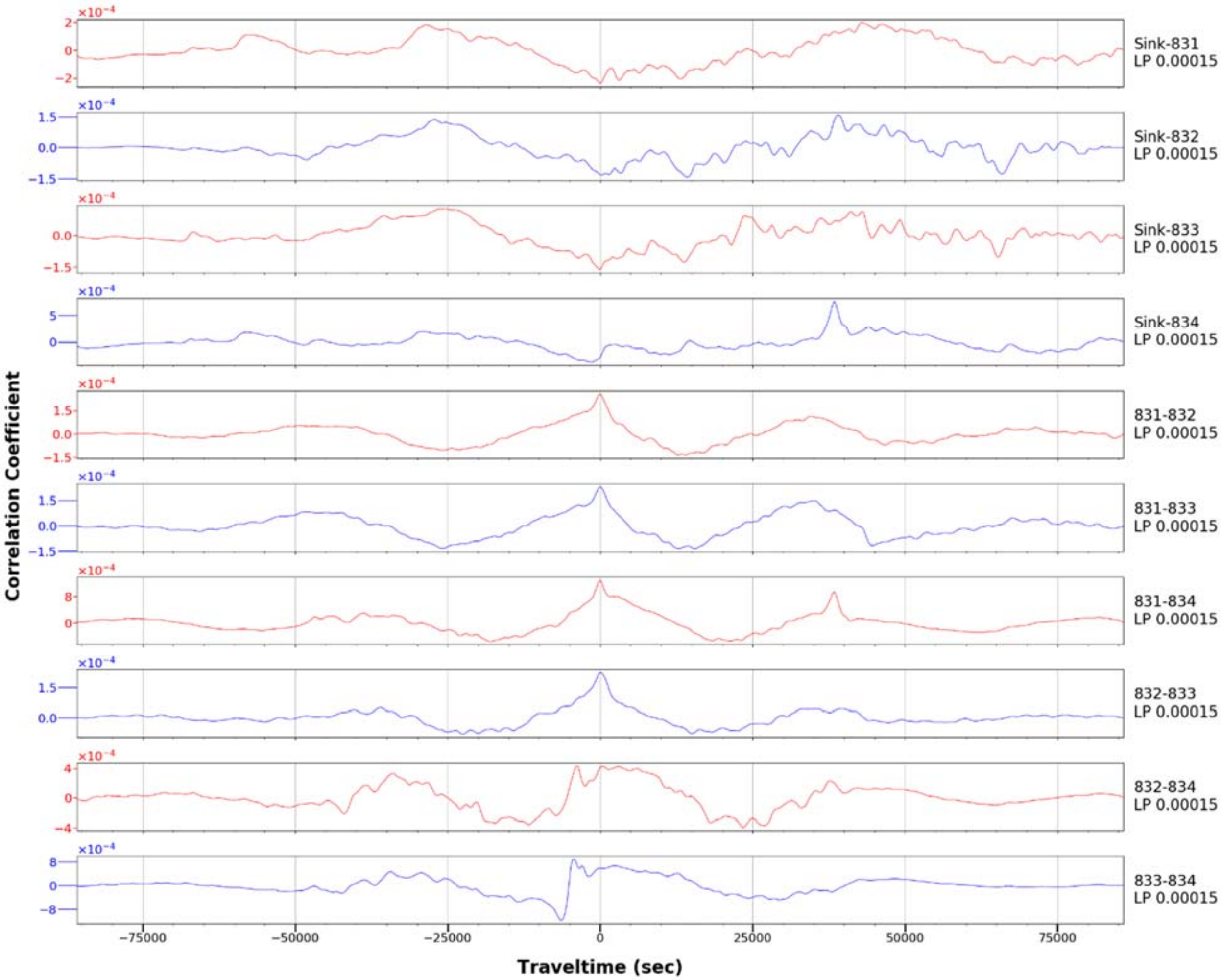

Figure A- 140. Stacked cross-correlograms from pumping-period-only daily data segment lengths with preserved water level amplitudes (not normalized). Correlograms were low-pass (LP) filtered with a corner frequency of 0.00015 Hz, or a period of just under 2 hours, which is indicated to the right of each panel.